



24018459



This is to certify that the

thesis entitled

Charge Transport Mechanisms in Layered Oxide and Polymeric Microsturctures: An Electrochemical Approach

presented by

Randal King

has been accepted towards fulfillment of the requirements for

Ph.D. degree in <u>Chemistry</u>

Date 8 August 1989

O-7639

MSU is an Affirmative Action/Equal Opportunity Institution

PLACE IN RETURN BOX to remove this checkout from your record. TO AVOID FINES return on or before date due.

	DATE DUE	DATE DUE
OCT 1 8 199 304		
	·	

MSU Is An Affirmative Action/Equal Opportunity Institution

CHARGE TRANSPORT MECHANISMS IN LAYERED OXIDE AND POLYMERIC MICROSTRUCTURES: AN ELECTROCHEMICAL APPROACH

Вy

Randal Daniel King

A DISSERTATION

Submitted to
Michigan State University
in partial fulfillment of the requirements
for the degree of

DOCTOR OF PHILOSOPHY

Department of Chemistry

1989

ABSTRACT

CHARGE TRANSPORT MECHANISMS IN LAYERED OXIDE AND POLYMERIC MICROSTRUCTURES: AN ELECTROCHEMICAL APPROACH

Вy

Randal Daniel King

complete electrochemical characterization of The the mechanisms controlling charge transport in layered oxides and polypyridinium based polymers is established. Synthetic design of these microstructures on the microscopic level is systematically developed for the purpose of achieving specific functions. The nature of the electroactive sites in layered oxides (clays) is established and characterized. Redox ions incorporated into clays have, on the microscopic level, several possible locations: (i) electrostatically bound in the galleries between clay layers; (ii) electrostatically bound on the outer edges of the clay platelets; (iii) in voids around the clay particles; and (iv) adsorbed onto the outer edges of the clay layers as ion-pairs in excess of the charge exchange capacity (CEC) of the clay. Only the ions which are present in the voids of clay films display electroactivity. On the macroscopic level, clay platelets stack in random orientation near the electrode and a more highly ordered orientation away from the electrode. The observed electroactivity

arises only from redox ions in voids created by the random face to edge stacking of clay platelets near the electrode. The amount of electroactivity from clay films can be increased by electropolymerization of vinyl containing inorganic complexes. Significantly the redox ions in the galleries of clays can become activated by using intersalated clay to tailor the clay microstructure.

Polymeric microstructures can also be manipulated with synthetic design which is established as a useful method for the controlling charge transport within modified electrode films. The rate of charge propagation of redox anions ion-exchanged in several poly-pyridinium films is observed to be dominated by electrostatic interactions involving cationic binding sites in the polymers. As the charge density of these binding sites increases so does their ability to interact with anions incorporated into their polymer matrix, thus slowing down the diffusion rate of the anion. In this way the rate at which anions diffuse in polycationic polymers soaking in nonaqueous solvents can be mediated with the synthetic design of cationic binding sites in polymers. This procedure is exploited by establishing a 2,2'-bipyridinium based polymer which possess an extremely high charge density binding pocket.

Electrodes modified with 2,2'-bipyridinium films are developed into a novel electroanalytical sensor. This sensor displays unprecedented ability to extract anions from dilute solutions. Furthermore, many crucial features necessary to the successful development of electrochemical sensors in aqueous and nonaqueous

Randal Daniel King

solvents, which heretofore have eluded characterization, have been realized for 2,2'-bipyridinium polymer modified electrodes.

ACKNOWLEDGEMENTS

Many endeared friends have helped me survive the past five years. Of course, academically on the top of my list of friends to thank is Dan Nocera. I have learned a great deal about technical writing and oral presentations from Dan. His guidance towards receiving a PhD is greatly appreciated. In the early part of my research I also received useful advice and assistance from Thom Pinnavaia which is also appreciated. Additionally, I would like to acknowledge and express my gratitude to Bob Mussell for working with me for many hours to become accustomed with electrochemical instrumentation and the Nocera lab.

Of my friends I would like to thank for their support, my gratitude to my best friend, Michele is beyond words. She has stood by my side through my entire career at Michigan State, with continuous words of encouragement and mountains of affection. I also thank God for the wonderful gift of our daughter, Emily who has helped me maintain my sanity. I would also like to express my delight with working for a man who I not only can learn from but also enjoy his companionship at sporting events, picnics, tailgate parties, bars, and yes even A.C.S. meetings. The memories I will maintain from my graduate school experience throughout my life will be the fun times with my fellow students and Dan. I am certain that Bob, Mark, and Colleen were the direct cause of my taking five years to graduate. Although, they are also the reason I enjoyed myself. Recently our lab has acquired an assortment of friendly graduate students and Janice. They seem strange at first but after

you get to know them you become certain they are good friends. Thank you all for your company in the lab and particularly to Janice for her delightful words of encouragement and Colleen for always being in a good mood.

Finally, I would like to thank my Family, most importantly my parents for their continual support throughout my college career. I cannot express how grateful to my family I am for their constant encouragement and love over the past 10 years.

TABLE OF CONTENTS

					rage
LIST	r of ta	ABLES			хi
LIST	OF FI	GURE	S		xiii
I	INT	RODU	CTION		1
ΙΙ	EXP	ERIMI	ENTAL	······································	41
	A.	Prep	aration	of Compounds	41
		1.	Inorg	ganic Metal Complexes	41
			a.	General Procedures	41
			b.	Synthesis of Fe(bpy) ₃ (SO ₄),	
				$Fe(phen)_3(SO_4)$, and $Fe(vbpy)_3(SO_4)$	41
			c.	Synthesis of (PPN) ₂ Fe(bpy)(CN) ₄	41
			d.	Synthesis of Os(bpy) ₃ (ClO ₄) ₂	42
			e.	Synthesis of Ru(bpy) ₃ (ClO ₄) ₂	43
			f.	Synthesis of (NBu) ₄ Mo ₆ Cl ₁₄	43
			g.	Synthesis of (NBu) ₄ W ₆ Br ₁₄	43
		2.	Orga	anic Polymers and Monomers	44
			a.	General Procedures	44
			b.	Synthesis of N-methylpolyvinyl-	
				pyridinium hexafluorophosphate (PVP ⁺ —Me/PF ₆ ⁻) 1	45
			c.	Synthesis of $\{N,N'\text{-bis}[-3-(\text{tri-}$	
				methoxysilyl)propyl]-4,4'-	
				bipyridinium}diiodide (PQ ²⁺ /2I ⁻), 2	45
			d.	Synthesis of 4-vinyl-4'-methyl-	
				2,2'-bipyridine (vbpy), 3	46

			Page
		e. Synthesis of 4-vinyl-4'-methyl-	
		N,N'-1,2-ethylene-2,2' bipyridinium	
		(EVDQ ²⁺), 4	46
		f. Synthesis of 4-vinyl-4'-methyl-	
		N,N'-1,3-propylene-2,2'-bipyridinium	
		(PVDQ ²⁺), 5	47
		g. Synthesis of 4-vinyl-4'-methyl-	
		N,N'-1,4-butylene-2,2'-bipyridinium	
		(BVDQ ²⁺), 6	48
	3.	Synthesis, Modification, Purification of	
		Layered Oxides	48
		a. Sodium Montmorillonite	
		(Wyoming)	48
		b. Synthetic Hectorite (Laponite)	48
		c. Fluorohectorite	49
		d. Reduced Charge Montmorillonite	49
		e. Intercalates	49
		f. Intersalated Montmorillonite	49
	4.	Supporting Electrolytes	50
	5 .	Solvents	50
B.	Meth	ods and Procedures	51
	1.	Electrochemical Measurements	51
	2.	Preparation of Modified Electrodes	51
	3.	Spectroscopic Characterization and	
		Instrumentation	53
	4.	Determination of Diffusion Coefficients	54

				Page
	C	Cons	struction and Cleaning of Working Electrodes	56
		1.	Pyrolytic Graphite	56
			a. Graphite Disc Electrodes	56
			b. Planer Graphite Electrodes	56
		2.	Platinum and Glassy Carbon Disk	
			Electrodes	. 56
		3.	Platinum Oxide Disc Electrodes	57
		4.	Preparation of Tin Oxide Electrodes	57
III	CLA	Y MOI	DIFIED ELECTRODES	. 58
	A.	Back	ground	. 58
	В.	Resu	ilts and Discussion	66
		1.	Nature of the Electroactive Sites	66
		2.	Elucidation of Clay Microstructural	
			Control of Electroactivity	90
		3.	Electrocatalytic Activity of	
			Clay/Polymer films	97
		4.	Intersalated Clay Films	118
	C	Conc	clusion	. 136
IV	POL	YPYR	IDINIUM BASED MODIFIED ELECTRODES	. 138
	A.	Back	ground	138
	B.	Resu	ilts and Discussion	150
		1.	PVP+_Me Polymer Modified Films	150
		2.	PQ ²⁺ Polymer Modified Films	169
		3.	EVDQ ²⁺ Polymer Modified Films	178
		4.	Comparison of EVDQ ²⁺ , PVDQ ²⁺ ,BVDQ ²⁺	
			Polymer Modified Films	190

		I	Page
	C	Conclusion	204
V	DEV	ELOPMENT OF AN ELECTROCHEMICAL SENSOR	206
	A.	Background	206
	B.	Results and Discussion	207
		1. Development of an Electroanalytical	
		Anionic Sensor for Nonaqueous Solvents	207
		2. Characterization of Anionic Effects on	
		the Microstructure of EVDQ ²⁺	213
	C	Conclusion	221
VΙ	REF	ERENCES	222

LIST OF TABLES

		Page
1	Conducting Silanes Used to Modify Oxide Surfaces	5
2	Monolayers of Electroactive Organics Attached to	
	Carbon Electrodes	10,11
3	Class I Polmers with a Polyvinyl Backbone	16-18
4	Electroactive Organic Monomers Used to Form Class	
	I Polymers	19,20
5	Class III Insulating Polyionic Polymers	22,23
6	Time Required to Reach Maximum Current	
	Response for Different Films Soaked in 0.2 mM	
	Os(bpy) ₃ ²⁺	81
7	Amount of Electroactivity From Different Clay Films	
	of Varying Thickness After Soaking in Aqueous	
	Fe(bpy) ₃ ²⁺ Solutions Containing 0.1 M Na ₂ SO ₄	91
8	Amount of Electroactivity from 0.38 μm	
	Montmorillonite Films Resulting from Incorporated	
	or Polymerized Fe(vbpy) ₃ ²⁺	111

		Page
9	Amount of Electroactivity from Different Clay Films after Soaking in 5.1 mM Fe(bpy) ₃ ²⁺	123
10	Diffusion Coefficients of W ₆ Br ₁₄ ² in Acetonitrile	
	Determined by Different Electrochemical	
	Techniques	164
11	Apparent Diffusion Coefficients and FWHM Values	
	for EVDQ ²⁺ Films With Varying Thicknesses	214
12	Apparent Diffusion Coefficients and FWHM Values	
	for PVDQ ²⁺ Films With Varying Thicknesses	215
13	Apparent Diffusion Coefficients for EVDQ ²⁺ and	
	PVDQ ²⁺ Films w/wo Added W ₆ Br ₁₄ ²⁻	219

LIST OF FIGURES

		Page
1	General reaction scheme for the reaction between organo-silanes and hydroxy functional groups on metal and semiconductor surfaces	4
2	Reactive pathways that are used to convert insulating silanes, which are covalently attached to electrodes, into conducting films	7
3	Reaction schemes for attaching organic monolayers to carboxylic acid functional groups on carbon surfaces	9
4	Schematic depicting three classes of conducting polymers: (i) Class I possess the redox active site in the polymer backbone; (ii) Class II have redox material covalently linked to a moeity on the polymer chain; and (iii) Class III possess electrostatically bound redox ions within a charged polymer matrix.	15
5	Ideal cyclic voltammogram obtained from a thin film of electroactive material attached to an electrode	. 27

		Page
6	Ideal cyclic voltammogram obtained from W ₆ Br ₁₄ ²	
	freely diffusing through an acetonitrile solution	
	containing 0.2 M TEAP	. 33
7	Idealized structure of smectite clay with a	
	hydrated cation between layers	60
8	Model of a clay film on an electrode containing ion-	
	exchanged polypyridyl metal complexes and	
	electrolyte	. 64
9	Increasing cyclic voltammetric response from Os(bpy) ₃ ²⁺ incoporating into a montmorillonite film	
	coated on graphite in an aqueous solution	
	containing 0.2 M sodium acetate and 0.2 mM	
	Os(bpy) ₃ ²⁺	. 68
10	Cyclic votammograms of a 80 % pre-exchanged	
	montmorillonite film on pyrolytic graphite: (a)	
	soaking in an aqueous solution containing 0.1 M	
	Na ₂ SO ₄ ; and (b) electrode from above placed in an	
	aqueous solution containing 0.1 M Na ₂ SO ₄ and 0.2	
	mM Os(bpy) ₃ ²⁺	. 71

		Page
1 1	A reaction scheme devised to oxidize Os(bpy) ₃ ²⁺	
	located in the galleries, with utilization of	
	Fe(bpy) ₃ ²⁺ as a redox charge shuttle agent	75
1 2	Reversible cyclic votammogram upon the first	
	oxidation scan of Fe(bpy) ₃ ²⁺ ion-exchanged into a	
	montmorillonite film containing pre-exchanged	
	Os(bpy) ₃ ²⁺ while soaking in an aqueous solution	
	containing 0.1 M Na ₂ SO ₄	77
13	Current responses obtained from Os(bpy) ₃ ²⁺	
	exchanged into montmorillonite films from an	
	aqueous solution containing 0.2 sodium acetate and	
	$0.2 \text{ mM Os(bpy)}_3^{2+}$: (a) 78 % pre-exchanged	
	$Os(bpy)_3^{2+}$; (b) 38 % pre-exchanged $Os(bpy)_3^{2+}$; (c)	
	Na ⁺ -exchanged (humidified); (d) Na ⁺ -exchanged (air	
	dried); and (e) reduced charge	80
1 4	SEM images of Na ⁺ -exchanged montmorillonite films	
	on pyrolytic graphite, (a) 1000 x and (b) 7800 x	84
1 5	The current response obtained as a function of time	
	from various clay films adsorbed onto graphite	
	soaking in 0.2 M sodium acetate and 0.2 mM	
	Os(bpy) ₃ ²⁺ : (a) laponite; (b) montmorillonite; and (c)	
	fluorohectorite	88

		Page
16	Model depicting locations of electroactive and non-	
	electroactive polypyridyl metal complexes within a	
	clay film	96
17	Growth of poly-Fe(vbpy) ₃ ²⁺ at 10 min intervals in	
	montmorillonite adsorbed onto pyrolytic graphite	
	while soaking in an acetonitrile solution containing	
	0.2 M TEAP and 2.0 mM Fe(vbpy) ₃ ²⁺	100
18	Cyclic voltammetric waves obtained from a poly-	
	Fe(vbpy) ₃ ²⁺ /montmorillonite electrode in	
	acetonitrile containing 0.2 M TEAP: (a) upon	
	scanning the electrodes potential from 0.00 V to	
	+1.20 V, to -1.80 V, and back to 0.00 V νs . SCE; (b)	
	after the reduction waves had been scanned once	
	prior to measurement; and (c) after the oxidation	
	wave had been cycled once prior to measurement	102
19	Cyclic voltammogram of poly-Fe(vbpy) ₃ ²⁺ adsorbed	
	onto pyrolytic graphite while soaking in an	
	acetonitrile solution containing 0.2 M TEAP: (a) upon	
	scanning the electrodes potential from 0.00 V to	
	+1.20 V, to -1.80 V, and back to 0.00 V vs. SCE; (b)	
	after the reduction waves had been scanned once	
	prior to measurement; and (c) after the oxidation	
	wave had been cycled once prior to measurement	105

		Page
20	A plot of the peak height $i_{p,a}$ (μ A) vs. the scan rate	
	(mV/sec) for the CV reproduced in Figure 18	109
21	Cyclic votammograms scanned at 2 mV/sec, of a	
	clay/poly-Fe(vbpy) ₃ ²⁺ film soaking in an aqueous	
	solution containing 0.2 M LiClO ₄ : (a) after the	
	addition of 4.2 mM Fe(CN) ₆ ⁴ and; (b) before the	
	addition of 4.2 mM Fe(CN) ₆ ⁴	. 115
22	Model depicting origins of electrocatalysis from a	
	clay/poly-Fe(vbpy) ₃ ²⁺ film on an electrode	117
23	The first two cyclic voltammograms of a Fe(bpy) ₃ ²⁺	
	intersalated montmorillonite film on pyrolytic	
	graphite immersed in a dichloromethane solution	
	containing 0.2 M TBAP	. 121
24	The X-ray diffraction patterns obtained from	
	Fe(bpy) ₃ ²⁺ intersalated films on pyrolytic graphite:	
	(a) before the electrolysis of the film; and (b) after	
	the electrolysis of the film in a dichloromethane	
	solution containing 0.2 M TBAP	126

		Page
25	Cyclic voltammetric waves of a polymerized	
	Fe(vbpy) ₃ ²⁺ /intersalated montmorillonite film	
	adsorbed onto pyrolytic graphite while soaking in	
	an acetonitrile solution containing 0.2 M TEAP	129
26	A plot of the peak height $i_{p,a}$ (μ A) vs. the scan rate	
	(mV/sec) for the CV reproduced in Figure 25	132
27	The X-ray diffraction patterns obtained from	
	polymerized Fe(bpy) ₃ ²⁺ /intersalated	
	montmorillonite films on pyrolytic graphite: (a)	
	before the electrolysis of the film; and (b) after the	
	electrolysis of the film in a acetnitrile solution	
	containing 0.2 M TEAP	134
28	Annihilation reaction between oxidized M ₆ X ₁₄ ⁻	
	cluster and reduced pyridinium ions to produce	
	cluster in its emissive excited state or ground state	141
29	Distance dependence of the differential bimolecular	
	rate constant for the excited-state (es) and ground-	
	state (gs) electron-transfer channels for the	
	reaction between Mo ₆ Cl ₁₄ and one electron	
	reduced 4-cyano-N-methylpyridinium	143

		Page
30	Reaction scheme for generation of excited state M ₆ X ₁₄ ^{-*} cluster upon annihilation of oxidized	
	cluster ion and a one-electron reduced poly-	
	pyridinium based polymer	147
3 1	A 250 MHz NMR spectrum of N-methylpolyvinyl	
	pyridinium hexafluorophosphate in CD ₃ CN	153
3 2	Cyclic voltammograms of: (a) W ₆ Br ₁₄ ²⁻ dissolved in	
	acetonitrile containing 0.2 M TBAPF ₆ at a bare	
	platinum electrode; (b) a PVP+Me film with a	
	surface coverage = $2.2 \times 10^{-6} \text{ mol/cm}^2$ absorbed	
	onto a platinum electrode immersed in an	
	acetonitrile solution containing 0.2 M TBAPF ₆ ; and	
	(c) a PVP ⁺ -Me film ion-exchanged with W ₆ Br ₁₄ ²	
	immersed in an acetonitrile solution containing	
	0.2 M TBAPF ₆	157
33	A plot of peak height $i_{p,a}$ (μ A) vs. the scan rate	
	(mV/s) for the anodic wave of the CV reproduced in	
	Figure 32c	159
34	The rate of W ₆ Br ₁₄ ² ion departure from an PVP+	
	Me film on a platinum electrode after potential	
	steps to +1.3 V vs. SCE for	
	increasing times	. 168

		Page
39	Cyclic voltammograms of a platinum electrode	
	coated with a EVDQ ²⁺ film (surface coverage = 1.7 x	
	10 ⁻⁸ mol/cm ²) and dipped into an acetonitrile	
	solution containing 0.2 M TEAP upon scanning the	
	potential: (a) past the one electron reduction waves	
	of EVDQ ²⁺ ; (b) past the one electron reduction	
	waves of EVDQ ²⁺ after addition of 15 μ M W ₆ Br ₁₄ ²⁻	
	to the acetonitrile solution; and (c) past the	
	oxidation of W ₆ Br ₁₄ ² - after incorporation into the	
	EVDQ ²⁺ film	. 185
40	Cyclic voltammograms of W ₆ Br ₁₄ ² - incorporated	
	into a EVDQ ²⁺ film adsorbed onto a platinum	
	electrode (surface coverage = 1.7 x 10 ⁻⁸ mol/cm ²)	
	immersed in an acetonitrile solution containing 0.2	
	M TEAP recorded at (a) 10 V/s and (b) 33V/s	188
41	Cyclic votammogram of a PVDQ ²⁺ film adsorbed	
	onto a platinum electrode (surface coverage = 4.0 x	
	10 ⁻⁹ mol/cm ²) immersed in an acetonitrile solution	
	containing 0.2 M TEAP	193

		Page
42	Cyclic voltammetric waves obtained from a PVDQ ²⁺	
	film coated onto a platinum electrode (surface	
	coverage = $1.1 \times 10^{-8} \text{ mol/cm}^2$) dipped into an	
	acetonitrile solution containing 0.2 M TEAP and 20	
	μ M W ₆ Br ₁₄ ² : (a) upon scanning the electrodes	
	potential from 0.00 V to +1.40 V to -1.10 V and	
	back to 0.00 V vs. SCE; (b) after the reduction	
	waves for the PVDQ ²⁺ polymer had been scanned	
	once prior to measurement; and (c) after the	
	oxidation wave of W ₆ Br ₁₄ ² - had been cycled once	
	prior to measurement	. 195
43	Cyclic votammogram of a PVDQ ²⁺ film on a	
	platinum electrode soaking in an acetonitrile	
	solution containing 0.2 M TBAPF ₆ ,	
	25 μ M W ₆ Br ₁₄ ²⁻ and 50 μ M IrCl ₆ ²⁻	198
44	A plot of the apparent diffusion coefficients, D _{app}	
	for W ₆ Br ₁₄ ² - incorporated into PVP+Me, PQ ²⁺ ,	
	BVDQ ²⁺ , PVDQ ²⁺ , and EVDQ ²⁺ polymeric films as a	
	function of the number of	
	hinding sites	201

45	A plot of the distribution coefficients K_D for	
	W ₆ Br ₁₄ ² - incorporated into PVP—Me, PQ ²⁺ , BVDQ ²⁺ ,	
	PVDQ ²⁺ , and EVDQ ²⁺ polymeric films as a function	
	of the number of binding sites	203
46	Cyclic voltammogram of W ₆ Br ₁₄ ² - incorporated	
	from an acetonitrile solution containing 0.2 M TEAP and 5 x 10 ⁻⁸ M W ₆ Br ₁₄ ²⁻ into a EVDQ ²⁺ film	
	adsorbed onto a platinum electrode (surface	
	coverage = 4.1 x 10 ⁻⁹ mol/cm ²)	210
47	A plot of the cyclic voltammetric peak current for	
	the oxidation of W ₆ Br ₁₄ ² - incorporated into EVDQ ²⁺	
	films as a function of the concentration of W ₆ Br ₁₄ ²	
	in the contacting acetonitrile solution for platinum	
	electrodes with surface coverages of, (a) 2.1 x 10 ⁻⁹	
	mol/cm^2 and (b) 1.1 x 10 ⁻⁹ mol/cm^2	212

CHAPTER I

INTRODUCTION

The investigation of modified electrodes has clearly been the most exciting and active area in electrochemistry over the past few decades. 1-6 Studies in this area have led to a clearer understanding of many aspects of electrochemistry including new insights about the electrode double layer and effects of adsorbed organics in the double layer, the effect of chemical modification of the electrode surface on heterogeneous electron transfer and diffusion rates, and a greater understanding of the role of distance, reorganizational energies, and electronic factors on homogeneous and heterogeneous electron transfer rates. These fundamental studies have had direct impact on the practical applications of organic and inorganic polymers in the areas of semiconductors, 7-12 electrocatalysis, 13-23 organic synthesis, 24-30 biochemical analysis, 31-38 electronics, 39-40 energy conversion, 41-50 electrochromic displays, 51-61 and redox-chemical sensors. 62-65

The area of modified electrodes was initiated in 1973 when Hubbard and Lane⁶⁶ deliberately adsorbed monolayers of organic olefins onto platinum electrodes for the purpose of modifying the electrode double layer. The olefins were either intrinsically electroactive or possessed a free coordination site that was used to bind electroactive inorganic ions. These studies provided the first insights into unique issues in regard to modified electrodes and their double layers. Since these pioneering experiments, the field of modified electrodes has steadily progressed from organic monolayers towards the development of more complex microstructures on the electrode surface, including multilayer amorphous organic polymers

and recently more highly ordered crystalline inorganic microstructures.

Techniques for covalently attaching monolayers to electrode surfaces first utilized condensation reactions on reactive SnO₂ surfaces.⁶⁷ Conducting silanes were coordinatively linked to this wide-bandgap semiconductor through Sn-O-Si linkages following the general reaction scheme shown in Figure 1. The silanization reaction works well with virtually any alkoxy- or chloro-silane and on all electrodes possessing an OH functional group. Examples of conducting silanes, electrodes, and reduction potentials of the silanized polymer films are listed in Table 1. An alternative approach to the preparation of electroactive silanized microstructures is to modify the electrode with nonconducting silanes that are subsequently converted to conducting films through chemical reactions. Some of these silanes and their respective reactions are shown in Figure 2.

Surface modification is not limited to hydroxylic functionalities but can include a variety of other organic groups as well. Miller et al. 88 demonstrated that carboxylic acid groups present on the surfaces of carbon can be functionalized with organic monolayers according to the reaction scheme shown in Figure 3a. Reactions 3b and 3c are two additional general reactions which have since been reported. 89-91 In almost all of these studies, the electroactivity of the film is generated by coordination of an inorganic complex to a functional group on the organic monolayer. Exemplary systems which have been reported in the literature, are presented in Table 2.

Figure 1

General reaction scheme for the reaction between organosilanes and hydroxy functional groups on metal and semiconductor surfaces.



M = Sn, In, Au, Pt, Ru, Ti, Ge, Ga, Si

R = CI, OMe, OEt

X, Y = see Table 1

Figure 1

Table 1
Conducting Silanes Used to Modify Oxide Surfaces

Silane ^a	Electrode	E ^o surf	Ref.
Fe[CpSi(OCH ₂ CH ₃) ₃] ₂	Pt/PtO Ge/GeO	+0.60 +0.45¢	68,69 70
FeCp ₂ (μ-SiCl ₂)	Au/AuO	+0.43	69
CpFeCpSiCl ₂	Si/SiO Pt/PtO Au/AuO	+0.08 ^c +0.51 +0.43	71-73 70 74
-(CH ₂ CH) _x (CH ₂ CH) _y 	Pt/PtO	+0.40	75
N—(CH ₂) ₃ Si(OCH ₃) ₃	Pt/PtO	+0.80d	76
(bpy) ₂ R u CH ₂ CH ₂ SiCl ₃	SnO ₂	+1.05	77,78

^aCp = cyclopentadienyl, bpy = bipyridine. ^bPotential in volts vs. SCE. ^cBroad waves. ^dChemically irreversible wave.

Figure 2

Reactive pathways that are used to convert insulating silanes, which are covalently attached to electrodes, into conducting films.

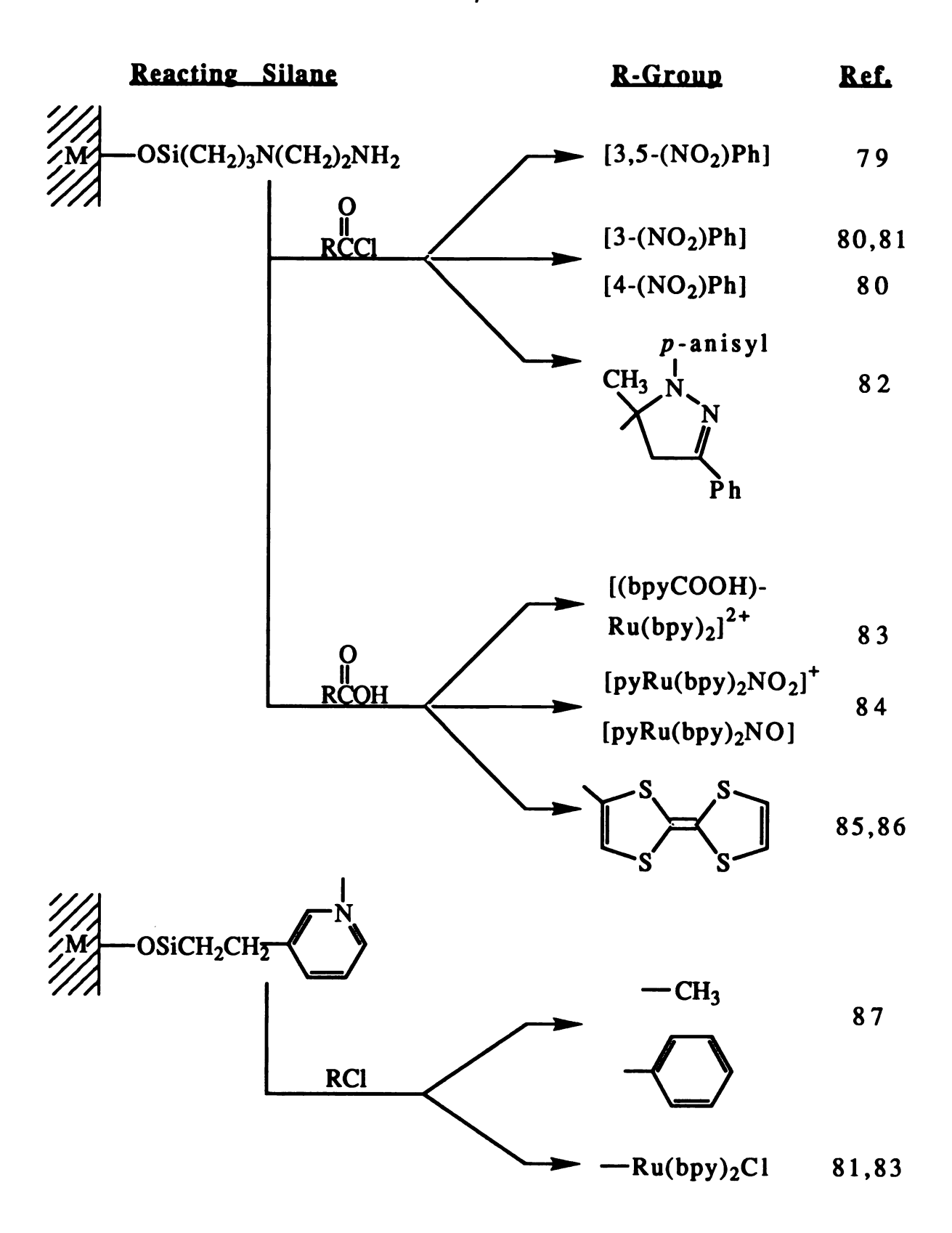
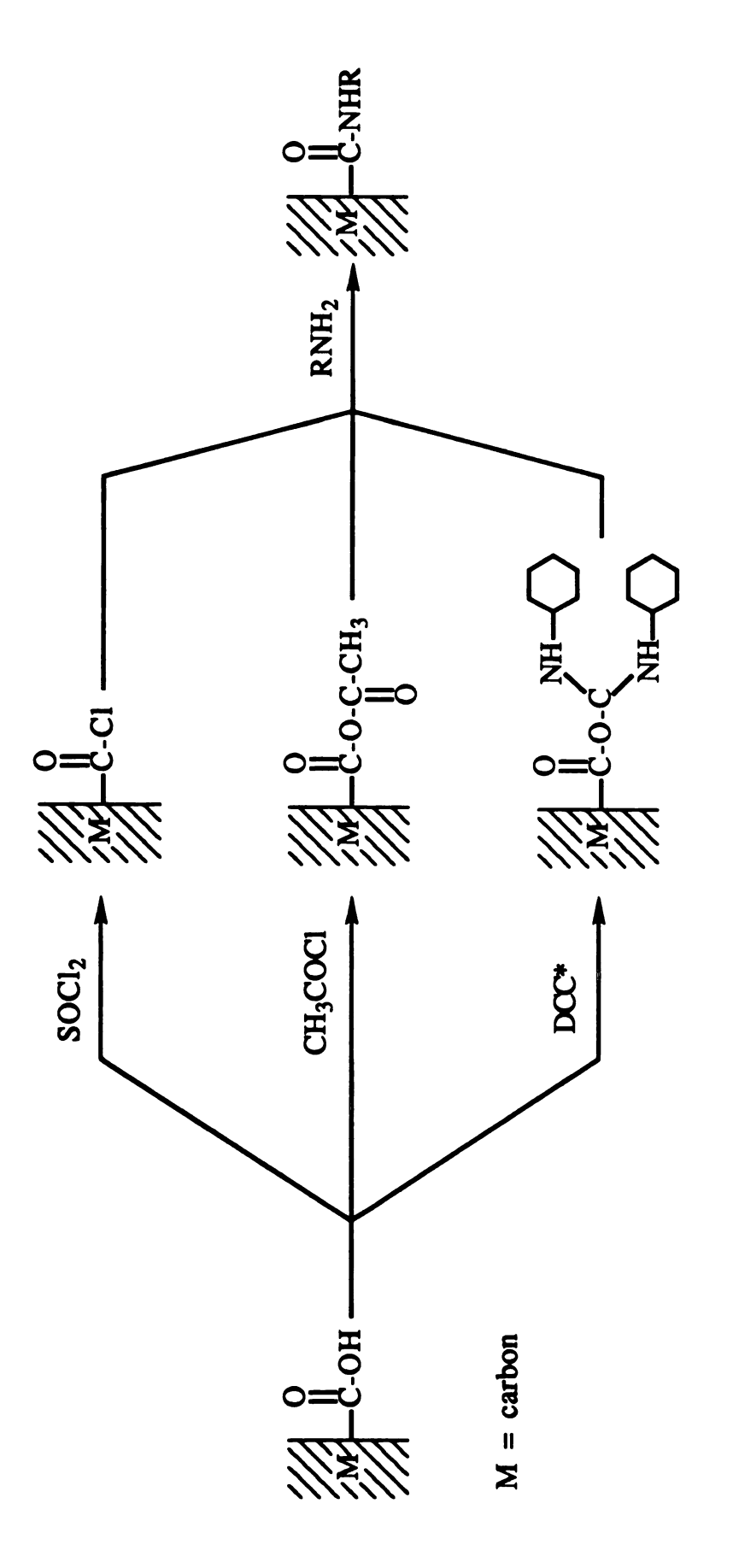


Figure 2

Figure 3

Reaction schemes for attaching organic monolayers to carboxylic acid functional groups on carbon surfaces.



* DCC = N,N'-dicyclohexylcarbodiimide

Figure 3

Table 2

Monolayers of Electroactive Organics Attached to Carbon Electrodes

Electrode/-C(O)Rb	$\mathbf{E^o}_{\mathbf{s}}$	E ^o surf	
R- modifying agent	1st wave	2nd wave	Ref.
-(m-NH ₂) ₄ TPP	-1.50	-1.45	92,93
-Fe(p-NH ₂) ₄ TPP	-0.18	-1.18	93,94
$-Co(m-NH_2)_4TPP$	+0.10	-0.86	93
$-Ni(p-NH_2)_4TPP$	-1.22	-1.80	93,94
-NH-CpFeCp	+0.44	-	93
-NH-CH ₂ N-Ru(EDTA)	-0.10	-	95

Table 2 (cont'd.)

E ⁰ s	a urf	
1st wave	2nd wave	Ref
+0.52	-	1 4
+0.20	-	96
-0.66	-	97
	+0.52 +0.20	+0.52 - +0.20 -

^aPotential in volts vs. SCE. ^bTPP = tetraphenylporphyrin, Cp = cyclopentadienyl, EDTA = ethylenedinitrilotetraacetate.

The modification of electrodes greatly expanded in scope and breadth with the advent of electrodes modified polymers.^{68,98-104} In contrast to the modified electrodes preceding polymer modification, polymer microstructures can be several hundred monolayers in thickness. There have been several methods developed to adhere polymers to electrode surfaces including physical adsorption, low solubility in the contacting solvent, and covalent attachment by using several different techniques. coating involves soaking the electrode in a dilute solution of the polymer for one hour to several days, 77,78,105-107 whereas droplet evaporation requires a solution of the polymer to be deposited directly onto the electrode surface followed by slow evaporation of the solvent or spin coating.^{75,108,109} Alternatively, the application of a radio frequency plasma discharge to gaseous organic monomers has been used to initiate polymerization directly on the electrode surface.89,103,110-112 Polymer modified electrodes can also be prepared by oxidative or reductive deposition. 101,113 This procedure takes advantage of changes in solubility which accompany electrochemically induced changes in ionic states. A different electrochemical technique utilizes free radical initiated polymerization of redox active organic monomers. 114-116 Upon their reduction or oxidation, many organic compounds will polymerize (e.g. phenols, anilines, pyrrole, and olefins) and produce strongly adhering films on electrodes.

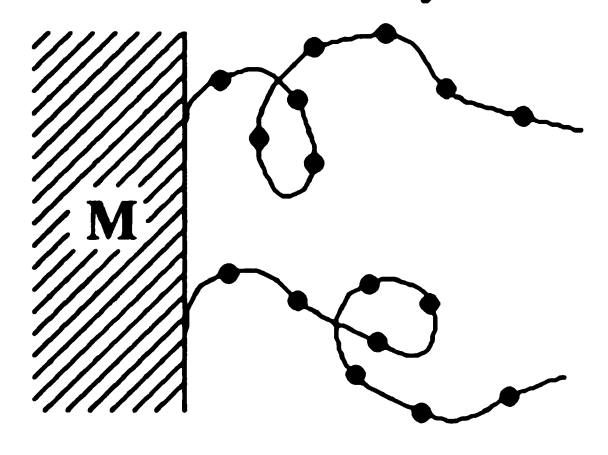
For all of these techniques the polymer is believed to adhere to the electrode surface by some combination of physical adsorption and insolubility in the contacting solvent. Polymer films can be covalently anchored to the electrode surface too by utilizing the same surface chemistry of hydroxyl groups with silanes as described in Figure 1. For this method the presence of water is required to initiate hydrolysis of the silane thereby resulting in polymer formation. 68,69,75,109

Polymers used to modify electrode surfaces can be subdivided into the three classes displayed in Figure 4: electrochemically active (Class I); insulating which are converted into conducting by covalent coordination of a electroactive species (Class II); and charged insulating which incorporate electroactive ions through ion-exchange processes (Class III). Class I polymers possess electroactive moieties built into the polymer backbone. The majority of investigations on Class I polymers to date have utilized polyvinyl backbones. Table 3 presents a selected listing of electrochemically active Class I polymers possessing a polyvinyl backbone and their respective reduction potentials. Additional Class I polymers which do not possess the vinyl backbone are listed in Table 4, along with their respective reduction potentials. Typically Class II polymers are converted to conducting by using a residue of the polymer as a ligand to covalently bind transition metal complexes. Class II polymers have been comprehensively reviewed in a recent article by Abruna.6 The first example of a metal complex coordinated to a polymer was by Oyama and Anson¹⁰⁷ who coordinated Ru(EDTA)⁻ $Ru(NH_3)_5^{2+}$ to the pyridine and nitrile groups of polyvinylpyridine and polyacrylonitrile, respectively. Several other studies utilizing the coordination chemistry of ruthenium-based metal complexes with polyvinylpyridine have since

Figure 4

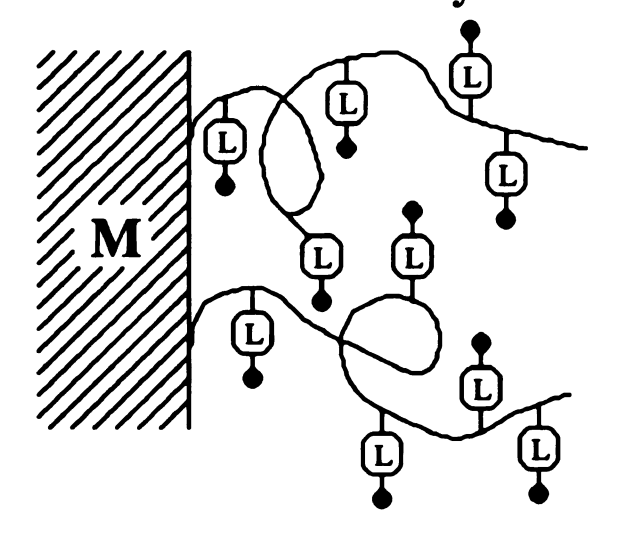
Schematic depicting three classes of conducting polymers: (i) Class I possess the redox active site in the polymer backbone; (ii) Class II have redox material covalently linked to a moeity on the polymer chain; and (iii) Class III possess electrostatically bound redox ions within a charged polymer matrix.

Class I Polymer



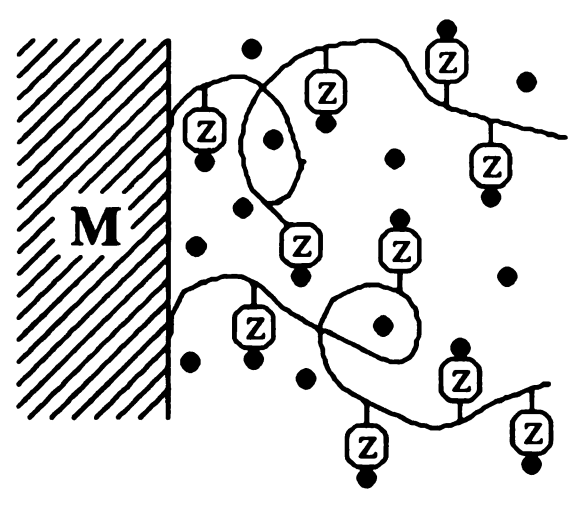
● - Electroactive Species

Class II Polymer



- L Coordination Site
- - Electroactive Species

Class III Polymer



- Z Charged Binding Site
- - Electroactive Species

Figure 4

Table 3

Class I Polymers with a Polyvinyl Backbone

-(CH ₂ -CHR)-	E ^o surf ^a 1st Wave	Method of Preparation	Ref.
Nitrobenzene	-1.60	Dip Coated	105,117
O C-NH-(CH ₂) ₂ OH Acryloyl Dopamine	+0.16	Dip Coated	118
-CpFeCp Ferrocene	+0.40	Electro- Deposited	101a
	+0.42	Plasma	103a,119
	+0.49	Droplet Evaporation	120
Carboxytetrathiafulvalene			

Table 3 (cont'd.).

-(CH ₂ -CHR)-	E ^o surf 1st Wave	Method of Preparation	Ref.
O N—CH ₃ 4-vinyloxycarbonyl- 1-methylpyridinium	-1.10 ^b	Droplet Evaporation	121
CH ₃ +N,N'-ethylene-4-methyl-2,2'-bipyridinium (EDQ ²⁺)	-0.45 ^c	Electro- Polymerized	122
9,10-diphenylanthracene	-1.88 ^d	Droplet Evaporation	123

Table 3 (cont'd.).

-(CH ₂ -CHR)-	E ^o surf 1st Wave	Method of Preparation	Ref.
**	-0.45 ^e	Droplet Evaporation	124,125
$- \left(\begin{array}{c} \\ \\ \\ \\ \end{array} \right) - \left(\begin{array}{c} \\ \\ \\ \end{array} \right) - \left(\begin{array}{c} \\ \\ \\ \end{array} \right)$	N—CH ₃		

N-methyl-N'-methylphenyl-4,4'-bipyridinium

^aPotential in volts vs. SCE. ^bA second reduction wave appears at -2.10 V vs. SCE. ^cA second reduction wave appears at -0.92 V vs. SCE. ^dAn oxidation wave appears at +1.40 V vs. SCE. ^eThe second reduction wave was not reported.

Table 4

Electroactive Organic Monomers Used to Form Class I Polymers

Electroactive	E ^o surf			
Organic Monomer	1st wave	2nd wave	Ref.	
$ \begin{bmatrix} H \\ NH \\ S \\ HN \\ n \end{bmatrix} $ 3,7-diaminophenothiazine	+0.070	-0.085 ^b	126,127	
Pyrrole	+1.20 ^b	+1.54 ^b	115b,12	
CH ₃ n 3-methylthiophene	+0.65 ^c	-	129,130	

Table 4 (cont'd.).

Electroactive Organic Monomer	E ^o surf		
	1st wave	2nd wave	Ref.
$\begin{bmatrix} CH_3 \\ I_+ \\ N \\ CH_3 \end{bmatrix}_n$ $N,N-dimethylaniline$	+0.80 ^c	-	131,132
·	-0.55	-0.95	133,134
OMe Si(CH ₂) ₃ -N OMe	$ \begin{array}{c} \text{MeO} \\ \text{H-}(\text{CH}_2)_3\text{Si} \\ \text{MeO} \end{array} $		
N,N'-bis(dimethoxysilyl)probipyridinium (PQ ²⁺)	ppyl-4,4'-		
	-0.42	-0.86	122
Si(CH ₂) ₂ —CH ₂ -N	N-CH ₃	$\left[\begin{array}{c} \\ \\ \end{array}\right]_{n}$	

N-methyl-N'-4-(2-methoxysilyl)-ethylbenzyl-4,4'-bipyridinium (BVSi²⁺)

^aPotential in volts vs. SCE. ^bChemically irreversible waves. ^cVery broad wave.

reported. 135-137 For the majority of the investigations in this area, formed via electroreductive backbone is polyvinyl polymerization of vinyl containing ligands that coordinate the In the initial studies utilizing this technique transition metal. Murray, Meyer, and coworkers electroreductively polymerized vinylpyridine and vinylbipyridine ligands coordinated to iron, osmium, and ruthenium. 114 A variety of vinyl-ligands coordinated with metal complexes have been polymerized, including vinylphenanthroline, vinyl-terpyridine, and pyrrole-pyridines. 138-141 This general technique can be applied to virtually any transition metal complex that possesses a pyridine based ligand. 142-145 In the case of Class III polymers, electroactivity within Class III polymers is typically obtained by electrostatically binding redox active ions. method of ion-exchanging redox species into polyionic films supported on electrodes was first introduced by Oyama and Anson in a now classic paper.¹⁴⁶ In this study protonated polyvinylpyridine (PVP) was used as the support to electrostatically bind polyanionic ions such as $IrCl_6^{2-}$ and $Fe(CN)_6^{3-}$. Several insulating polyionic polymers in conjunction with their incorporated ionic redox active counterparts are presented in Table 5. The unique ability of these films to indiscriminately incorporate a wide variety of ions make polyionic polymer modified electrodes a promising area for further investigations. Also it should be mentioned that some Class I and II polymers are polyionic and can electrostatically bind redox ions. this case Class I and II polymers behave identically to Class III polymers. However, this differentiation in Class III polymers will not be made for the sake of simplicity.

Table 5
Class III Insulating Polyionic Polymers

Polymer	Electrostatically Bound Redox Ions	Ref.
-(CH ₂ CH) _n - N+ R polyvinylpyridinium ^a	Fe(CN) ₆ ^{3-/4-} , Co(CN) ₆ ^{3-/4-} Ru(CN) ₆ ^{3-/4-} , Mo(CN) ₈ ^{3-/4-} IrCl ₆ ^{2-/3-}	147-149
O -(CH-C-NH) _n - (CH ₂) ₄ + NH ₃ poly(L-lysine)	$Mo(CN)_8^{3-/4-}$, $W(CN)_8^{3-/4-}$ $Fe(EDTA)^{-/2-}$, $Co(C_2O_4)_3^{3-/4-}$	150
-(CH ₂ -CH) _n - CH ₂ th Et-N-Et H	$Fe(CN)_6^{3-/4}$, $Zn(TPPS)^{3-/4}$ TPPS = meso-tetrakis- (4-sulfonatophenyl)porphine	151,152
poly-p-(diethylamino- methyl)styrene		

Table 5 (cont'd.).

	Electrostatically	
Polymer	Bound Redox Ions	Ref.
-(CH ₂ CH) _n -	$Os(bpy)_3^{3+/2+}$, $Ru(bpy)_3^{3+/2+}$	157,158
	$Co(bpy)_3^{3+/2+}$, $Ru(NH_3)_6^{3+/2+}$	
ŠO ₃ - polystyrenesulfonate		
$-(CF_2-CF_2)_{\overline{x}}-(CF-CF_2)_{y}-$	$Os(bpy)_3^{3+/2+}$, $Ru(bpy)_3^{3+/2+}$	153-156
O CF ₃ CF ₂ —CF	$Co(bpy)_3^{3+/2+}$, $Fe(bpy)_3^{3+/2+}$	
O CF ₂	Co(bpy) ₃ ^{3+/2+} , Fe(bpy) ₃ ^{3+/2+} Co(terpy) ₃ ^{3+/2+} , Ru(NH ₃) ₆ ^{3+/2+}	
CF ₂ SO ₃		
anionic perfluoropolymer (Nafion)		

 $^{^{\}mathbf{a}}$ R = H, Me, Ph.

Soon after it was established that conducting polymers could participate in electron transfer reactions with electrode surfaces, the forefront issue became the charge transport mechanism. As will be discussed later, the overall charge transport in polymer films can obey diffusional behavior. Therefore, eq 1 which describes the diffusion of ions in solution can be applied to the motion of charge in polymers,

$$x = \sqrt{Dt}$$
 (1)

where x (cm) is the distance an ion travels in time t (sec) with a rate of D (cm²/sec). Charge transport in polymers is aptly described by the diffusion coefficient D_{ct} (cm²/sec) which can replace D in eq 1. Therefore, eq 1 defines two limiting regimes for charge transport in modified electrodes. If the film thickness, d, is smaller than the displacement (d < x), then the entire film will be sampled in the time of the experiment. This limit represents so-called thin cell behavior. Alternatively, if the film thickness is greater than the displacement then diffusional behavior will be observed. Equation 1 is instructive because it illustrates that Class I and II polymers can demonstrate diffusional behavior despite the fact that the electroactive reagent is covalently anchored in the film and therefore unable to physically diffuse to the electrode. Indeed diffusional currents in Class I and II polymers have been observed for fast scan rates ν (small t), thick films (large d), and slow charge transport rates (small D_{ct}). $^{159-161}$ This behavior has also been observed for cross-linked polymeric films.75 Conversely, Class III polymers, in which electroactive species are free to physically diffuse to the electrode, do not necessarily exhibit diffusional currents. If the film thickness is small, thin cell behavior will be observed.

We next consider the mechanism and physical charge transport properties of Class I, II, and III polymers. Because electroactive sites are immobilized in Class I and II polymers, Kaufman and Engler¹⁶² proposed that the current is generated by electron transfer between neighboring electroactive sites thereby establishing a site-to-site electron hopping mechanism for charge transport. Further developments by Murray et al., 159 and Oyama and Anson 160 established that site-to-site electron exchange could be treated as a diffusive transport process. Although theoretical modeling has been crucial in correlating the rate of electron hopping Kex to charge transport diffusion constants D_{ct}, 163-165 isolation of the rate determining step in the overall charge transport process has proven to be difficult. Several different rate determining steps have been suggested including counter ion mobility required to maintain charge neutrality, 120 segmental motions and/or swelling of the polymer backbone, 159,160 and the intrinsic rate of electron self exchange between neighboring redox centers of the proper orientation. 166,167 The one crucial feature to have emerged with certainty from charge transport studies is that the rate determining step is intimately dependent on the type of polymer used.

Thin polymeric films and monolayers on electrodes exhibit the standard symmetrical shaped cyclic voltammogram obtained for thin cells (Figure 5). Surface bound behavior from films with the redox sites attached to the electrode arises from thin-film behavior. If this

Figure 5

Ideal cyclic voltammogram obatained from a thin film of electroactive material attached to an electrode.

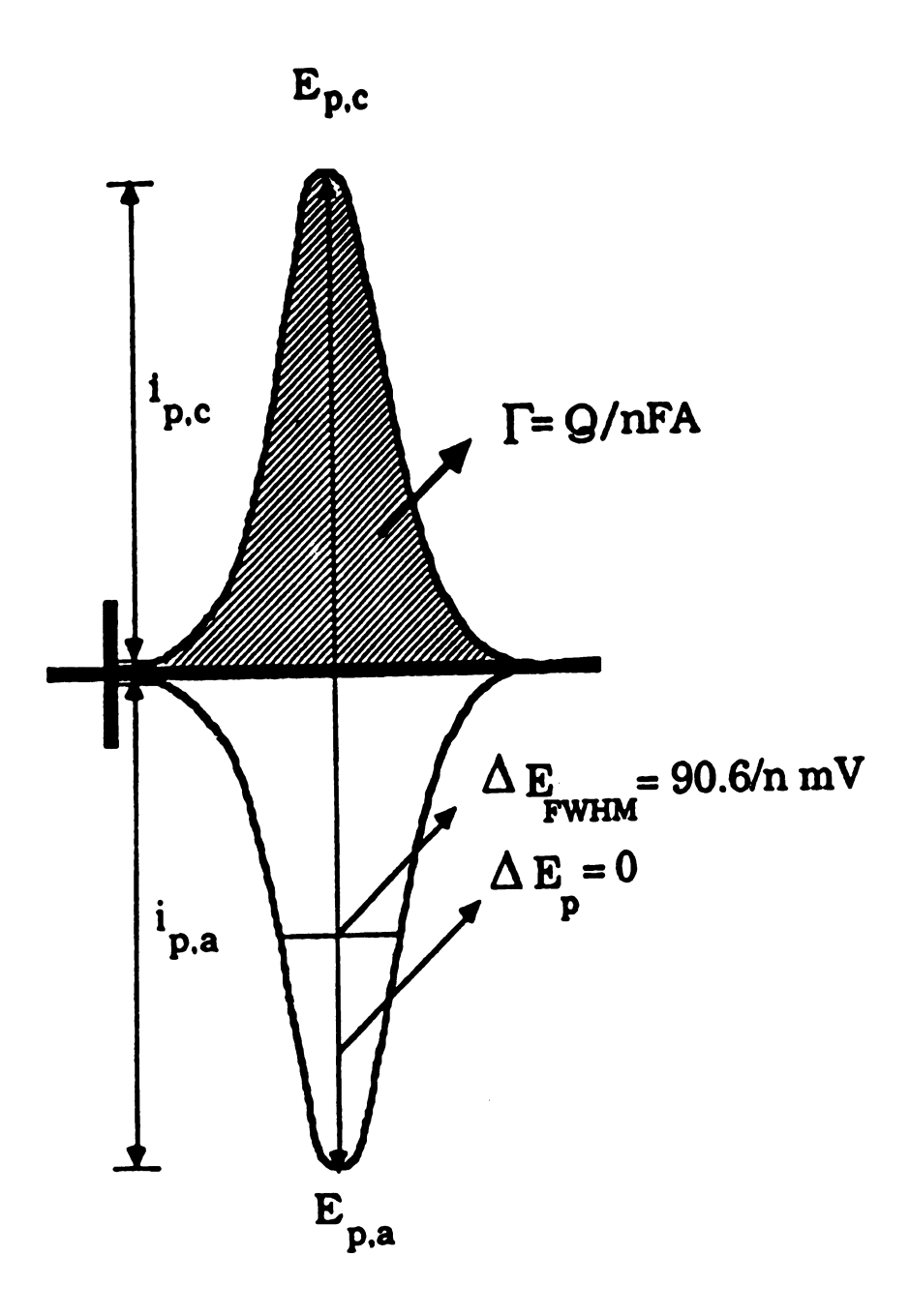


Figure 5

criterion is met, then the peak current, (defined in Figure 5) will follow eq 2,

$$i_{\mathbf{p}} = \frac{n^2 F^2 A \Gamma_{\mathbf{T}} \nu}{4RT} \tag{2}$$

where i_p (amps) is the maximum current of the peak, n is the number of electrons transferred, F is Faraday's constant, A (cm²) is the area of the electrode, Γ_T (moles/cm²) is the total coverage of electroactive material on the surface of the electrode, ν (mV/sec) is the scan rate, R is the gas constant, and T (K) is the absolute temperature. It is noteworthy that this equation predicts a plot of peak current $(i_p) \nu s$. scan rate (ν) should be linear with a y-intercept of zero. This prediction contrasts with the more common linear $i_p \nu s$. $\nu^{1/2}$ behavior for electroactive ions freely diffusing in homogeneous solutions.

When electrolysis of the entire polymer film is completed during the time of a cyclic experiment, the following relationship applies

$$Q = nFA\Gamma_{T}$$
 (3)

This equation reveals that the amount of charge (Q) under the cyclic voltammetric wave is independent of scan rate, and that the total coverage of electroactive material $\Gamma_{\rm T}$ can be directly obtained.

Ideally, adsorbed Class I and II polymers undergo reversible redox chemistry under Langmuir isotherm conditions. Therefore, the

anodic E_{p,a} and cathodic E_{p,c} peak potentials (from Figure 5) should, for an ideal system, appear at the same value, or $\Delta E_n = 0$. These results have been adhered to in a few studies^{66a,160,168} however, and more often deviations from this ideal behavior are observed. 169-172 The result of $\Delta E_p \neq 0$ in the case of adsorbed monolayers is normally attributed to slow heterogeneous electron transfer between the redox active species and the electrode surface. This explanation is invalid for Class I and II polymers however, because the observed peak separations are independent of scan rate. If slow heterogeneous electron transfer kinetics were involved, peak separations should increase with faster scan rates. Excluding isolated reports, 173 this is generally not the case. The origins of large peak separations obtained from films of Class I and II polymers attached to electrodes is still not agreed upon. Several groups have proposed that the large ΔE_p is a result of nonequilibrium between reduced and oxidized states (differences in the E^o values of the two redox partners) caused by either interfacial solvation or steric effects (conformational differences between reactant pairs).83 Alternatively others have attributed non-zero ΔE_p 's to uncompensated film resistance. 119,163,174

In addition to absolute peak separations, reversible redox couples bound to an electrode surface should also adhere to the following criterion for peak width:

$$\Delta E_{p,1/2} = E_{FWHM} = 3.53 \frac{RT}{nF} = \frac{90.6}{n} \text{ mV } (25 \text{ }^{\circ}\text{C})$$
 (4)

Although some full widths at half maximum (FWHM) equal to 90.6 mV have been reported for Class I and II polymers, 168,175,176 many studies have presented FWHM in the 100-250 mV range, $^{169-172,177-180}$ while still others have obtained FWHM values of less than 90.6 mV. $^{161,163,181-185}$ Two different explanations for this deviation from ideal behavior have been proposed: (i) Anson et al. 186 propose that differences in the activities of the bound redox couple (oxidized and reduced forms) will result in repulsive destabilizing interactions $E_{FWHM} > 90.6$ mV, whereas activity effects leading to attractive stabilizing interactions can yield $E_{FWHM} < 90.6$ mV; 186,187 (ii) alternatively, Peerce and Bard 163 have presented rather convincing evidence through digital simulations that multiple E^0 values in combination with activity effects can account for the observed deviations from the ideal E_{FWHM} of 90.6 mV.

The diffusional behavior sometimes observed for Class I and II polymers is analogous to that for freely diffusing ions; and the current in this case is described by

$$i_p = 2.65 \times 10^5 n^{3/2} A D_{ct}^{1/2} v^{1/2} C^*$$
 (5)

where C^* (moles/cm³) is the concentration of electroactive species in the bulk solution. Eq 5 predicts that a plot of peak current $(i_p) vs$. the square root of scan rate $(v^{1/2})$ should be linear with a y-

intercept passing through the origin. The diffusion coefficient for charge transport D_{ct} is obtained directly from the slope of this line.

In contrast to the cyclic voltammograms corresponding to thin cell behavior (Figure 5), diffusive voltammetric waves exhibit the characteristic tail shown in Figure 6. The cyclic voltammograms have non-zero theoretical peak separations given by,

$$|E_{p,a} - E_{p,c}| = 2.2 \frac{RT}{nF} = \frac{56.5}{n} \text{ mV (25 °C)}$$
 (6)

Experimentally determined values of ΔE_p often exceed 56.5/n mV. Explanations for the larger peak separations are uncompensated film resistance, 119,188 slow heterogeneous electron transfer, 189,190 and internal polymer effects (differences in swelling and or steric effects). 163 The accepted method for determining E^o values for both surface bound and diffusional waves has been to report the average of $E_{p,a}$ and $E_{p,c}$ measured from cyclic voltammetric studies. This procedure does not consider the possibility of slow kinetics which can cause unsymmetrical deviations in the locations of $E_{p,a}$ and $E_{p,c}$. Therefore, reported E^o values determined by averaging $E_{p,a}$ and $E_{p,c}$ for some polymer modified electrodes are not exact.

In contrast to Class I and II polymers, charge propagation in Class III polymers is complicated by the fact that charge transport mechanisms can include molecular diffusion in addition to electron hopping. This in itself does not make the determination of diffusion coefficients any more difficult because the process of physical diffusion is indistinguishable from electron hopping, and the sum of

Figure 6

Ideal cyclic voltammogram obtained from $W_6Br_{14}^{\ 2-}$ freely diffusing through an acetonitrile solution containing 0.2 M TEAP.

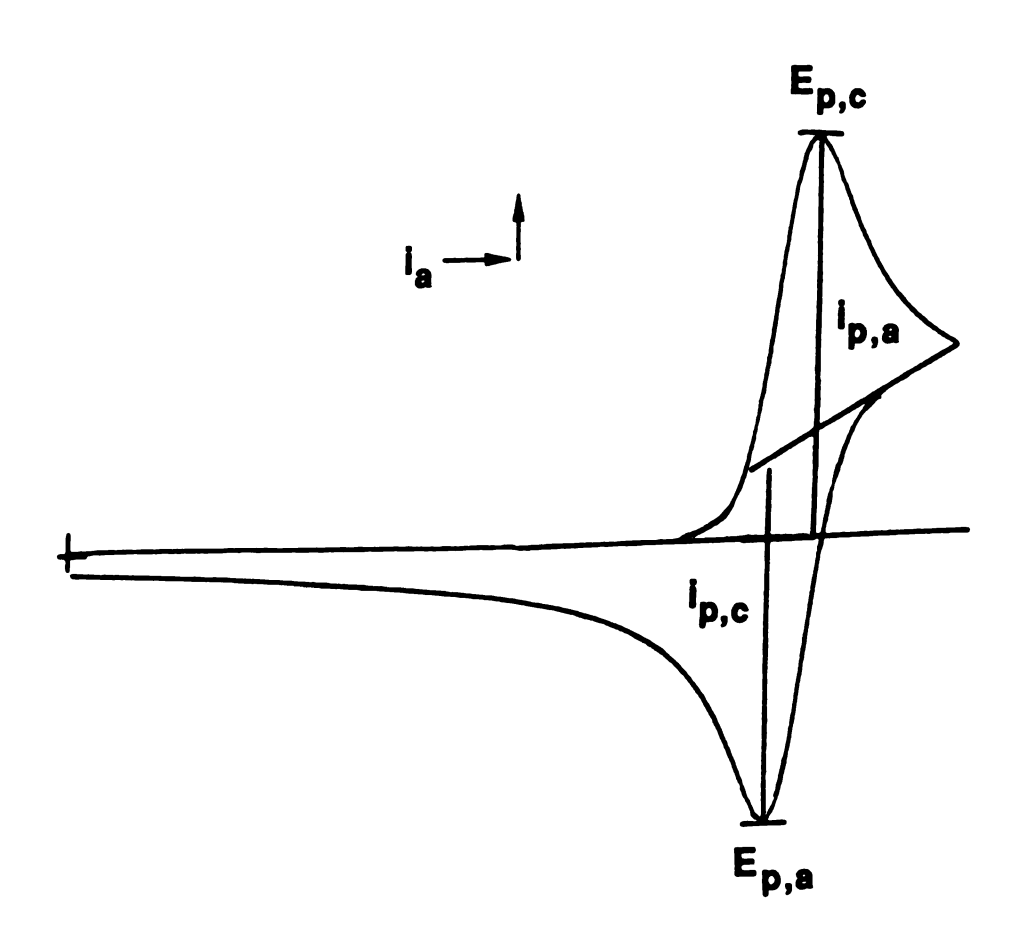


Figure 6

the two processes simply appears as a new overall diffusion coefficient. The difficulty arises because the diffusion of ions electrostatically bound within polyionic films is much slower than that for their counterparts freely diffusing in solution. Thus, self electron exchange between adjacent electroactive sites, which is negligible in solution, ¹⁹¹ becomes competitive with physical diffusion in the polymer. Several groups have proposed ^{164,165,192,193} that the Dahms ¹⁹¹ and Ruff ¹⁹⁴ treatment of freely diffusing ions in solution,

$$D_{exp} = D_o + D_{et} \tag{7}$$

also applies to ions electrostatically bound in polymers. In eq 7, D_{exp} (cm²/sec) is the experimentally determined diffusion coefficient (often referred to as the apparent diffusion coefficient, D_{app}), D_{o} (cm²/sec) is the diffusion coefficient which would be measured in the absence of any contribution from self electron exchange (essentially the corresponding value to D_{ct} for Class I and II polymers), and D_{et} is the diffusion coefficient for electron self exchange. The electron transfer term D_{et} can be expressed in the following form,

$$D_{et} = \frac{\pi k_{ex} \delta^2 C}{4}$$
 (8)

and D_{exp} can be rewritten as,

$$D_{exp} = D_o + \frac{\pi k_{ex} \delta^2 C}{4}$$
 (9)

where $k_{\rm ex}$ (M⁻¹s⁻¹) is the second order rate constant controlling electron self exchange, δ (cm) is the electron transfer distance, and C (mol/cm³) is the concentration of the co-reactant. This equation demonstrates that ions with large k_{ex} will contribute significantly to the overall charge transport process. This prediction, was confirmed with experiments conducted by Buttry and Anson, 195 Facci and Murray. 196 and later by Bard and coworkers using a more tenuous technique.¹⁹⁷ The Buttry and Anson experiment employed two structurally similar ions, Ru(bpy)₃²⁺ and Co(bpy)₃²⁺ in Nafion[®], possessing exchange rate constants k_{ex} differing by several orders of Although the values of D_{exp} for these two ions were magnitude. shown to be significantly different, implicating electron selfexchange as the possible cause, the experimentally determined diffusion coefficient D_{exp} did not exhibit a linear dependence on the concentration as expected (eq 9) for a diffusional process governed by electron self-exchange. In a now classic paper, Buttry and Anson 198 attributed this anomaly to the existence of hydrophilic and hydrophobic phases within the Nafion[®] film. Introduction of competing electron exchange in the hydrophobic phase, the hydrophilic phase, and across the two phase boundaries accounted for the charge transport properties of the film. This model for charge transport has experimentally been verified by using rotating disc voltammetry. 199-201 As an outgrowth of these studies, the overall charge transport for electroactive ions bound within polyionic films

is believed to be controlled by physical diffusion through the hydrophilic phase, electron or ion hopping through the hydrophobic phase (referred to as the Donnan domains), and/or cross-phase electron transfer or place exchange between the two phases.

Cyclic voltammetric behavior for Class III films is analogous to that observed for Class I or II polymers. For thin films, if electrolysis of the trapped ions is completed during the time required to traverse the cyclic wave, then thin cell behavior is observed; and for thick films or fast scan rates diffusional behavior is observed. Rotating disc electrodes have been most extensively used to determine rates of electron transfer for electrocatalysis, and for theoretical studies designed to elucidate the limiting steps of the charge transport process. 202-207

It is obvious from the above discussion that the accurate determination of diffusion rates (D_{ct} and D_{exp}) is crucial for the physical characterization of Class I, II, and III polymers. The electrochemical technique of choice for determining D_{ct} and D_{exp} is chronoamperometry. It has an intrinsic advantage over cyclic voltammetry because (i) D_{ct} can be determined for films which obey thin cell behavior (which is not the case for cyclic voltammetry, see eq 5) and (ii) uncompensated film resistance can be easily overcome through the application of a large overpotential. For this case, the current i(t) obtained from the polymer will obey the Cottrell equation 160,161

$$i(t) = \frac{nFAD_{ct}^{1/2}C^*}{\pi^{1/2}t^{1/2}}$$
 (10)

where i(t) (amps) is the diffusionally controlled current obtained at time t (sec). This equation is only valid at short times, (i.e. < 50 ms) for Class I and II polymeric films^{119,159,160,167,177} and Class III films which have low redox loading.²⁰⁸⁻²¹³ At longer times the concentration gradient within the film reaches the film-solution boundary, and the current is given by the finite diffusion relationship¹¹⁹

$$i(t) = \frac{nFAD_{ct}^{1/2}C^*}{\pi^{1/2}t^{1/2}} \left(\sum_{k=0}^{\infty} (-1)^k \left\{ exp(\frac{-k^2d^2}{D_{ct}t}) - exp[\frac{-(k+1)^2d^2}{D_{ct}t}] \right\} \right)$$
(11)

where k is an integral counter. The current time response for thin films of Class I polymers have been shown to conform to eq 11.119,159

Although chonoamperometry has been widely accepted as an accurate method for the determination of diffusion coefficients for all three classes of polymers, some discrepancies have been observed for diffusional currents. The most compelling data has been put forth by Majda and Faulkner, 214 who determined the diffusion coefficient $D_{\rm exp}$ for ${\rm Ru(bpy)_3}^{2+}$ in a Class III polymer (polystyrene sulfonate) by using a luminescence quenching technique. Values of $D_{\rm exp}$ that were 40-80 times larger than those determined with chronoamperometry were measured. Because the luminescence

technique precludes counter-ion motion as the rate limiting step in the charge transport process, the discrepancy in Dexp for the two methods suggests that either charge transport of ions within polystyrene sulfonate is limited by these counter-ion motions, or that using a transient perturbation technique such as chronoamperometry is flawed in the determination of D_{exp}. Although the former explanation has been embraced, presumably due to the fact that the majority of the D_{exp} and D_{ct} values been determined with chronoamperometry, recent studies by Faulkner et al. clearly demonstrate this technique to be fraught with error. Faulkner and his coworkers²¹⁵ have recently determined, with a steady state experiment involving a rotating ring disc electrode, that Os(bpy)₃²⁺ electrostatically bound within a Nafion® film actually diffuses 100 times faster than previously thought. The results clearly show that diffusion coefficients determined by using chronoamperometry should only be used to compare a series of data and absolute values of D_{exp} measured by chronoamperometry are tenuous at best.

As is evident from this chapter, charge transport mechanisms in polymer modified electrodes has been studied extensively and are fairly well understood. Investigations have primarily focussed on the intrinsic physical properties of charge propagation in polymers, rate determining steps, theoretical modeling, and applications with little regard on how charge transport properties of films are controlled by their microenvironment. The field of modified electrodes has matured to a level that researchers are now using the knowledge gained from existing polymeric systems to develop industrially useful devices. Although the amorphous nature of

poly diff adv w h Mid fili pr(of M CO m M S(

a

polymers makes the characterization of their microstructures difficult, systems with the most potential with regards to new advances require the ability to control polymer microstructures, which in turn require a clear understanding of polymer microenvironments and existing guest-host interactions within the The wide variety of covalent or electrostatic binding sites film. 39,40 provide a great deal of flexibility for controlling the microstructure of amorphous materials. Alternatively, preformed highly ordered microstructures deposited onto electrode surfaces can also provide convenient probe systems for establishing charge transport/ microenvironment relationships. Thus synthetically tailored polymer microstructures and the development of highly microstructures on electrode surfaces will significantly broaden the scope of modified electrochemistry.

This thesis presents fundamental studies that elucidate and clarify charge transport processes in polymeric and inorganic host matrices and utilizes this knowledge to design systems of practical applicability. Chapter III presents investigations that probe and define the charge transport processes within two-dimensional layered silicates (clays). By combining physical and electrochemical techniques, a unified model for electroactive clay films has been constructed. The nature of the electroactive sites can be manipulated by appropriate modifications of the clay film. With the information gained from these studies electrocatalytic activity has been observed from clay/polymer composites.

In Chapter IV investigations of the electrochemical behavior of inorganic cluster ions electrostatically bound within polymeric

pyridinium and bipyridinium films in nonaqueous solvents are presented. The charge propagation rates of cluster ions are shown to be controlled by electrostatic interactions within the polymer microenvironment. By systematically tailoring the binding site of the polymer, specific control of the charge transport rates mediated by the polymer backbone and the electrostatic cluster sites has been achieved. The systems presented in this Chapter provide benchmarks for microstructure/electroactivity relationships.

The structural design of the binding sites in bipyridinium microstructures of polymers is utilized to develop a novel electroanalytical sensor which is discussed in Chapter V. The sensor developed utilizes a 2,2'-bipyridinium based polymer which can detect extremely dilute concentrations of monoanions from both aqueous and nonaqueous solutions. Furthermore, electrolyte effects on the diffusion rates in these films support recently proposed charge propagation models dominated by migration effects.

CHAPTER II

EXPERIMENTAL

A. Preparation of Compounds

1. Inorganic Metal Complexes

- a. General Procedures. Potassium hexachloroiridate K_2IrCl_6 and potassium ferrocyanide trihydrate $K_4Fe(CN)_6 \cdot 3H_2O$, and hexaammineruthenium chloride $[Ru(NH_3)_6]Cl_2$ were obtained from commercial sources (Aldrich Chemical Company and Alfa) and were used without further purification. Ferrocene $(Cp)_2Fe$ (Aldrich) was purified by sublimation. Other reagents were purchased from Aldrich unless otherwise specified and were used as received. All inorganic complexes were characterized by UV-vis spectroscopy and cyclic voltammetry.
- b. Synthesis of $Fe(bpy)_3(SO_4)$, $Fe(phen)_3(SO_4)$, and $Fe(vbpy)_3(SO_4)$. Syntheses which relied on procedures similar to those previously reported were employed. An aqueous solution of ferrous sulfate was slowly added to an ethanolic solution containing 3.5 equivalents of polypyridyl ligand [2,2'-bipyridine (bpy), 1,10-phenanthroline (phen), or 4-vinyl-4'-methyl-2,2'-bipyridine (vbpy)]. The resulting mixture was stirred for 2 h. The red product was precipitated by addition of acetone, filtered, and washed with benzene to remove excess ligand. Highly crystalline solids of $Fe(bpy)_3(SO_4)$, $Fe(vbpy)_3(SO_4)$, and $Fe(phen)_3(SO_4)$ were recovered from ethanol/acetone and methanol/acetone solution mixtures respectively.
- c. Synthesis of $(PPN)_2Fe(bpy)(CN)_4$. The procedure described by Schilt²¹⁷ was followed with slight modifications. Stoichiometric amounts of ferrous ammonium sulfate hexahydrate

and 2,2'-bipyridine were added to distilled water and the solution was heated to a temperature just below boiling. A 15 molar excess of KCN was added to the warmed solution, which was stirred for 20 After 2 h red crystals of Fe(bpy)₂(CN)₂ formed. The product was filtered and washed several times with cold water, dissolved in hot water containing a 100 fold excess of KCN, and heated on a steam bath for 12 h. The dark orange-brown product $K_2Fe(bpy)(CN)_4$ was precipitated by the addition of an excess of acetone, filtered, washed water, and recrystallized from ethanol. The with cold bis(triphenylphosphoranylidene)ammonium(PPN+) salt was precipitated by addition of (PPN)Cl to an aqueous solution of K_2 Fe(bpy)(CN)₄.

d. Synthesis of Os(bpy)₃(ClO₄)₂. The procedure of Dwyer and Hogarth²¹⁸ was followed with several minor changes. Stoichiometric amounts of OsO₄ (Alpha) and FeCl₂·6H₂O were added to a solution of concentrated HCl and the mixture was heated for 2 h on a steam bath. After the solution changed color to dark red, the green complex K₂OsCl₆ was precipitated by addition of excess KCl. The solution was cooled and the precipitate was collected by filtration, washed several times with absolute ethanol, and dried. The precipitate was dissolved in glycerol containing an equal molar amount of 2,2'-bipyridine, and this solution was heated to 240 °C for 1 h. The solution was doubled in volume with distilled water and an excess of NaClO₄ was added to precipitate Os(bpy)₃(ClO₄)₂. The product was filtered, washed with cold water, and recrystallized from acetonitrile.

- e. Synthesis of Ru(bpy)₃(ClO₄)₂. Metathesis of Ru(bpy)₃(Cl)₂, with NaClO₄ yielded the perchlorate salt, which was recrystallized from aqueous solution.
- f. Synthesis of $(NBu_4)_2Mo_6Cl_{14}$. Molybdenum dichloride (Cerac Inc.) was dissolved in hot 6 M HCl, and the resulting solution was filtered. Addition of NBu_4Cl immediately caused the yellow solid $(NBu_4)_2Mo_6Cl_{14}$ to precipitate, which was subsequently collected, washed several times with water and ethanol, and recrystallized from spectral grade (Burdick & Jackson) dichloromethane by slow evaporation.
- Synthesis of (NBu₄)₂W₆Br₁₄. The procedure g. Dorman and McCarley²¹⁹ was followed with slight modifications. In a drybox, 15.0 g of WBr₅ (Alpha), 0.72 g of Al metal (fine turnings obtained by shaving a 99.999 % pure aluminum rod with a tungsten carbide tip), 13.0 g of AlBr₃ (Alpha), and 7.50 g of NaBr were added to a quartz reaction tube. The neck of the tube was cleaned and capped with a rubber septum. The tube was removed from the drybox and connected to a high vacuum manifold, evacuated for several hours, (until the pressure was below 1x10⁻⁴ torr) and then flame sealed under dynamic vacuum. The contents were thoroughly mixed and the quartz tube was wrapped in asbestos and inserted in a steel pipe, which was placed into a high temperature furnace. reaction vessel was heated to 200 °C for 3 h with the steel pipe being rotated at 20 min intervals. The temperature was then raised to 450 ^OC over a 3 h period, held at 450 °C for 9 h, and finally raised to 550 ^oC where it was held for 30 h (with the steel pipe being rotated at 30 min intervals). The tube was allowed to cool to room temperature

and wrapped in several layers of paper towel. The tube was carefully broken with a blunt object (Caution: violent explosions have occurred). Most of the glass was removed and the black fused solid was ground into a fine powder and added to a hot 9 M HBr/EtOH 50:50 mixture. The black powder was recollected and washed several times with 95 % ethanol, and then added to a 50:50 solution of EtOH and 9 M HBr. This mixture was heated with stirring for 12 h. The black powder and ground glass were removed by filtration. Addition of NBu₄Br to the yellow EtOH/HBr solution produced the yellow (NBu₄)₂W₆Br₁₄, which was recrystallized from spectral grade acetonitrile.

2. Organic Polymers and Monomers

a. General Procedures. All reagents, including methylviologen (MV²⁺), were purchased from Aldrich unless otherwise specified, and were used as received. The organic polymers and monomers were characterized by proton NMR spectroscopy and by cyclic voltammetry. Elemental analysis was performed by Galbraith Laboratories.

b. Synthesis of N-methylpolyvinylpyridinium hexafluorophosphate $(PVP^{+}Me/PF_{6}^{-})$, 1.

Stoichiometric amounts of polyvinylpyridine (PVP) and methyl iodide were added to methanol. The mixture was heated under nitrogen and in the dark to 60 °C for 10 h. The iodide salt of (PVP+—Me) precipitated from solution and was collected by filtration and washed several times with cold ethanol. The hexafluorophosphate salt was prepared by the addition of NaPF₆ to an aqueous solution of (PVP-Me)I. The white precipitate was washed with water and recrystallized from acetonitrile containing an excess of NaPF₆.

c. Synthesis of $\{N, N' - bis[-3 - (trimethoxysilyl) propyl] - 4,4' - bipyridinium \ diiodide \ (PQ^{2+}/2I'), 2.$

$$\left[(MeO)_{3}Si(CH_{2})_{3}^{+} \cdot N - (CH_{2})_{3}Si(OMe)_{3} \right] 2I^{-}$$
2.

The procedure of Bookbinder and Wrighton²²⁰ was followed with slight modifications. A 75 fold molar excess of 1-iodo-3-

trimethoxysilypropane (Petrach Company) was added to dry acetonitrile containing 4,4'-bipyridine. The mixture was refluxed for 24 h, cooled to room temperature, filtered, and washed several times with cold acetonitrile. The light orange precipitate, (PQ²⁺) was used without further purification.

d. Synthesis of 4-vinyl-4'-methyl-2,2'-bipyridine (vbpy), 3.

The method of Abruna, Breikss, and Collum²²¹ was followed with the modification that the final product (vbpy) was further purified by low temperature sublimation.

e. Synthesis of 4-vinyl-4'-methyl-N,N'-ethylene-2,2'-bipyridinium (EVDQ²⁺), 4.

Vinyl-bipyridine (vbpy) was added to freshly distilled 1,2-dibromoethane and heated under nitrogen and in the dark to 60 °C for 8 h. A light green precipitate was collected and the filtrate was

placed back into the reaction flask. This procedure was repeated five times producing high yields of the precipitate each time except the last. Solids collected from successive precipitations were combined and washed several times with ether. The hexafluorophosphate salt of EVDQ²⁺ was obtained by the addition of ammonium hexafluorophosphate to an aqueous solution of the light green precipitate. The light blue hexafluorophosphate salt was collected, washed with water, and dried *in vacuo*. The monomer was characterized by elemental analysis.

f. Synthesis of 4-vinyl-4'-methyl-N, N'-1, 3-propylene-2,2'-bipyridinium (PVDQ²⁺), 5.

The preparation of the hexafluorophosphate salt of $(PVDQ^{2+})$ followed the same procedure as that described for $EVDQ^{2+}$, except that 1,3-diiodopropane was substituted as the alkylating agent.

g. Synthesis of 4-vinyl-4'-methyl-N, N'-1, 4-butylene-2,2'-bipyridinium (BVDQ²⁺), 6.

The preparation of the hexafluorophosphate salt of $(BVDQ^{2+})$ followed the same procedure as that for $EVDQ^{2+}$, except that 1,4-diiodobutane was substituted as the alkylating agent.

3. Synthesis, Modification, and Purification of Layered Oxides

- a. Sodium Montmorillonite (Wyoming). Sodium montmorillonite $Na_{0.60}[Al_{3.23}Fe_{0.42}Mg_{0.47}](Si_{7.87}Al_{0.13})O_{20}(OH)_4$ was obtained from the Clay Minerals Repository (University of Missouri, Columbia, MO). The mineral was purified by sedimentation to collect the < 0.2 μ m fraction, and subsequently washed with HSO_4^- to remove carbonate and with dithionite to remove free iron oxides. The charge exchange capacity (CEC) of the montmorillonite was 80 meq of charge/100 g of clay. The platelet size was < 200 nm.
- b. Synthetic Hectorite (Laponite[®]). Laponite[®]
 Na_{0.22}Li_{0.14}[Mg_{5.64}Li_{0.36}](Si_{8.00})O₂₀(OH)₄ was purchased from Laporte
 Industries Ltd. and used as received. The CEC and platelet size of this Laponite[®] were 55 meq/100 g and < 50 nm, respectively.

- c. Fluorohectorite. Fluorohectorite $\text{Li}_{1.60}[\text{Mg}_{4.40}\text{Li}_{1.60}]$ (Si_{8.00})O₂₀(F)₄ was a synthetic product similar to that previously described by Barrer²²² and was obtained from Corning Glass Works. The CEC and platelet size of this fluorohectorite were 190 meq/100 g and > 1000 nm, respectively.
- Montmorillonite. A 5 mL d. Reduced Charge suspension of a 2 % slurry of sodium montmorillonite was sealed in dialysis tubing with 2 mL of 1 M LiCl. After 24 h, the dialysis tubing was suspended in freshly distilled water, and over the next 48 h the lithium-exchanged water was changed everv 8 h. The montmorillonite was removed from the dialysis tubing and deposited onto graphite electrodes, evaporated, and the resulting films were heated to 250 °C for 2 h.
- e. Intercalates. The desired inorganic cation was added to a aqueous suspension (2 % by weight) of clay. The amount of cation added depended on the desired loading and was calculated by using the CEC of the smectite clay used.
- f. Intersalated Montmorillonite. A 2.0 % by weight aqueous montmorillonite suspension was sonicated (this pretreatment of the clay sample is the crucial step of the synthesis) and rapidly added to an aqueous solution containing 3-5 CEC of $FeL_3(SO_4)$ (L=bpy, vbpy), followed by stirring for 2 h.

The amount of $Fe(bpy)_3^{2+}$ in excess of bound material was determined by centrifuging the intersalated sample and quantifying the concentration of $Fe(bpy)_3^{2+}$ in the supernatant by UV-vis spectroscopy. The molar absorptivity was determined to be 7040 M⁻¹ cm⁻¹ from a 10 point Beer-Lambert plot with a correlation

coefficient of 0.9987. The determination of the $Fe(bpy)_3^2$ + concentration of the supernatant (5.1 mM) was in accordance with the value calculated by assuming a $Fe(bpy)_3^2$ loading of 2 CEC (4.8 mM).

4. Supporting Electrolyte

Tetrabutylammonium hexafluorophosphate $(TBAPF_6,$ Southwestern Analytical Chemicals) and tetrabutylammonium tetrafluoroborate (TBABF₄, Aldrich) were dissolved in ethyl acetate containing MgSO₄, filtered, and then recrystallized by the addition of These salts were dried in vacuo at 90 °C for 10 h. ether. Tetrabutylammonium (TBAP, Southwestern Analytical Chemicals) tetraethylammonium perchlorate (TEAP, Southwestern Analytical Chemicals) were recrystallized from water and dried in vacuo at 30 °C for 12 h. Metathesis of potassium hexafluoroarsenate (TBAAsF₆, Ozark-Mahoning) with NBu₄Br yielded tetrabutylammonium salt which was collected and dried in vacuo at 60 °C for 12 h. Lithium perchlorate (LiClO₄, Fisher) was recrystallized from acetonitrile and dried in vacuo at 100 °C for 6 h. Sodium acetate (Aldrich) was recrystallized from twice distilled glacial acetic acid. All other supporting electrolytes were reagent grade and used as received.

5. Solvents

Acetonitrile purchased from Burdick & Jackson Laboratories (distilled in glass grade), was subjected to four freeze-pump-thaw (fpt) cycles and then vacuum distilled onto 3-Å activated molecular

sieves, dried for 6 h, distilled onto CaH₂, and finally vacuum distilled into a sealed flask. Distilled water was passed through a column of activated charcoal and two columns of mixed-bed ion exchange resin.

B. Methods and Procedures

1. Electrochemical Measurements.

Cyclic voltammetry, chonopotentiometry, and bulk electrolysis experiments were conducted by using a Princeton Applied Research (PAR) Model 173 potentiostat, 175 universal programmer, 179 digital coulometer, and a Houston Instruments Model 2000 X-Y chart Chronoamperometric experiments were performed with a Bioanalytical Systems (BAS) 100A multianalyzer. The nonaqueous experiments were performed in a Vacuum Atmospheres HE-453 double-sided glove box. Electrochemical experiments employed a conventional H-cell equipped with a working electrode (pyrolytic graphite, glassy carbon, platinum, or antimony doped tin oxide coated glass), counter-electrode (Pt gauze), and a reference electrode (aqueous/saturated calomel and acetonitrile/silver wire). determined in acetonitrile were converted to the SCE reference scale using the ferrocenium/ferrocene couple of +0.31 V vs. SCE as an internal standard.

2. Preparation of Modified Electrodes

Clay modified electrodes were prepared by droplet evaporation of the desired clay suspension on the electrode surface. Best results

were obtained by maintaining the concentration of the clay suspension between 1-2 weight percent. The Na⁺-exchanged and Fe(bpy)₃²⁺ pre-exchanged experiments employed 0.31 mg/cm² of clay on the electrodes; this coverage corresponds to a film thickness of 1.75 μm. In the experiments conducted for the purpose of comparison to intersalated montmorillonite, the amount of clay deposited on the electrode was 0.07 mg/cm² corresponding to a film thickness of 0.40 μm. The incorporated electroactive cations were ion-exchanged into the clay films by either soaking the clay modified electrode in an aqueous solution containing electroactive ions or by pre-exchanging polypyridyl metal complexes into the clay samples (as described in Section II.A.3) before the films were cast. The metal polypyridyl pre-exchanged and intersalated clay samples cast uniform strongly adhering films in the range of 0.1-0.8 CEC and 3-5 CEC, respectively.

Polyvinylpyridinium films were cast by droplet evaporation of a 1% (PVP—Me)PF₆ acetonitrile solution on the electrode surface.

Poly-PQ²⁺ films were prepared according to the procedures of Wrighton et al.²²⁰ with a few modifications. The best results were obtained by using a 1 mM concentration of monomer. It was necessary, to apply a potential step of -0.76 V vs. SCE for 3-10 minutes in order to observe film growth.

Poly-EVDQ²⁺ and poly-PVDQ²⁺ were prepared by the methods of Willman and Murray.¹²² However, the preparation of stable films were best accomplished in the glovebox.

Poly-Fe(vbpy)₃⁺²/clay films were prepared by cycling montmorillonite films (Na⁺-exchanged and intersalated) in an acetonitrile solution containing Fe(vbpy)₃⁺² and TEAP following published procedures.¹¹⁴ The polymerization was only successful if the electrolyte was TEAP. Attempts to produce the polymer by using other electrolytes (TBAP, TBAPF₆, and LiClO₄) failed.

Electroactive inorganic anions were ion-exchanged into the polymeric films by soaking the modified electrodes in dilute solutions containing the anion of interest.

3. Spectroscopic Characterization and Instrumentation

Electronic spectra were recorded on a Varian Associates Cary Model-2300 UV-visible spectrometer. NMR spectra were recorded on a Bruker Model WH 250 MHz instrument. The chemical shifts were measured with respect to the solvent signal.

X-ray diffraction studies, used to determine the d(001) basal spacings, employed either Philips X-ray or Siemens Crystalloflex-4 Diffractometers. Both instruments were equipped with Ni filtered Cuka radiation sources. The samples were prepared by evaporating a 1% aqueous suspension of intersalated clay onto either a glass slide or thinly shaved planar graphite.

Scanning electron micrographs were recorded on a JEOL JSM 35C SEM at the Center for Electron Optics at Michigan State University. The samples were prepared by allowing an aqueous clay suspension to air dry onto pyrolytic graphite. The clay coated graphite was mounted, and sputter coated with a thin layer of gold. Measurements were made by Dr. Stan Flegler.

Film thicknesses of modified electrodes were determined by cutting films cast on SnO₂ electrodes, with a razor blade and

measuring the height differential between the film and glass support with a Sloan Dektak Surface Profilometer.

The molecular weights of EVDQ²⁺, PVDQ²⁺, and BVDQ²⁺ were determined by Fast Atom Bombardment Mass Spectrometry (FABMS) using a JEOL HX 110 double focusing mass spectrometer, which is housed in National Institute of Health/ Michigan State University Mass Spectrometry Facility. Samples of EVDQ²⁺, PVDQ²⁺ and PVDQ²⁺ were dissolved in glycerol matrices.

4. Determination of Diffusion Coefficients

Polymer modified electrodes have been shown to obey semiinfinite linear diffusion at short times < 50 msec. 119, 223, 224 Accordingly, diffusion coefficients of multilayer modified electrodes can be determined by chronoamperometry by using the Cottrell The diffusion coefficient for charge equation (equation 10). propagation, D, (cm²/s) is obtained by using the slope of the line from a plot of current vs. time. The values for the constants in equation 10 were easily obtained; n is the number of electrons transferred during the redox event, F (coul/mole) is Faraday's constant, and A (cm²) is the area of the electrode. This latter value was also determined by chronoamperometry by using ferrocyanide as a standard because of it's well documented diffusion coefficient.²²⁵ The value for the concentration of electroactive material C* (moles/cm³) was obtained by converting C* into the form Γ/d , where Γ (moles/cm²) is the surface coverage of the modifying layer, and d (cm) is the film thickness. By combining constants into a new term K

and changing the form of concentration, the Cottrell equation can be rewritten as

$$i(t)t^{1/2} = slope = \frac{KD^{1/2}\Gamma}{d}$$
 (12)

The surface coverage Γ of electroactive polymeric films was determined by integrating the area under cyclic voltametric wave for a one electron reduction. Alternatively Γ of electroactive inorganic complexes ion-exchanged into both clay and polymeric films were ascertained by measurement of the number of coulombs passed on a slow (< 10 mV/sec) cyclic voltammetric scan. Film thicknesses for polymers were determined using surface profilometery. Errors in the calculation of diffusion coefficients arise primarily from inability to measure the thickness of fully hydrated films, because these films lose solvent during thickness measurements and tear easily. Therefore, we were obligated to measure thicknesses of dry films. Wrighton and coworkers²²⁰ have determined the error in diffusion coefficients calculated using the Cottrell equation resulting from dry film thickness measurements is \pm 20 %. Thicknesses of clay films were determined from density measurements.

C. Construction and Cleaning of Working Electrodes

1. Pyrolytic Graphite Electrodes

- a. Graphite Disc Electrodes. Cylinders (0.476 cm in diameter) were machined from a block of pyrolytic graphite (Union Carbide). The cylinder axis was colinear with the c-axis of the graphite. The cylinders were sealed with heat shrink tubing onto the end of glass tubes containing copper wire. Electrical contact between the copper wire and graphite was made with mercury, which was confined within the tubing by parafilm wax. For each experiment a fresh surface was obtained by cleaving a thin layer of the graphite with a razor blade.
- b. Planar Graphite Electrodes. A thin plane of graphite was cleaved with a razor blade from a 2x1x1 cm³ block of graphite along the basal surface. Electrical contact between the graphite and a copper wire was made with conducting silver epoxy (Tra Con Corp).

2. Platinum and Glassy Carbon Disk Electrodes

Electrodes were constructed by sealing a platinum cylinder (1.6 mm diameter) or a glassy carbon cylinder (3.2 mm diameter) into a Teflon shroud purchased from BAS. The Pt electrode was polished with 1 μ m diamond paste and with 0.05 μ m alumina, both purchased from BAS. The electrode was thoroughly washed with water and methanol. This same procedure was used for glassy carbon electrodes with the exclusion of the diamond paste polishing.

3. Platinum Oxide Disc Electrodes

The preparation of platinum oxide electrodes utilized the Pt disc electrode (BAS). The Pt electrodes were pretreated by initially polishing according to the described procedures in Section II.C.2. The electrode was then soaked in 1 M sulfuric acid for 10 h. The electrode was removed from solution and potentiostated in an aqueous 0.5 M sulfuric acid solution at +1.9 V vs. SCE for 10 min, cycled between -0.15 and +1.2 V vs. SCE for 2 h, anodized at +1.1 V vs. SCE for 60 sec, and finally washed thoroughly with water and air dried.

4. Preparation of Tin Oxide Electrodes

Antimony doped tin oxide coated glass (80 ohms/square) was generously donated by Pittsburgh Plate and Glass (PPG). The larger sheets of glass were annealed and cut into rectangles 9 x 15 mm². Ohmic contact between the semiconductor surface and a copper wire was made by using conducting silver epoxy, which was further coated with insulating epoxy resin (Dexter Corp.).

CHAPTER III

CLAY MODIFIED ELECTRODES

A. Background

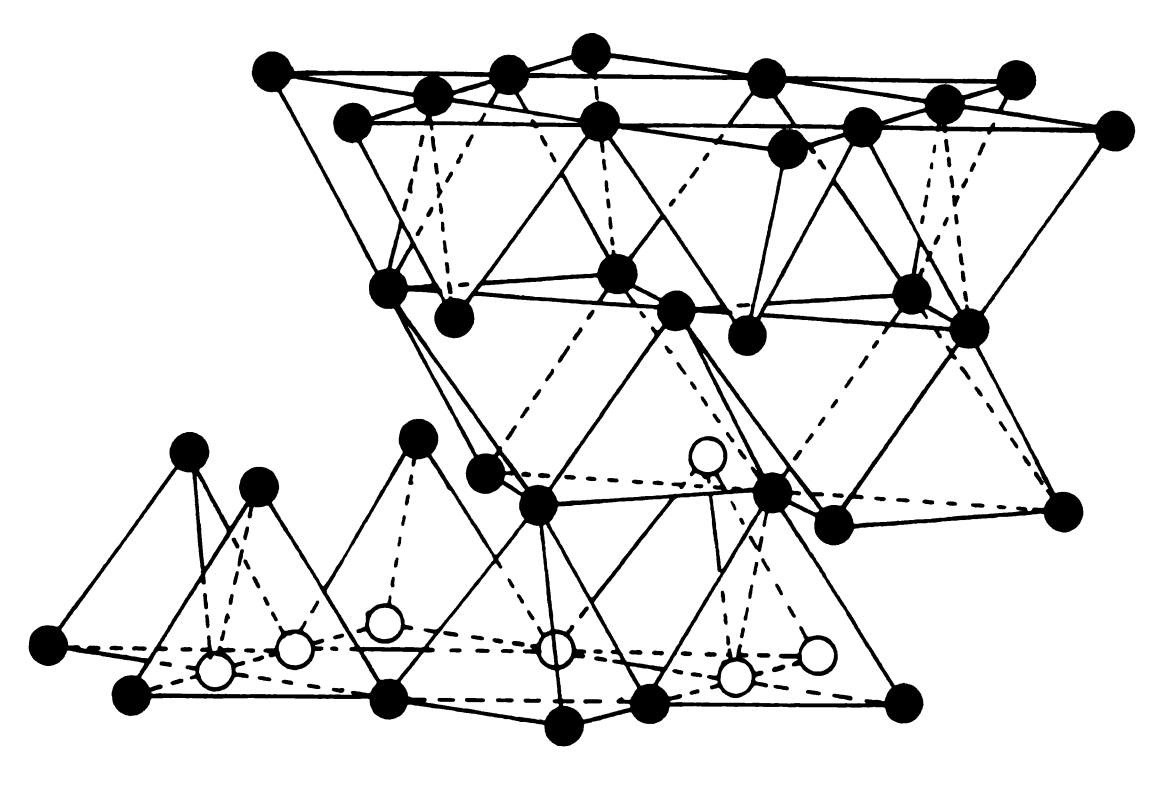
The modification of electrode surfaces with inorganic crystalline supports provides improved microstructural stability, the potential for increased heterogeneous catalytic activity, and well-defined microstructures. Ghosh and Bard's²²⁶ observation of electrochemical activity from transition metal complexes incorporated within treated clay adsorbed onto a platinum electrode represented the first report of an inorganic modified electrode. Since this seminal paper, a wide variety of inorganic modified electrodes have been reported including clays,²²⁷⁻²³¹ hydrotalcite,^{232,233} sepolite,²³⁴ bentonite,²³⁵ porous aluminum oxide,^{236,237} sol gels,²³⁸ zeolites,²³⁹⁻²⁴³ layered Zr-phosphates,²⁴⁴ polyoxometalates,²⁴⁵⁻²⁴⁷ tungsten oxide bronzes,²⁴⁸ and transition metal cyanides.²⁴⁹

Clays are inorganic supports possessing good thermal and chemical stability. The acidic clay interlayers (often called the gallery), make clays potentially useful as size and shape selective catalysts, and catalyst supports. 250-252 These properties in conjunction with the ability of clays to behave as cation-exchangers have led to numerous studies on clay modified electrodes, some of which have demonstrated their utility in the areas of organic synthesis, 253 energy conversion, 254,255 electrocatalysis, 256,257 photocatalysis, 258,259 and chromatography. 260

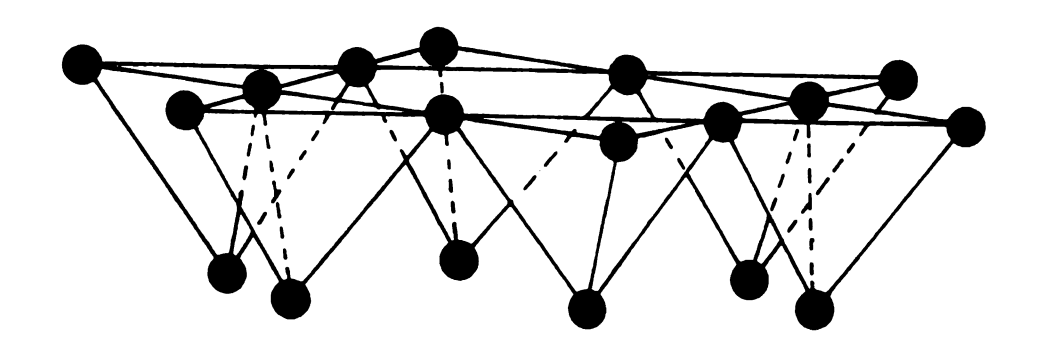
The idealized structure of a smectite clay is shown in Figure 7.

These 2:1 aluminosilicates have structures consisting of an octahedral layer sandwiched between two inverted tetrahedral layers. The tetrahedral layers consist of a oxygen framework with silicon

Idealized structure of smectite clay with a hydrated cation between layers.



 $M^{n+} \cdot xH_2O$



- Hydroxyl Groups
- Oxygen Atoms

Figure 7

occupying the tetrahedral sites. The various smectites are differentiated from one another by the cations residing in the octahedral sites. As an example, montmorillonite, which has aluminum ions occupying 2/3 of the octahedral sites, acquires an overall negative charge on the clay layers by isomorphous substitution of Mg²⁺ for Al³⁺, which is stoichiometric and uniform throughout the clay. The resulting negative charge is counterbalanced by hydrated cations located between the silicate layers. The charge equivalence is quantified by the cation exchange capacity (CEC) which is defined as the molar equivalence of charge per quantity of clay.

Ghosh and Bard's²²⁶ initial work established that $Ru(bpy)_3^{2+}$, $Fe(bpy)_3^{2+}$, and $Fe(Cp)_2^+$ could be incorporated into clay/PVA films and that these ions could participate in electron transfer with the underlying platinum electrode. The scope of clay modified electrodes was expanded with subsequent studies by Liu and Anson²²⁸ who reported that metal polypyridyl complexes, $Ru(NH_3)_6^{2+}$, and $Ru(NH_3)_5py^{2+}$ could be ion-exchanged into free standing clay films on pyrolytic graphite electrodes.

Interestingly, polypyridyl metal complexes and meyhylviologen (MV²⁺) bind in clays at a 100-fold excess over the concentration of the contacting solution. Whereas the polypyridyl metal complexes require many hours to be extracted from clay films, $Ru(NH_3)_6^{2+}$ is leached from films within minutes.^{227,228} In accordance with these observations the experimentally determined diffusion coefficient of $Ru(NH_3)_6^{2+}$ is a factor of 300 larger than that for polypyridyl metal complexes within montmorillonite films.²⁶¹

These results have been interpreted as evidence of the importance of hydrophobic interactions between the clay layers and electrostatically exchanged organophilic cations in the binding process.

Further insight into the origins of electroactivity of clay films is provided by coulometric experiments. Quantitative studies show that only a fraction (15-30 %) of the total complex confined in clay films is electrochemically active. 227,228 Moreover, electrodes displaying activity will lose electroactive ions from the film when soaked in an aqueous solution containing only electrolyte, yet the film retains the color of the inorganic ion. The degree of electroactivity in general correlates with the external surface area of the clay, thereby suggesting that externally adsorbed complex is the contributor to charge transport in clay-modified electrodes.²⁶¹ Moreover, Fe(CN)₆³⁻ and other negative ions (C₂O₄²⁻, Mo(CN)₈⁴-, I⁻) readily penetrate clay films and their diffusion is strongly dependent on the electrolyte concentration and pH of the solution. 227,230b,231 Because these ions should be repelled by the permanent negative charge of the clay layers, the presence of electroactive channels between the clay particles has been proposed.²²⁷

The above results have lead to the general model for electroactive clay films shown in Figure 8. Ions reside in clay galleries, micropores, and on the clay particle surfaces with most of the ions exchanged in the clay film being electrochemically silent. Organophilic cations, bound tightly within the clay film, are for the most part electrochemically inactive due to their immobility while

Model of a clay film on an electrode containing ion-exchanged polypyridyl metal complexes and electrolyte.

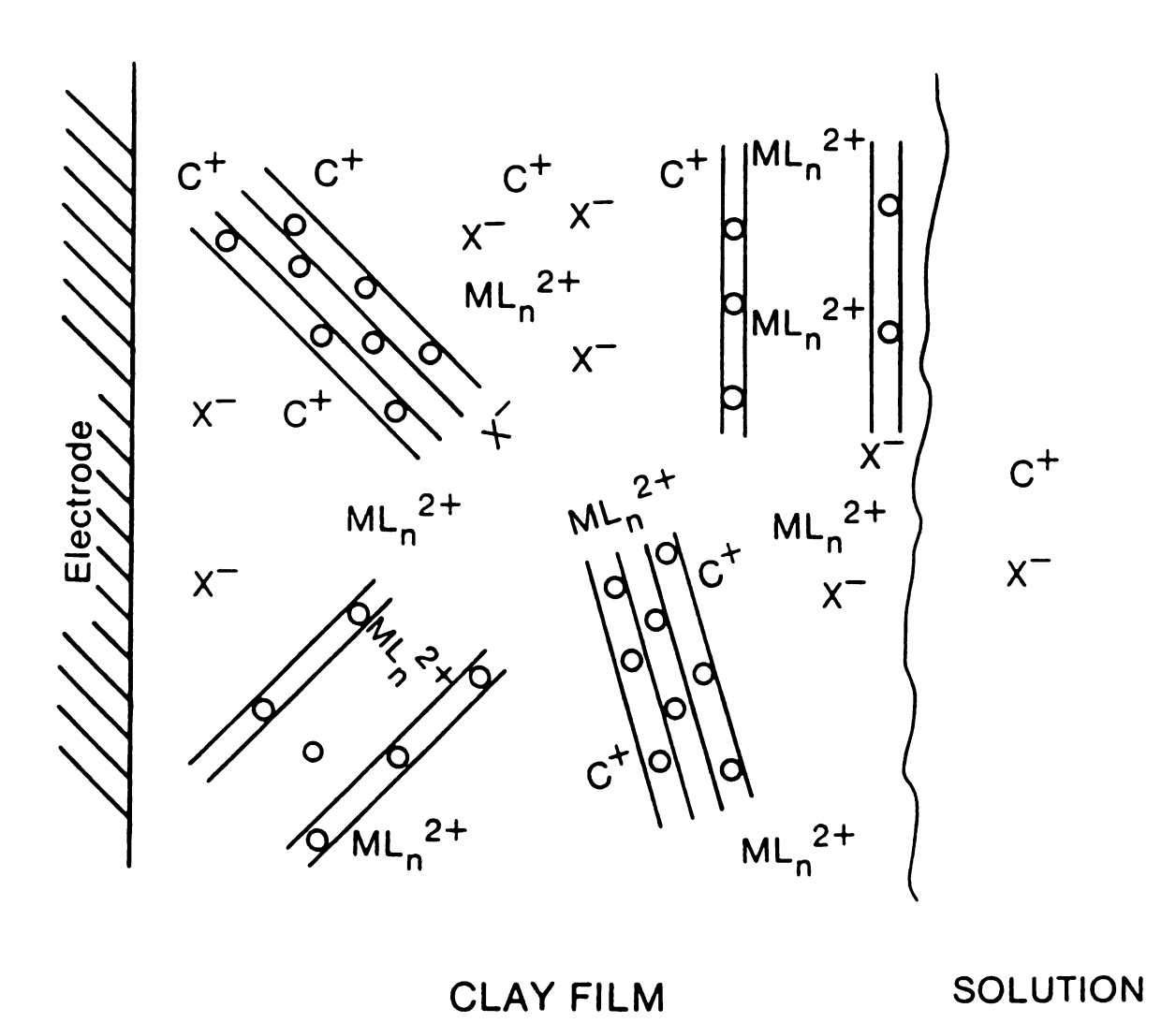


Figure 8

purely inorganic ions are very mobile, with the degree of electrochemical activity correlating to the external surface area of the clay. Because ions reach the electrode surface by diffusing through channels around clay particles, the swelling of the clay plays an important role in the observed electrochemical activity.

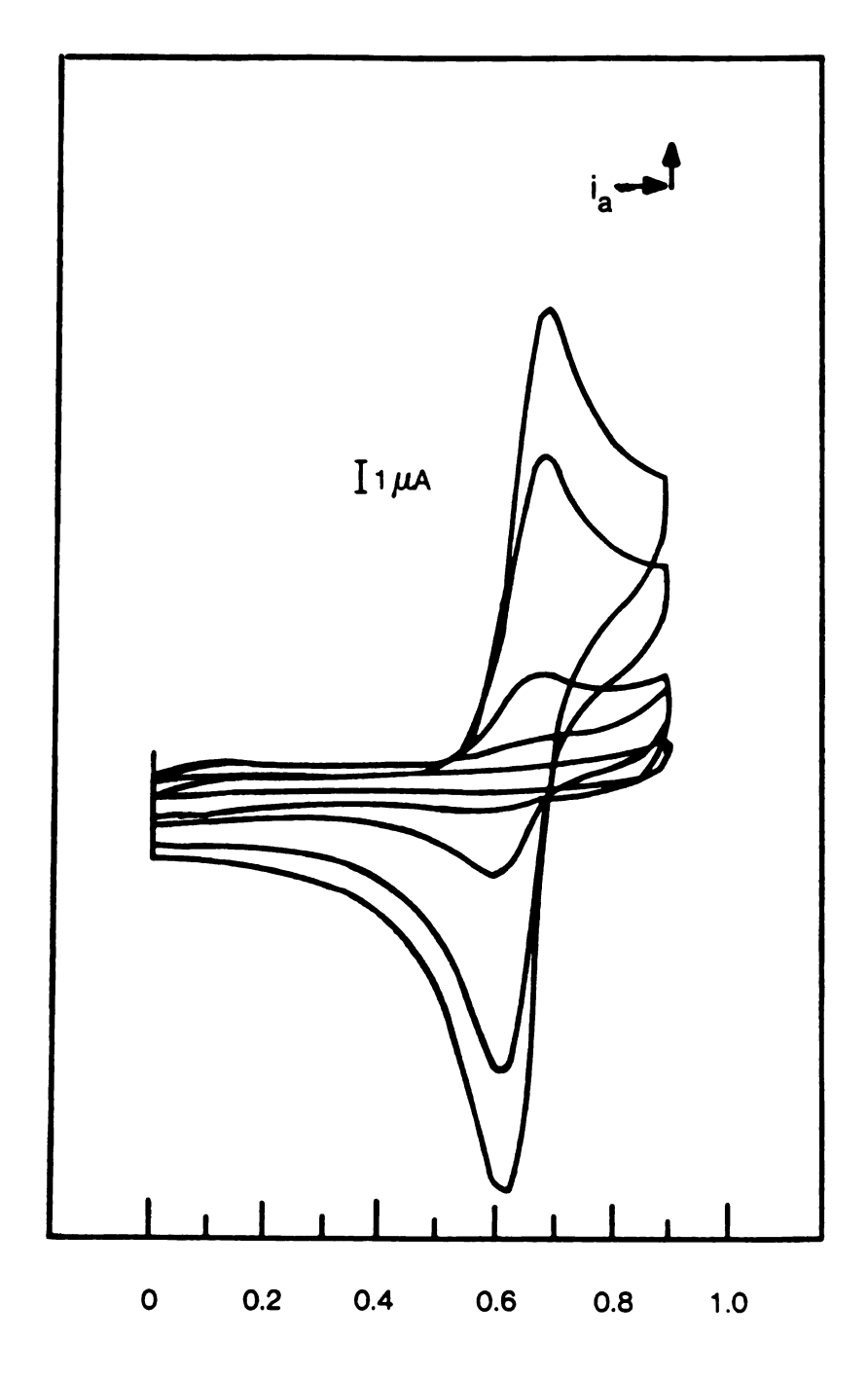
Although the qualitative aspects of the electroactivity in clay films have begun to emerge, the quantitative nature of the electroactive sites and charge transport mechanisms have yet to be Ion-exchanged electroactive ions M⁺ have potentially determined. three distinct locations within the film (Figure 8): (i) voids or channels around the clay platelets; (ii) outer edges of the clay layers; and (iii) the galleries between clay layers. Because one objective of clay studies is to derive electrocatalytic activity from ions between clay interlayers, the elucidation of the electroactive sites within the clay film is of paramount importance, particularly in lieu of the initial studies on clay-modified electrodes which have indicated that rigorously bound between clay layers might electrochemically silent. Conventional electrochemical approaches utilized to date have not provided sufficient insight into many of these crucial issues of clay modified electroactivity. Therefore. unique studies designed to probe the clay's microstructure and its effects on the observed electrochemical activity of bound redox ions were undertaken. With the information garnered from these studies, clay-modified electrodes can begin to be systematically designed.

B. Results and Discussion

1. Nature of the Electroactive Sites.

All previously reported studies on clay modified electrodes utilized the Na⁺-exchanged form of the clay to cast films on conducting metal oxide, metal, or carbon surfaces. Because Na⁺smectites are totally delaminated in aqueous suspension the formation of continuous, crack-free films capable of imbibing electroactive species is facilitated. For instance, a graphite electrode coated with Na⁺-exchanged montmorillonite (0.31 mg/cm^2). immersed in solution of $M(bpy)_3^{2+}$ (M = Fe, Ru, Os), produces cyclic voltammograms exhibiting well-defined $M(bpy)_3^{3+/2+}$ waves. As previously observed,^{227,228} the intensity of the wave increases monotonically with electrode immersion time, and the functional dependence of the peak current on scan rate is characteristic of a diffusional process. Figure 9 shows the waves obtained at 10 min intervals for a Na⁺-exchanged montmorillonite film in a 0.2 mM Os(bpy)₃²⁺ solution containing 0.1 M Na₂SO₄ when the electrode potential is continuously cycled between 0.00 and +0.90 V vs. SCE. After soaking the electrode for 2 h, during which the electrode becomes golden upon incorporation of Os(bpy)₃²⁺ in the film, the voltammetric response reaches a plateau. Direct transfer of the electrode to solutions containing pure electrolyte causes the peak currents to be attenuated only slightly. With continued soaking, however, the electrode response decreases, indicating that the electroactive dipositive cation is displaced from the film. Significantly, although the current response is virtually eliminated

Increasing cyclic voltammetric response from $Os(bpy)_3^2$ incoporating into a montmorillonite film coated on graphite in an aqueous solution containing 0.2 M sodium acetate and 0.2 mM $Os(bpy)_3^{2+}$.



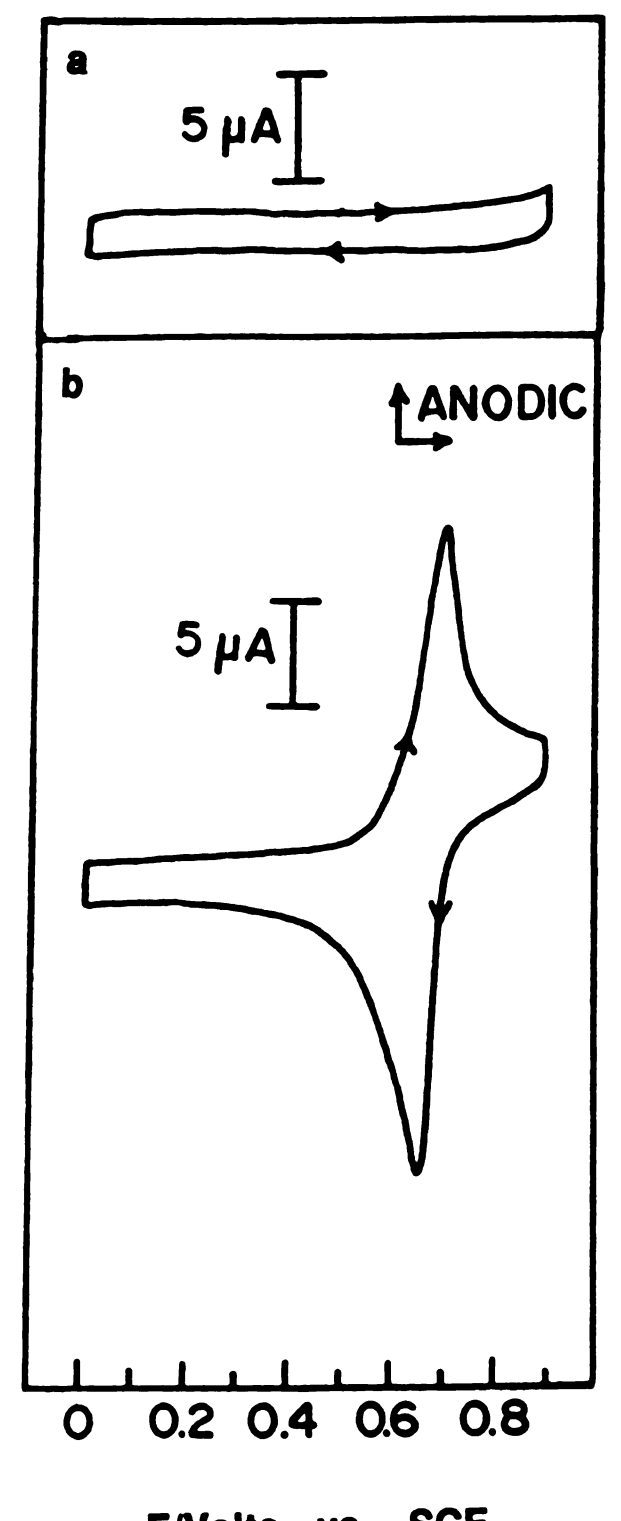
E/Volts vs. SCE

Figure 9

after soaking the electrode for 24 h in pure electrolyte solution, the film retains the deep golden color of $Os(bpy)_3^{2+}$.

As mentioned above these results indicate that only a fraction of the total ML₃²⁺ cations that are present in the clay film are electroactive, a fact recognized by all earlier workers. However, the extent to which ML_3^{2+} ions at the exchange sites of the clay contribute to the voltammetric response heretofore has remained an unresolved question of fundamental significance. One simple yet incisive approach to this issue is to examine the behavior of films from pre-exchanged Os(bpy)₃²⁺-montmorillonite. Accordingly, montmorillonite electrode films in which 25, 50, 80 and 100 % of the Na⁺ ions had been replaced by Os(bpy)₃²⁺ were prepared. In this way, Os(bpy)₃²⁺ is present on exchange sites both within the intracrystalline galleries and on the external surfaces. No evidence for an $Os(bpy)_3^{3+/2+}$ wave is observed for any of these electrodes when immersed in solutions containing only pure Figure 10a shows the electrochemical response of an electrode coated with 80 percent Os(bpy)32+-exchanged montmorillonite after 2 h of continually scanning the electrode potential at 50 mV/sec between 0.00 and +0.90 V vs. SCE. An Os(bpy)₃²⁺ wave is not detected even at high current sensitivities. Electrodes coated with pre-exchanged Ru(bpy)₃²⁺-, Fe(bpy)₃²⁺-, Fe(phen)₃²⁺-, and MV²⁺-montmorillonite films similarly failed to yield voltammetric responses. It is clear from these results that ML₃²⁺ and MV²⁺ cations electrostatically bound in the galleries and external surfaces of smectite clays are rigorously electroinactive.

Cyclic votammograms of a 80 % pre-exchanged montmorillonite film on pyrolytic graphite: (a) soaking in an aqueous solution containing 0.1 M Na_2SO_4 ; and (b) electrode from above placed in an aqueous solution containing 0.1 M Na_2SO_4 and 0.2 mM $Os(bpy)_3^{2+}$.



E/Volts vs. SCE

Figure 10

Pre-exchanged ML₃²⁺-montmorillonite films are similar to Na⁺montmorillonite in their ability to incorporate redox active cations. Dipping a 80 % Os(bpy)₃²⁺-exchanged montmorillonite coated electrode into 0.2 mM solutions of Os(bpy)₃²⁺ yields the appropriate cyclic voltammetric wave. As in the case of Na⁺-exchanged films, the current response is attenuated when the electrode is transferred to pure electrolyte solution. Figure 10b shows the limiting cyclic voltammetric response of the film in pure electrolyte solution. cyclic voltammogram has the same shape, potential characteristics, and limiting current response obtained with Na⁺-exchanged montmorillonite films; however, the peak current of the Os(bpy)₃²⁺exchanged film grows at a rate five times as fast as that obtained for Na^+ -exchanged montmorillonite films. Thus, while ML_3^{2+} and MV^{2+} ions within clay galleries do not communicate with the electrode surface, dipping the pre-exchanged ML₃²⁺-clay electrode in solutions of electroactive ions does promote electrochemical activity.

Although $\mathrm{ML_3}^{2+}$ cations at exchange sites do not communicate with the electrode surface, one might expect freely diffusing ions incorporated in clay films to transfer electrons to the electrostatically bound surface cations. Like the function of $\mathrm{Ru}(\mathrm{NH_3})_6^{2+}$ as a charge transport ion between the electrode and immobile cobalt tetraphenylporphyrin in Nafion®-coated polymer films, 262 mobile electroactive ions are potentially capable of shuttling charge between ions incorporated in the clay gallery and the electrode surface. In this context, the large self-exchange rate constants, 263 appropriate half-wave potentials of the 3+/2+ couples, and structural similarities of the osmium and iron bipyridyl complexes establish $\mathrm{Fe}(\mathrm{bpy})_3^{2+}$ as a

convenient probe of oxidation-reduction processes in Os(bpy)₃²⁺exchanged clay films. The charge shuttle scheme referred to here is graphically shown in Figure 11. A graphite electrode coated with Os(bpy)₃²⁺-exchanged montmorillonite (80 % of the charge exchange capacity) was placed into a solution of Fe(bpy)₃²⁺, rinsed once in water, placed in a cell containing 0.05 M Na₂SO₄ as the electrolyte, and scanned between 0 and +1.10 V vs. SCE. As shown in Figure 12, the initial cyclic voltammogram of the electrode gave a well-defined, reversible $Fe(bpy)_3^{2+}$ wave with a peak current ratio, $i_{p,a}/i_{p,c}$ of The initial $i_{p,a}/i_{p,c}$ value was independent of scan rates unity. between 2.0 and 200 mV/sec. This result is not consistent with a charge shuttle mechanism. If charge were being shuttled between the clay gallery and electrode, then Fe(bpy)₃³⁺ formed by oxidation at the electrode would be reduced by Os(bpy)₃²⁺ at the clay Therefore, cyclic voltammograms of Fe(bpy)₃^{3+/2+} would exhibit behavior characteristic of a catalytic EC' mechanism (i.e., $i_{p,a}$ > Under no conditions, even when the Fe(bpy)₃²⁺ solution concentration is increased to 0.05 M, is current flow attributable to Os(bpy)₃²⁺ oxidation observed.

The incorporation rate obtained for pre-exchanged clay is five times faster than for the Na⁺-exchanged form. This indicates that the method of preparation of the clay affects it's electrochemical properties. Because the gallery ions are electrochemically inert, the only significant difference between these samples is that the pre-exchanged clay is swollen to a greater degree than the Na⁺-exchanged form. The effect swelling has on the incorporation rate of Os(bpy)₃²⁺ into various forms of montmorillonite was determined

A reaction scheme devised to oxidize $Os(bpy)_3^{2+}$ located in the galleries, with utilization of $Fe(bpy)_3^{2+}$ as a redox charge shuttle agent.

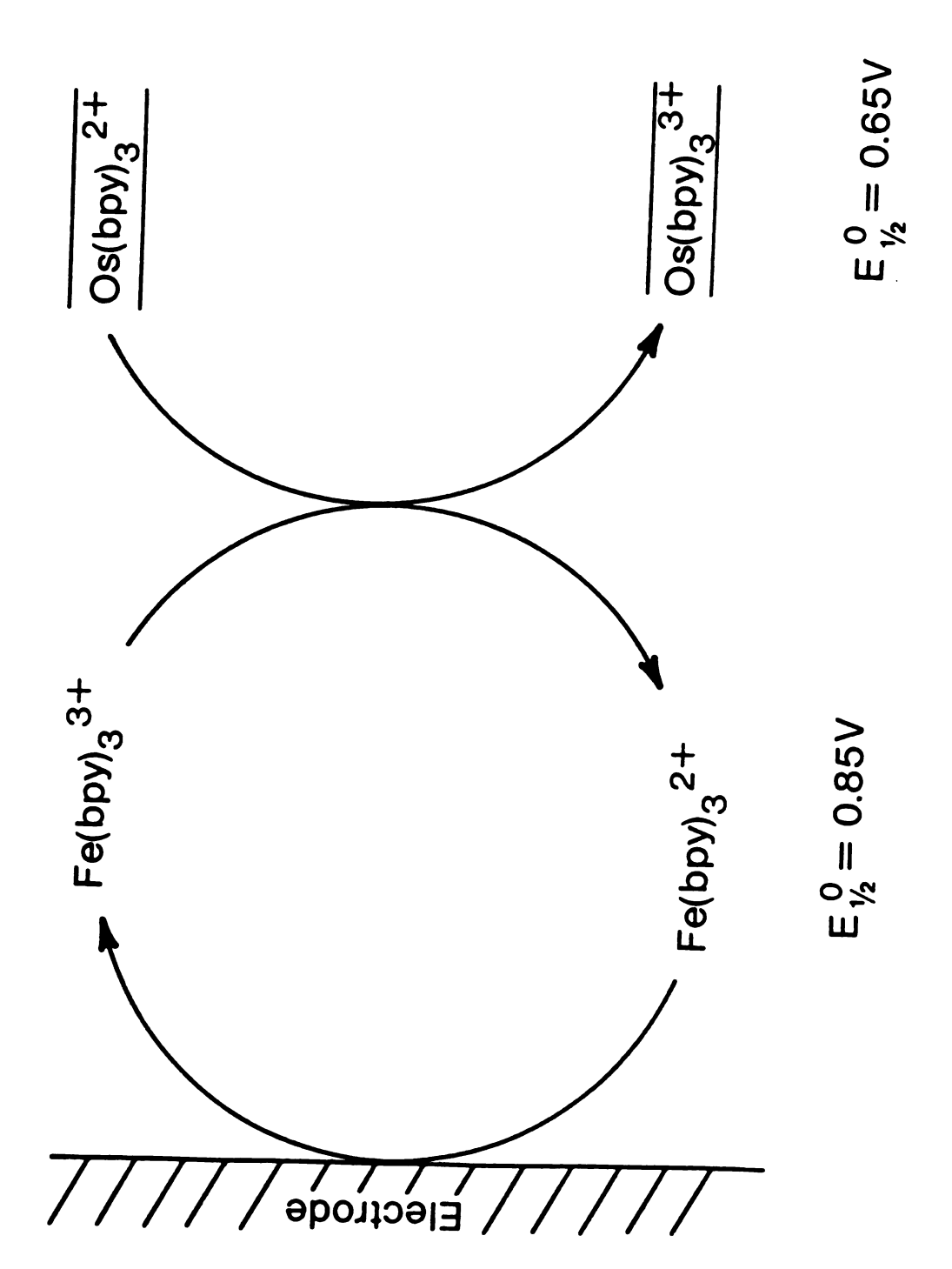


Figure 11

Reversible cyclic votammogram upon the first oxidation scan of $Fe(bpy)_3^{2+}$ ion-exchanged into a montmorillonite film containing pre-exchanged $Os(bpy)_3^{2+}$ while soaking in an aqueous solution containing 0.1 M Na_2SO_4 .

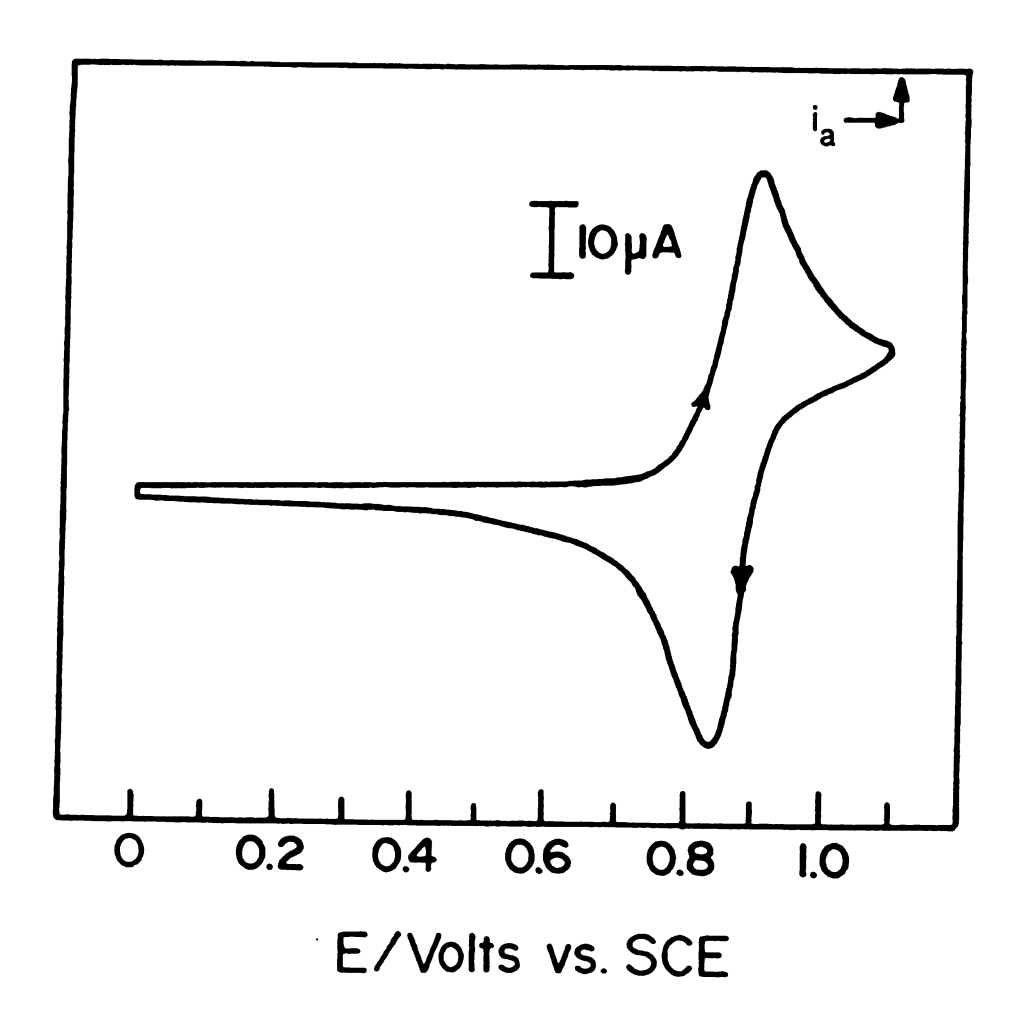


Figure 12

with the preparation of five montmorillonite films: a) 78% preexchanged Os(bpy)₃²⁺, b) 38% pre-exchanged Os(bpy)₃²⁺, c) Na⁺exchanged placed in 100% humidity for 24 h, d) Na⁺-exchanged air dried for 4 h and e) reduced charge (collapsed) films. As previously mentioned, the 78% pre-exchanged film should swell the most, followed by the 38% pre-exchanged film, and then the humidified and air dried films. The collapsed clay film should not swell. current response obtained at various times for the five clay samples while soaking in an aqueous solution containing 0.2 mM Os(bpy)₃²⁺ and 0.2 M Na⁺-acetate is shown in Figure 13. The incorporation rates parallel the degree of swelling for these films. The films maximum loading and time required to attain them are listed in Table 6. These results, which demonstrate that the preparation and resulting swelling of clay films have a pronounced effect on the incorporation rates of ML₃²⁺ metal complexes are further supported by investigations with Al, Zr, Fe, and Si pillared clays. 261,265 Increased diffusion rates for Fe(bpy)₃²⁺ in pillared clay films over Na⁺exchanged clay have been reported. In addition pillared clays incorporate polypyridyl cations from nonaqueous solutions whereas Na⁺-exchanged clay films do not. Presumably the large fixed dspacing of pillared clays resulting from the molecular props in their clay galleries causes the films to behave as if they were fully swollen.²⁶⁵

As previously mentioned Bard and coworkers²⁶¹ have suggested that the electrochemical response obtained for anionic complexes arises from the presence of microchannels which are filled by solution containing the redox active anion. Such microchannels

Current responses obtained from $Os(bpy)_3^{2+}$ exchanged into montmorillonite films from an aqueous solution containing 0.2 sodium acetate and 0.2 mM $Os(bpy)_3^{2+}$: (a) 78 % pre-exchanged $Os(bpy)_3^{2+}$; (b) 38 % pre-exchanged $Os(bpy)_3^{2+}$; (c) $Os(bpy)_3^{2+}$; (d) $Os(bpy)_3^{2+}$; (e) $Os(bpy)_3^{2+}$; (e) Os(bpy

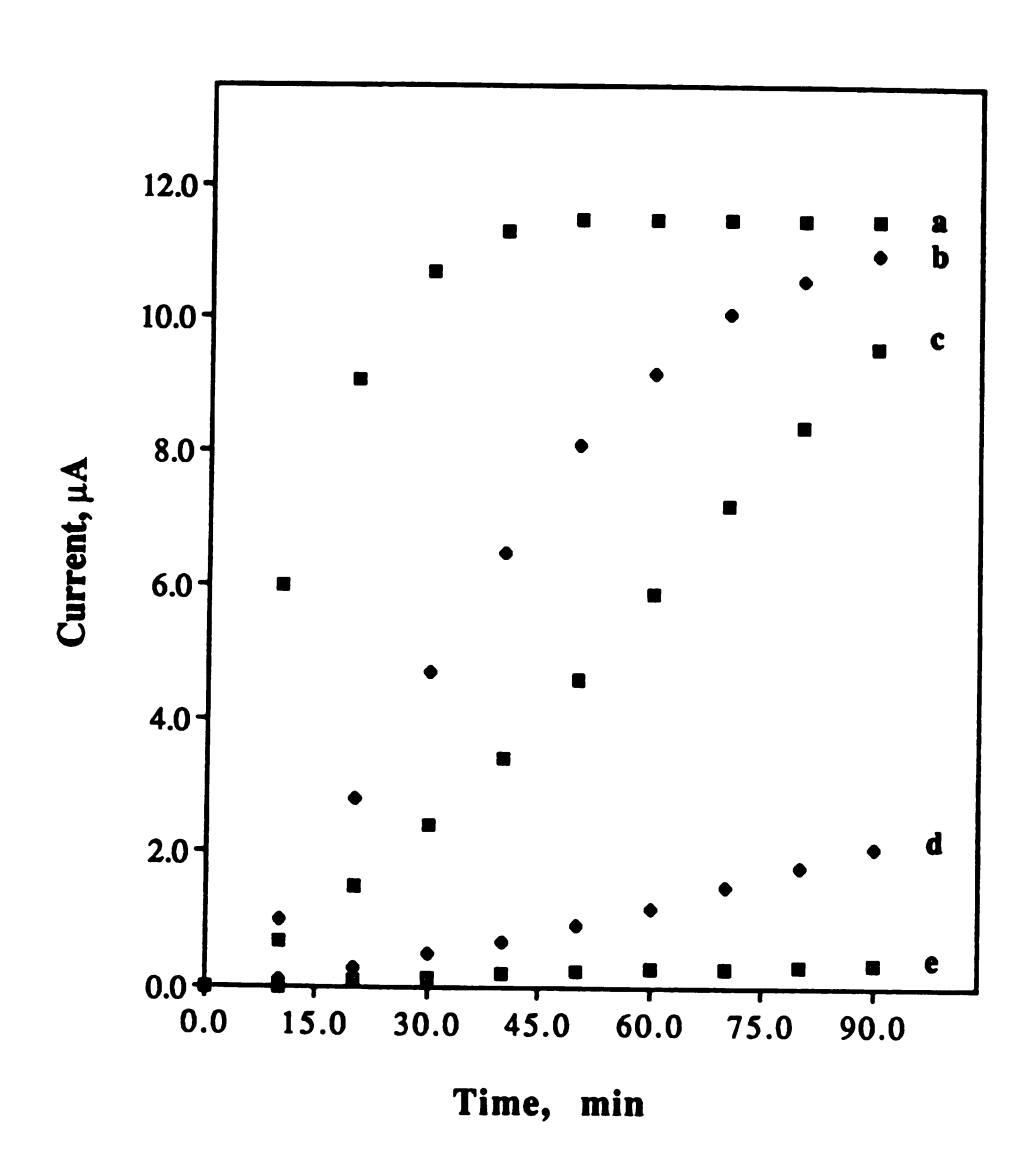


Figure 13

Table 6

Time Required to Reach Maximum Current Response for Different Films Soaked in 0.2 mM Os(bpy)₃²⁺

Sample	Montmorillonite Film	t(i _{max})/min	i _{max} /μA
a	80% pre-exchanged with Os(bpy) ₃ ²⁺	4 2	11.9
b	38% pre-exchanged with Os(bpy) ₃ ²⁺	90	11.4
c	Na ⁺ -exchanged humidified	130	13.2
đ	Na ⁺ -exchanged air dried 4 h	360	10.6
e	reduced charge (collapsed)	300	0.60

would also contribute to the activity observed for polypyridyl complexes and methylviologen cations. To obtain more direct evidence for microchannels, we have investigated the texture of montmorillonite films deposited on graphite by scanning electron microscopy. The low-magnification SEM image shown in Figure 14a reveals the characteristic waffle-like surface formed by the deposition of clay into interconnected domains of ridges and valleys. At higher magnification (Figure 14b) one can detect grain boundaries formed by the imperfect stacking of tactoids with a rag-like texture. These grain boundaries may represent the channels where redox active ions in solution can invade the film.

Despite the above evidence for microchannels in clay films, the simple solution-filling of such channels cannot be the sole mechanism responsible for the electroactivity of clay films. It has been shown that the effective concentration of electroactive $\mathrm{ML_3}^{2+}$ cations in clay films (10^{-1} M) is substantially higher than the concentration of cations in the soaking solution (10^{-3} M). This suggests that the cations are being concentrated in the film by interactions with the clay surface. Also, Yamagishi and Aramata have demonstrated enantioselectivity for oxidation of racemic $\mathrm{Co}(\mathrm{phen})_3^{2+}$ at a SnO_2 glass electrode coated with $\Delta - \mathrm{Ru}(\mathrm{phen})_3^{2+}$ -montmorillonite. 96,253 This latter result also establishes that the redox active polypyridyl complex communicates with the clay surface. Yet, we must keep in mind that ions bound to external surfaces, are rigorously electroinactive. How can these facts be reconciled?

It is proposed that the electroactive ML_3^{2+} and MV^{2+} cations in Clay modified electrodes in part are bound as ion pairs to the

SEM images of Na^+ -exchanged montmorillonite films on pyrolytic graphite, (a) 1000 x and (b) 7800 x.

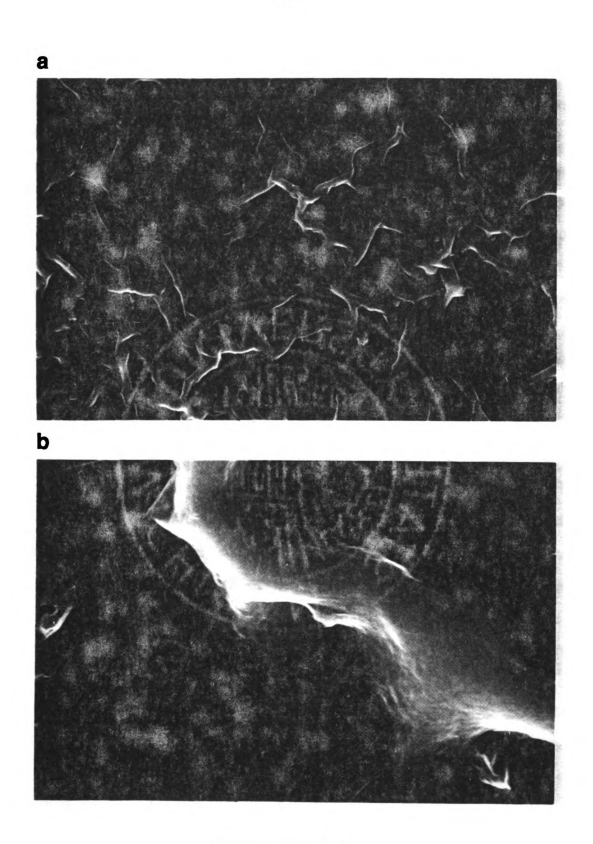


Figure 14

surfaces of the clay particles which border the microchannels. Although anions should normally be repelled by the surfaces of smectite clays, polypyridyl complexes are known to be exceptionally effective in promoting anion binding through ion pair formation. The driving force for ion pairing is facilitated by strong physical adsorption of the polypyridyl complexes to the organophilic surface and by the ability of the large organocation to shield the accompanying anion from the negative charge of the clay. Methylviologen cations and related organic dye cations which have also been shown to be electroactive in clay films, share many of the same properties of polypyridyl complexes in promoting ion pair formation.

The distinction between inactive, electrostatically bound complexes at exchange sites and active complexes bound by ion pairing is that in the former case the counter anion is the clay itself, whereas in the latter case the counterions are the anions of the electrolyte. Thus the electroactive cations are those which bind to the clay surface in excess of the cation exchange capacity by an ion pairing mechanism. Support for ion pairing is provided by the fact that peak currents are dependent on the anion of the supporting electrolyte. For instance, the limiting peak current for a Os(bpy)₃^{3+/2+} wave with Na₂SO₄ as electrolyte is 1.4 to 3.0 times as large as the currents observed with NaC₂H₃O₂ as the electrolyte over the ionic strength range 0.05-0.30 M. Related electrolyte effects have been noted by Bard and his co-workers.^{261,265}

In order to determine the relative importance of ion pair formation on basal surfaces and edge surfaces, the cyclic voltammetric properties of clay films with different morphological properties have been investigated. Specifically, we have examined laponite and fluorohectorite, synthetic clays with particle sizes larger and smaller than that of montmorillonite. The clay platelet sizes decrease along the series fluorohectorite (> 1000 nm). montmorillonite (< 200nm), and laponite (< 50 nm). Decreasing the platelet size should increase the edge surface area greatly without altering the total basal surface area within the oriented film. Thus, the edge surface area of laponite should be more than twenty times as large as the edge surface area of fluorohectorite. As Figure 15 illustrates, the incorporation rate and limiting current response for Os(bpy)₃²⁺ in Na⁺-smectite films is correlated with clay particle size. The limiting currents after 24 h are 24.3 μ A for laponite, 12.6 μ A for montmorillonite, and 4.6 μ A for fluorohectorite. To make certain that these differences were not associated with the diffusion of ions through these films, the apparent diffusion coefficients (Dapp) for the three films using slow scan cyclic voltammetry were determined by methods described by Anson et al.²²⁸ The D_{app} values obtained, as expected were very similar for all three clay films, (5.5 x 10⁻¹¹ cm²/sec for laponite, 3.3 x 10⁻¹¹ cm²/sec for montmorillonite, and $2.8 \times 10^{-11} \,\mathrm{cm}^2/\mathrm{sec}$ for fluorohectorite) and were also in good agreement with the D_{app} of $Os(bpy)_3^{2+}$ (3.5 x 10^{-11} cm²/sec) in a montmorillonite film.²²⁸ The same relative results are obtained for clays pre-exchanged with Os(bpy)₃²⁺.

The results thus far establish that ML_3^{2+} and MV^{2+} cations electrostatically bound to the exchange sites of smectite clay do not

The current response obtained as a function of time from various clay films adsorbed onto graphite soaking in 0.2 M sodium acetate and 0.2 mM Os(bpy)₃²⁺: (a) laponite; (b) montmorillonite; and (c) fluorohectorite.

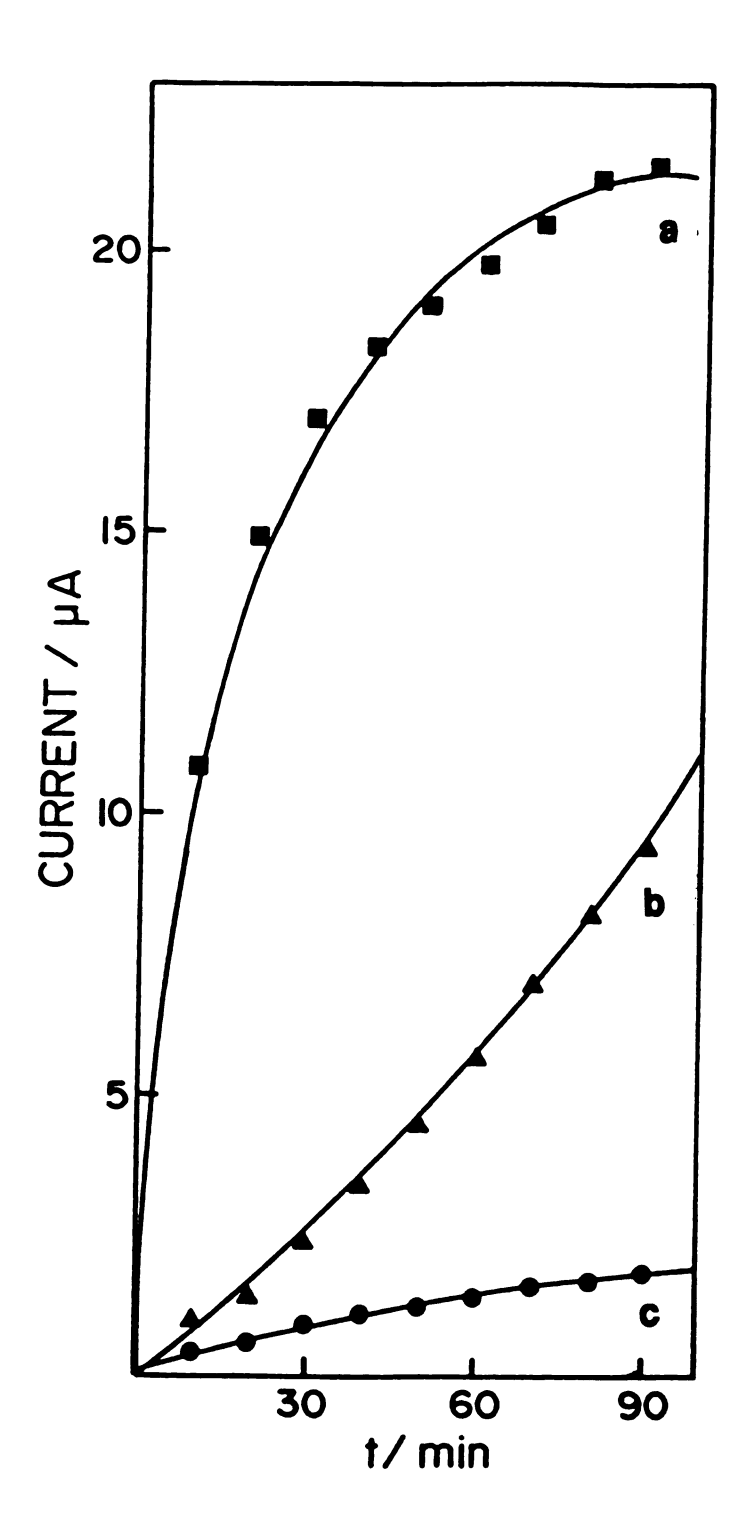


Figure 15

undergo electron transfer with the electrode surface or with freely diffusing cations contained in the microchannels. This is a result of an unfavorable exchange equilibrium with counterions required to maintain charge neutrality after electron transfer has occurred. In order to oxidize metal polypyridyl complexes electrostatically bound to clays one of two processes must accompany the electron transfer step: ejection of a metal complex from the clay or uptake of a negative counterion. Polypyridyl complex ions bind very strongly to montmorillonite, as reaction 13 is known to proceed essentially to completion.

$$(2 \text{ Na}^+)_{\text{clay}} + [\text{ML}_3^{2+}]_{\text{soln}} \xrightarrow{-e^-} (\text{ML}_3^{2+})_{\text{clay}} + [2 \text{ Na}^+]_{\text{soln}}$$
 (13)

Thus, the desorption of ML_3^{2+} from montmorillonite upon electrolytic oxidation of ML_3^{2+} to ML_3^{3+} , as expressed in equations 14 and 15, is unfavorable and electron transfer is impeded.

$$(2 \text{ ML}_3^{2+})_{\text{clay}} + [\text{Na}^+]_{\text{soln}} \xrightarrow{-e^-} (\text{ML}_3^{3+})_{\text{clay}} + (\text{Na}^+)_{\text{clay}} + [\text{ML}_3^{2+}]_{\text{soln}}$$
 (14)

$$(3 \text{ ML}_3^{2+})_{\text{clay}} \xrightarrow{-2e^-} (2 \text{ ML}_3^{3+})_{\text{clay}} + [\text{ML}_3^{2+}]_{\text{soln}}$$
 (15)

The alternative mechanism, counterion uptake is thermodynamically a highly unfavorable process. A large driving force would be required to overcome the energy required for the uptake of a negative ion into negative clay layers. Because electron-self exchange between ML_3^{2+} and ML_3^{3+} has a driving force

approximately equal to zero, (even the cross reaction between $Os(bpy)_3^{2+}$ and $Fe(bpy)_3^{3+}$ only has a driving force ~ 0.2 eV) the system does not possess enough energy to overcome this barrier.

Thus, of the three possible locations for ML_3^{2+} ions within the clay microstructure (Figure 8), only those ions freely diffusing in voids around clay particles are electrochemically active while electrostatically bound ions are electrochemically inert, presumably due to unfavorable thermodynamics required to maintain charge neutrality during the redox event.

2. Elucidation of Clay Microstructural Control of Electroactivity.

Having established that electrochemical responses arise from excess complex around clay platelets, important issues include: are the electrochemically active ions equally distributed throughout the clay film?; and which of these ions have electrochemical access to the electrode?

The first issue of interest is the determination of the percentage of material outside the clay platelets that is electrochemically active. Shown in Table 7 is the number of coulombs (after subtracting background coulombs) for the oxidation of Fe(bpy)₃²⁺ measured by slow scan cyclic voltammetry for various montmorillonite film thicknesses on graphite electrodes. The samples were prepared by soaking the clay modified electrodes in several different concentrations of Fe(bpy)₃²⁺ until equilibrium was established, with subsequent transfer to an aqueous solution containing 0.1 M Na₂SO₄. It is important to maintain a common

Table 7

Amount of Electroactivity From Different Clay Films of Varying Thickness After Soaking in Aqueous Fe(bpy)₃²⁺

Solutions Containing 0.1 M Na₂SO₄

Montmorillonite Film	Thickness (µm)	Concentration Fe(L) ₃ ²⁺ (mM) ^a	Coulombs x 10 ^{4 b, c}
Na ⁺ -exchanged	1.27	0.2	0.93 d
<u> </u>	0.76	0.2	1.01 ^e
	0.76	2.0	1.35
	0.38	2.0	1.18
	1.27	5.0	3.31
	0.38	5.0	3.42 ^f
	1.27	10.0	3.61
Pre-exchanged 80% of	1.27	0.2	0.97 ^g
CEC with Fe(bpy) ₃ ²⁺	1.27	5.0	3.21
(17/3	0.76	2.0	1.56 ^h
	0.38	5.0	3.11 ^h

^aL = bipyridine. ^bThe number of coulombs under reduction wave after subtracting background. ^cStandard deviation for three separate identical experiments: $^{d}\pm 0.08$, $^{e}\pm 0.09$, $^{f}\pm 0.26$, $^{g}\pm 0.11$. ^hThe clay was pre-exchanged with 88 % of the CEC.

electrolyte with identical concentrations for each system studied, because as mentioned in Section III.B.1, the anion of the electrolyte plays an intimate role in the ion-exchange process. The amount of $Fe(bpy)_3^{2+}$ incorporated active electrochemically montmorillonite at a given concentration of Fe(bpy)₃²⁺ is independent of film thickness, within the error of the experiment. The amount of electroactive Fe(bpy)₃²⁺ in these films monotonically increases with the concentration of Fe(bpy)₃²⁺ in the soaking solution and reaches a maximum value at = 5 mM. Importantly the clay films which were prepared by pre-exchanging 80 % and 88 % of the CEC with Fe(bpy)₃²⁺ behave similarly to the Na⁺-exchanged form. These results are consistent with those listed in Table 6 and illustrated in Figure 13.

The fact that the observed electroactivity does not increase with thicker films suggests that only the Fe(bpy)₃²⁺ near the electrode is electrochemically active. This conclusion is further supported by electroactivity / morphology relationships of the clay microstructure on the electrode. The casting of montmorillonite films from aqueous suspensions onto flat substrates results in 90 % of the clay platelets being oriented parallel to the surface, where the remaining 10 % make up so-called defect zones.²⁶⁹ In the defect zone clay particles are jumbled and owing to the random stacking of clay platelets, cavities and voids are more likely to form. In conjunction with our previous results, this implies that the observed electroactivity should increase with the creation of more defect zones in the clay microstructure. One approach to creating defect sites is to impart disorder in the microstructure by using the electrode surface

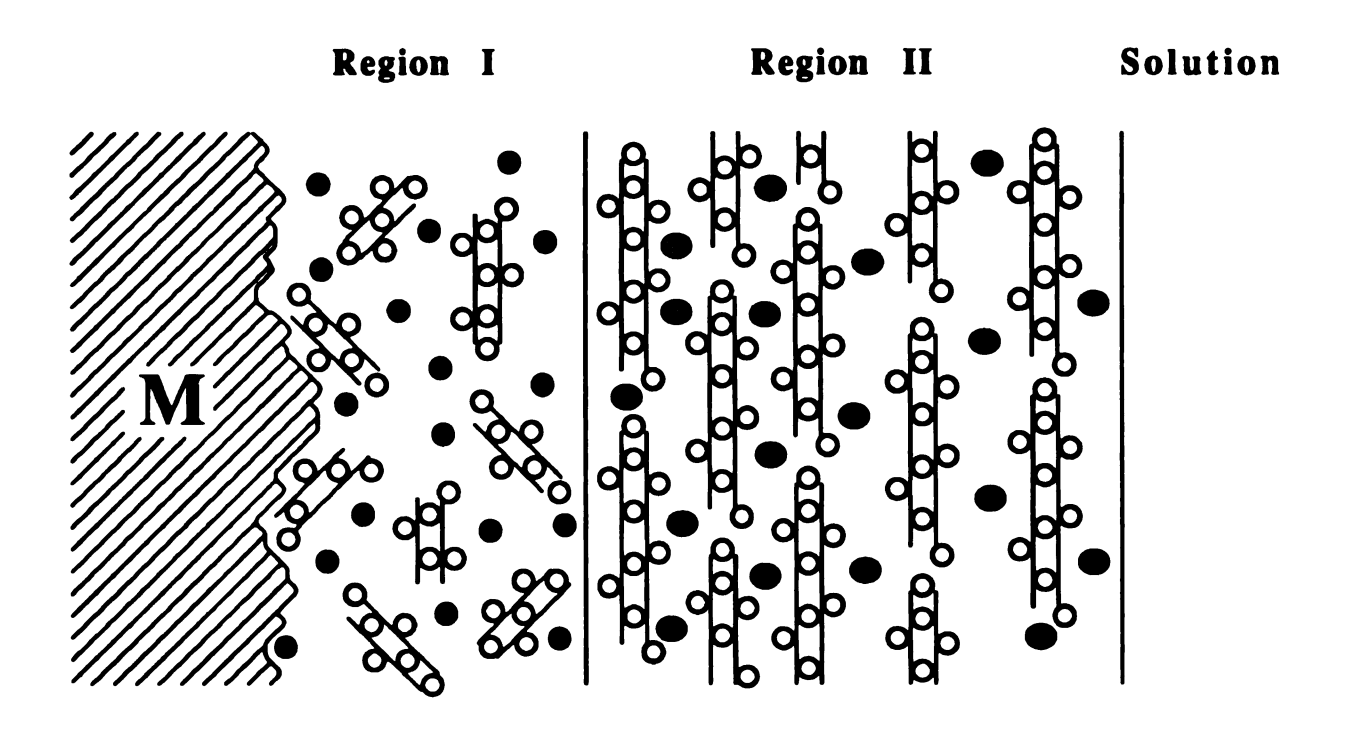
Increased roughness of the electrode surface should as a template. enhance the production of additional defect zones by inducing edge to face stacking of the clay platelets. This would be most pronounced near the electrode surface, while normal stacking of the clay platelets occurs with increased distance from the electrode. Within this framework the electrochemical responses of several electrode Pyrolytic graphite electrodes microstructures can be understood. which possess a visibly rough surface, with rocking curves of 6.41°, incorporate a larger quantity of electroactive Fe(bpy)₃²⁺ than smooth surface electrodes. For example 0.3 um montmorillonite films on SnO_2 ,²²⁷ and Pt^{231} display current densities of 30 μ A/cm² and 60 μA/cm² respectively, whereas the same films on pyrolytic graphite have current densities in the range of 100-120 μ A/cm². In addition the incorporation rates for ML_3^{2+} into clay films on Pt, SnO_2 , and glassy carbon are very dependent on the thickness of the clay film and incorporate ML_3^{2+} ions at a rate between 3-7 times slower (depending on the film thickness) than for identical films on pyrolytic graphite.

The common practices of rapidly heating clay films on smooth electrodes and the use of polyvinylalcohol (PVA) to increase the measured electrochemical activity^{227,230,231,271,274,275} are also consistent with increasing disorder of the clay microstructure. The former procedure prevents formation of parallel aligned platelets, thereby increasing the amount of edge to face stacking in the clay microstructure²⁷⁰ and the latter procedure prevents platelet alignment by requiring the platelets to conform to the amorphous polymer structure.

These results permit the model for clay electroactivity to be modified as shown in Figure 16. This model, which is consistent with all of our results to date, separates the clay film into two regions: one which electrochemically communicates with the electrode surface and one that does not. As discussed above, the electroactive ML_3^{2+} ions are located in defect zones (previously referred to as channels or voids) throughout the clay film. But only those ions in Region I with access to the electrode surface either by direct contact or charge shuttling through open pathways display electroactivity. At further distances away from the electrode surface the amount of parallel stacking of clay platelets increases resulting in the more ordered microstructures represented by Region II. This increased order reduces the basal volume and eliminates electrochemical pathways to the electrode surface thereby resulting in electrochemically isolated ML₃²⁺ ions. Substrates with smooth surfaces have a smaller quantity of the defect zones, at least near the electrode surface, and thus Region I for these electrodes will not extend as far away from the electrode surface as for pyrolytic graphite.

In the context of these results, one final note of interest here bears on the common practice in the literature of reporting the amount of electroactivity as a function of the CEC for the clay sample. Because the amount of $\mathrm{ML_3}^{2+}$ incorporated into clay does not depend directly on film thickness and at some distance from the electrode ions are electroinactive, normalizing the electroactivity observed from exchanged redox ions to the quantity of clay on the electrode is problematic. On the basis of this work, it is advised that activities

Model depicting locations of electroactive and non-electroactive polypyridyl metal complexes within a clay film.



- O Non-Electroactive ions
- - Electroactive ions
- Isolated potentially active ions

Figure 16

should be reported as charge/cm² where the charge is measured from electrolysis experiments. In our studies we report only the charge because our electrode area remains constant 0.178 cm². In light of the complexities involved with reporting consistent data from clay modified electrodes, the necessity to perform control experiments is of paramount importance.

3. Electrocatalytic Activity of Clay/Polymer Films

The model described in Figure 16 shows the electroactive ML₃²⁺ ions incorporated into clay films to be confined to a small volume in the microstructure. The isolated ions in Region II should become electroactivated if a pathway to the electrode is established. This might be accomplished by the formation of a conductive polymer network throughout the clay film. In this manner, electron/hole transport from the electrode surface to Region II may The preparation of conductive polymers in clay films be achieved. by electrochemical methods has been established with the formation methylviologen $(MV^{2+})^{271}$ of tetrathiafulvalenium (TTF⁺)²⁷² in montmorillonite. Heterogeneous electrochemical initiated polymerization of pyrrole^{273,274} and aniline²⁷⁵ has since been achieved.

Our effort of electrochemically accessing the isolated ions in Region II with conductive polymers was initiated with the reductive polymerization of transition metal complexes containing vinyl bearing ligands, which have been ion-exchanged into the clay. This method of polymerization was first described by Meyer, Murray and coworkers.¹¹⁴ The polymerization proceeds via a radical-radical

coupling process involving pairs of vinyl groups. 276,277 incorporation of $Fe(vbpy)_3^{2+}$ (vbpy = 4-methyl-4'-vinyl-2,2'bipyridine) into montmorillonite films of Na⁺-exchanged and 80 % pre-exchanged Fe(vbpy)₃²⁺ from an acetonitrile solution containing 2 mM Fe(vbpy)₃²⁺ was achieved with limited success. Upon transfer of these electrodes to acetonitrile solutions containing only electrolyte the incorporated complex was completely leached from the film on the first cycle. However, continuously cycling the potential of montmorillonite modified electrodes between -1.70 and +1.35 V vs. SCE, while soaking in an acetonitrile solution containing 0.2 M tetraethylammonium perchlorate (TEAP) and 0.5 $Fe(vbpy)_3(ClO_4)_2$, promotes the incorporation of metal complex as shown in Figure 17. These data were recorded at 10 min intervals for a duration of 1 h. Film growth continued for several hours thereafter providing oxygen was rigorously excluded from solutions. The electrode was washed extensively with acetonitrile and transferred to an acetonitrile solution containing 0.2 M TEAP. Figure 18a shows the CV for an electrode whose potential was cycled sequentially from 0.00 to -1.85 V, to +1.45 V and back to 0.00 V vs. The anodic wave at +0.97 V vs. SCE. arises from the 2+/3+SCE. couple of the metal center, whereas the two cathodic waves at -1.46 and -1.58 V originate from the sequential one-electron reduction of the vinylbipyridine ligands. The $i_{p,a}/i_{p,c} = 1.25$ for the oxidation wave is greater than the expected value of 1.00. Conversely the opposite behavior is observed for the cathodic waves which display $i_{p,a}/i_{p,c} < 1.00$. As shown in Figure 18, $i_{p,a}/i_{p,c}$ ratios will be unity upon consecutively cycling (two times) the potential between 0.00

Growth of poly-Fe(vbpy) $_3^{2+}$ at 10 min intervals in montmorillonite adsorbed onto pyrolytic graphite while soaking in an acetonitrile solution containing 0.2 M TEAP and 2.0 mM Fe(vbpy) $_3^{2+}$.

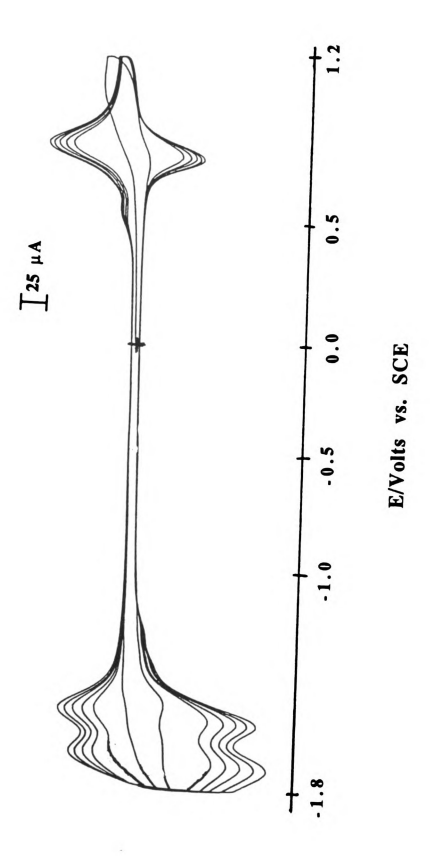
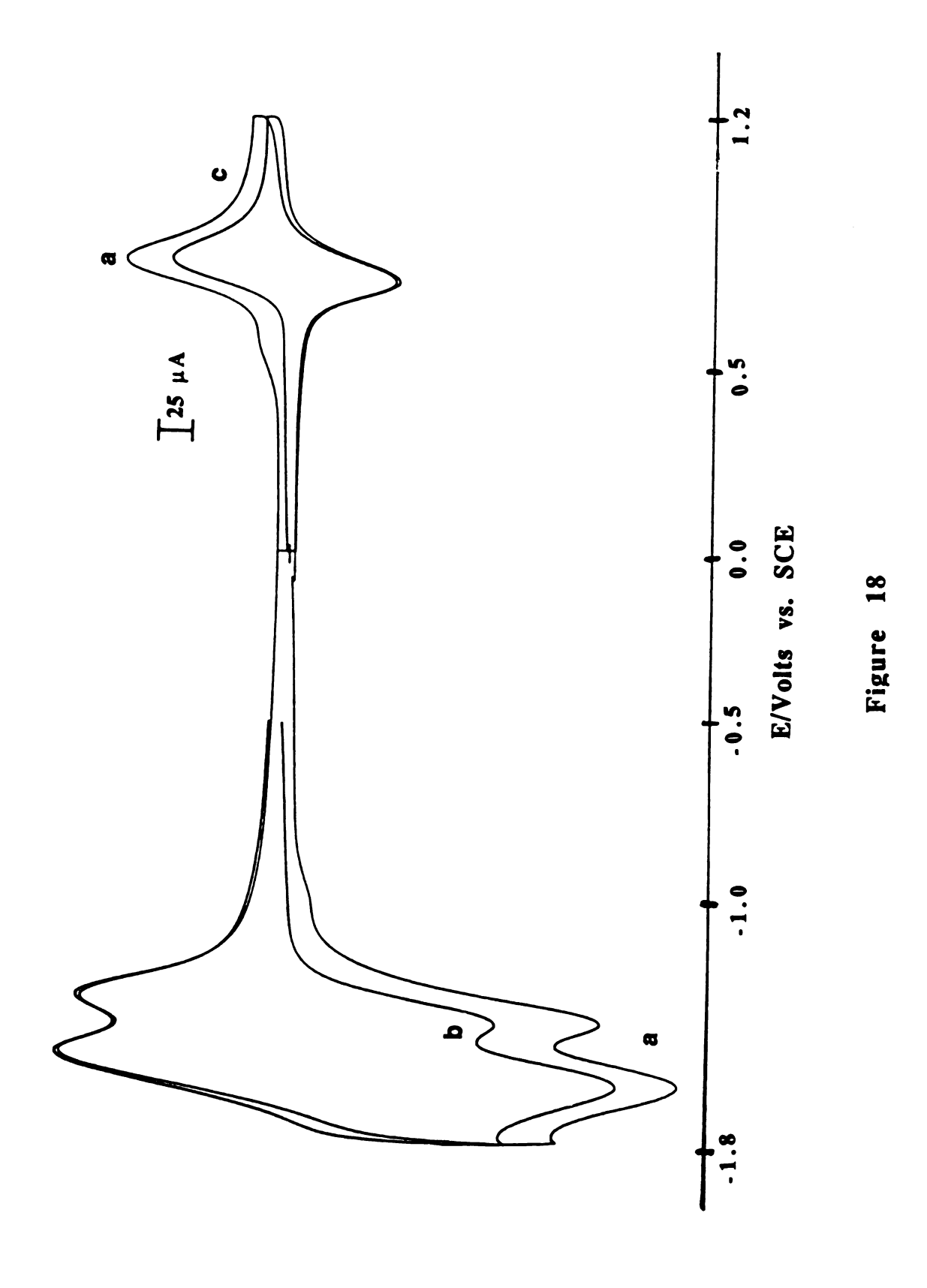


Figure 17

Cyclic voltammetric waves obtained from a poly-Fe(vbpy)₃²⁺/montmorillonite electrode in acetonitrile containing 0.2 M TEAP: (a) upon scanning the electrodes potential from 0.00 V to +1.20 V, to -1.80 V, and back to 0.00 V vs. SCE; (b) after the reduction waves had been scanned once prior to measurement; and (c) after the oxidation wave had been cycled once prior to measurement.

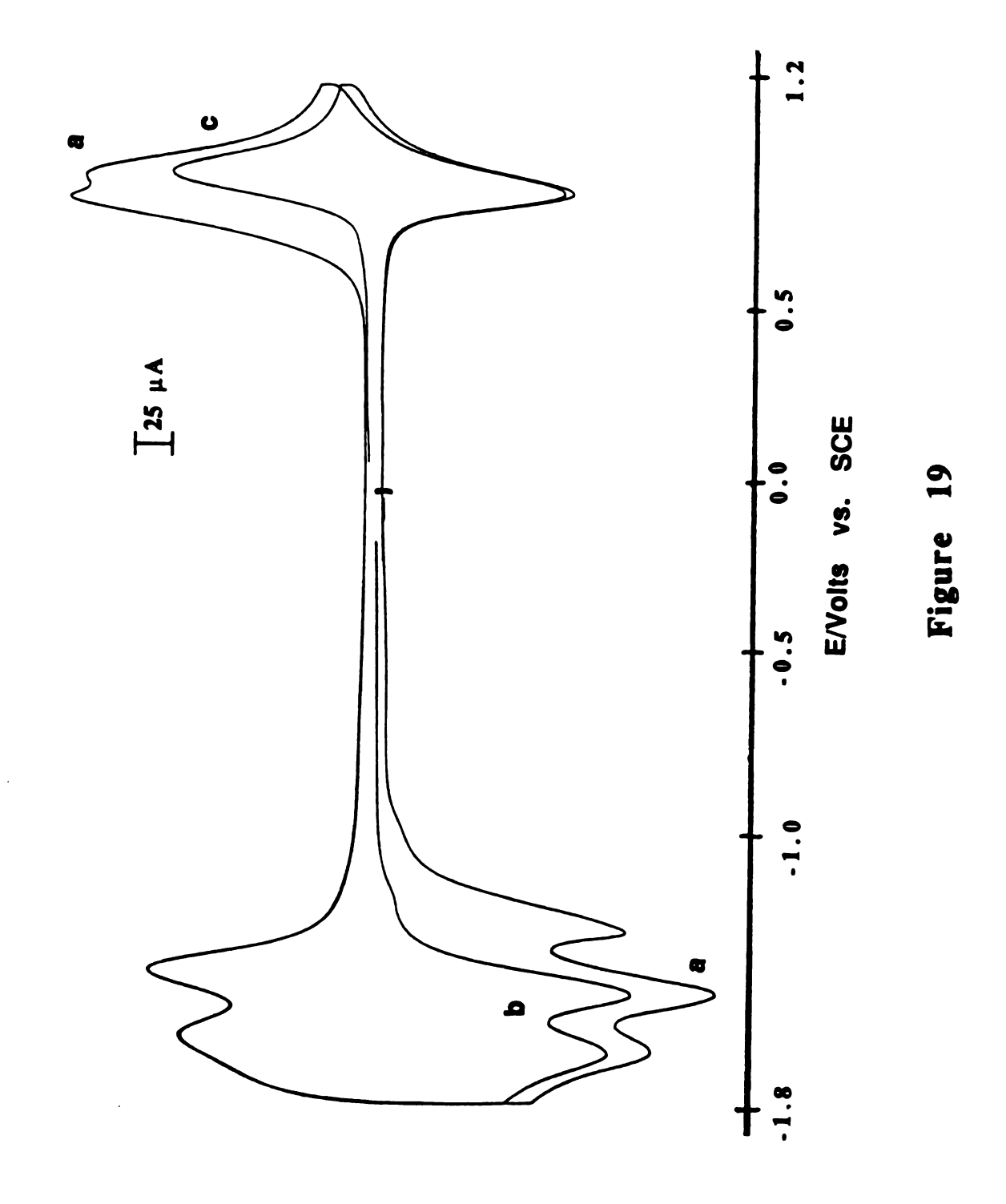


and +1.45 V. Similarly $i_{p,c}/i_{p,a} = 1.00$ for both reduction waves (Figure 18c) after cycling the potential two times between 0.00 and -1.85 V.

In an effort to elucidate the origins for $i_{p,a} \neq i_{p,c}$ on the first scan, an identical experiment was conducted at a bare graphite The potential sequence was 0.00 to -1.80 V, to +1.20 V, and back to 0.00 V vs. SCE. Figure 19a shows a prewave spike before the oxidation wave and the first reduction wave. The prewaves are eliminated (Figure 19b and 19c) by performing the parallel experiments used to obtain the CV's shown in Figure 18b and 18c. These prewaves are clearly stable and associated with one another; once one spike is cycled it does not reappear until after the other is Thus these waves represent the anodic and cathodic branches of the same redox couple. Although the origin of these prewaves obtained at the bare electrode has not unequivocally been established possible explanations have been presented. Observed prewaves at bare electrodes have been attributed to isolated sites of damaged polymer, which are either to dilute or too immobile to undergo direct electron transfer with the electrode. 176 Guarr and Anson have proposed prewaves to arise from the partial reduction of ligands which have been protonated causing the metal complex to have a significantly more negative III/II redox couple.¹⁴⁵

Although the clay/polymer composite modified electrode is similar to the polymer at the bare electrode with regards to $i_{p,a} \neq i_{p,c}$, the absence of the prewave spikes for the former suggests the clay microenvironment is altering the polymerization process. Further support for clay mediated polymerization comes from observations

Cyclic voltammogram of poly-Fe(vbpy)₃²⁺ adsorbed onto pyrolytic graphite while soaking in an acetonitrile solution containing 0.2 M TEAP: (a) upon scanning the electrodes potential from 0.00 V to +1.20 V, to -1.80 V, and back to 0.00 V vs. SCE; (b) after the reduction waves had been scanned once prior to measurement; and (c) after the oxidation wave had been cycled once prior to measurement.



that the growth rate of the polymer at the bare graphite electrode is 2.5-3.0 times faster in acetonitrile solutions containing equal concentrations of Fe(vbpy)₃²⁺ than that for Na⁺-exchanged modified Because the radical initiated polymerization process requires Fe(vbpy)₃²⁺ from solution to approach and react with reduced polymer already formed on the electrode, unfavorable electrostatic interactions between the positively charged diffusing ion and the positively charged polymer must be overcome for polymerization to occur. The negatively charged clay layers may electrostatically facilitate this process. The nature of the defect site for clay mediated polymerization will be different than that of a bare It is important to note that the inability to observe prewave spikes from clay/polymer microstructures does preclude their existence. Indeed, the fact that $i_{p,a} \neq i_{p,c}$ for the clay/polymer composite suggests that isolated defect sites are present in this system. The prewaves arising from these defect sites may be shifted in potential such that they fall under the waves of the bulk polymer.

Clay/polymer films are very stable to oxidation in acetonitrile solutions containing electrolyte, but rapid loss of activity occurs if the films are reduced over several cycles. For example the film whose CV is shown in Figure 18 loses only 6 % of its activity, upon cycling the electrode potential past the oxidation wave continuously for 2 h and films soaked (48 h) in acetonitrile solutions containing 0.2 M TEAP, which are not cycled, demonstrate no measurable loss of activity. Conversely, activity is lost within a few cycles over the reduction waves of the polymer. The cause for the degradation of

these films upon reduction in fresh acetonitrile solutions is not clear. These acetonitrile solutions are not dry and water, which is required to assist in swelling of the films, can be reduced at the high negative potentials needed for the reduction of the $Fe(vbpy)_3^{2+}$ polymer. It is possible that the reduced polymer is attacked by OH^- produced from the reduction of H_2O . Another interesting result is that the oxidation wave stops growing after about 3 h of cycling the potential of the clay modified electrode in 0.5 mM $Fe(vbpy)_3^{2+}$. However, the reduction waves continue to grow and shift to more negative potentials. This result implies the presence of a chemically induced polymerization initiated by cathodic currents.

The current response for the clay/poly-Fe(vbpy)₃²⁺ film indicates thin cell behavior. Figure 20 displays a linear dependence of current with scan rate, for the clay/poly-Fe(vbpy)₃²⁺ film. Additional support for thin cell behavior is provided by the symmetrical shape of the cyclic voltammogram for the Fe(vbpy)₃²⁺ oxidation wave (Figure 18c). The peak currents of the reduction waves and E_{p,c} for the metal-centered oxidation wave appear at identical potentials for the polymer at bare graphite and within clay. However, E_{p,a} for the oxidation wave of the polymer incorporated in clay films is shifted 40 mV positive of the E_{p,a} for the polymer on graphite. This shift in potential could result from interactions of the positively charged polymer with negative sites within the clay producing an energy barrier which must be overcome for electron transfer to occur. Peak separations of 81 mV for the oxidation wave of Fe(vbpy)₃²⁺ (100 mV/sec) and a FWHM of 125 mV are greater than predicted and most likely result from resistive effects.

A plot of the peak height $i_{p,a}$ (μA) νs . the scan rate (mV/sec) for the CV reproduced in Figure 18.

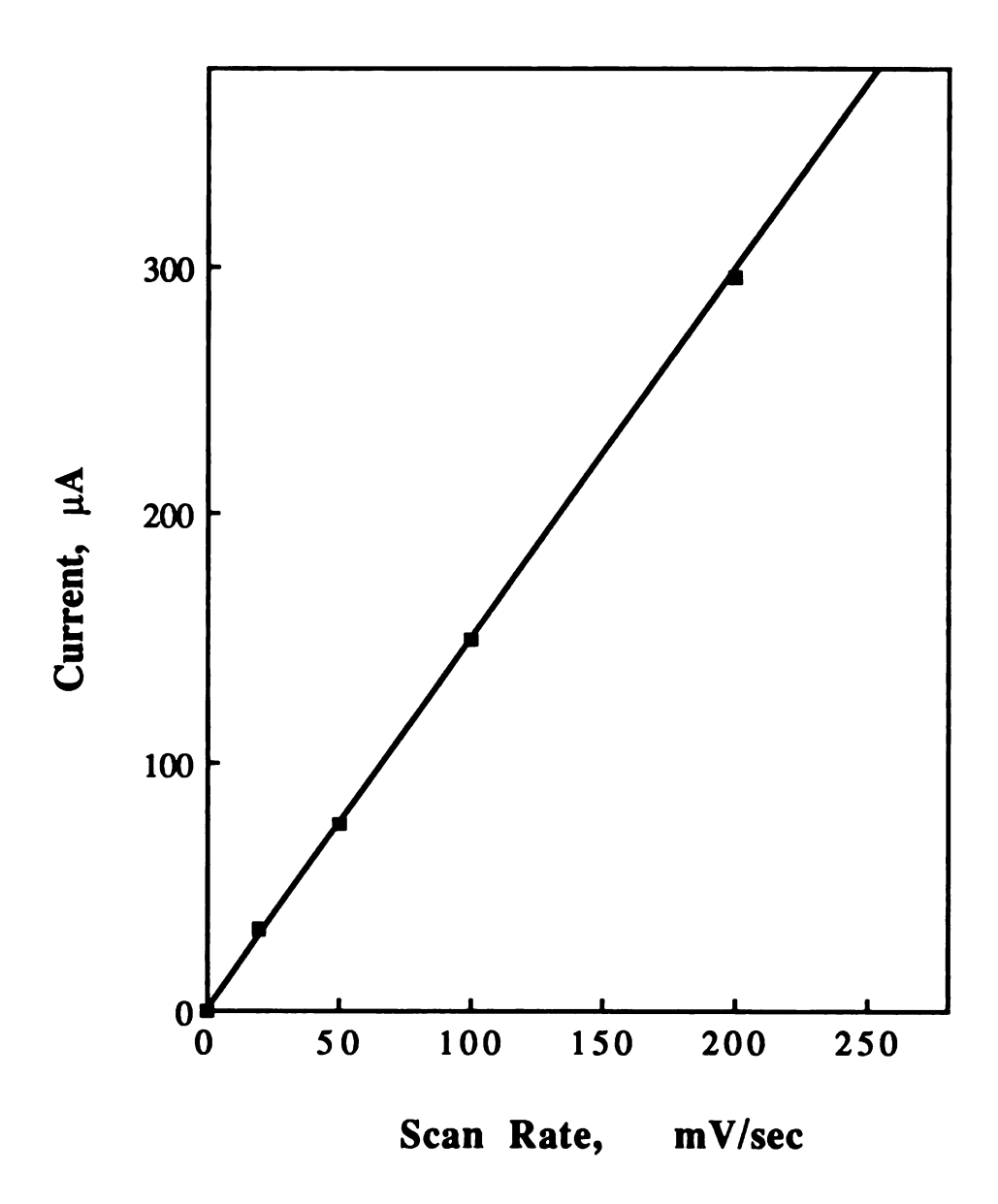


Figure 20

Although thin film behavior does not unequivocally establish the $Fe(vbpy)_3^{2+}$ to be polymerized, it is noteworthy that clay films incorporating comparable loadings of electrolyzed $Fe(bpy)_3^{2+}$ (30 % of CEC for $Fe(bpy)_3^{2+}$ clay film active / 34 % of CEC for $Fe(vbpy)_3^{2+}$ clay film active) demonstrate diffusional behavior (ip is linear with the square root of scan rate $v^{1/2}$ and diffusional tail is observed in CV). Thus thin cell behavior appears to be specific to poly- $Fe(vbpy)_3^{2+}$ attached to the electrode. Moreover electroactive ions do not leach from this film even after days of soaking in water and/or acetonitrile solutions containing electrolyte. These results strongly suggest that $Fe(vbpy)_3^{2+}$ is polymerized in the clay.

With the formation of a polymerized film established, the possibility of extending electroactivity into Region II can be investigated. The polymerization of Fe(vbpy)₃²⁺ in Na⁺-exchanged and 88 % Fe(vbpy)₃²⁺ pre-exchanged montmorillonite films on graphite was performed in acetonitrile solutions containing 2.0 mM Fe(vbpy)₃²⁺ and 0.2 M TEAP. Table 8 lists the number of coulombs of charge accessed during a slow voltammetric scan from the cathodic portion of the oxidation wave of polymerized Fe(vbpy)₃²⁺ in clay that has been transferred to acetonitrile solutions containing 0.2 M TEAP. Almost identical values of 2.2 and 2.1 x 10⁻⁴ coulombs for the polymerized films indicate that the gallery height does not greatly affect electroactivity, a result which supports earlier conclusions. For the purpose of comparison Table 8 also lists the coulombs obtained from Na⁺-exchanged and 88 % Fe(vbpy)₃²⁺ preexchanged montmorillonite films identically prepared to those above; polymerized films were soaked in 2.0 mM solutions of Fe(vbpy)₃²⁺

Film	Solution Fe(L) ₃ ²⁺ Extracted from ^a	Solution Coul. Measured in ^b	Coulombs x 10 ^{4 c}
Na ⁺ -exchanged			
polymerized	acetonitrile	acetonitrile	2.2
soaked	acetonitrile	acetonitrile	•
	acetonitrile	water	0.3
	water	water	1.2
Pre-exchanged 88 % CEC ^d			
polymerized	acetonitrile	acetonitrile	2.1
soaked	acetonitrile	acetonitrile	•
	acetonitrile	water	0.7
	water	water	1.3

^aL = vinyl-bipyridine, and the solution contains 2 mM Fe(vbpy)₃²⁺.

^bThe soaking solution contains just electrolyte. ^cThe number of coulombs under reduction wave after subtracting background. ^dThe exchanged ion is Fe(vbpy)₃²⁺.

for 8 h and transferred to either acetonitrile or aqueous solutions containing 0.2 M TEAP and 0.2 M LiClO₄, respectively. Significantly diminished responses from these films results from the poor swelling ability of clays in acetonitrile. Comparison of the electroactivity from Fe(vbpy)₃²⁺ polymerized in clay films as opposed to incorporation by soaking clearly shows that polymerization enhances swelling. additional comparison, these same Na⁺-exchanged and 88 Fe(vbpy)₃²⁺ pre-exchanged montmorillonite films were soaked in aqueous solutions containing 2.0 mM Fe(vbpy)₃²⁺ and 0.2 M LiClO₄ for 8 h and then transferred to aqueous solutions containing 0.2 M The coulomb data listed in Table 8 demonstrate that even films soaked in aqueous solutions, which completely eliminates swelling effects, have a diminished response over the polymerized clay films. The electroactivity data in Table 8 corresponds to 0.26 of the CEC for the films soaked in aqueous Fe(vbpy)₃²⁺ solutions and 0.48 of the CEC for the films polymerized in acetonitrile Fe(vbpy)₃²⁺ The results are clear. The polymerized films display solutions. almost twice the electroactivity over films which extract ions from We therefore conclude that polymerized Fe(vbpy)₃²⁺ in clay films effectively extends Region I further away from the electrode by accessing previously isolated Fe(vbpy)₃²⁺ in Region II. Nevertheless all of the Fe(vbpy)₃²⁺ from Region II is not activated in the clay/polymer films because doubling the film thickness does not increase the amount of activated Fe(vbpy)₃²⁺. Thus Region I activity can be enhanced by creating a mode for charge propagation into Region II by polymerizing Fe(vbpy)₃²⁺ in the clay film, although much of Region II is still electroinactive.

Clay/poly-Fe(vbpy)₃²⁺ films exhibit unique electrocatalytic A clay/polymer modified electrode was placed in an aqueous solution containing 0.2 M LiClO₄ and 4.2 mM Fe(CN)₆⁴⁻ and its potential was cycled from - 0.10 to + 1.20 V vs. SCE at 2 mV/s. The resulting voltammogram (Figure 21a) demonstrates the characteristic S-shaped voltammetric response expected from electrocatalytic systems. Presumably the Fe(vbpy)₃²⁺ polymer is oxidized during the forward oxidation scan and before Fe(vbpy)₃³⁺ can be reduced at the electrode on the reverse cycle, it is reduced by $Fe(CN)_6^{4-}$ to generate $Fe(CN)_6^{3-}$ and $Fe(vbpy)_3^{2+}$, which in turn becomes reoxidized at the electrode. The large excess of Fe(CN)₆⁴present in solution coupled with the slow scan rate enables a steady state response to develop which is manifested in the S shape of the The efficiency of this catalytic cycle is evidenced by the magnitude of the difference in current responses from the clay/poly-Fe(vbpy)₃²⁺ in the presence (Figure 21a) and absence (Figure 21b) of added Fe(CN)₆⁴. In order to observe catalytic behavior the Fe(CN)₆⁴ must necessarily come in contact with Fe(vbpy)₃³⁺. Fe(CN)₆⁴- must either penetrate through the clay/polymer film or react at the edges of the film in Region I and/or Region II (Figure The former pathway would result in a buildup of Fe(CN)₆³ within the clay/polymer film. Yet Figure 21b shows no evidence of $Fe(CN)_6^{3-/4}$ in the film (the redox couple for $Fe(CN)_6^{3-/4}$ appears at ≈ +0.3 V) suggesting that catalysis is occurring at the edge of the clay/polymer film in either Region I or Region II (Figure 22). Because electroactivity from clay films arises only from ions near the electrode in Region I, and isolated ions further from the electrode in

Cyclic votammograms scanned at 2 mV/sec, of a clay/poly- $Fe(vbpy)_3^{2+}$ film soaking in an aqueous solution containing 0.2 M $LiClO_4$: (a) after the addition of 4.2 mM $Fe(CN)_6^{4-}$ and; (b) before the addition of 4.2 mM $Fe(CN)_6^{4-}$.

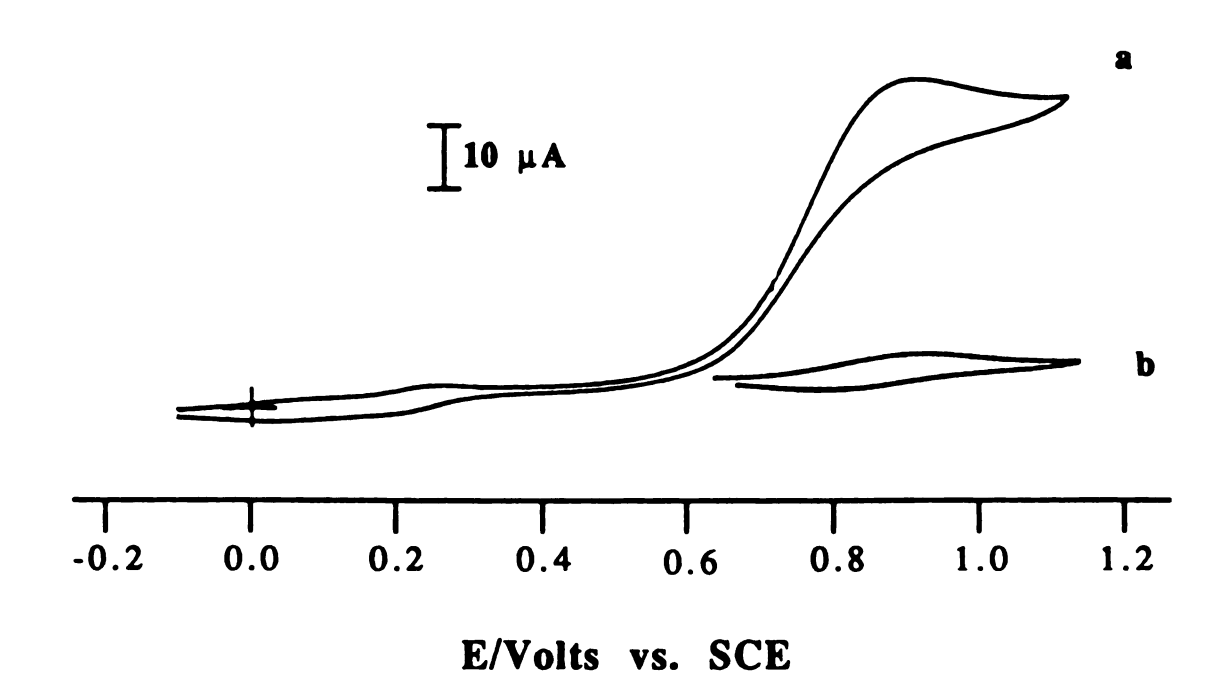


Figure 21

Model depicting origins of electrocatalysis from a clay/poly-Fe(vbpy)₃²⁺ film on an electrode.

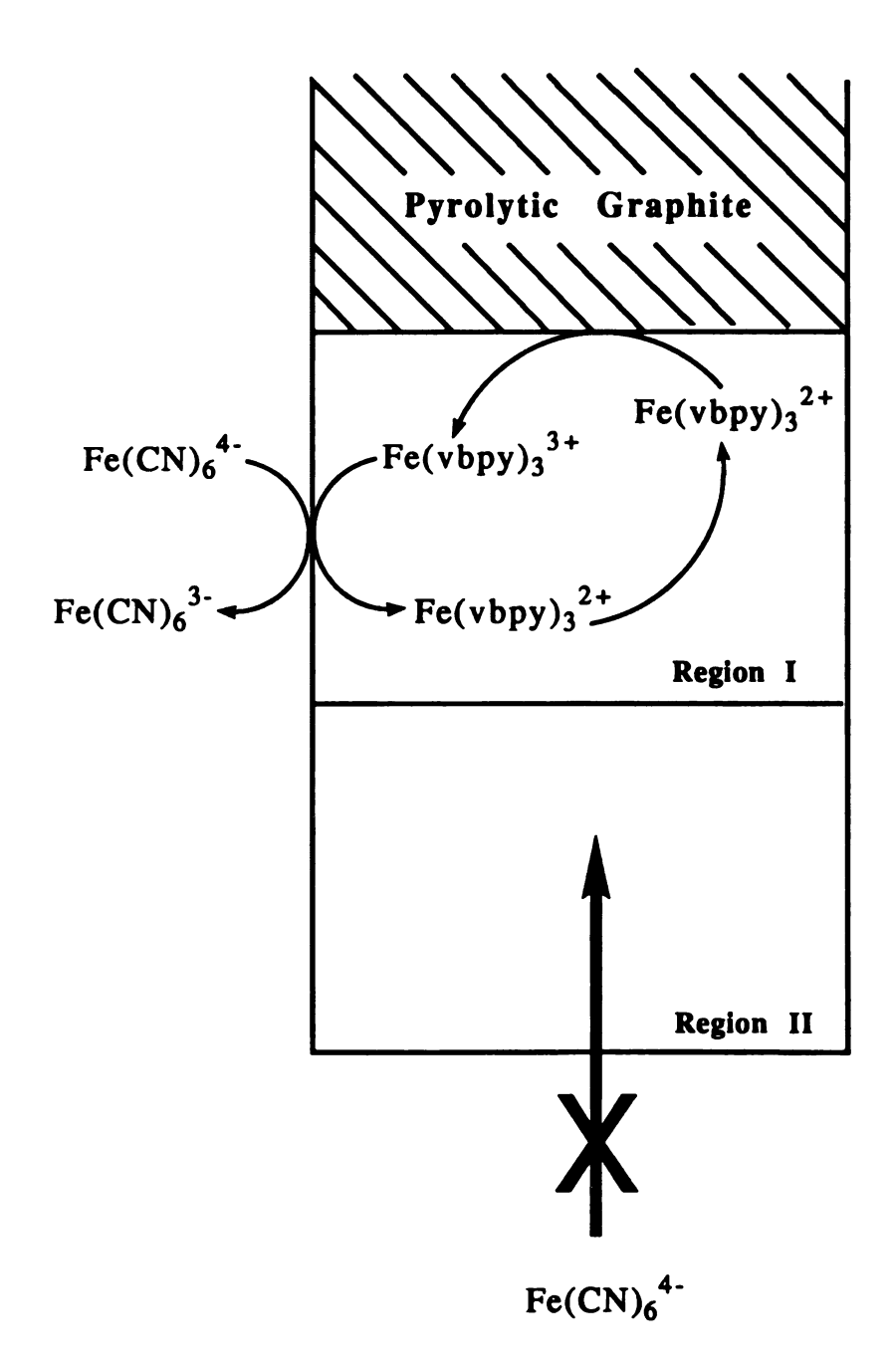


Figure 22

Region II are electroinactive, necessarily implies communication between $Fe(CN)_6^{4-}$ and $Fe(vbpy)_3^{3+}$ to occur at Region I edges. Thus as graphically displayed by the model proposed in Figure 22, electrocatalysis from the clay/poly- $Fe(vbpy)_3^{3+}$ film is believed to arise from the edges of Region I.

4. Intersalated Clay Films

With the studies described heretofore, electroactivity from ions in clay galleries has not been realized. As discussed in Section III.B.1, inactivity of ions in the the clay galleries results from unfavorable thermodynamics arising from the inability to maintain charge neutrality during electrolysis. The requirement of mobile negative ions within the clay galleries can, in principle, be achieved with intersalated clays. The general structure of montmorillonite intersalated with Fe(bpy)₃²⁺ is given below by structure 6.

Negat	ively Charged	Clay	Layer
	Fe(bpy) ₃ ²	F	
Fe(bpy) ₃ ²⁺	SO ₄ ²⁻		Fe(bpy) ₃ ²⁺
SO ₄ ²	Fe(bpy) ₃ ²⁺		SO ₄ ²⁻
Fe(bpy) ₃ ²⁺			Fe(bpy) ₃ ²⁺
Negat	ively Charged	Clay	Layer

6

An intersalated clay, prepared by adding the clay to 5 CEC of a polypyridyl metal complex in the presence of dianions of the form

 XO_4^{2-} (X = S, Mo, W), is distinguished by its incorporation of twice the CEC in the clay galleries. One CEC balances the charge of the clay layers while the additional CEC is present as an ion pair between the metal complex and the XO_4^{2} -counterion. The additional 3 CEC is external to the clay gallery (i.e. on surface layers and in voids around the clay platelets) and is required to maintain a favorable equilibrium for intersalate formation. This excess loading of the galleries is reflected by increased d-spacings. The d-spacing obtained for montmorillonite films with 1 CEC loading of Fe(bpy)₃²⁺ is 18.4 Å whereas ion incorporation from solutions of 5 CEC yields intersalates with d-spacings of 29.5 Å. The sulfate ions of intersalates are mobile and can be easily displaced with different anions.²⁶⁸ Because intersalated clays should allow for total activity of all redox cations within the clay film, the unfavorable thermodynamics associated with the maintenance of charge neutrality should be circumvented. Accordingly electrochemical studies were undertaken with the goal of observing electroactivity from ions electrostatically bound between clay layers.

Intersalated modified electrodes were prepared by air drying a dilute suspension of intersalate onto a pyrolytic graphite electrode. Figure 23 shows the first two scans of an intersalated modified electrode immersed in a dichloromethane solution containing 0.2 M tetrabutylammonium perchlorate (TBAP). The quantity of $Fe(bpy)_3^{2+}$ oxidized on the first scan, as determined by coulometry, corresponds to ~3 CEC of the montmorillonite film. However, the amount of metal complex electrolyzed upon the subsequent scan is greatly reduced and continues to decrease with continued scanning

The first two cyclic voltammograms of a Fe(bpy)₃²⁺ intersalated montmorillonite film on pyrolytic graphite immersed in a dichloromethane solution containing 0.2 M TBAP.

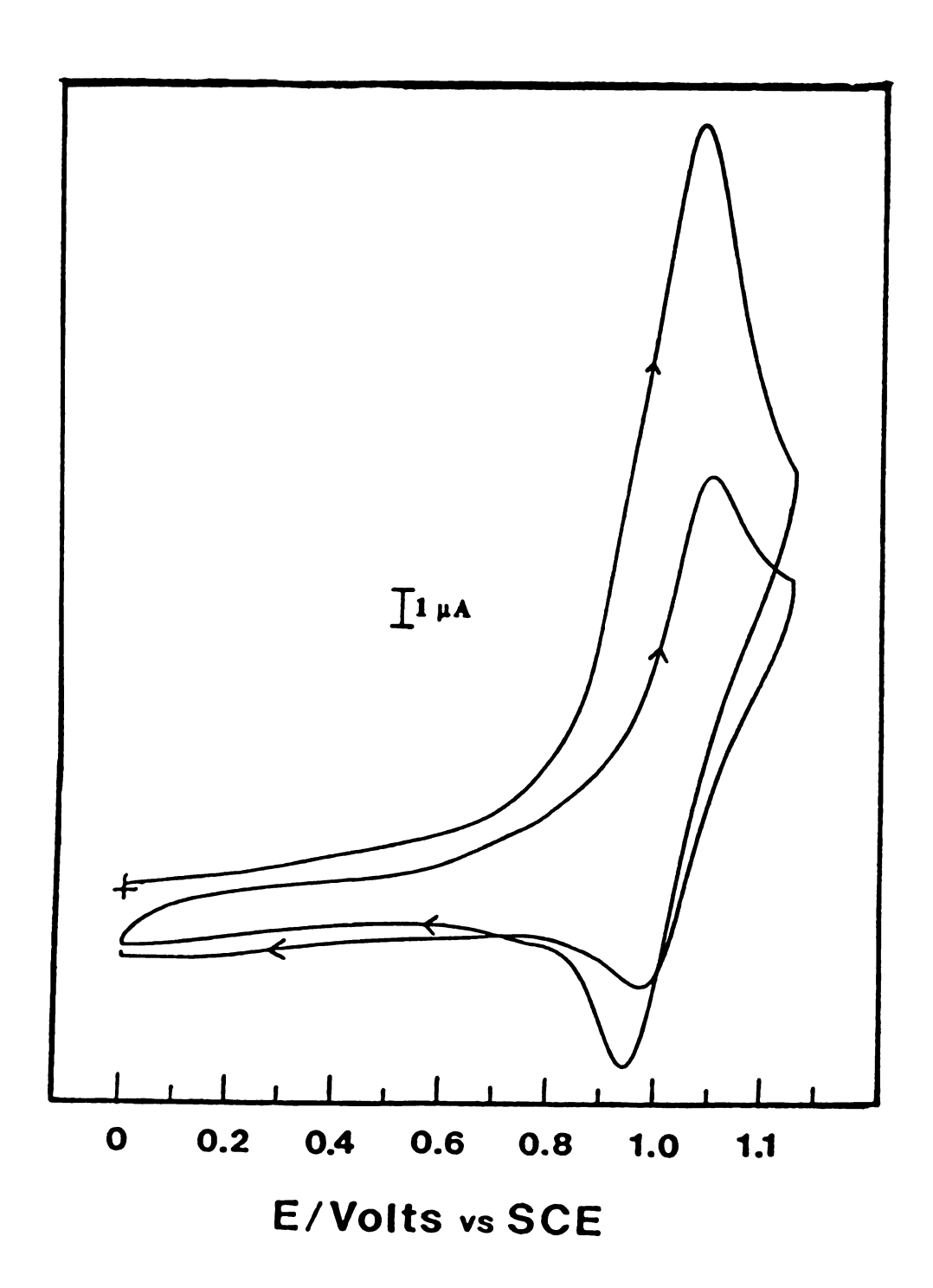


Figure 23

of the oxidation wave. To ensure that this result was not caused by the collapse of the clay in dichloromethane, the same experiment was conducted in a saturated aqueous solution of sodium sulfate. Almost identical results were obtained.

Although the increased electrochemical response of the intersalates is encouraging, current attributed to a totally activated intersalated film is not observed. The total number of coulombs of intersalates should correspond to 5 CEC. Noting that of the 5 CEC in intersalated films, 2 CEC are in the clay galleries and 3 CEC are external to the galleries, the observation of current corresponding to 3 CEC may reflect electroactivity from only Fe(bpy)₃²⁺ outside of the clay particles. In this case, the ultimate incorporation of Fe(bpy)₃²⁺ into an 88% pre-exchanged Fe(bpy)₃²⁺ montmorillonite film soaked in a 5.1 mM solution (the concentration of the 3 CEC excess Fe(bpy)₃²⁺ in intersalate suspensions as determined in Section II.A.3.f) should be the same as that for the intersalate because the total amount of electroactive Fe(bpy)₃²⁺ incorporated in clay films is independent of the d-spacing. As shown in Table 9 the number of coulombs measured on the 1st and 20th scans of an 88% preexchanged Fe(bpy)₃²⁺ film, which has been soaked in 5.1 mM Fe(bpy)₃²⁺ for 3 h and transferred to a dichloromethane solution containing 0.1 M TBAP, corresponds to the Na⁺-exchanged film and not to the intersalate. The values in Table 9 were determined for the reduction rather than the oxidation of Fe(bpy)₃²⁺ because the former excludes charge arising from the oxidation of water. As one additional control experiment, 3 CEC of Fe(bpy)₃²⁺ was added to an 88 % pre-exchanged montmorillonite slurry before the film was cast.

Table 9

Amount of Electroactivity from Different Clay Films after Soaking in 5.1 mM Fe(bpy)₃²⁺

	# of coulombs		
Montmorillonite Film	1 st scan	20 th scan	
Intersalated + 5 CEC	13.5 x 10 ^{-4 a}	3.0 x 10 ^{-4 a}	
of Fe(bpy) ₃ ²⁺	$4.4 \times 10^{-4} \text{ b}$	$2.5 \times 10^{-4} \text{ b}$	
Pre-exchanged with 88% CEC of Fe(bpy) ₃ ²⁺	1.4 x 10 ^{-4 b}	1.0 x 10 ^{-4 b}	
Na ⁺ -exchanged	1.3 x 10 ^{-4 b}	0.9 x 10 ^{-4 b}	
Pre-exchanged with 88 %	3.9 x 10 ^{-4 a}	1.5 x 10 ^{-4 a}	
CEC of $Fe(bpy)_3^{2+} + 3$ CEC of $Fe(bpy)_3^{2+}$ c	3.7 x 10 ^{-4 b}	1.2 x 10 ^{-4 b}	

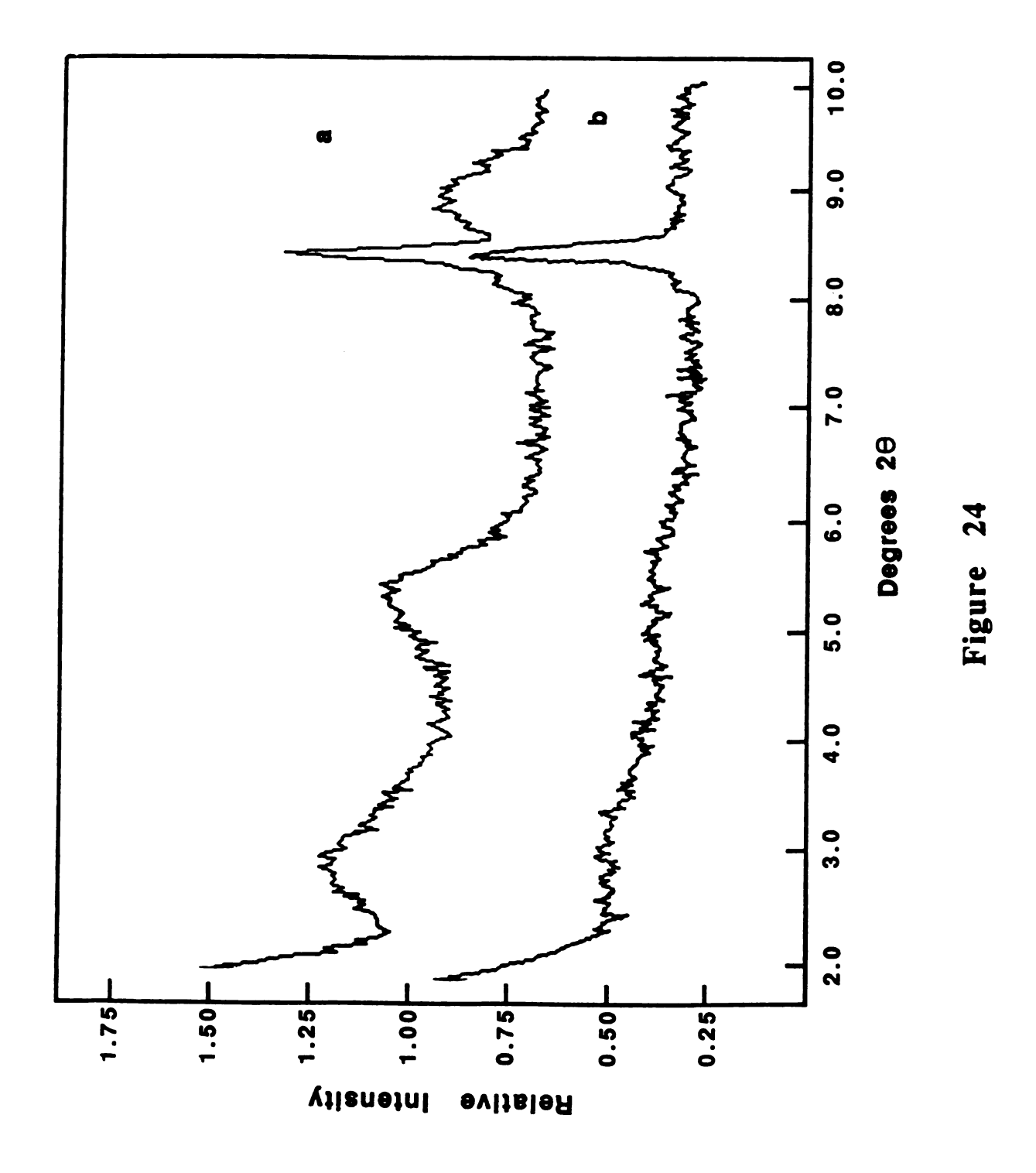
^aThe number of coulombs under oxidation wave after subtracting background. ^bThe number of coulombs under reduction wave after subtracting background. ^cThis film was not soaked in a 5.1 mM Fe(bpy)₃²⁺ solution.

Initial electroactivation is ~ 3 times that obtained for pre-exchanged films (Table 9) soaked in $Fe(bpy)_3^{2+}$. Nevertheless, the activity on the first oxidation for the intersalate is ~ 10 times this value. In addition, by the 20^{th} scan the responses from both pre-exchanged films are basically the same whereas the intersalate activates about 3 times more $Fe(bpy)_3^{2+}$. Thus excess activity is clearly observed for intersalates.

The decrease in electroactivity from intersalates after the first scan suggests significant and irreversible perturbation of the microstructure upon passing current into the film. This could mean that $Fe(bpy)_3^{3+}$ is not stable when exchanged into clay galleries. Previous experiments by Oyama, Oyama and Anson^{278,279} and Rudzinski and Bard²⁶¹ have demonstrated that structural iron located in the clay octahedral sites is redox active. Could the $Fe(bpy)_3^{3+}$ produced upon oxidation of the intersalate react with the clay structure thereby leading to its degradation in the clay gallery? UV-vis spectroscopy in combination with bulk electrolytic experiments suggest otherwise. Electronic absorption spectra show only the presence of $Fe(bpy)_3^{2+}$ and $Fe(bpy)_3^{3+}$ and CV's display only the reversible 3+/2+ couple. Therefore, instability of intersalates under electrolytic conditions must result from a different source.

X-ray patterns of the intersalated clay sample on graphite before and after electrolysis are enlightening. Figure 24a shows the expected diffraction profile for an intersalated clay on pyrolytic graphite; the appropriate d-spacing of 29.4 Å is observed. The pattern changes significantly upon electrolysis of a single oxidative scan. As shown in Figure 24b, the order of the clay film is almost

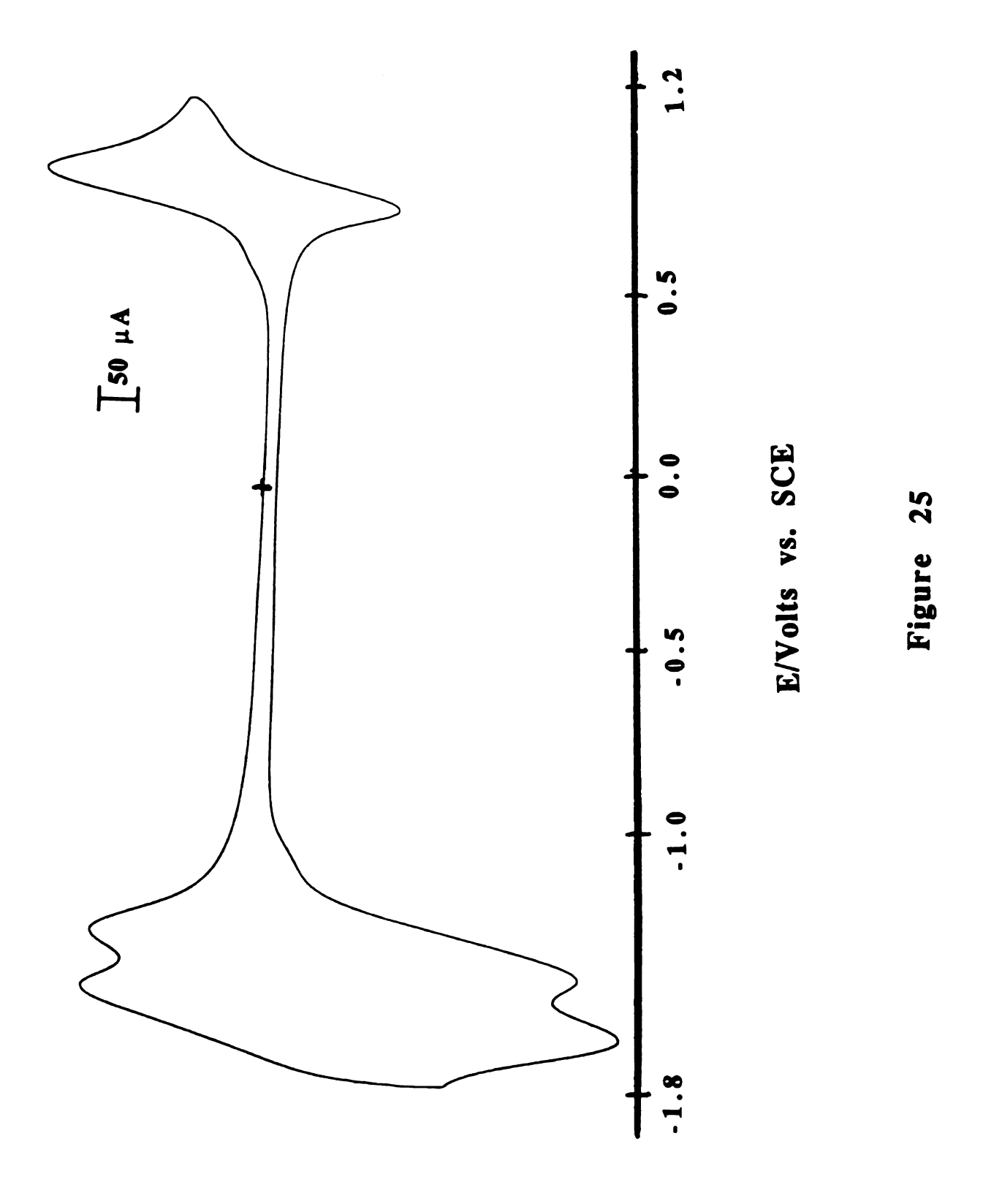
The X-ray diffraction patterns obtained from Fe(bpy)₃²⁺ intersalated films on pyrolytic graphite: (a) before the electrolysis of the film; and (b) after the electrolysis of the film in a dichloromethane solution containing 0.2 M TBAP.



completely lost; only the sharp peak corresponding to crystalline Fe(bpy)₃²⁺, present in the regions outside of the clay particles, is present. This x-ray data suggests that upon electrolysis the intersalate is collapsing to a monolayer with the rapid ejection of Fe(bpy)₃³⁺ from the galleries. Significantly, the diffraction pattern in Figure 24b indicates that the clay platelets are no longer stacked in an ordered manner. Increased activity of intersalate on the 20th scan is consistent with our previous data which suggests the manifestation of disorder in increased electroactivity owing to a larger basal volume for electroactive ions. Collapse of the intersalate will create large void volumes which will be occupied by the ejected ions. The greater volume of voids in Region I should allow the incorporation of more cations and hence greater electroactivity.

These results clearly show that in order to sustain electroactivity from intersalated species, the metal complex must be immobilized within the galleries as an intersalate to prevent ejection of the ion upon electrolysis. This can be achieved with the electrochemical polymerization of a clay film intersalated with Fe(vbpy)₃²⁺. A Fe(vbpy)₃²⁺ intersalated montmorillonite film was cast on graphite, placed into a acetonitrile solution containing 2.0 mM Fe(vbpy)₃²⁺ and 0.2 M TEAP, and the oxidation and reduction waves were cycled for 1 h to induce polymerization. Figure 25 reproduces the oxidation and reduction waves for this film in acetonitrile containing 0.2 M TEAP. The amount of material oxidized as determined by coulometry corresponds to 1.55 CEC of the clay. The current response vs. scan rate for this intersalated clay/polymer film shows thin cell behavior at slow scan rates but negative deviation at

Cyclic voltammetric waves of a polymerized Fe(vbpy)₃²⁺/intersalated montmorillonite film adsorbed onto pyrolytic graphite while soaking in an acetonitrile solution containing 0.2 M TEAP.



higher scan rates is observed (Figure 26). Likewise the voltammogram exhibits intermediate behavior, exhibiting a symmetrical shape at slow scans with increasing diffusional contributions at faster scan rates. The intersalated/polymer films are very stable towards prolonged soaking in acetonitrile or aqueous solutions and are also stable to oxidation. But these films are even more sensitive to cathodic degradation than observed for the Na⁺-exchanged or Fe(vbpy)₃²⁺ pre-exchanged forms.

X-ray patterns of the intersalated clay before and after electrolysis were obtained in order to better understand the effect of electropolymerization on the microstructure of the intersalated clay. 27a shows the expected diffraction profile montmorillonite intersalated with Fe(vbpy)₃²⁺ on pyrolytic graphite; the appropriate d-spacing of 30.1 Å is observed. Upon electrolysis (Figure 27b) the second and third order diffraction peaks are lost and the first order peak broadens, and shifts to a value corresponding approximately to 22 Å. The sample has clearly lost Although the film is no longer totally intersalated, it is also swollen beyond the d-spacing expected for one CEC of Fe(vbpy)₃²⁺, (the d-spacings for montmorillonite containing one CEC of Fe(bpy)₃²⁺ or Fe(phen)₃²⁺ are approximately 18 Å).^{266,267} Either the film is not lying on the electrode with the order observed prior to electrolysis or more likely a wide variety of d-spacings exist throughout the film. The observation that some order is maintained after the electrolysis of Fe(vbpy)₃²⁺ intersalated films directly contrasts the results of intersalated films of Fe(bpy)₃²⁺ which show total loss of order upon electrolysis (Figure 24b).

A plot of the peak height $i_{p,a}$ (μA) vs. the scan rate (mV/sec) for the CV reproduced in Figure 25.

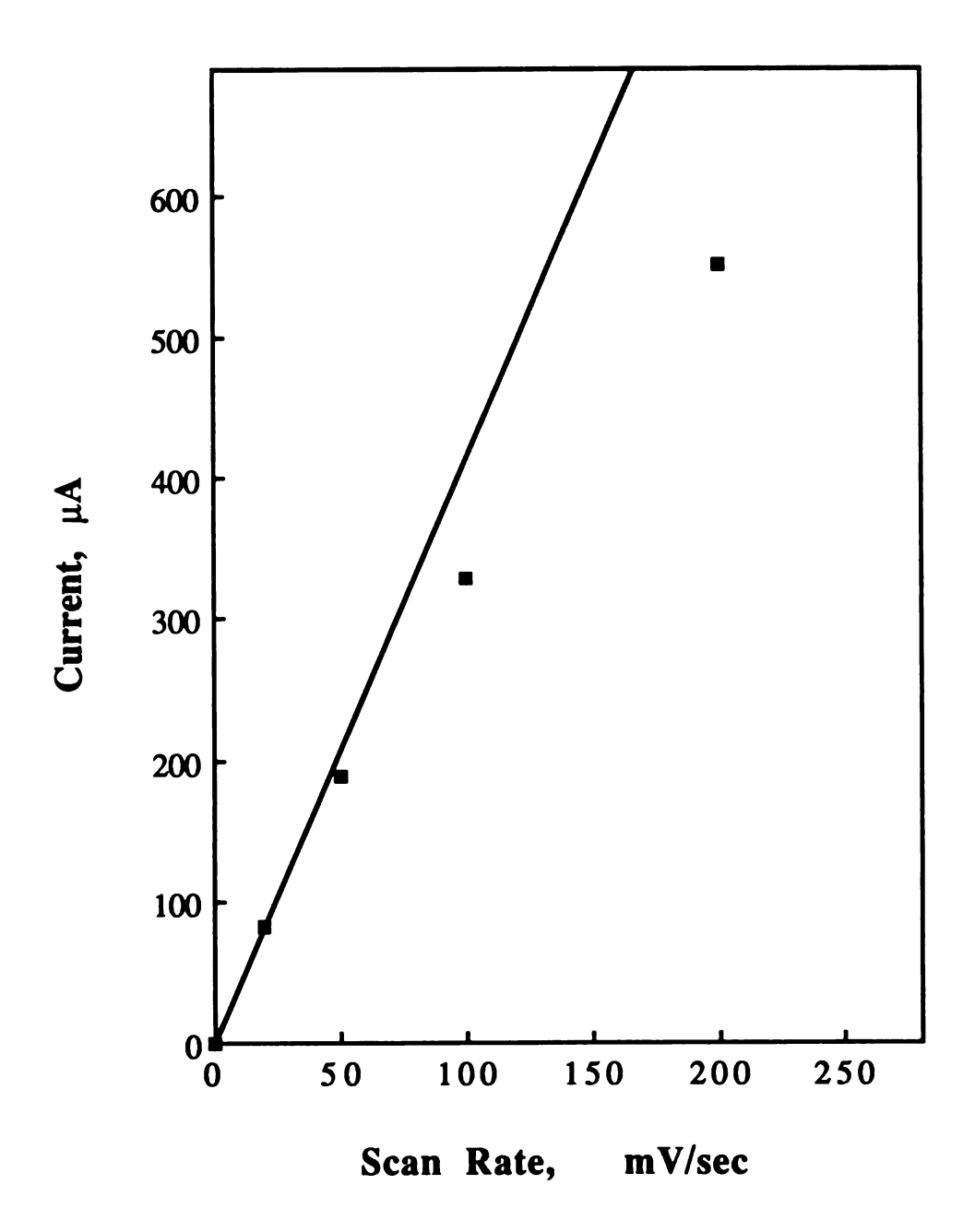
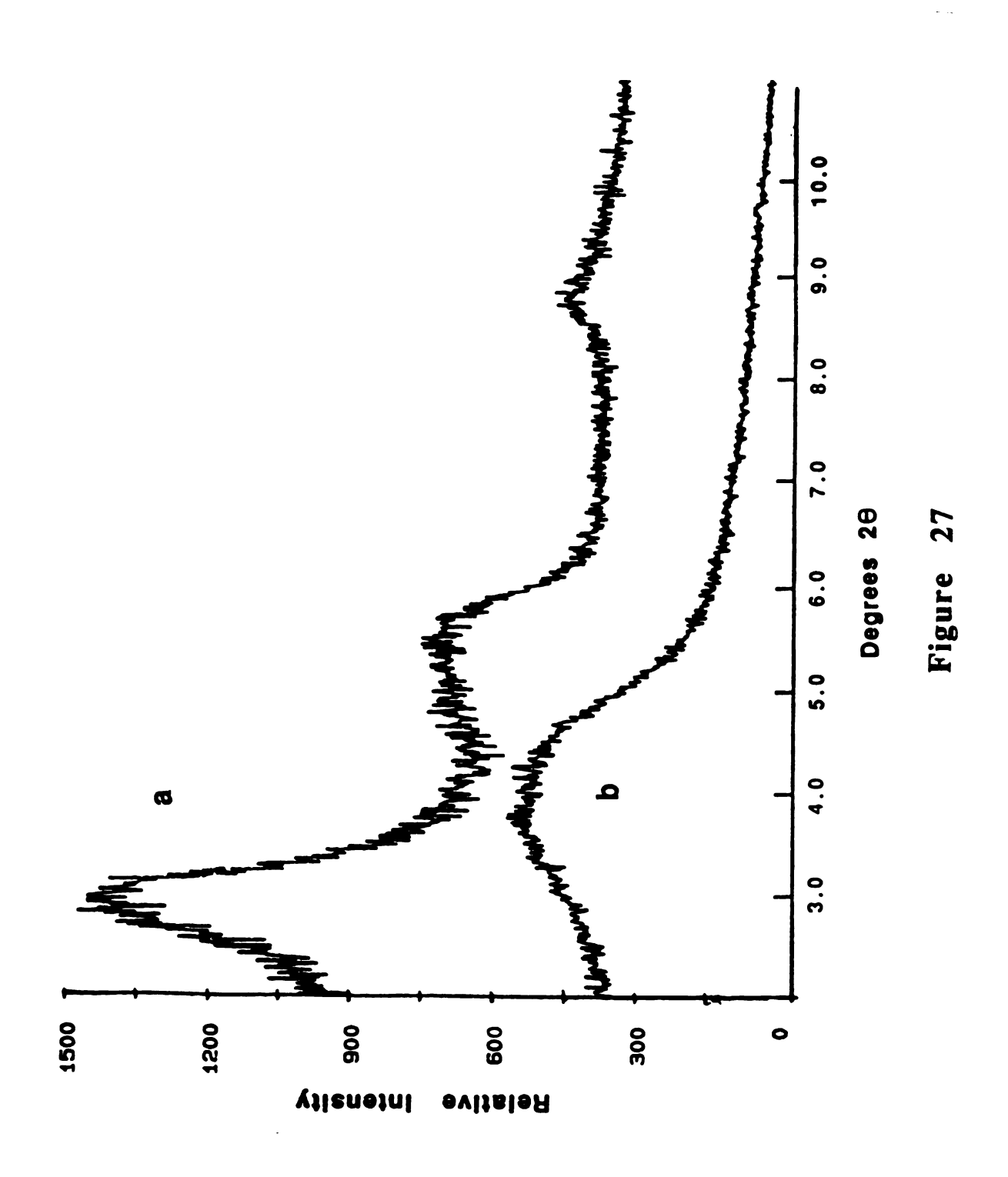


Figure 26

The X-ray diffraction patterns obtained from polymerized Fe(bpy)₃²⁺/intersalated montmorillonite films on pyrolytic graphite: (a) before the electrolysis of the film; and (b) after the electrolysis of the film in a acetnitrile solution containing 0.2 M TEAP.



How can we explain these results? In the Fe(bpy)₃²⁺ intersalate experiments, the oxidation of 2.8 CEC of Fe(bpy)₃²⁺ suggests ions in clay galleries are activated. As previously determined the electroactive material is not evenly distributed throughout the clay film but rather located in Region I. Therefore, 3 CEC cannot correspond to only external Fe(bpy)₃²⁺ but must include contributions from ions in clay galleries as well. The intersalate can maintain charge neutrality by simply ejecting cations. This process accounts for the loss of order from intersalated Fe(vbpy)₃²⁺ films and rationalizes the increased electroactivity from these films. case where Fe(vbpy)₃²⁺ is the intersalate, electrolysis entails the reduction of Fe(vbpy)₃²⁺ which subsequently initiates polymerization. The accompanying process of maintaining charge neutrality by cation uptake or ejection of anions can not involve Fe(vbpy)₃²⁺, which should remain in the gallery. The thermodynamics of ejecting a polymer from the gallery to maintain charge neutrality upon oxidation of Fe(vbpy)₃²⁺ should be significantly less favorable than uptake of an anion. supported by the X-ray diffraction pattern having Fe(vbpy)₃²⁺ present in the galleries at quantities greater than 1 CEC. Moreover, activation of ions in the gallery from intersalated films is further in evidence by the comparison of the films prepared by the electropolymerization of Fe(vbpy)₃²⁺ in 0.38 µm films of intersalated, 88 % Fe(vbpy)₃²⁺ pre-exchanged and Na⁺-exchanged montmorillonite using 10 mM Fe(vbpy)₃²⁺. The limiting currents obtained from intersalated, pre-exchanged and Na⁺-exchanged films corresponded to 1.1 x 10⁻³ coulombs which is 2.4 of the CEC, 4.2 x 10⁻⁴ coulombs

which is 0.9 of the CEC, and 3.3 x 10⁻⁴ coulombs which is 0.7 of the CEC respectively. The electroactivity of the polymerized Fe(vbpy)₃²⁺ intersalated film (2.5 CEC) corresponds closely to that measured on the first scan from of an intersalated Fe(bpy)₃²⁺ film (2.8 CEC). The similarity in the electrochemical responses on the initial scans for these films is satisfying because the overall microstructures should be initially similar. However, the electroactivity observed from the polymerized film is prolonged because the metal complex can not escape from the gallery.

C. Conclusion

Voltammetric investigations demonstrate unequivocally that tris(bipyridyl) metal complexes and methylviologen cations bound electrostatically to the exchange sites of montmorillonite are rigorously electroinactive. This electroinactivity is believed to result from the inability of ions to move in and out of the gallery region between the clay layers, which is required in order to maintain charge neutrality after electron transfer has occurred. Alternatively, electroactivity is observed from ions located in defect zones in the clay film near the electrode (Region I) whereas ions in isolated areas further from the electrode (Region II) are inactive. The amount of electroactivity from these films can be increased if Fe(vbpy)₃²⁺ is electropolymerized within the clay film, presumably resulting from extension of Region I by providing a means to shuttle charge to remote ions. By forming intersalates, counterion motion through the galleries between the clay layers is permitted. Although intersalated ions appear to be electrochemically active owing to the observation of 3 CEC activation in the films; the metal complexes are rapidly expelled from the galleries of intersalate upon electrolysis. Immobilization of ions within intersalated montmorillonite can be accomplished by the electrochemical polymerization of Fe(vbpy)₃²⁺. Similar electroactivity is obtained from the $Fe(vbpy)_3^2$ intersalated/polymer films (2.5 of the CEC) as that for Fe(bpy)₂²⁺ However, for the former the X-ray diffraction pattern intersalates. obtained after electrolysis of an intersalated film suggests that metal complex is retained within the clay galleries. The combination of the X-ray and coulometric data strongly supports the hypothesis that gallery ions can be activated in intersalated clay/poly-Fe(vbpy)₃²⁺ These clay/poly-Fe(vbpy)₃²⁺ composites are very stable to prolonged electrochemical oxidation and have been shown to demonstrate electrocatalytic activity similar to poly-Fe(vbpy)₃²⁺ films on bare electrodes.

CHAPTER IV

POLYPYRIDINIUM BASED MODIFIED ELECTRODES

A. Background

Electron transfer reactions between highly exergonic intermediates provide a means of generating excited states which cannot readily be prepared via photoexcitation. Electrogenerated chemiluminescence (ecl) arises from the electron transfer reactions of electrochemically generated oxidized and reduced intermediates (often called an annihilation reaction) with sufficient energy to populate an emisive excited state of one product. A major advantage of ecl is that the production of high energy intermediates required for luminescence occurs at an electrode, whereas chemiluminescence (cl) requires sacrificial destruction of an added species. Although sufficient electrochemical excitation energy is a necessary requirement for ecl, it is not sufficient. For example, most organic systems have enough energy to populate excited states, yet low excited state production yields Φ_{es} are observed, $^{280-282}$ (Φ_{es} is defined as the equivalents of excited states produced per electron Typically a nonemissive triplet intermediate is transferred). populated and subsequent triplet-triplet annihilation yields the emitting singlet state. Because triplet-triplet annihilations are inherently inefficient, low Φ_{ex} are often observed.²⁸³

Conversely, most inorganic complexes have low lying emissive excited states that can directly be populated upon annihilation. Inorganic ecl systems should therefore possess higher excited state production yields Φ_{es} than their organic counterparts. Despite the discovery of several inorganic systems possessing ecl chemistry, 284 - 289 measured excited state production yields of few systems

approach unity.^{290,291} The origin of these low yields is sometimes known (i.e. decomposition of one or both of the electrogenerated reactants),.²⁹²⁻²⁹⁴ but for many systems these explanations are not applicable. Low yields are nevertheless observed. Recently, Mussell and Nocera²⁹⁵ accounted for the low excited state production yields of highly exergonic inorganic systems by employing current electron The general reaction scheme summarizing this transfer theories. analysis is shown in Figure 28. Annihilation between oxidized hexanuclear cluster Mo₆Cl₁₄ and reduced pyridinium compounds (D) results in production of Mo₆Cl₁₄²- in its electronically excited state (reaction 1) or ground state (reaction 2). An excited state production yield of ≈ 8 % was observed. For highly exergonic systems such as these ($\Delta G^{\circ} \ge 2.2 \text{ eV}$) electron transfer can occur at distances greater than closest contact. Long distance electron transfer is shown to circumvent excited state production (reaction 1) and facilitate reaction to ground state (reaction 2). By using the steady-state equilibrium pair distribution model for electron transfer, the dependence of the excited state k_{es} and ground state k_{gs} rates on the distance at which electron transfer occurs, is shown in Figure 29. An increase in distance is accompanied by a steady diminution of k_{es} owing to an increase in the outer-sphere reorganizational energy (λ_0) and accompanying decrease in electronic coupling (H_{AB}) between reactant pairs. Conversely opposite behavior is observed Because annihilation to produce ground state reactants occurs in the inverted region, an increase in distance is manifested in a monotonic decrease of the outer sphere reorganizational energy and hence increase in rate. This rate increase originating from the

Annihilation reaction between oxidized $M_6X_{14}^-$ cluster and reduced pyridinium ions to produce cluster in its emissive excited state or ground state.

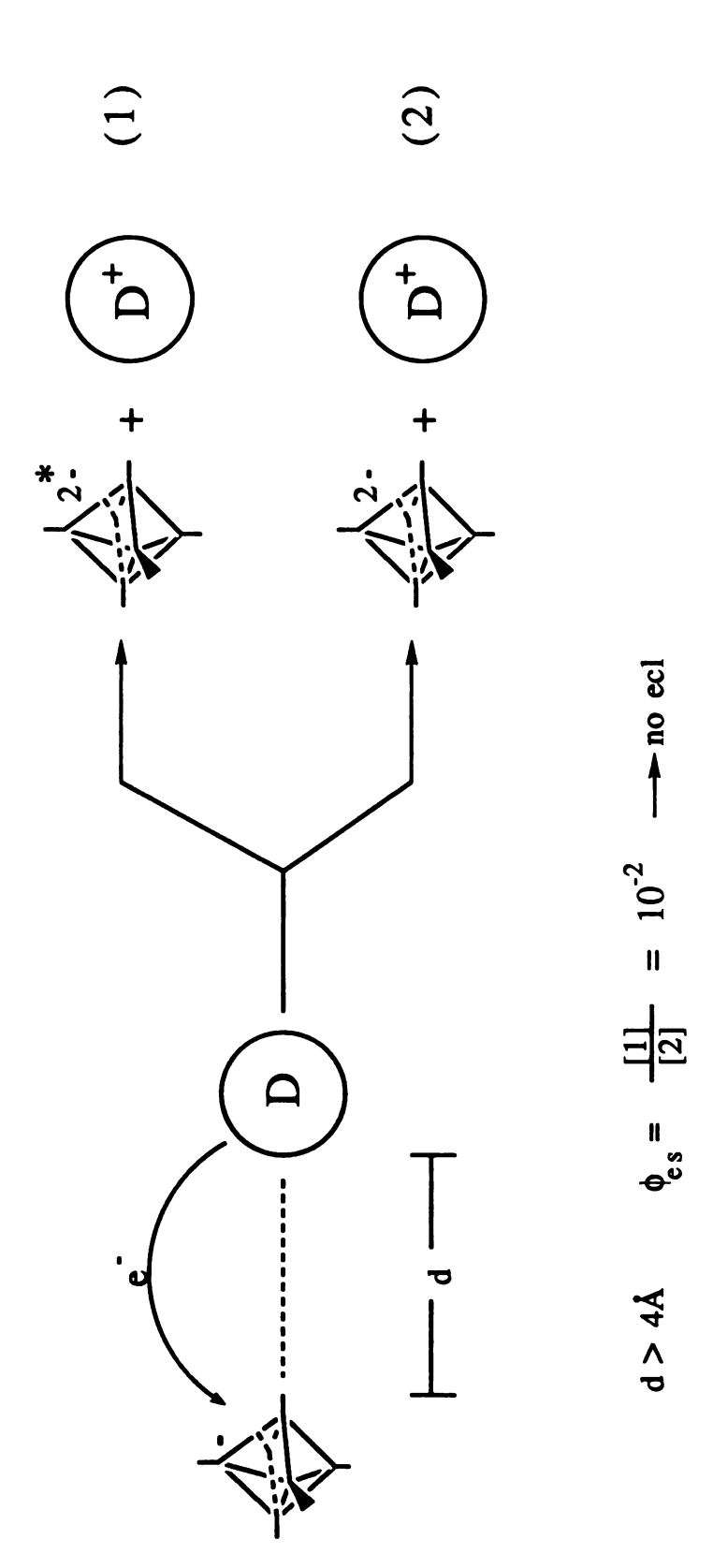


Figure 28

Distance dependence of the differential bimolecular rate constant for the excited-state (es) and ground-state (gs) electron-transfer channels for the reaction between $Mo_6Cl_{14}^-$ and one electron reduced 4-cyano-N-methylpyridinium.

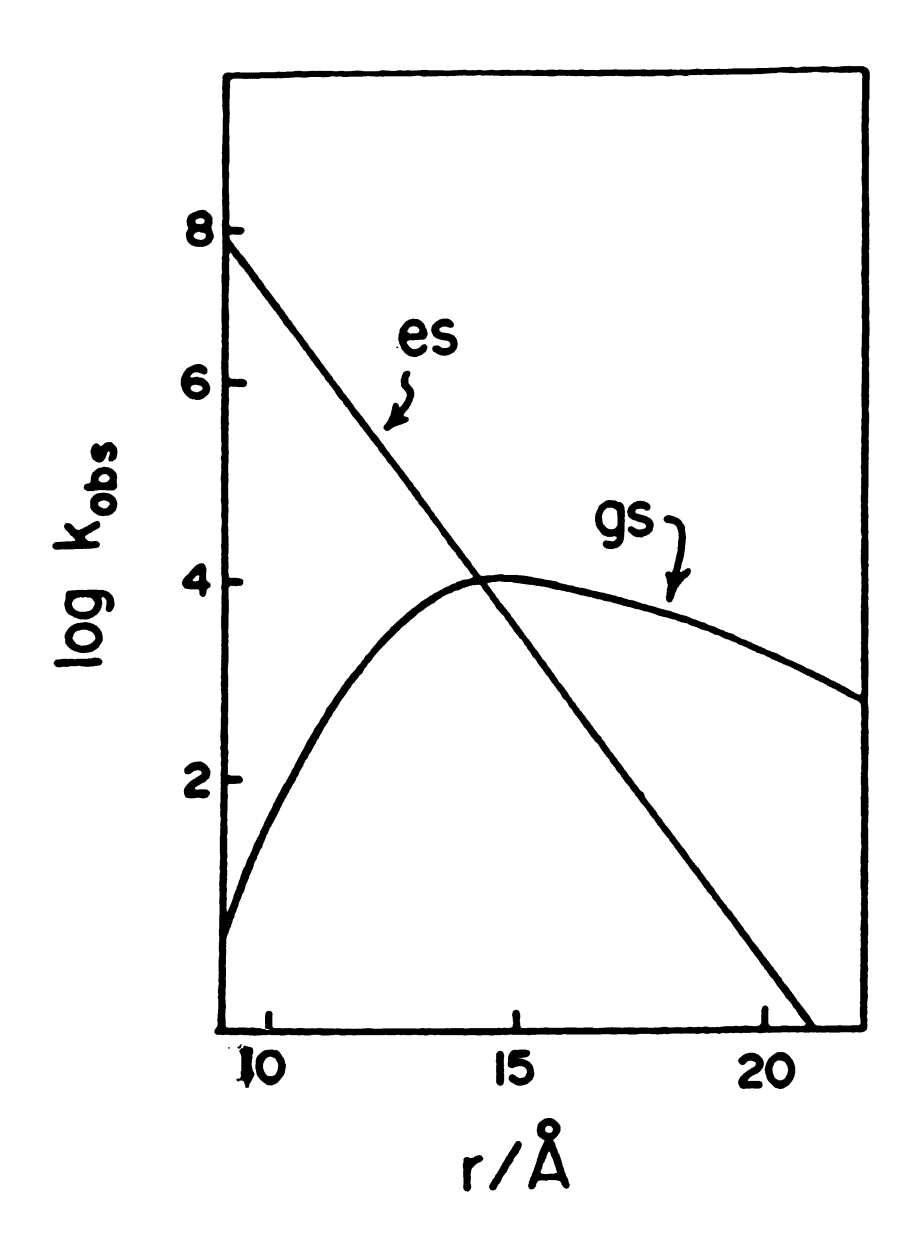


Figure 29

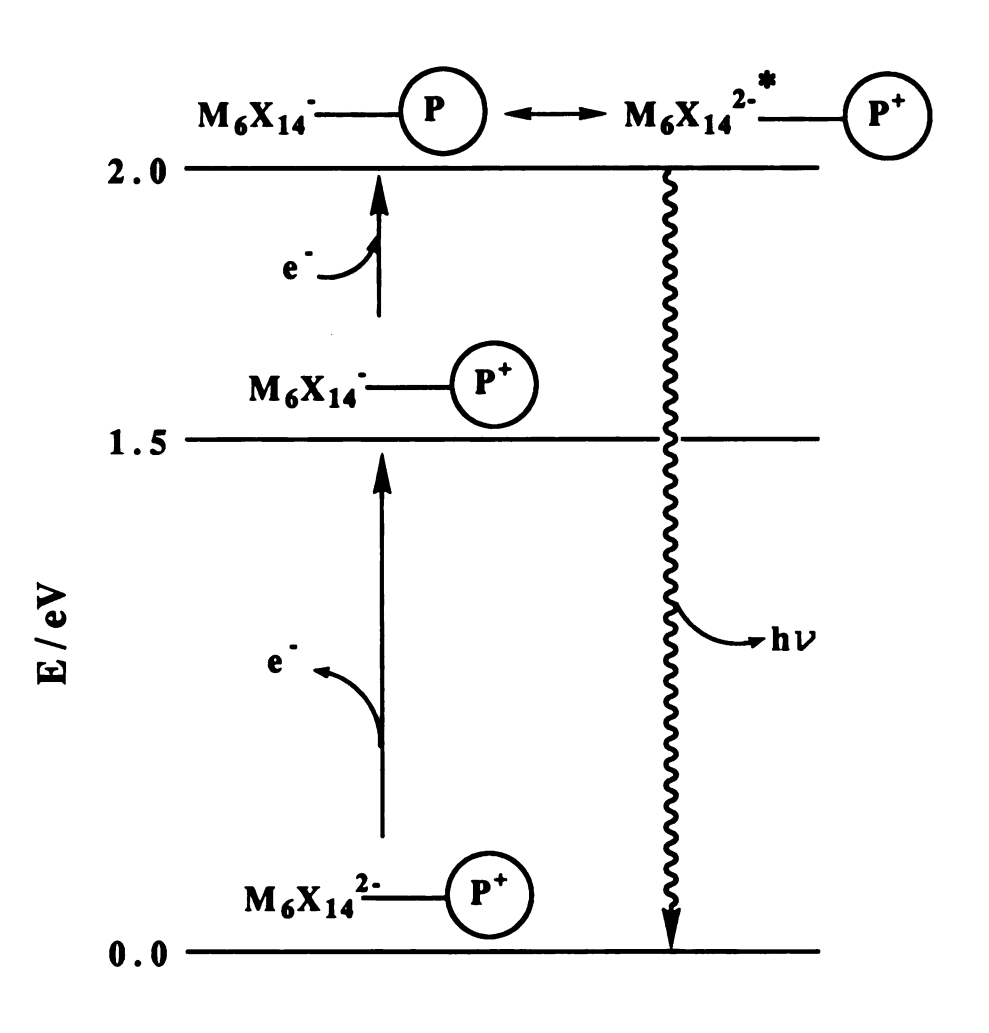
outer sphere reorganizational energy competes with a decrease in rate resulting from attenuated electronic coupling with distance. The net result is that $k_{\rm gs}$ will increase and maximize at electron transfer distances greater than closest contact. In this case reaction to ground state will prevail and low $\Phi_{\rm es}$ will be observed. Significantly, this model predicts unit excited state production efficiencies for annihilation in which the reactant pairs are confined to closest contact during electron transfer.²⁹⁵

Control of the electron transfer distances in ecl reactions may be accomplished in polymer modified microstructures. The ability to obtain ecl from a luminescent inorganic ion, electrostatically bound within a polymer (Nafion®, a sulfonate based polymer) has been established. 296-300 In these systems, ecl is obtained from electron transfer between oxidized Ru(bpy)₃³⁺ and a sacrificial electron donor $C_2O_4^{\ 2}$; the polymer does not participate in the annihilation reaction (Nafion[®] is an insulator). In this regard the ability to produce ecl from covalently linked poly-Ru(vbpy)₃²⁺³⁰¹ and polyvinyl-9,10-diphenylanthracene³⁰² attached to electrodes has been described. These systems however do not exhibit unit excited state production yields even though they are covalently linked and electron transfer can occur between neighbors on the same chain. Presumably the floppiness of the polymer backbone does not fix the neighboring reactant pairs at closest contact and annihilation reactions occur at long distances.

This problem should be overcome by juxtaposing reactants by the formation of a tight ion-pair. This might be achieved by substituting the pyridiniums of Figure 28 with polymer bound pyridinium and bipyridinium ions. One electron reduction of the bipyridinium ion will maintain a favorable electrostatic interaction between negatively charged oxidized cluster and monovalent bipyridinium radical cation. Indeed, addition of bipyridinium cations to solutions containing $Mo_6Cl_{14}^{2-}$ result in the immediate precipitation of an insoluble salt thereby suggesting that polymeric films containing pyridinium and bipyridinium groups attached to electrodes may tightly bind clusters by ion-pair formation.

An ecl reaction scheme for $M_6 X_{14}^{2}$ -/pyridinium bipyridinium systems is shown in Figure 30. The electrode is poised to a value positive enough to oxidize cluster, and then rapidly stepped to a value sufficiently negative to reduce the pyridinium or The resulting electron transfer bipyridinium based polymer. between oxidized cluster and reduced polymer can populate the excited state of the cluster (providing the polymer has a reduction potential of at least -0.64 V vs. SCE) which in turn can emit light. The use of both conducting and insulating polyionic polymers, which electrostatically bind electroactive organic and inorganic ions by ionexchange processes is well established.¹⁻⁶ Typically, the polymeric film is cast onto the electrode and ion exchange is accomplished by soaking the electrode in a dilute solution containing the ion of The electrode is then transferred to a solution containing interest. just electrolyte (actually most investigations have maintained a very low concentration, 10⁻⁵ M of the exchanged ion in the electrolyte prevent reverse ion exchange from occurring) and solution electrochemical studies are performed.

Reaction scheme for generation of excited state M_6X_{14} -cluster upon annihilation of oxidized cluster ion and a one-electron reduced poly-pyridinium based polymer.



 $M_6X_{14}^{2-}$: (M = Mo, W; X = Cl, Br)

P + : (pyridinium or bipyridiniumbased polymer)

Figure 30

Of course the success of controlling electron transfer in $M_6X_{14}^{2}$ /pyridinium or bipyridinium based polymers requires microscopic design of the polymer microstructure. Polymer microstructures have synthetically been tailored to accomplish specific functions. example cobalt tetraphenylporphyrin is known to catalyze the reduction of molecular oxygen to hydrogen peroxide, which makes it The expense and difficulty associated useful in fuel cell schemes. with its preparation stimulated attempts to immobilize small quantities of the porphyrin on electrode surfaces. However, free standing films of the porphyrin do not adhere to the electrode, and when confined within polymers the porphyrin does not communicate with the underlying electrode. This problem was resolved by Buttry and Anson who introduced redox active ions into polymers to shuttle charge between the electrode an isolated redox species.^{262,303} To this end, the polymer microstructure has crudely been manipulated. More precise control of polymer microstructures is seen in Wrighton's use of polymer modified small band-gap semiconductor electrodes to catalyze hydrogen evolution. 304-307 Silicon is modified with a positively charged bipyridinium polymer. Incorporation of PtCl₆²⁻ by ion-exchange and subsequent reduction to Pt^o permits the surface area for electrochemical contact to be increased thereby enhancing the rates for catalytic reduction of water in these microstructures. This procedure for converting polymers into porous been exploited by several other research electrodes has groups. 125,308,309

Perhaps the most specific case of synthetically designing polymer microstructures arises from the possibility of using

polymers as semi-conductors or molecular wires. Many polymers are conductors in their oxidized or reduced states, such as polypyrrole. However, these systems are of limited use because their switching times are several orders of magnitude slower than those of conventional solid state electronics, because the rate limiting step for switching the potential is counterion uptake. This problem has recently been eliminated by synthetic design of a new class of self-doped conducting polymers. These polymers eliminate charge compensation as the rate limiting step by covalently attaching an oppositely charged functional group onto the redox active moiety. Therefore, when the polymer is electrochemically activated, a zwitter-ion results and thus switching times are intrinsically faster.

Presented here are our investigations of the charge transport processes of hexanuclear cluster complexes ion-exchanged into polyionic films. Unit excited state production yields of synthetically designed M₆X₁₄²-/poly- pyridinium or bipyridinium based polymeric microstructures might be attained if the cluster ion is completely immobilized at the polymer redox site. The mechanism for ecl with the oxidized cluster/reduced pyridinium based polymer systems, (Figure 30) requires rapidly stepping the electrode potential past their respective redox couples resulting in electron transfer between This scheme operates well if the charge propagation reactant pairs. rates for cluster ions and polymer redox sites are equal. this will only occur if their rate limiting steps are the same (i.e. motions of the polymer backbone or counter-ion movement). potential problem with unequal propagation rates is demonstrated here, in a typical experiment the electrode is first biased to an oxidizing potential generating M_6X_{14} then rapidly switched to a negative enough potential to produce reduced polymer, although this potential can also reduce M_6X_{14} back to $M_6X_{14}^{2-}$. Therefore, if the charge propagation rate of the cluster is significantly faster then for the polymer the cluster will be reduced by the electrode and not by the polymer. This could be avoided by reducing the polymer first, (this scenario could be reversed with the polymer charge propagation rate being faster than the cluster). Thus a complete understanding of the mechanisms of charge transport within these films is required in order to establish that tight binding is occurring in these systems and that the appropriate annihilation reaction be established for ecl chemistry.

B. Results and Discussion

1. PVP+Me Polymer Modified Films

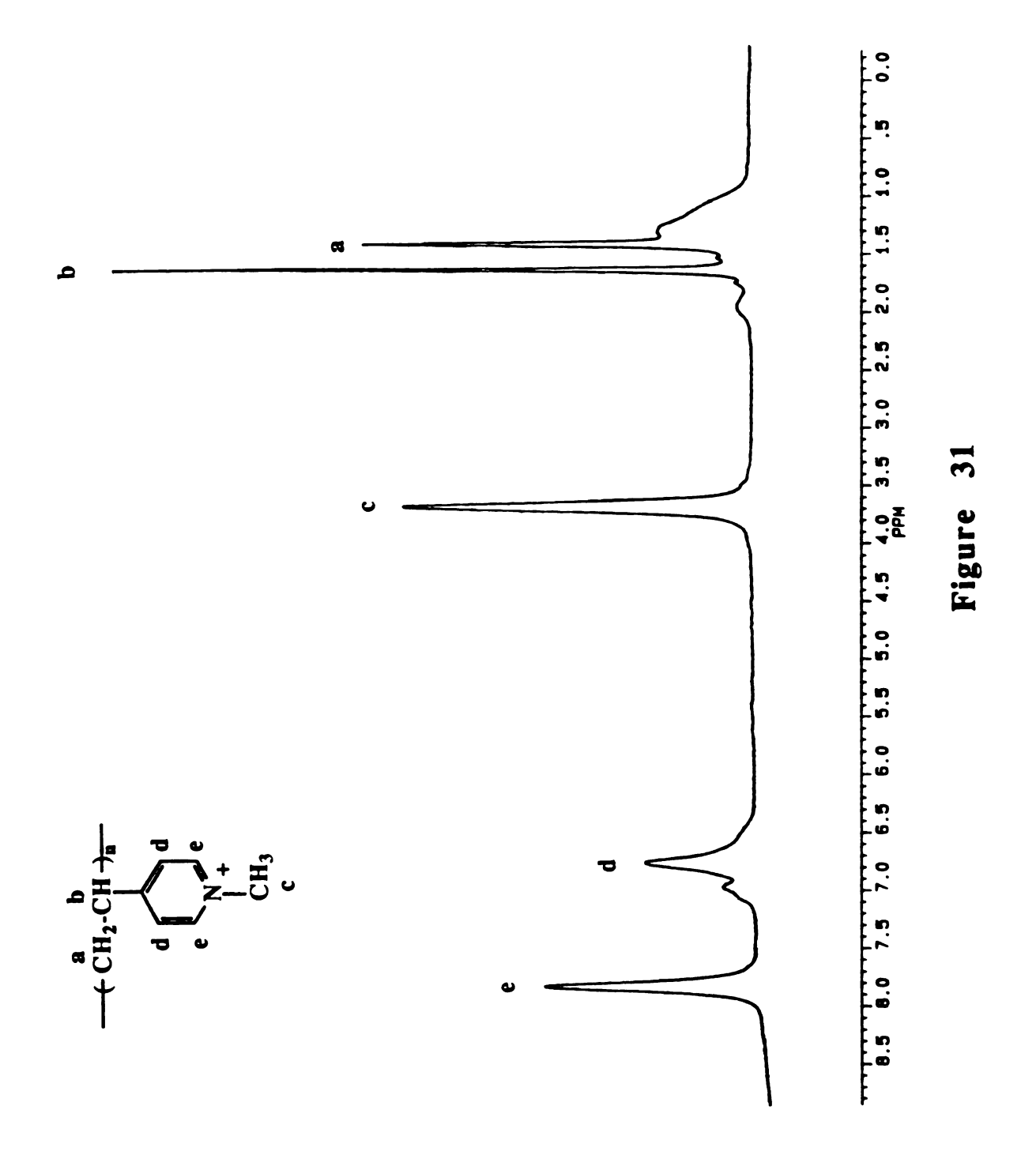
Polyvinylpyridine (PVP) coordinates inorganic metal complexes 107,174,182,224 and in acidic solutions electrostatically binds multicharged inorganic anions. $^{313-316}$ In addition to protonation the nitrogen of the PVP moiety is easily quaternized with alkyl halides. $^{147,317-319}$ Quaternized PVP is ideal for our studies because the polymer will retain it's positive charge in nonaqueous solvents. Furthermore, an ion-pair can be formed between the $M_6X_{14}^{2-}$ ion and two quaternized PVP units. Prior attempts to incorporate negative ions into these films in acetonitrile have failed. 147 Interestingly we have found that by choosing appropriate experimental conditions,

negative ions can be exchanged into these films and the immobilized anions display electrochemical activity.

Initial investigations utilized N-methyl-4-polyvinylpyridinium (PVP+Me), 1 as the polymer backbone. The NMR spectrum of (PVP-Me)PF₆ prepared as described in Section II.A.2.b in CD₃CN is shown in Figure 31. The peak assignments are δ (peak shape, number of protons from integration): 7.8(b, 2H), 6.5-7.0(b, 2H), 3.6(b, 3H), 1.6(s, 2H), 1.3(b, -). A contaminant present at 1.1-1.2 ppm, prohibits the accurate integration of the peak at 1.3 ppm and cannot be eliminated, even after three recrystallizations of PVP+Me. Although it's origin is unclear, this impurity is electrochemically inert. The bump at 1.93 ppm is from the solvent and is used as the reference peak. The broadness of these peaks is common for polymers and is the result of dipolar broadening from neighboring protons.³²⁰

Although any $M_6X_{14}^{2-}$ (M = Mo, W and X = Cl, Br) cluster ion can be ion-exchanged into PVP⁺—Me, $W_6Br_{14}^{2-}$ was employed as the probe ion of choice for the charge transport characterization because $W_6Br_{14}^{2-}$ possesses an easily accessed, reversible oxidation couple $E_{1/2}$ ($W_6Br_{14}^{-/2-}$ = +0.98 V vs. SCE in acetonitrile). Films were prepared by droplet evaporation of a methanol solution containing 1.3 % of (PVP—Me)PF₆ (cluster does not incorporate if the films are cast from aqueous solutions) on platinum or glassy carbon electrodes. Modified electrodes were soaked in a acetonitrile solution containing 2.0 mM $W_6Br_{14}^{2-}$ followed by several washings with acetonitrile. If the surface coverage of the polymer is less than 1 x 10⁻⁶ moles/cm², the cluster completely leaches from the film within several cyclic voltammetric scans. However, thicker films retain $W_6Br_{14}^{2-}$ for over

A 250 MHz NMR spectrum of N-methylpolyvinylpyridinium hexafluorophosphate in CD_3CN .



24 hours of continuous soaking in acetonitrile. In the following studies platinum electrodes were employed although glassy carbon also work as well.

Figure 32 shows the cyclic voltammograms of $W_6 Br_{14}^{\ 2}$ in acetonitrile containing 0.2 M TBAPF₆, PVP+Me film adsorbed on platinum with a surface coverage of 2.2 x 10⁻⁶ mol/cm², and an ionexchanged W₆Br₁₄²-/PVP⁺-Me film. For the native film two chemically irreversible waves appear at -1.31 V and -1.45 V vs. SCE attributable to multiple E^o values for the reduction of pyridiniums in different microenviornments. The irreversibility of these waves may arise from dimerization of PVP rings in the 2-position upon reduction; the dimerization of a monolayer of N-methyl-2polyvinylpyridinium is known to occur in the four position at a potential of -1.32 V vs. SCE.87 The reduction waves, which persist for several scans, correspond to activation of only 0.5 % of the pyridinium sites in the polymer as determined by coulometry. Limited electrochemical response from these films is a signature of poor swelling of the polymer by acetonitrile producing an energy barrier for electron hopping. The polymer reduction waves are attenuated and broadened upon incorporation of W₆Br₁₄²- into the film. Moreover, both of these observations are consistent with ionpairing in the polymer film. For the latter a tighter ion-pair between PVP+ Me and W₆Br₁₄² as opposed to PF₆ results in stiffening of the polymer chains, which restricts the polymer motions required for site-to-site electron hopping. The enhanced decay of the polymer response upon incorporation of cluster is consistent with the cluster

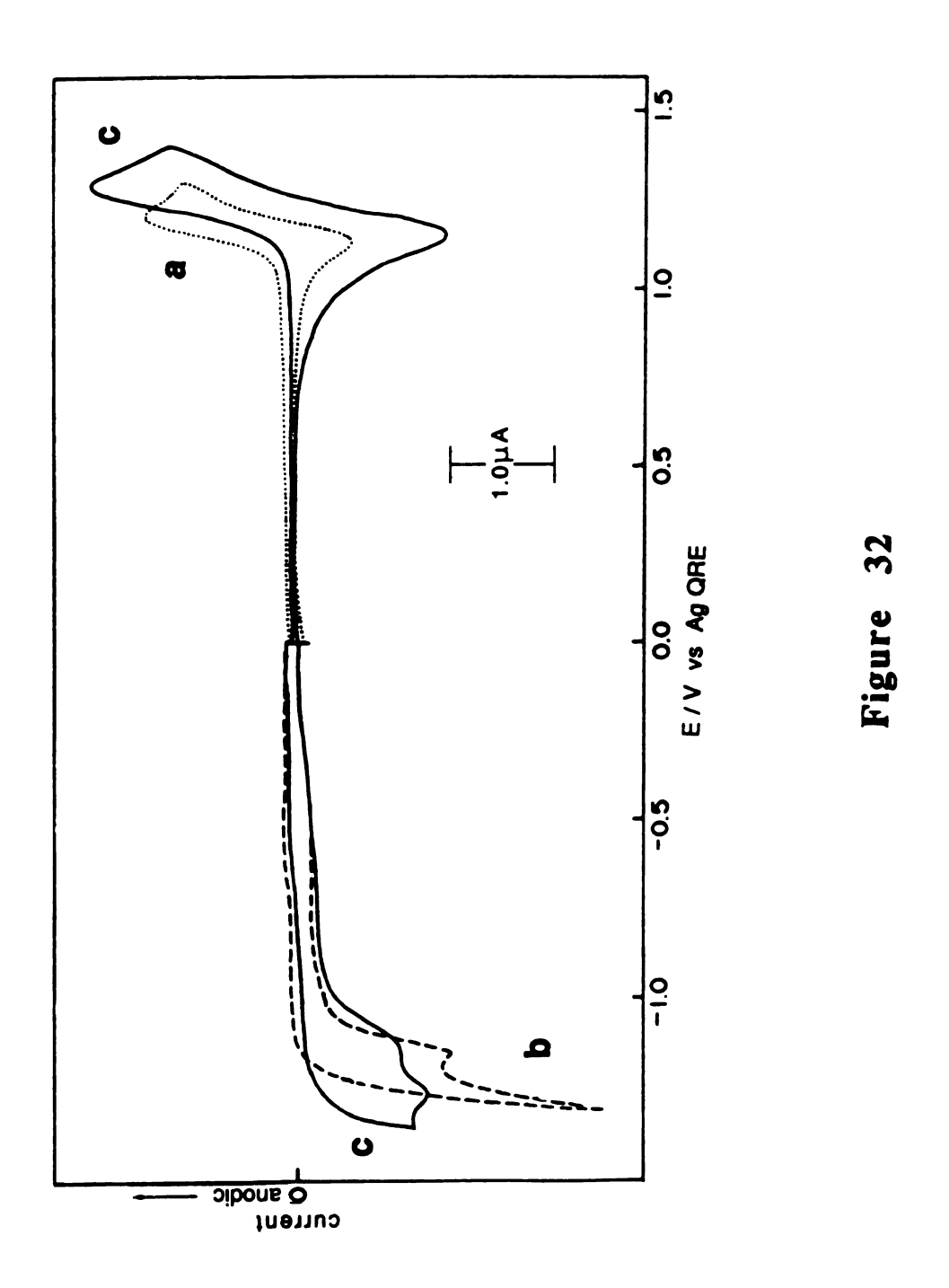
anion bringing two pyridinium sites together, thereby facilitating dimerization in the polymer.

The reversible oxidation of the W₆Br₁₄²- ion is preserved in PVP $^+$ Me films. A measured $E^{o}_{1/2} = +1.05$ V (Figure 32c) is shifted 60 mV positive to the value observed at the bare electrode (Figure This shift is expected on the basis of simple ion-pair considerations. The binding of the cluster anions to the positively charged polymer will stabilize the negative charge of the cluster making it thermodynamically more difficult to oxidize. The oxidation wave of W₆Br₁₄²- displays diffusional behavior (diffusional tail). A peak separation ($\Delta E = 130 \text{ mV}$) greater than the expected 59 mV is probably due to uncompensated film resistance because increasing the electrolyte concentration is accompanied by a resultant decrease Further support for diffusional behavior is provided by the linear relationship between the cyclic voltammetric peak current ip and the square root of the scan rate $v^{1/2}$ (Figure 33). The amount of electroactive W₆Br₁₄²-, determined by coulometry, corresponds to a 15 % loading (assuming 93 % of the pyridinium sites are methylated as determined by NMR spectroscopy). The concentration of electroactive W₆Br₁₄² (mol/L) in the film C_{cluster} can be determined bу

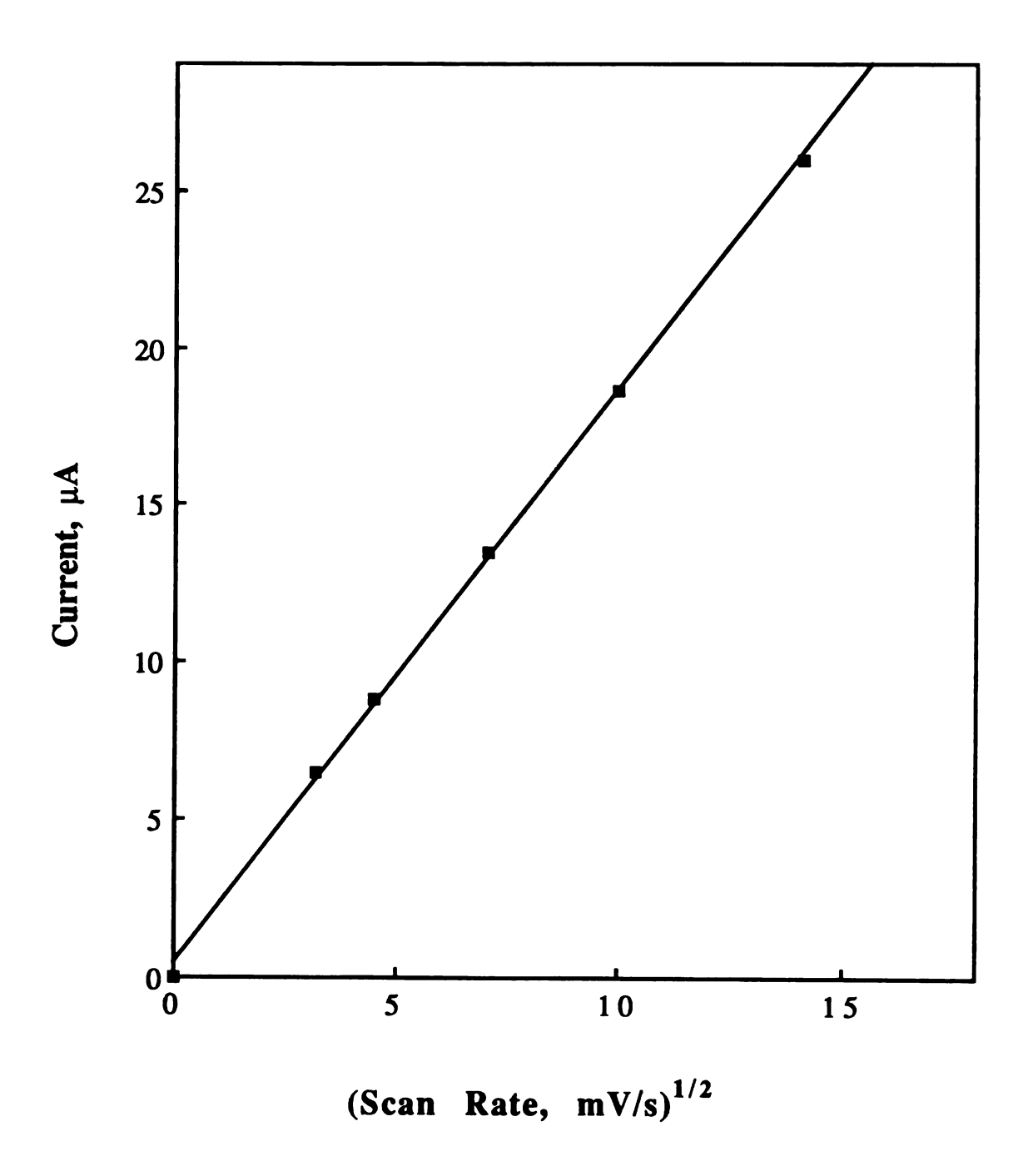
$$C_{\text{cluster}} = \frac{Q_{\text{cluster}} \rho 10^3}{F(\text{wt}_{\text{polymer}})}$$
 (16)

where $Q_{cluster}$ is the coulombs of $W_6Br_{14}^{2-}$ determined by coulometry, ρ is polymer density (g/cm³), F is Faraday's constant,

Cyclic voltammograms of: (a) $W_6Br_{14}^{2-}$ dissolved in acetonitrile containing 0.2 M TBAPF₆ at a bare platinum electrode; (b) a PVP⁺—Me film with a surface coverage = 2.2 x 10^{-6} mol/cm² absorbed onto a platinum electrode immersed in an acetonitrile solution containing 0.2 M TBAPF₆; and (c) a PVP⁺—Me film ion-exchanged with $W_6Br_{14}^{2-}$ immersed in an acetonitrile solution containing 0.2 M TBAPF₆.



A plot of peak height $i_{p,a}$ (μA) vs. the scan rate (mV/s) for the anodic wave of the CV reproduced in Figure 32c.



Fugure 33

and wtpolymer is the weight (g) of PVP+Me deposited onto the electrode. A polymer density of 0.91 ± 0.02 g/cm³ was determined by dissolving a known quantity of polymer into a known volume of acetonitrile and accurately measuring the volume change. A density of = 1.0 g/cm³ was independently determined by dividing the film surface coverage mol/cm² by the film thickness (the thickness determined by profilometry is equal to 5.6 µm). However, because the film must be dry for profilometry measurements, the density measurement of 0.91 g/cm³ is deemed more accurate. interesting to note that the density determined by using the dry film thickness corresponds to a 15 % error due to swelling effects, which is in good agreement with other polymeric systems studied.^{220,321} On the basis of 0.91 g/cm³, a maximum cluster concentration of 0.70 M is calculated from eq 16. This value falls into the 0.1-5.0 M range calculated for most polymeric films containing redox ions. 1 During the characterization of W₆Br₁₄²-/PVP+-Me films it was noticed that upon cycling the potential, the peak current for the W₆Br₁₄² wave decreases in a regular manner. The decrease in the peak current is more pronounced at slower scan rates. However, if the electrode was soaked without cycling for extended lengths of time, for a given scan rate, much smaller attenuation was observed. Thus scanning the film promotes a loss in electroactivity, and this loss is most prominent at slow scan rates. Possibly cluster ion in the dianion form binds tightly in the film whereas the monoanion diffuses freely, exits the film, and is lost to bulk solution. This mechanism would require a corresponding uptake of anions from the electrolyte and therefore, should be affected by electrolyte concentration. Although, increasing

th of

the concentration of electrolyte did not dramatically perturb the loss of electroactivity of the film, an additional attenuation of 10 % was observed when the TBAPF₆ concentration was increased from 0.2 M to 0.8 M. By taking into account the fact that increased electrolyte concentrations also increase the leaching rate without cycling the potential, an effective increase in rate of cluster departure from the film upon oxidation in a 0.8 M TBAPF₆ solution is 8 %. Interestingly Mortimer and Anson³²¹ observed the opposite behavior, for the 2-/3- and 3-/4- reductions of inorganic ions exchanged into bipyridinium films in aqueous solutions. In their case, the more negatively charged ion leached from the film. They attribute this behavior to the necessity of maintaining charge neutrality within the This explanation does not apply here because the oxidation of the cluster would induce cluster anion uptake and not its ejection. Moreover, in Mortimer and Anson's study the redox couples were polyionic in both oxidized and reduced forms and thus can electrostatically crosslink the polymer in either form. Differences in electrostatic interactions, therefore, should not perturb the polymer significantly upon oxidation or reduction. In these investigations, the monoanion W₆Br₁₄ can not electrostatically crosslink the polymer and therefore unlike it's polyanion W₆Br₁₄²-counterpart will not have the effect of crosslinking to hinder its diffusion from the film.

The electrostatic binding of the cluster ions within PVP^{+} —Me will be reflected in the diffusion coefficients of $W_6Br_{14}^{2-}$ and $W_6Br_{14}^{-}$. Before these values can be determined for $W_6Br_{14}^{2-}$ in a polymer matrix swelled by acetonitrile, the diffusion coefficient of $W_6Br_{14}^{2-}$ in acetonitrile at a bare electrode needs to be determined.

Un in

et ic

e

1

Unfortunately very few determinations of diffusion coefficients for inorganic ions in nonaqueous solutions have been reported. et al. have demonstrated that diffusion coefficients of many organic ions determined by chronoamperometry in low viscosity solvents are inaccurate.^{225,323} Errors in the value of n_T (the apparent number of electrons transferred considering slow kinetics), undetermined side reactions with impurities, and film formation on the electrode surface are all causes for the anomalous measurements of diffusion coefficients of organic ions. Although these problems do not exist in most inorganic studies, diffusion coefficients of inorganic ions in nonaqueous solvents vary significantly with methodology of For example reported diffusion coefficients for ferrocene determined in acetonitrile varies from 7.0×10^{-6} to 2.4×10^{-6} 10^{-5} cm²/s.³²⁴⁻³²⁶ Thus it is instructive to examine the diffusion coefficients obtained for W₆Br₁₄²- in acetonitrile by several different techniques.

$$\tau^{1/2} = \frac{nFAD^{1/2}\pi^{1/2}C^*}{2i}$$
 (17)

where τ (s) is the transition time (the amount of time required for the concentration C^* of redox material to drop to zero at the

electrode) resulting from the application of a constant applied current i (amps) to the electrode. The slope of the line obtained by plots of τ at different applied currents directly yields D. Finally, rotating disc voltammetry is a very accurate technique for determining diffusion coefficients. The limiting current i_1 (amps) is related to $D^{2/3}$ by the Levich equation

$$i_1 = \frac{0.620 \text{ nFAD}^{2/3} \omega^{1/2} C^*}{12^{1/6}}$$
 (18)

where ω is the angular rotation rate (s), and ν the kinematic viscosity (cm²/s, for acetonitrile ν is equal to 4.67 cm²/s at 25 ^oC).³²⁷ Plots of the i(t) vs. $t^{1/2}$, i_p vs. $v^{1/2}$, $\tau^{1/2}$ vs. 1/i, and i_l vs. $\omega^{1/2}$ were linear with correlation coefficients of at least 0.9998. The diffusion coefficients obtained for W₆Br₁₄²- in acetonitrile by these different techniques are summarized in Table 10. The values are in good agreement with each other with an average value of 10.1 ± 0.9 x 10⁻⁶ cm²/s. Of these techniques, cyclic voltammetry is believed to be the least reliable because the value of the Randles-Sevcik constant depends on the electrode and varies between 2.52 - 2.72 x 10⁵, errors in the diffusion coefficient as high as 16 % can result. Chronopotentiometry suffers from large double layer charging effects resulting from continual change in potential and the large potential steps required in chronoamperometry causes significant transient perturbations. Rotating disc voltammetry is reliable because large potential or current steps are not required, steady state is achieved very rapidly, and most importantly the Levich equation is rigorously

Table~10 $Diffusion~Coefficients~of~W_6 Br_{14}^{~2-}~in~Acetonitrile$ Determined~by~Different~Electrochemical~Techniques.

Concentration of W ₆ Br ₁₄ ²⁻ (m M)	Electrochemical Technique	Diffusion Coeff. x 10 ⁶ (cm ² /s)
2.26	Cyclic Voltammetry	8.9
3.17	Cyclic Voltammetry	9.0
1.02	Rotating Disc Voltammetr	y 9.4
3.34	Chronoamperometry	10.2
2.80	Chronopotentiometry	11.9

derived from hydrodynamics; diffusion coefficients can be determined to \pm 1 %. Therefore, we believe the diffusion coefficient of 9.4 x 10^{-6} cm²/s obtained from rotating disc experiments to be the most dependable measurement of $W_6Br_{14}^{2-}$ in PVP⁺—Me. This value agrees very well with the diffusion coefficients measured for $Fe(bpy)_3^{2+}$ (D = 1.10 x 10^{-5} cm²/s) and $Fe(phen)_3^{2+}$ (D = 1.08 x 10^{-5} cm²/s) in acetonitrile.³²⁷ Both $W_6Br_{14}^{2-}$ and $Fe(L)_3^{2+}$ ions have charges z = 2, and similar ionic diameters $d(Fe(bpy)_3^{2+} = 10.5 \text{ Å}$, $d(Fe(phen)_3^{2+}) = 10.8 \text{ Å}$, and $d(W_6Br_{14}^{2-}) = 12.0 \text{ Å}$. Thus similar diffusion coefficients for these systems is expected with the larger size of the cluster explaining it's slightly slower diffusion.

apparent diffusion coefficient D_{app} for W₆Br₁₄² electrostatically bound within PVP+Me can be determined most easily by chronoamperometry using the Cottrell equation (eq 10) providing the film thickness and quantity of cluster inside the polymer are known. The film thickness was determined from the above mentioned density measurements, and the amount of exchanged cluster was determined by coulometry. The calculated D_{app} for $W_6Br_{14}^{2-}$ is 9.1 x 10^{-9} cm²/s. The diffusion coefficient for W₆Br₁₄ is provided by reverse step chronoamperometry. This technique involves the application of a potential step to the mass controlled region for a known amount of time, τ (s), and then the electrode potential is stepped back to zero. For reversible reactions the diffusion coefficient can be determined by the relation,

$$i_{r}(t) = \frac{nFAD^{1/2}C^{*}}{\pi^{1/2}} \left(\frac{1}{(t-\tau)^{1/2}} - \frac{1}{t^{1/2}} \right)$$
 (19)

and is found to be 1.8 x 10^{-8} cm²/s for W₆Br₁₄. This value is more than twice that obtained for W₆Br₁₄² in the polymer film and provides strong evidence in support of the prediction that the W₆Br₁₄² cluster is bound more tightly than W₆Br₁₄ in the film.

Substitution of the measured diffusion coefficient and the PVP film thickness into eq 4 (Section I) permits the approximate amount of time required for the W₆Br₁₄ to reach the outer edge of the polymer film to be assessed. For D = 1.8 x 10^{-8} cm²/s and d = 5.6 μ m a value of 8.7 s is obtained. In other terms, if the potential of the electrode is stepped to a oxidizing enough value to ensure mass transfer controlled diffusion, a significant loss of redox material should occur at 8.7 seconds. Although cluster is always leaching from the film, the leaching process levels off once the loading of the film reaches approximately 4 %. At this value, cluster exits the film very slowly, unless the potential is cycled. A plot of the the amount of material lost (as determined by coulometry) when the potential of the electrode is stepped to +1.2 V for increasing times is shown in Figure 34. The transition time of ~ 12 s agrees surprisingly well with the predicted value of 8.7 s when one considers the errors associated in determination of the film thickness. For example, assuming that swelling of the film increases the thickness by 15 %, the predicted transition time would increase to 11.5 seconds. Thus, $W_6Br_{14}^{2}$ is bound strongly whereas W₆Br₁₄ can freely diffuse and exit the film, resulting in attenuated currents.

The rate of $W_6Br_{14}^{2-}$ ion departure from an PVP+Me film on a platinum electrode after potential steps to +1.3 V vs. SCE for increasing times.

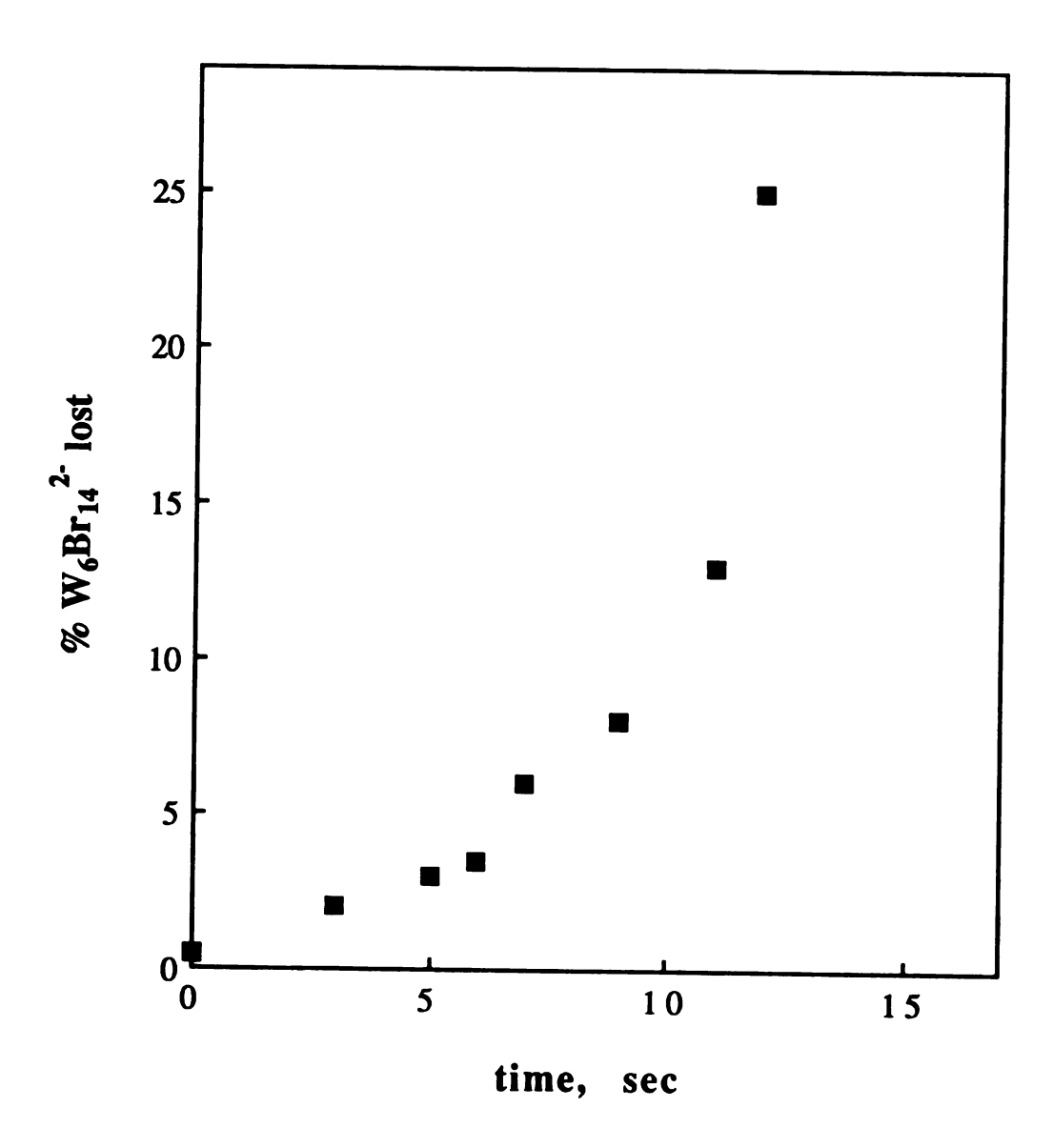


Figure 34

2. PQ2+ Polymer Modified Films

Cluster ions can be incorporated into PVP $^+$ —Me polymers and undergo electron transfer with the underlying electrode. However, the original goal of a tight ion-pair is not achieved. The favorable binding of $W_6Br_{14}^{2-}$ within the polymeric support is vitiated upon cluster oxidation. The measured diffusion coefficients and time traversal studies clearly establish a freely diffusing $W_6Br_{14}^{-}$ ion within the PVP $^+$ —Me microstructure. A tighter binding of the cluster in it's oxidized form might be achieved by utilizing a polymer with more highly localized positive charge density. Accordingly, the 4,4'-bipyridinium based polymer, N,N'-bis[-3-(trimethoxysilyl)propyl]-4,4'-bipyridinium, (PQ^{2+}) , 2, first developed by Bookbinder and Wrighton, 328 was investigated.

The NMR spectrum of PQ^{2+} prepared as described in Section II.A.2.c in D_2O is shown in Figure 35. The peak assignments are δ (peak shape, number of protons from integration, coupling constants): 9.17(4H, d, J = 7 Hz), 8.61(4H, D, J = 7 Hz), 4.77(4H, t, J = 7 Hz), 3.36(18H, s), 2.24(4H, q, J = 7 Hz), 0.84(4H, t, J = 7 Hz). Polymeric films were prepared by electrochemically depositing monomeric PQ^{2+} onto platinum oxide and tin oxide electrodes (Section II.B.2).

The cyclic voltammogram of PQ^{2+} (surface coverage 5.2 x 10^{-9} mol/cm²) in an acetonitrile solution containing 0.2 M LiClO₄ is given in Figure 36a. Two waves corresponding to the consecutive one-electron reductions of the PQ^{2+} to PQ^{+} to PQ^{0} are observed. A $\Delta E_p = 28$ mV and FWHM for both $E_{p,c}$ and $E_{p,a} = 90$ mV for the $PQ^{2+/+}$ wave is clearly indicative of thin cell behavior. However, this

A 250 MHz NMR spectrum of N, N - b is [-3-(trimethoxysilyl)propyl]-4,4'-bipyridinium diiodide in D_2O .

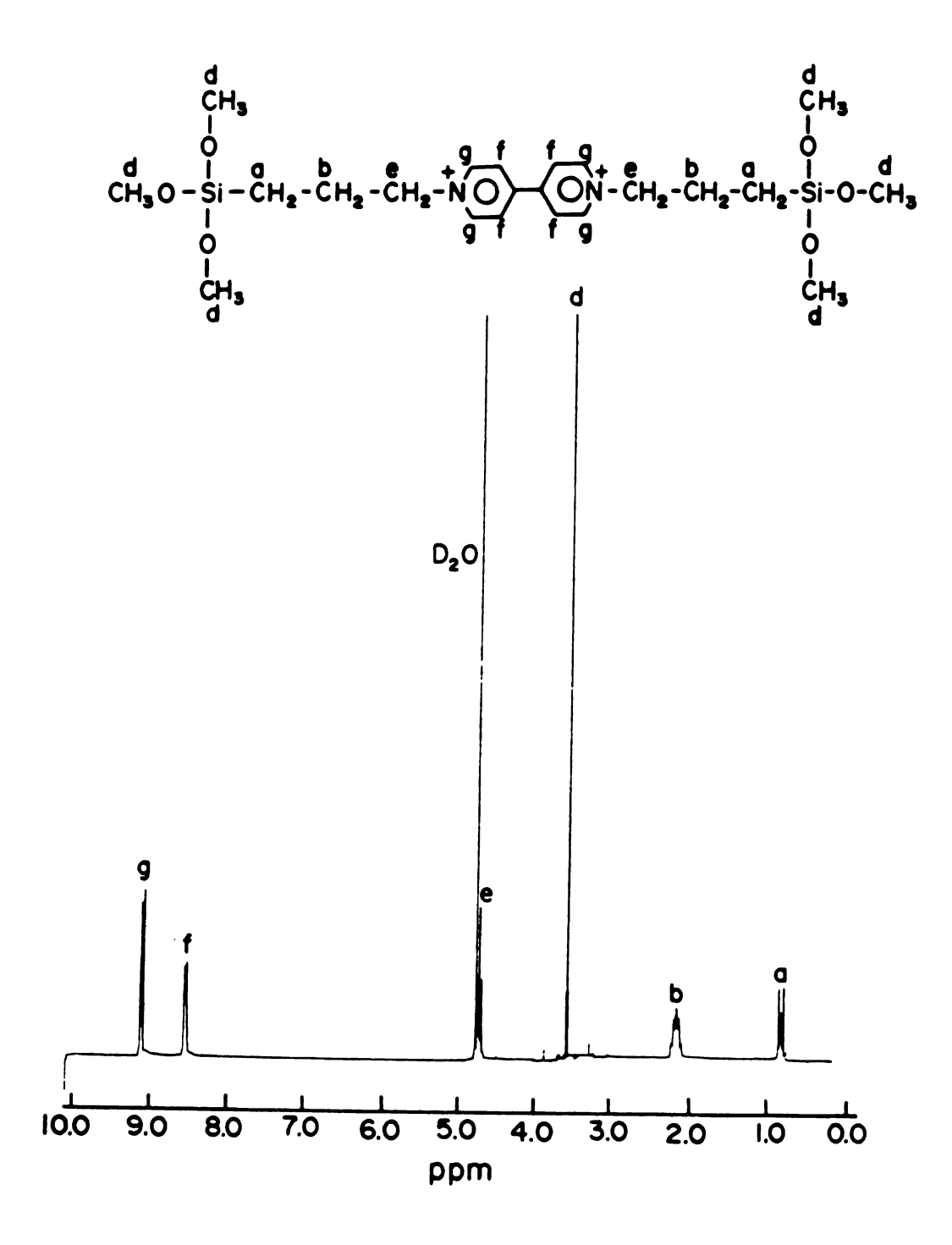
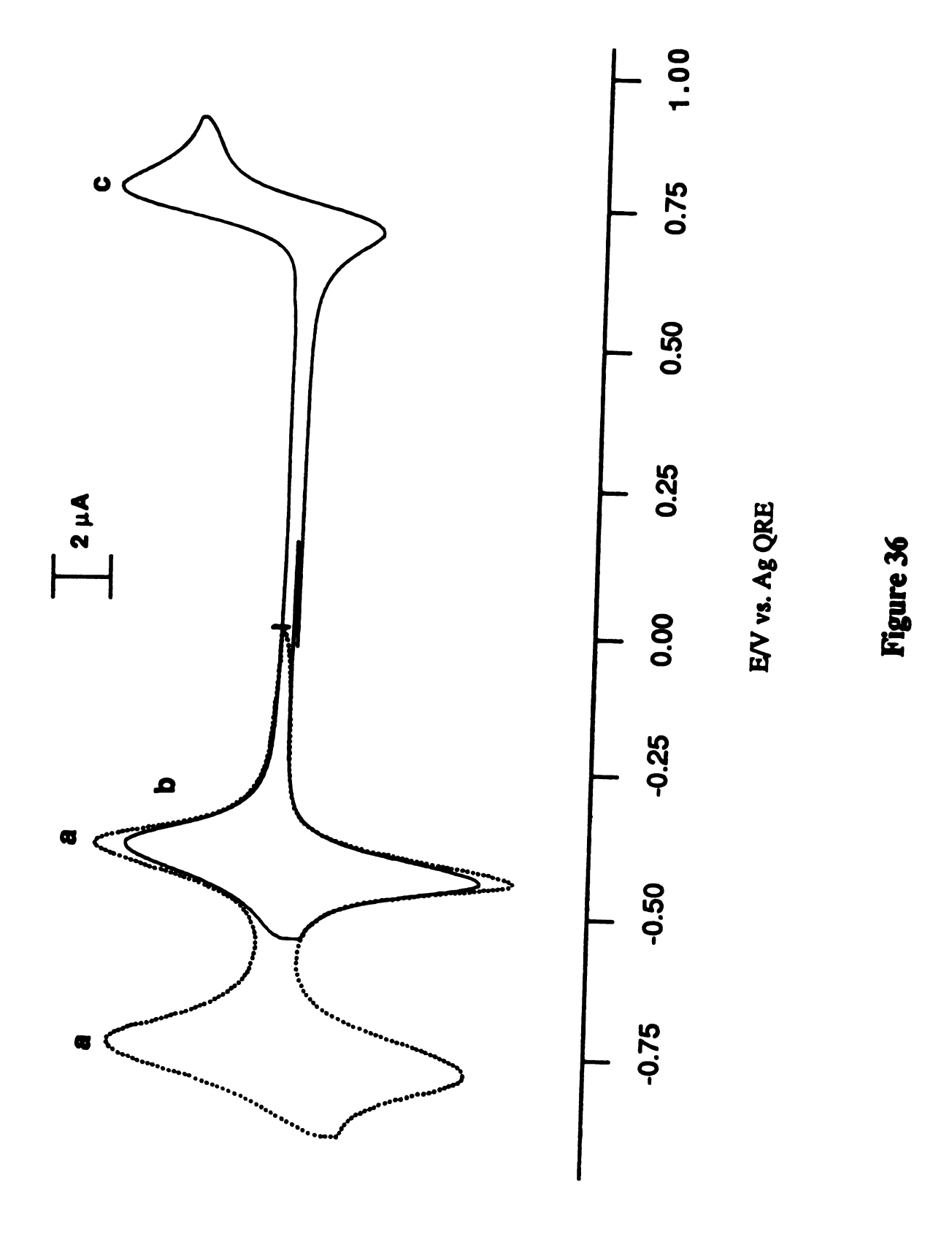


Figure 35

Cyclic voltammograms of a platinum oxide electrode modified with a PQ^{2+} film (surface coverage = 5.2 x 10^{-9} mol/cm²) immersed in an acetonitrile solution containing 0.2 M LiClO₄ upon scanning the potential: (a) past the one electron reduction waves of PQ^{2+} ; (b) past the one electron reduction waves of PQ^{2+} after addition of 50 μ M $W_6Br_{14}^{2-}$ to the acetonitrile solution; and (c) past the oxidation of $W_6Br_{14}^{2-}$ after incorporation of the cluster ion into the PQ^{2+} film.



behavior is not observed when the film is transferred to a solution containing 75 μ M $W_6Br_{14}^{2-}$. As shown in Figure 36b, ΔE_p increases to 45 mV and the FWHM of anodic component of the wave increases to 140 mV but the 90 mV FWHM cathodic component of the wave is preserved. The increased peak separation is expected for tighter ion-pairing of the polymer with the cluster than with the supporting electrolyte ClO_4^{-} . The unusual behavior of the FWHM values for the anodic and cathodic components of the reduction wave are most probably related to the microstructure. The wave for the $W_6Br_{14}^{-/2-}$ couple is diffusional in shape and behavior (Figure 36c), with a peak separation ΔE_p of 75 mV and peak current directly proportional to the square root of the scan rate.

No electrochemical responses from incorporated cluster was observed if the film coverages of PQ²⁺ were greater then 1.5 x 10⁻⁸ mol/cm². This is in direct contrast to PVP polymeric films, which require thick films for prolonged electrochemical responses. The difference between the two systems is believed to originate from the much tighter binding of the cluster in PQ²⁺ polymer films which will be manifested in a more rigid polymer network. Thus PQ²⁺ films in a 0.2 M LiClO₄ acetonitrile solution with a coverage of 1.5 x 10⁻⁸ mol/cm² display reversible thin cell behavior. However addition of 50 µM W₆Br₁₄²⁻ to the contacting acetonitrile solution shuts down the current due to polymer reduction after four potential scans (Figure 37). Therefore, investigations of charge transport of anions exchanged into PQ²⁺ polymer films from acetonitrile must utilize thin films.

The first four consecutive cyclic voltammograms of a PQ^{2+} film attached to a platinum oxide electrode (surface coverage = 1.5 x 10^{-8} mol/cm²) placed into an acetonitrile solution containing 0.2 M LiClO₄ and 5 μ M W₆Br₁₄²⁻.

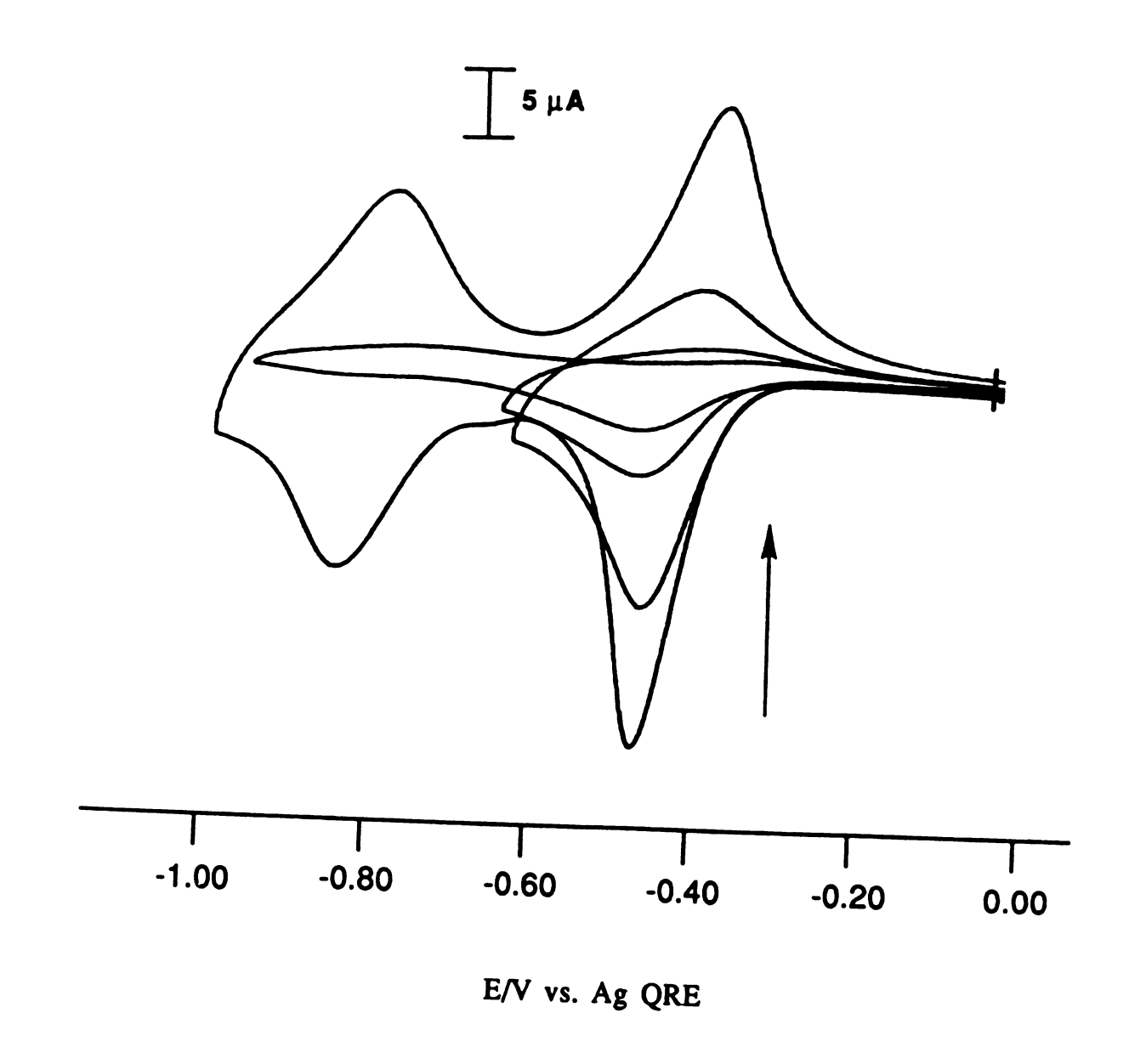


Figure 37

The electrochemistry of PQ2+ films has been studied extensively in both aqueous and nonaqueous solutions. 133,134,220,306-308,,322,328-331 However, to our knowledge the diffusion coefficient for charge propagation (D_{ct}) for PQ²⁺ films in nonaqueous solvents have not been reported. This value can be calculated using the Cottrell equation (eq 10) providing the area of the electrode, surface coverage Γ (mol/cm²), and film thickness are known. The surface area of PtO electrodes measured by electrochemical techniques are slightly larger than the areas calculated from physical dimensions of the electrode. For example, the PtO electrodes have a measured area of 0.020 cm², while the electrochemically determined area using Fe(CN)₆⁴- as the standard is 0.028 cm²; for the latter, the surface coverage was determined by dividing the coulombs under the reduction wave by both Faraday's constant and the electrochemically determined area of the electrode (the common practice in the literature, when this procedure is used, is to report the surface coverage as Γ_{corr} where corr stands for corrected value). thickness values were determined by profilometry. The D_{ct} for the reduction of PQ²⁺ by chronoamperometry could not be determined because potential steps large enough to overcome resistive effects could not be achieved. Therefore, the potential was initially stepped past the reduction wave for several seconds to ensure complete reduction of the film, and after the potential was stepped back to zero volts the current response as a function of time was measured. The charge transfer diffusion rates D_{ct} for PQ²⁺ were determined for films immersed in acetonitrile solutions containing 1.0 M LiClO₄ as described in Section II.B.4. The average diffusion coefficient D_{ct} of $6.3 \pm 0.4 \times 10^{-11} \text{ cm}^2/\text{s}$ was obtained from three independent measurements of films ranging in coverages Γ_{corr} from 9.2×10^{-9} to $1.2 \times 10^{-8} \text{ cm}^2/\text{s}$ in acetonitrile. The D_{ct} for PQ^{2+} obtained in aqueous solutions containing 1.0 M LiClO₄ is $11.0 \times 10^{-11} \text{ cm}^2/\text{s}.^{220}$ The fact that the propagation of charge for PQ^{2+} is twice as fast in water as it is in acetonitrile suggests that polymer motions or counter-ion mobility is the rate limiting step for charge transport because water will swell PQ^{2+} to a much greater extent than acetonitrile.

The apparent diffusion coefficient D_{app} for $W_6Br_{14}^{2-}$ electrostatically bound within PQ^{2+} can be determined from the Cottrell equation according to the procedure described in Section II.B.4. The calculated values of D_{app} for $W_6Br_{14}^{2-}$ and $Mo_6Cl_{14}^{2-}$ are 8.7 x 10^{-11} and 8.9 x 10^{-11} cm²/s respectively. This value is over 2 orders of magnitude slower than is observed for $W_6Br_{14}^{2-}$ electrostatically bound in PVP^{+-} Me. Clearly the tighter binding pocket in the PQ^{2+} polymer film causes more restricted movement of the cluster dianion.

3. EVDQ2+ Polymer Modified Films

Although, PQ^{2+} films display stronger binding towards $W_6Br_{14}^{2-}$ than PVP^{+-} Me, cluster ions are still leached from PQ^{2+} films upon cycling the potential several times in acetonitrile solutions containing only electrolyte. This observation provided motivation for the design of a polymer with even tighter binding sites. Inspection of the PQ^{2+} unit reveals the distance between the nitrogen atoms in 4,4'-bipyridine is 7.1 Å. 332 The positive charge can be concentrated

by bringing the nitrogens into the 2,2' position of the bipyridine where the nitrogens are only separated by 2.8 Å.³³² Therefore, the charge density of the electrostatic pocket for a 2,2'-bipyridinium based polymer should be larger than that for a 4,4'-bipyridinium based polymer and the cluster should be more tightly bound.

Accordingly, electrochemical investigations turned to 4-vinyl-4'-methyl-N,N'-ethylene-2,2'-bipyridinium (EVDQ²⁺), 4, which was first described by Murray and coworkers. 122,177,277,335 Preparation of EVDQ²⁺ is described in (Section II.A.2.e). The starting material for the synthesis of EVDQ²⁺ is 4-vinyl-4'-methyl-2,2'-bipyridinium (VDQ), 3, (Section II.A.2.d). Low temperature sublimation of the product as the final step in the purification procedure eliminates all starting materials and produces a highly purified product as demonstrated by elemental analysis (Anal. Calc. (Found)) for $C_{13}H_{12}N_2 \cdot 1/4H_2O$: C, 77.81 (78.51); H, 6.29 (6.30); and N, 13.96 (13.95) and NMR spectroscopy. The NMR spectrum of VDO prepared as described in Section II.A.2.d in CD₃CN is shown in Figure 38. The peak assignments are δ (peak shape, number of protons from integration): 8.47 (1H, d), 8.36 (1H, d), 8.21 (1H, s), 8.05 (1H, s), 7.14 (1H, d), 6.97 (1H, d), 6.61 (1H, q), 5.94 (1H, d), 5.40 (1H, d), 2.33 (3H, s) which agree well with the literature. 221,333,334

The characterization of $EVDQ^{2+}$ is more difficult. The NMR spectrum in both D_2O and CD_3OD produces broad and uninformative peaks. That the initial light green $EVDQ^{2+}$ turns a deep purple upon dissolution in water suggesting the presence of radical impurities, a fact confirmed by EPR data. Elemental analyses are in poor agreement with the values expected for $EVDQ^{2+}$ (Anal. Calc. (Found))

A 250 MHz NMR spectrum of 4-vinyl-4'-methyl-2,2'-bipyridinium in CD₃CN.

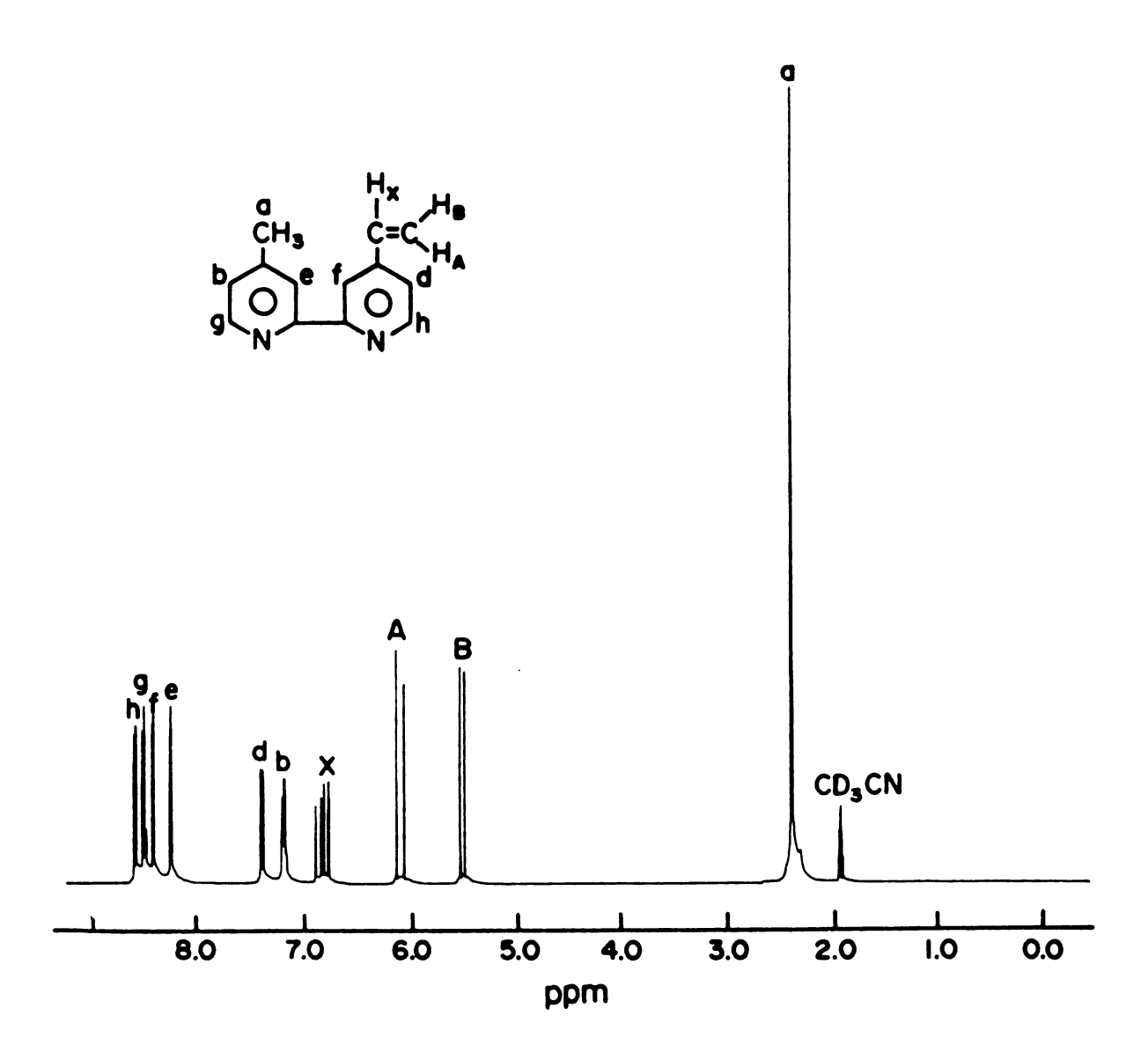


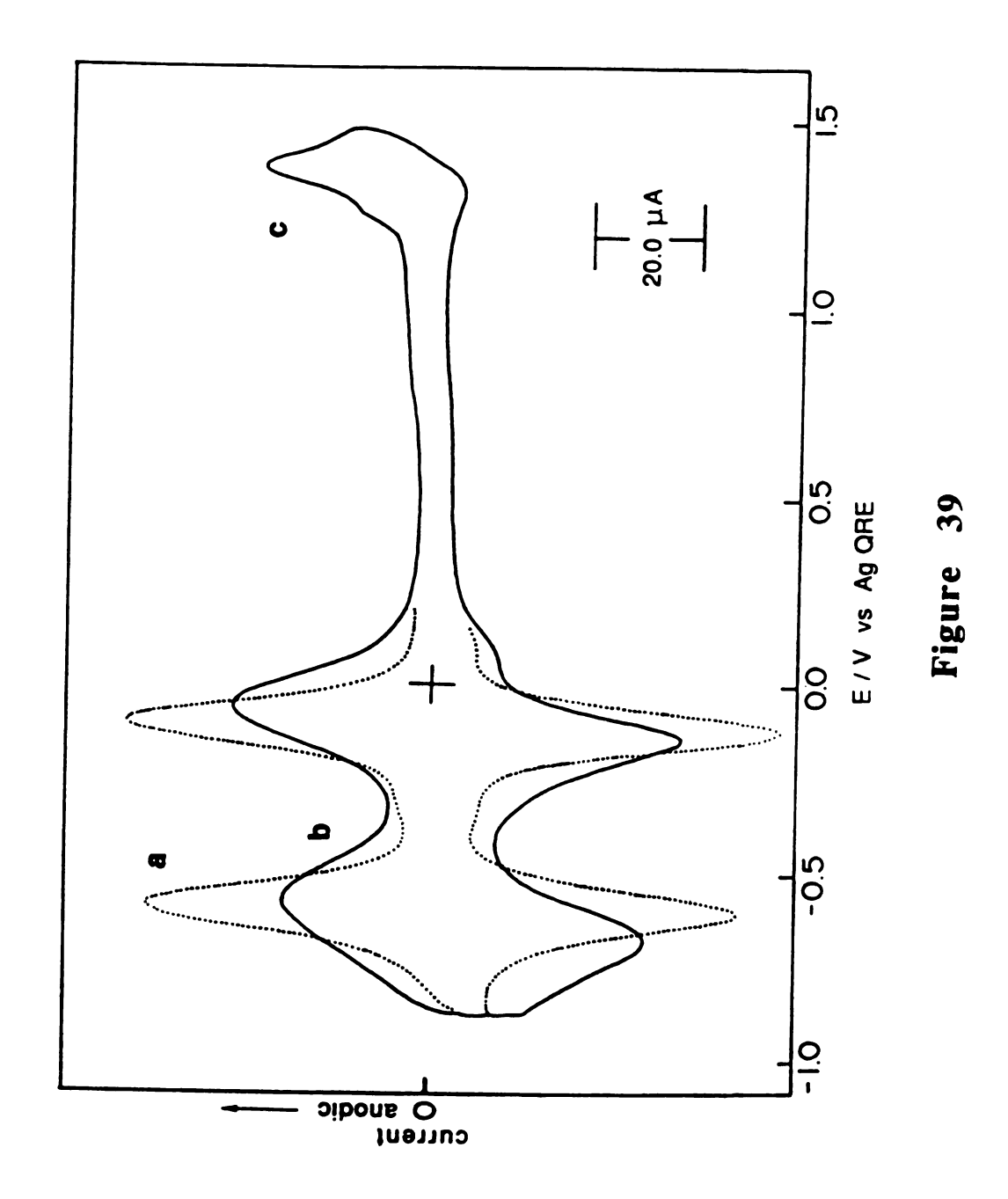
Figure 38

for $C_{15}H_{16}N_2 \cdot H_2O$: C, 44.80 (42.08); H, 4.51 (4.52); and N, 6.97 (6.63). Fast Atom Bombardment Mass Spectrometry (FABMS) display a parent peak at 243 corresponding to the molecular weight of EVDQ²⁺ plus a water of hydration.

The polymerization of EVDQ²⁺ has been reported to occur via free radical initiation of the vinyl group at the electrode. 122 However, we believe that the overall process is more complicated and probably involves contributions from electro-deposition as well. Neutral EVDQ is less soluble in acetonitrile than EVDQ²⁺ and readily Evidence for electro-deposition is adsorbs onto the electrode. predicated on the fact that polymeric films are not formed with the one electron reduction of EVDQ²⁺ but rather require the cycling of both reduction waves; vinvl centered free radical polymerization usually requires only one-electron reductions. In addition growth of the polymer in TBAP, TBAPF₆, TMAP₆, and TEAP (at high concentrations of EVDQ²⁺) all display absorptive postwave spikes after the second reduction wave which is characteristic of electrodeposition. 101,113 Postwave spikes are not observed for dilute concentrations of EVDO²⁺ in TEAP previously reported in the literature¹²², and hence have previously escaped detection. Also only thin films can be grown (the thickest film obtainable was 2.1 x 10⁻⁸ mol/cm²) which is also characteristic of electro-deposition. Nevertheless, film growth does include a polymerization component. No film is obtained from the monomer without the vinyl group 4.4'dimethyl-2,2'-bipyridinium (EDQ²⁺). Considering the extent of π aromaticity of EDQ²⁺ it is unlikely that the vinyl group is needed for electro-deposition but it does provide the site for free radical polymerization. Additionally, film growth requires the presence of Br or I and the rate of film formation can be increased in presence of excess Br or using the I. The rate increase for a polymerization process is expected because free radical polymerization requires a positively charged diffusing EVDQ²⁺ ion to come in contact with a positively charged polymer chain and these halides are known to form charge transfer complexes which can stabilize this process.³³⁶

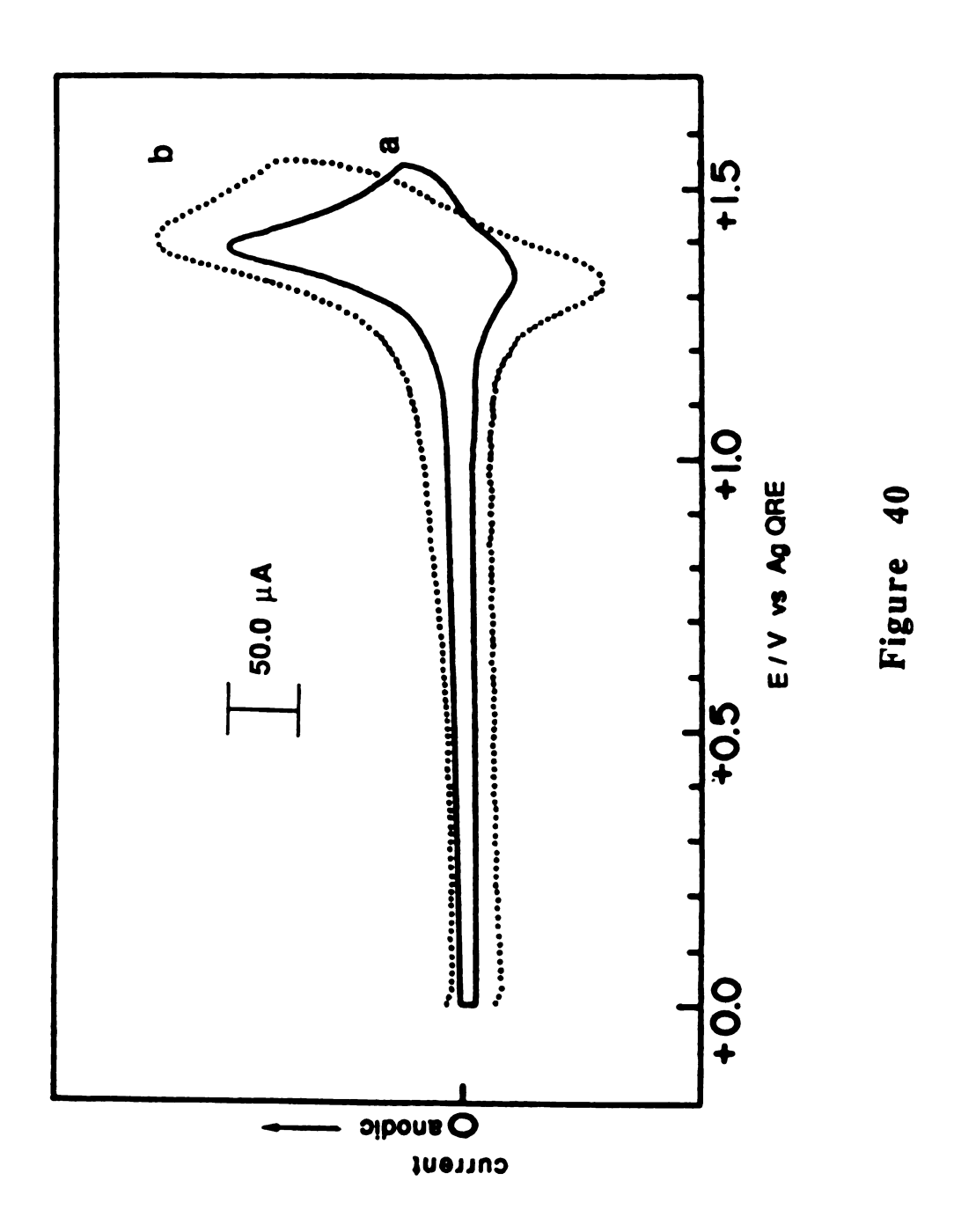
The cyclic voltammogram of a EVDQ²⁺ film on a platinum electrode with a surface coverage of 1.7 x 10⁻⁸ mol/cm² in acetonitrile containing 0.1 M TEAP is shown on Figure 39a. The two reduction waves corresponding to consecutive one-electron $(E_{p,1} = -0.54 \text{ V and } E_{p,2} = -1.02 \text{ V } vs. \text{ SCE}) \text{ of the}$ reductions pyridinium display reversible thin cell behavior, ($\Delta E = 20 \text{ mV}$, FWHM = 90 mV, and peak currents are directly proportional to the scan rate). In accordance with previous observations of the PQ²⁺ system, transferral of this electrode to a acetonitrile solution containing 15 μ M $W_6Br_{14}^{2}$ (a concentration too low to observe at the bare electrode) and 0.1 M TBAPF₆ causes the reduction waves to broaden (Figure 39b), again presumably due to tight ion-pairing of W₆Br₁₄² in the tight diaquat pocket. The oxidation wave of the W₆Br₁₄²- is reversible at fast scan rates. A diffusional tail (Figure 39c) is not observed and peak currents are directly proportional to the scan rate. Because these films are thin, these observations alone do not prove that the cluster ion is immobilized. However, this film does not lose cluster upon soaking in a acetonitrile solution containing only electrolyte for over 24 h. The combination of these results suggest that cluster is tightly bound within EVDQ²⁺.

Cyclic voltammograms of a platinum electrode coated with a $EVDQ^{2+}$ film (surface coverage = 1.7 x 10^{-8} mol/cm²) and dipped into an acetonitrile solution containing 0.2 M TEAP upon scanning the potential: (a) past the one electron reduction waves of $EVDQ^{2+}$; (b) past the one electron reduction waves of $EVDQ^{2+}$ after addition of 15 μ M $W_6Br_{14}^{2-}$ to the acetonitrile solution; and (c) past the oxidation of $W_6Br_{14}^{2-}$ after incorporation into the $EVDQ^{2+}$ film.



The oxidation wave of the cluster becomes electrochemically irreversible at slow scan rates. In Figure 40, the wave clearly shows irreversible behavior at 10 V/s. The enhanced reversibility at faster scan rates is possibly due to irreversible chemical reaction of the oxidized cluster which is circumvented by faster scan rates. However, W₆Br₁₄² is completely reversible at a bare platinum electrode in acetonitrile ($i_{p,a} = i_{p,c}$ and i_pC^* is constant from cyclic voltammetry; it 1/2 is constant for chornoamperometry (short times); and $\tau_r = \tau_f/3$ for reverse chronopotentiometry) and we have no evidence that decomposition of the monoanion is promoted by the polymer film. Alternatively, the presence of prewave humps on both the first reduction wave of EVDO²⁺ and the oxidation wave of $W_6Br_{14}^{2}$ (Figure 39) provide a clue as to the origins of the electrochemical irreversibility, this unusual behavior. Similar to the prewave spikes described in Section III.B for Fe(vbpy)₃²⁺, the prewaves in Figure 39 are associated with one another and correspond to the anodic and cathodic components of a redox couple. This behavior is consistent with the oxidized cluster becoming trapped in an inaccessible region of the polymer and therefore being unable to return to the electrode $(i_{p,a} > i_{p,c})$. By increasing the scan rate, the W₆Br₁₄ ion does not have enough time to diffuse into the isolated domains resulting in $i_{p,a} = i_{p,c}$. On this basis the possibility exists that the redox sites of the polymer might be able to shuttle charge to the isolated W₆Br₁₄. If this does occur we would expect that scanning the reduction waves of the polymer subsequent to scanning the oxidation wave of the cluster should result in an enhanced response from the cathodic portion of the polymer

Cyclic voltammograms of $W_6Br_{14}^{2-}$ incorporated into a EVDQ²⁺ film adsorbed onto a platinum electrode (surface coverage = 1.7 x 10^{-8} mol/cm²) immersed in an acetonitrile solution containing 0.2 M TEAP recorded at (a) 10 V/s and (b) 33V/s.



reduction wave. It is noteworthy that the polymer reduction wave is reversible if the oxidation wave of cluster is not scanned. expected because isolated oxidized cluster is not present for the polymer to shuttle charge to, unless W₆Br₁₄ is produced. Similarly the anodic portion of the oxidation wave for the cluster should be significantly diminished upon its second scan without cycling the polymer reduction waves because the oxidized cluster in the isolated regions of the polymer can not communicate directly with the Without activation of the polymer, isolated cluster ions electrode. can not be reduced. Indeed these are the observed results. Enhanced response from the polymer reduction wave is observed with attenuated responses of the cluster oxidation wave. In a typical experiment, the number of coulombs lost on subsequent scans of the cluster oxidation wave appear almost identically as an increased response for the cathodic current of the polymer wave. The ratio of these experimentally determined differences in the cluster and polymer waves is 1.18 ±.04 (for three separate films). This value is close to unity and suggests that the polymer mediates electron transfer to isolated W₆Br₁₄.

Therefore, while $W_6Br_{14}^{2-}$ is tightly bound within the polymer, $W_6Br_{14}^{-}$ freely diffuses. The apparent diffusion coefficient of $W_6Br_{14}^{2-}$ incorporated within EVDQ²⁺ films determined by using the procedure described in Section II.B.4 is 1.8 x 10^{-11} cm²/s (accurate determination of the diffusion coefficient of $W_6Br_{14}^{-}$ was impossible because of its rapid exodus to the isolated regions of the polymer). This value is significantly smaller than the value obtained for the

 PQ^{2+} system (8.7 x 10^{-11} cm²/s) suggesting even tighter binding for $W_6Br_{14}^{2-}$ in the 2,2' over the 4,4' bipyridinium films.

4. Comparison of EVDQ²⁺, PVDQ²⁺, and BVDQ²⁺ Polymer Modified Films

The charge density of the cationic binding site increases along the series PVP+Me, PQ²⁺, and EVDQ²⁺ and a corresponding decrease in the diffusion coefficient of W₆Br₁₄²- is observed. The ability to control the diffusion rates of ions within polymeric films by specifically designing polymers with varying charge density binding sites is a novel and potentially useful concept. However, in addition to the binding site, other significant differences in the polymer microstructures exist. Therefore, in an effort to unequivocally assess the role of the binding site in determining charge transport in the pyridinium and bipyridinium films it was of interest to investigate the diffusion rates of cluster in structurally similar polymers with binding sites of varying charge density. The 2,2'-bipyridinium systems provides the opportunity to undertake such studies. increasing the length of the linkage between the nitrogen groups, the effective charge density of the dication binding site can be altered. The interplanar angle of the pyridine rings in N,N'-ethylene-2,2'bipyridinium (EDQ²⁺) is 9° , whereas for N,N'-1,3-propylene-2,2'- (PDQ^{2+}) is 60° and for N, N'-1, 4-butylene-2, 2'bipyridinium bipyridinium (BDQ²⁺) is 80°.³³⁷ Therefore, polymers formed from the vinyl containing analogs of these monomers should possess progressively weaker binding pockets as the interplanar angle increases, while maintaining structural uniformity in the overall polymer microstructure.

The physical properties of 4-vinyl-4'-methyl-N,N'-propylene-2,2'-bipyridinium (PVDQ²⁺) 5 and 4-vinyl-4'-methyl-N,N'-butylene-2,2'-bipyridinium (BVDQ²⁺) 6, synthesized as described in Sections II.A.2.f and II.A.2.g, were identical to EVDQ²⁺. FABMS exhibited parent peaks which correspond to their prospective molecular weights with a water of hydration. The same polymerization procedure for EVDQ²⁺ was employed with the exception that the I-salts were used.

The cyclic voltammogram of PVDQ²⁺ on a platinum electrode with a surface coverage of 4.0 x 10^{-9} mol/cm² in acetonitrile containing 0.1 M TBAP is shown in Figure 41. The cathodic peak potentials are $E_{p,1}=-0.76$ V and $E_{p,2}=-1.04$ V vs. SCE. The shift in the first reduction wave to more negative potentials as compared to $EVDQ^{2+}$ is attributed to the decreased delocalization of the π -system arising from the torqued pyridinium rings of $PVDQ^{2+}$. The second reduction wave is relatively insensitive to changes in structure as evidenced by their values only differing by 20 mV. The two reduction waves for $PVDQ^{2+}$ (Figure 41) display reversible thin cell behavior ($\Delta E = 20$ mV, FWHM = 90 mV) and peak currents are directly proportional to the scan rate.

A PVDQ²⁺ modified platinum electrode (surface coverage = 1.06 x 10^{-8} mol/cm²) readily incorporates cluster from an acetonitrile solution containing 20 μ M $W_6Br_{14}^{\ 2-}$ and 0.2 M TBAPF₆ as shown in Figure 42a. The oxidation wave does not have a diffusional tail and peak currents are directly proportional to scan rate. Ion-exchanged

Cyclic votammogram of a $PVDQ^{2+}$ film adsorbed onto a platinum electrode (surface coverage = $4.0 \times 10^{-9} \text{ mol/cm}^2$) immersed in an acetonitrile solution containing 0.2 M TEAP

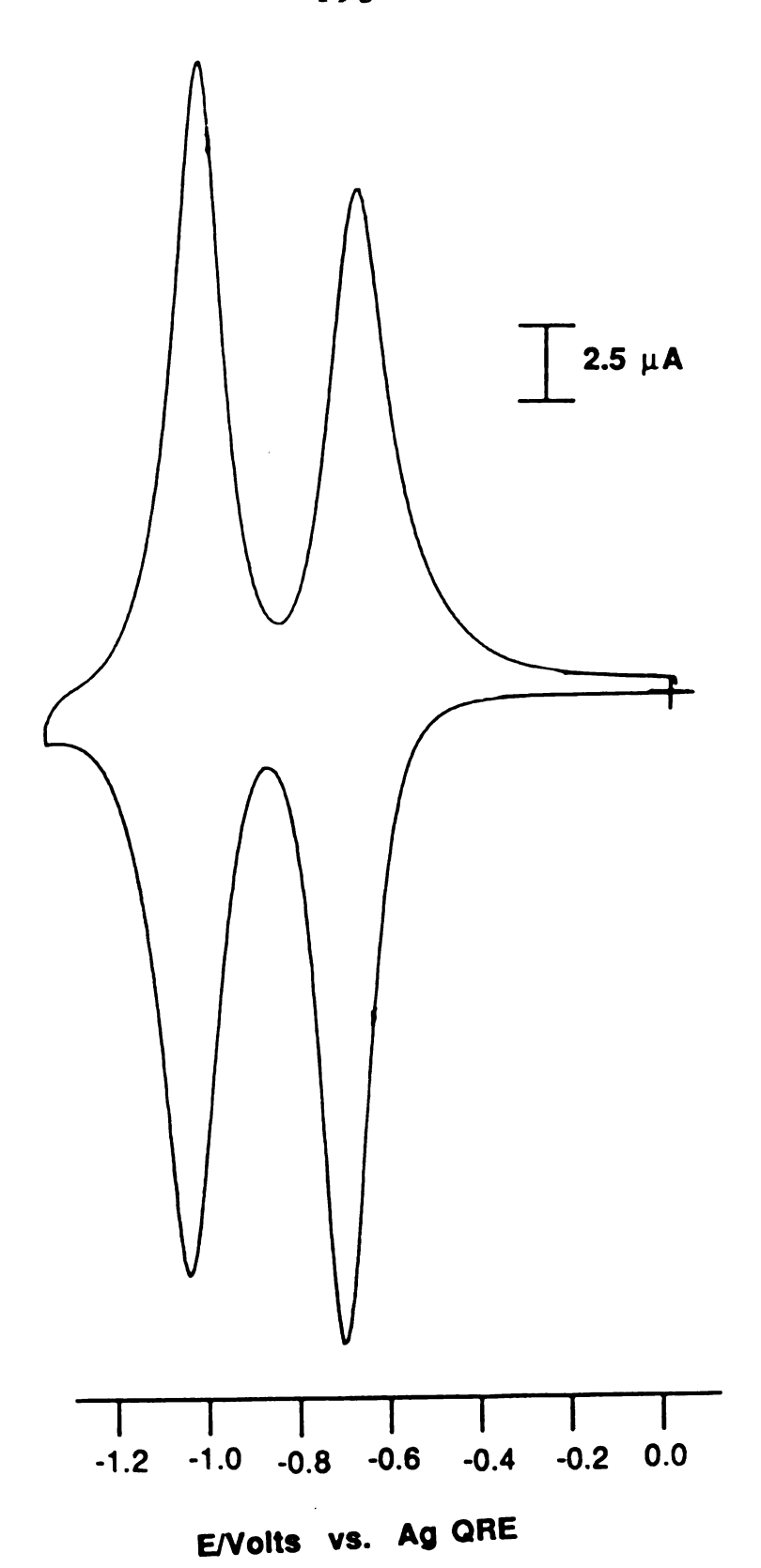
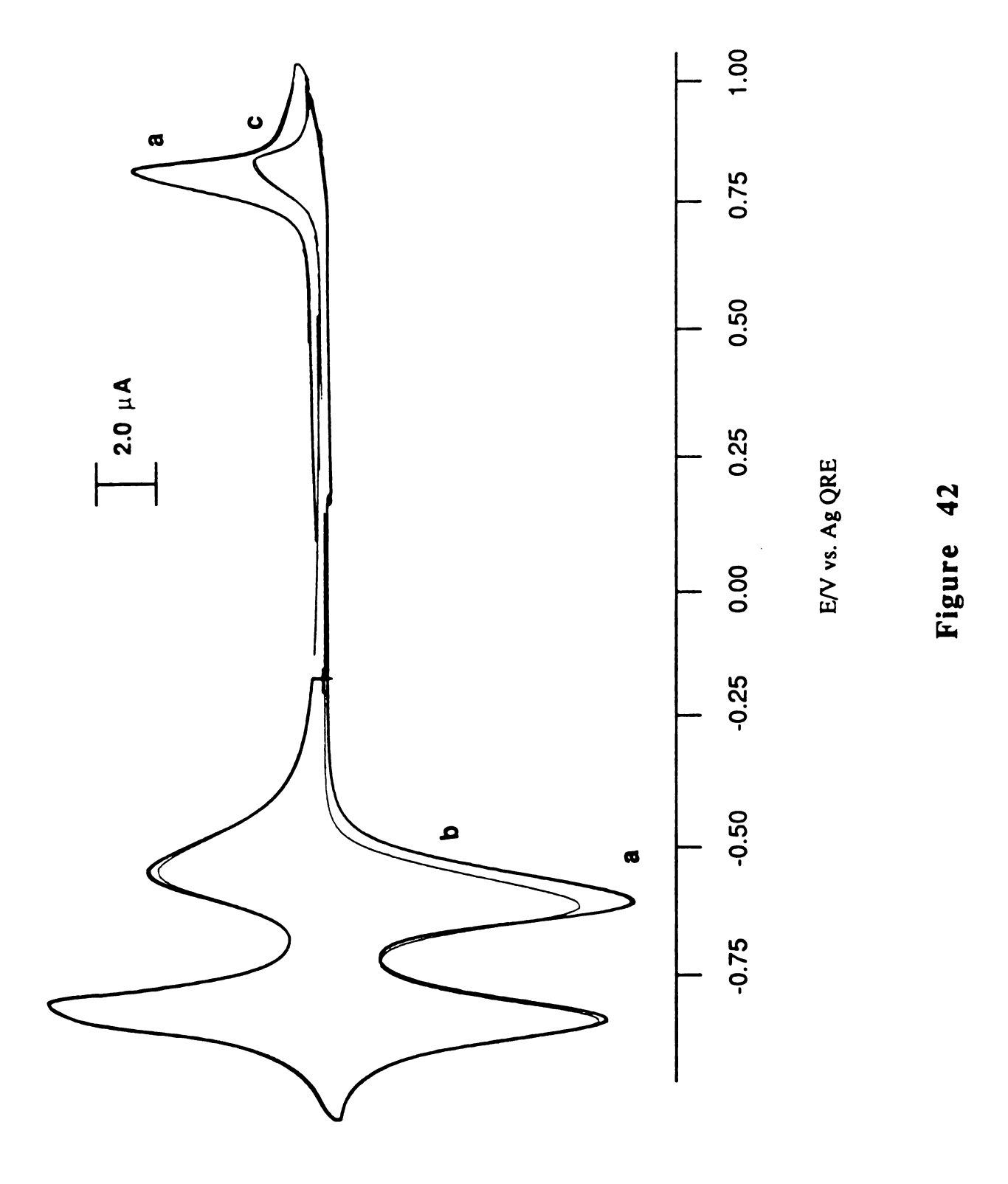


Figure 41

Cyclic voltammetric waves obtained from a PVDQ²⁺ film coated onto a platinum electrode (surface coverage = $1.1 \times 10^{-8} \, \text{mol/cm}^2$) dipped into an acetonitrile solution containing 0.2 M TEAP and 20 μ M W₆Br₁₄²⁻: (a) upon scanning the electrodes potential from 0.00 V to +1.40 V to -1.10 V and back to 0.00 V vs. SCE; (b) after the reduction waves for the PVDQ²⁺ polymer had been scanned once prior to measurement; and (c) after the oxidation wave of W₆Br₁₄²⁻ had been cycled once prior to measurement.



cluster in PVDQ²⁺ shows no evidence of a return wave even at scan rates as fast as 50 V/s. In this regard the PVDQ²⁺ behaves similarly to EVDQ²⁺ in that W₆Br₁₄- diffuses to isolated sites within the PVDQ²⁺ microstructure, as shown in Figure 42a. Scanning the oxidation wave two consecutive times results in a decreased electroactive response Subsequent scans of the reduction waves of the (Figure 42b). PVDQ²⁺ polymer film show an enriched response of the cathodic portion of the polymer reduction wave on the first scan $(i_{p,c} > i_{p,a})$ on first scan, $i_{p,c} = i_{p,a}$ on second scan). If the increased response of the cathodic portion of the reduction wave results from the polymer film shuttling charge to isolated cluster ions, then the differences in electroresponses for the oxidation of cluster and reduction of polymer from Figure 42 should correspond to the same number of coulombs. Integration of these waves establishes that this is clearly the case (the ratio for the number of excess coulombs for polymer reduction divided by the number of lost coulombs for the oxidation of cluster = $1.04 \pm .03$).

This model is further substantiated by charge shuttling experiments. Reactivation of isolated oxidized cluster ions which cannot directly communicate with the electrode surface, is not necessarily related to polymer but can be accomplished by a variety of freely diffusing shuttle reagents. The reduction of isolated cluster ions by $IrCl_6^{3-}$ is shown in Figure 43. $IrCl_6^{3-}$ initially generated at the electrode is in evidence by a cathodic component of the $IrCl_6^{2-/3-}$ couple. Of course in a charge shuttle mechanism the anodic component of the couple is not observed because the $IrCl_6^{3-}$ diffuses to isolated $W_6Br_{14}^{-}$, reduces it, and the $IrCl_6^{2-}$ generated by this

Cyclic votammogram of a PVDQ²⁺ film on a platinum electrode soaking in an acetonitrile solution containing 0.2 M TBAPF₆, 25 μ M W₆Br₁₄²⁻ and 50 μ M IrCl₆²⁻.

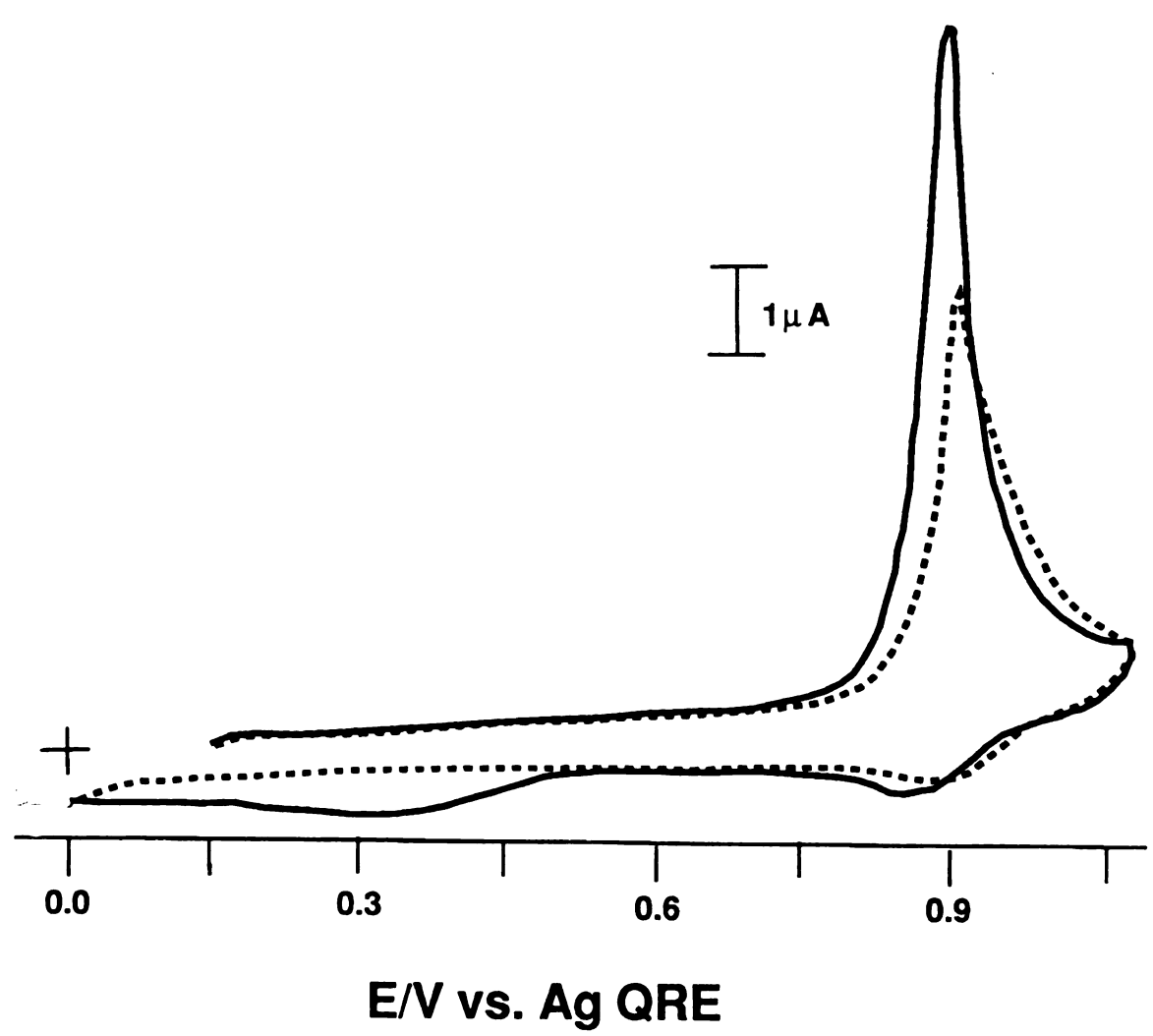


Figure 43

reaction diffuses back to the electrode and becomes rereduced whereupon it diffuses to another oxidized cluster thereby establishing a catalytic cycle. This mechanism is borne out by the absence of an oxidation wave for $IrCl_6^{2-}$. These results establish that $W_6Br_{14}^{-}$ ions freely diffuse within the PVDQ²⁺ microstructure and become confined in an isolated region of the film which can only be accessed by the use of intrinsic and extrinsic charge mediators.

The reduction wave for BVDQ²⁺ polymerized onto platinum produces one very broad reduction wave at approximately -0.95 V vs. SCE. The first reduction wave is evidently shifted far enough negative that it engulfs the second reduction wave. Thin films of BVDQ²⁺ formed onto platinum extract cluster ions from a acetonitrile solution containing 10 μ M W₆Br₁₄²⁻. The oxidation waves for W₆Br₁₄²⁻ exchanged into BVDQ²⁺ and PVDQ²⁺ display almost identical behavior.

Apparent diffusion coefficients for W₆Br₁₄²⁻ electrostatically bound within PVDQ²⁺ and BVDQ²⁺, determined as described in Section II.B.4 are 3.0 x 10⁻¹¹ cm²/s and 4.1 x 10⁻¹¹ cm²/s respectively. The D_{app} values for PVDQ²⁺ and BVDQ²⁺ are more similar to each other than for EVDQ²⁺ because the interplanar angles are more closely correlated. The apparent diffusion coefficients D_{app} of cluster in PVP⁺—Me, PQ²⁺, EVDQ²⁺, PVDQ²⁺, and BVDQ²⁺ are graphically summarized in Figure 44. These data clearly demonstrate that the diffusion rate of exchanged W₆Br₁₄²⁻ ion decreases with increasing charge density of the binding sites. Moreover this conclusion is further evidenced by determinations of the distribution coefficient K_D (the concentration of redox ion in the

A plot of the apparent diffusion coefficients, D_{app} for $W_6Br_{14}^{2-}$ incorporated into PVP+Me, PQ²⁺, BVDQ²⁺, PVDQ²⁺, and EVDQ²⁺ polymeric films as a function of the number of binding sites.

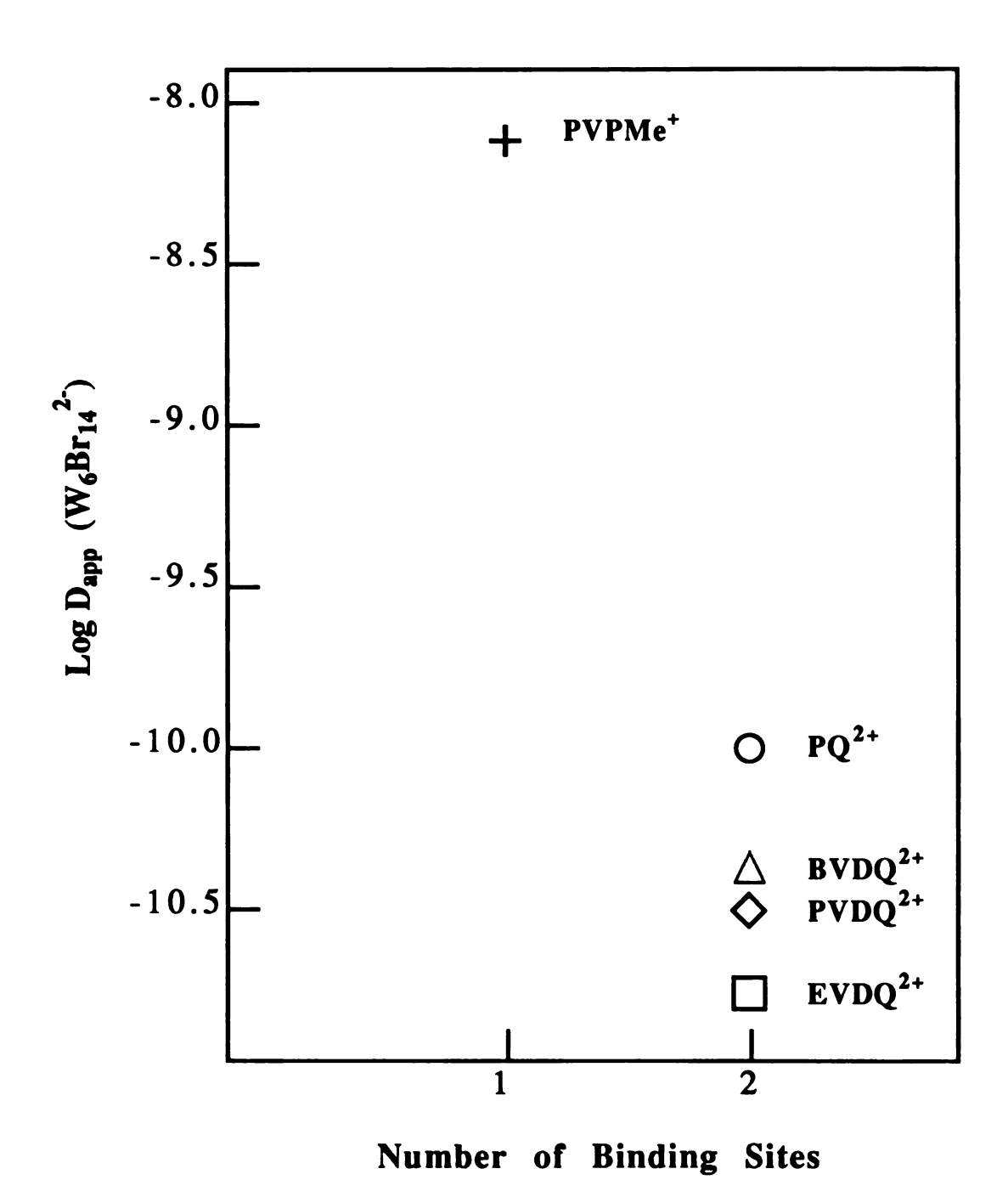


Figure 44

A plot of the distribution coefficients K_D for $W_6Br_{14}^2$ incorporated into PVP^+ Me, PQ^{2+} , $BVDQ^{2+}$, $PVDQ^{2+}$, and $EVDQ^{2+}$ polymeric films as a function of the number of binding sites.

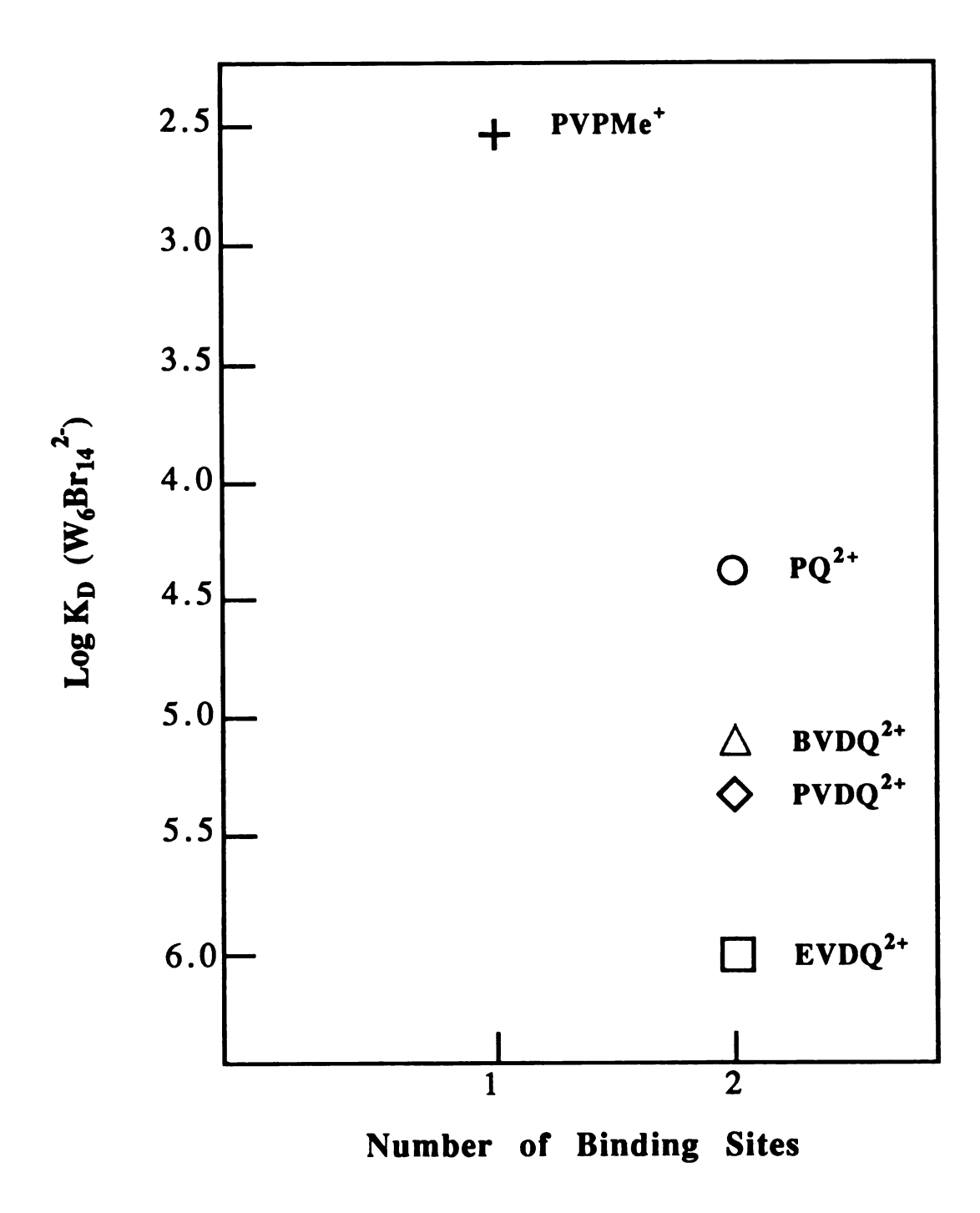


Figure 45

polymer film divided by the concentration in the soaking solution) 109 for $W_6Br_{14}^{\ 2^-}$ incorporated into the polymers. As shown in Figure 45 the K_D values for the five polymers investigated monotonically increase as a function of binding site charge density in a parallel manner to the apparent diffusion coefficients lending further evidence to our conclusion that in acetonitrile, electrostatic binding in ionic polymers is directly related to the charge density of the binding site..

C. Conclusion

These studies demonstrate that the diffusion rates of ions exchanged into polyionic polymer films can be influenced by the design of the polymer microstructure. The binding pocket of PVP^{+} —Me requiring the juxtaposition of two pyridinium rings per cluster ion is structurally floppy and $W_6Br_{14}^{\ 2^-}$ is mobile. The diffusion coefficient of cluster is suppressed by several orders of magnitude by bringing the individual positive charges of the PVP^{+} —Me sites into a single pocket in PQ^{2+} . By localizing the charge even further into the 2,2' position of the bipyridinium ring the ion-pairing is further enhanced. As originally inferred from structural considerations, the diffusion coefficients of $W_6Br_{14}^{\ 2^-}$ decrease along the the series $BVDQ^{2+}$, $PVDQ^{2+}$, and $EVDQ^{2+}$ owing to the tilt angle between the bipyridinium rings. This correlation of the diffusion rates among the pyridinium and bipyridinium series, and parallel behavior of K_D and D_{app} strongly suggests that the primary perturbation on the charge

transport in these films is the nature of the binding site and that the macroscopic polymer structure plays at most only a secondary role.

In each polymer system investigated the W₆Br₁₄²- ions are immobile in tight ion-pairs, however, the oxidation of cluster or reduction of polymer binding sites to +1 reduces ion-pair interactions significantly, such that W₆Br₁₄ becomes mobile. Hence fixed site distance for ecl reaction between oxidized cluster and reduced polymer will not be maintained. On this basis the ecl yields for these cluster/polymer systems similar are expected to be cluster/pyridinium ions in solution. This is the case. Thus in order accomplish fixed distance electron transfer in polymer microstructures, reactant pairs will have to be covalently liked to each other to ensure they do not diffuse apart. This can be accomplished by preassembling the system. For example, Mo₆Cl₁₃LL' modified with the bidentate ligand L,L' will enable W₆Br₁₃ to be Production of oxidized tungsten bromide cluster and coordinated. reduced molybdenum chloride cluster in the charge rectification sense will establish an ecl annihilation reaction at closest contact.

CHAPTER V

DEVELOPMENT OF AN ELECTROANALYTICAL SENSOR

A. Background

One of the major challenges facing analytical chemists is the ability to quantify trace and ultratrace quantities of materials from multicomponent samples. The best-known electroanalytical stripping analysis,³³⁹ whereby a trace metal is technique is electrolytically deposited onto an electrode thus satisfying the dual purpose of concentration and isolation of the analyte from the The analysis is conducted by electrochemically complex matrix. stripping, in one potential step, the deposited metal from the electrode surface, resulting in a enhanced current response from the electrode over that which would be observed if no analyte was deposited onto the electrode surface. This technique is virtually limited to metal ions as the analyte and mercury electrodes because most organics and inorganic complexes cannot be electrodeposited and solid electrodes become easily fouled.³³⁹

The area of voltammetry following nonelectrolytic concentration has been established as a technique with tremendous potential for trace analysis of electroactive analytes.³⁴⁰ The most recent development in this field has been the use of modified electrodes. The methods developed to confine analytes within polymers on electrodes have been: (i) complexation which utilizes functional groups on the polymer backbone to coordinate the analyte; (ii) covalent attachment of the analyte to the polymer backbone; and (iii) electrostatic binding of the analyte within a polyionic polymer.³⁴⁰ Of these techniques electrostatic binding of analytes is the most versatile because specific reactions between the analyte

and polymer are not required. The analysis of multicharged electroactive analytes has been achieved in many systems. $^{1-6}$ Although there has been a report in the literature claiming to detect Ag⁺ at concentrations as low as 1 x 10^{-11} M³⁴¹ the majority of the polyionic sensors have detection limits in the range of 1 x 10^{-6} to 1 x 10^{-9} M with linear calibration curves over approximately 2 orders of concentration. $^{342-348}$

The desired features for an electroanalytical sensor for analyte are: (i) rapid equilibration between contacting solution and polymer; (ii) low detection limits with large concentration ranges of linear current responses; (iii) efficient operation over a large pH range; (iv) detectability of monocharged species; (v) ability to reversibly establish the sensor (i. e. reverse ion-exchange can be accomplished); (vi) operation in both aqueous and nonaqueous solvents; and (vii) the ability to discriminate the desired analyte from complex mixtures. The sensing systems developed heretofore achieve only a few of these goals. Therefore the development of new sensors is of major interest. Described herein is a novel electroanalytical sensor which realizes the above goals.

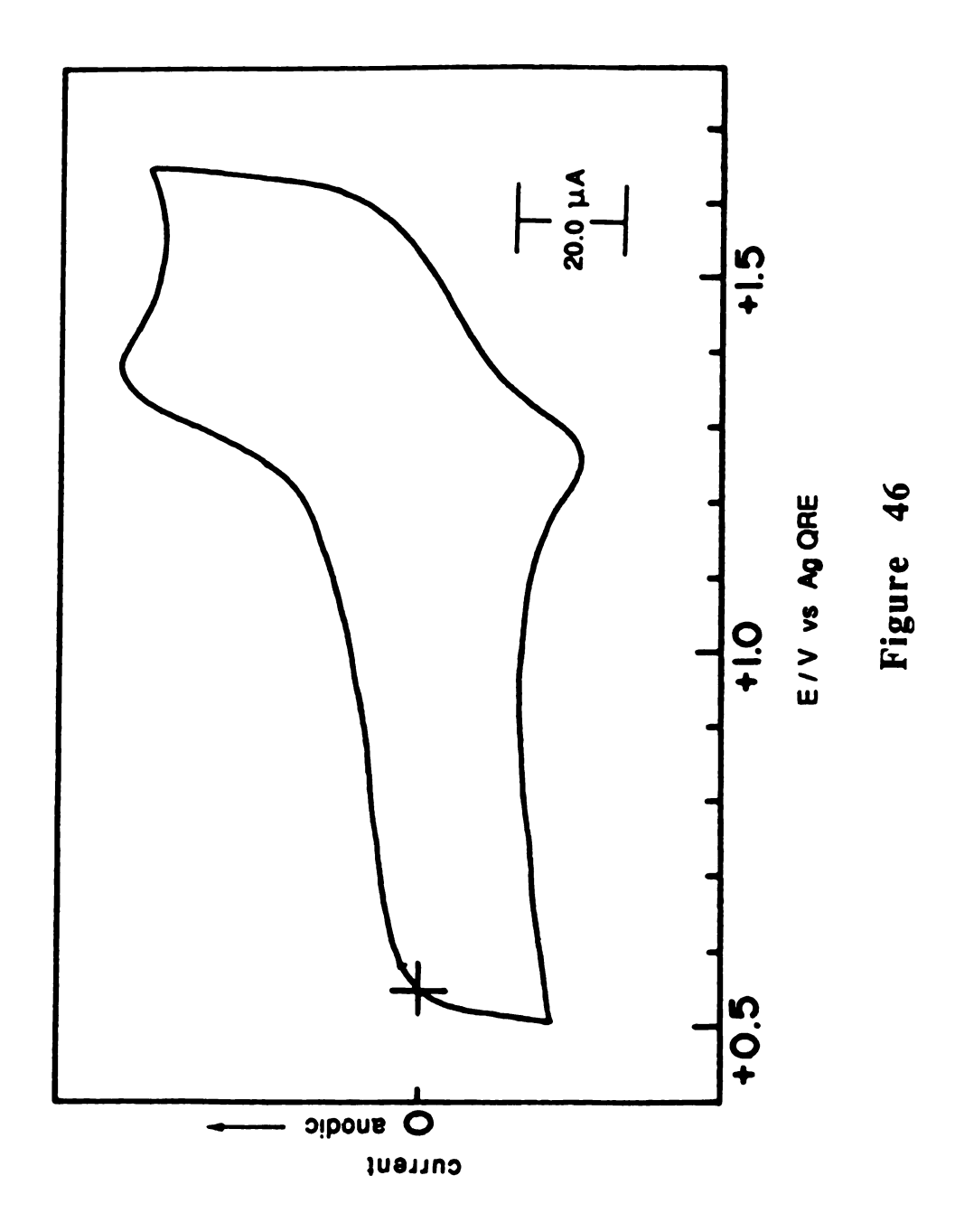
B. Results and Discussion

1. Development of an Electroanalytical Anionic Sensor for use in Nonaqueous Solvents

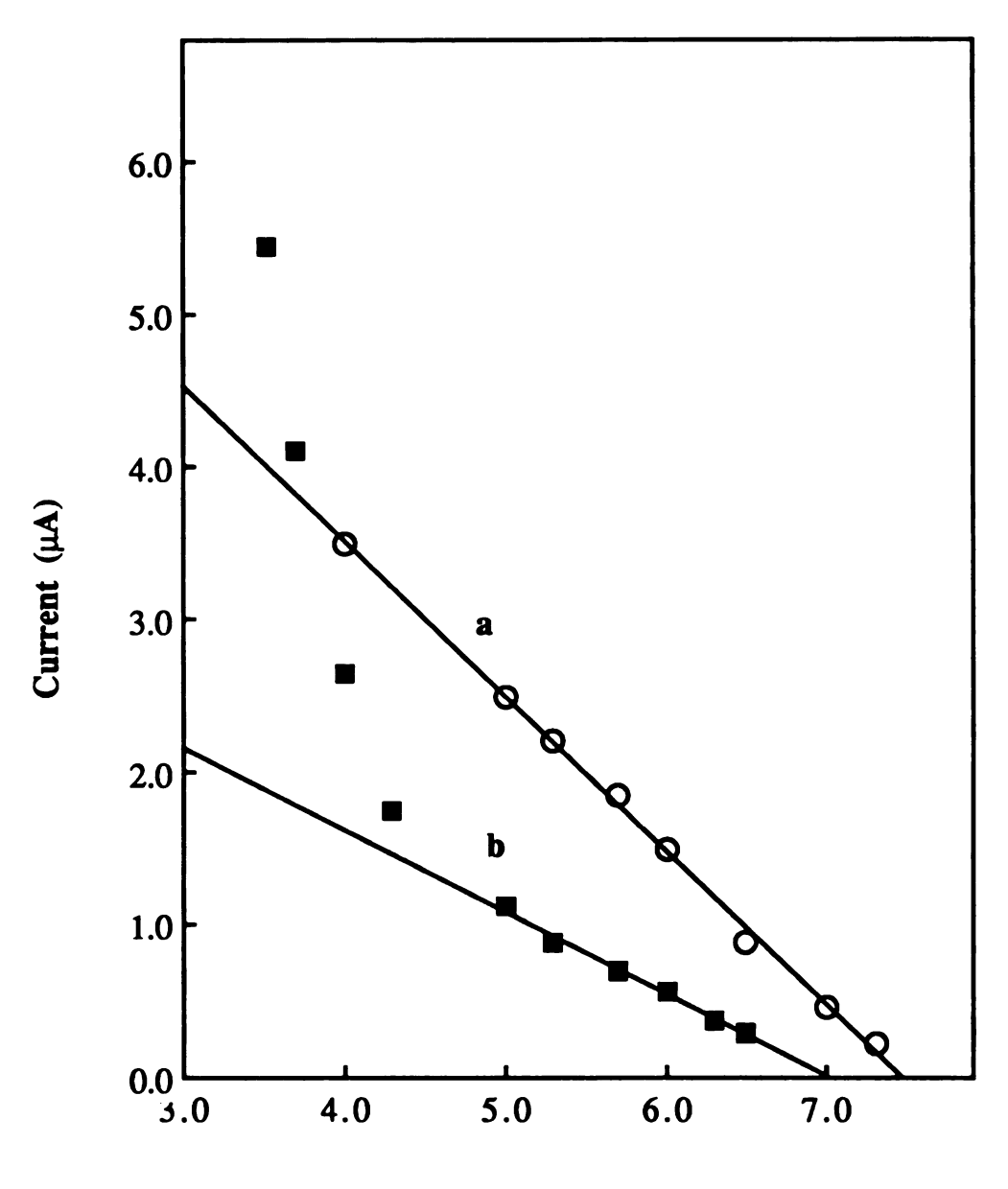
The EVDQ²⁺ polymer films extract and concentrate anions from very dilute solutions. Therefore, these films are viable candidates as electrochemical sensors for anion detection in nonaqueous solutions.

For example the unprecedented detection of a dianion (W₆Br₁₄²-) at concentrations as low as 5 x 10⁻⁸ M in acetonitrile by cyclic voltammetry is shown in Figure 46. The detection limit for W₆Br₁₄²with a film of EVDQ²⁺ (surface coverage 2.1 x 10⁻⁹ mol/cm²) is 3 x 10⁻⁸ M as determined from the anodic peak current of the cyclic voltammogram and would presumably be even greater by using a more sensitive technique such as differential pulse polarography. Moreover, the anodic peak current for the detection of W₆Br₁₄² is linear over 3.5 orders of magnitude (Figure 47a). Unfortunately the peak current is dependent on the surface coverage of the film as evidenced by Figure 47b which shows that a film with a surface coverage of 1.1 x 10⁻⁹ mol/cm² has a limit of detection of 1 x 10⁻⁷ M and displays linear responses only over 2.5 orders of magnitude. The sharp rise in peak currents in Figure 47b corresponds to currents which would be attained from a bare electrode at the same concentration indicating the film is not altering the electroresponse at higher concentrations. Films thicker than 4.5 x 10⁻⁹ mol/cm² also display diminished ability to detect low concentrations of W₆Br₁₄²-. Film coverages between $2.0 \times 10^{-9} \text{ mol/cm}^2$ and $4.0 \times 10^{-9} \text{ mol/cm}^2$ yielded the greatest sensitivity and accompanying linear range of detection for the cluster anions. The fact that the magnitude of peak currents are affected by the film coverage of EVDQ²⁺ is a drawback because these films must be calibrated before they can be used to quantify electroactive material in solution. Importantly, the high sensitivity for anion binding and detection have also been observed for anions other than cluster including Fe(CN)₆³-, Fe(CN)₄bpy⁻, IrCl₆²-, I', and Br'. These films have tremendous potential for the

Cyclic voltammogram of $W_6Br_{14}^{2-}$ incorporated from an acetonitrile solution containing 0.2 M TEAP and 5 x 10^{-8} M $W_6Br_{14}^{2-}$ into a EVDQ²⁺ film adsorbed onto a platinum electrode (surface coverage = 4.1 x 10^{-9} mol/cm²).



A plot of the cyclic voltammetric peak current for the oxidation of $W_6Br_{14}^{2-}$ incorporated into $EVDQ^{2+}$ films as a function of the concentration of $W_6Br_{14}^{2-}$ in the contacting acetonitrile solution for platinum electrodes with surface coverages of, (a) $2.1 \times 10^{-9} \text{ mol/cm}^2$ and (b) $1.1 \times 10^{-9} \text{ mol/cm}^2$.



-Log (Concentration M) W₆Br₁₄²-

Figure 47

electrochemical detection of trace quantities of anions in nonaqueous solvents.

2. Characterization of Anionic Effects on the Microstructure of EVDQ²⁺

Seldom is the analysis of a pure sample required and most often extraction and detection of analyte from a complex mixture is required. For EVDQ²⁺ polymer films, anions other than the analyte, have the most potential to interfere with the function of the film as a sensor. Thus the examination of anion effects on the charge transport rates of EVDQ²⁺ modified electrodes was undertaken.

The D_{ct} for the reduction of EVDQ²⁺ and PVDQ²⁺ could not be determined because potential steps large enough to overcome resistive effects can not be achieved. The potential was stepped past the reduction wave for several seconds to ensure complete reduction of the film, and after the potential was stepped back to 0.0 V vs. SCE the current response as a function of time was measured. The charge transfer diffusion rates D_{ct} for EVDQ²⁺ and PVDQ²⁺ films soaking in acetonitrile solutions containing different electrolytes are given in Tables 11 and 12, respectively. These D_{ct} values are clearly sensitive to the supporting electrolyte.

The D_{ct} values are determined for the oxidation of +1 polymers to +2, which necessarily requires accompanying cation ejection or anion uptake. The role cations play in the charge neutrality process can in part be understood by comparison of the D_{ct} values for the perchlorates (Tables 11 and 12). The rate of charge transport decreases along the series $LiClO_4 > TBAP \ge TEAP$. Clearly no obvious

Table 11

Apparent Diffusion Coefficients and FWHM Values for EVDQ²⁺ Films With Varying Thicknesses

$\Gamma_{\rm corr} \times 10^9$ moles/cm ² a	0.2 M Electrolyte	FWHM ^b mV		D _{ct} x 10 ¹¹
		i _{p,c}	i _{p,a}	c m ² /sec ^c
5.6	LiClO ₄	90	110	3.61
5.6	ТВАР	91	114	2.61
14.3	TBAP	120	153	2.80
5.6	TEAP	90	115	2.54
12.9	TEAP	115	144	2.50
14.3	TEAP	110	140	2.45
5.6	TBAPF ₆	130	146	1.49
12.9	TBAPF ₆	140	170	1.50
14.3	TBAPF ₆	151	179	1.41
14.3	TBABF ₄	162	190	0.57
14.3	TBAAsF ₆	185	236	0.43

^a The film coverage Γ_{corr} was determined using the electrochemically determined area of the Pt electrode. ^bFull width at half maximum of the cyclic voltammetric peak for the first one electron reduction of EVDQ²⁺. ^cD_{ct} is the apparent diffusion coefficient from EVDQ²⁺ films.

Table 12

Apparent Diffusion Coefficients and FWHM Values for PVDQ²⁺ Films With Varying Thicknesses

Γ _{corr} x 10 ⁹ moles/cm ² a	0.2 M Electrolyte	FWHM ^b mV		D _{ct} x 10 ¹¹
		i _{p,c}	i _{p,a}	c m ² /sec ^c
9.7	LiClO ₄	120	146	2.34
12.0	LiClO ₄	117	150	2.69
3.5	ТВАР	90	115	1.69
9.7	TBAP	135	166	1.60
12.0	TBAP	140	160	1.65
2.4	TEAP	90	124	1.37
9.7	TEAP	151	183	1.35
10.0	TEAP	146	180	1.41
2.4	TBAPF ₆	124	152	0.48
3.5	TBAPF	130	155	0.48
9.7	TBAPF ₆	176	204	0.53
1.0	TBAPF ₆	180	210	0.41
3.5	TBABF₄	155	176	0.32
9.7	TBABF ₄	220	255	0.39
9.7	TBAAsF ₆	240	306	0.31

^a The film coverage Γ_{corr} was determined using the electrochemically determined area of the Pt electrode. ^bFull width at half maximum of the cyclic voltammetric peak for the first one electron reduction of EVDQ²⁺. ^cD_{ct} is the apparent diffusion coefficient from EVDQ²⁺ films.

trend between the size of the cation and D_{ct} rates exists. observations implicate anion uptake as the process responsible for The D_{ct} values for the anions in maintaining charge neutrality. Tables 11 and 12 follow the order $ClO_4^- > PF_6^- > BF_4^- > AsF_6^-$. With the exception of BF₄, this series parallels hard/soft acid/base formalisms with the hardest base $\mathrm{ClO_4}^-$ (smallest least polarizable anion) producing the fastest D_{ct} rate and the softest base AsF₆ (largest most polarizable anion) producing the slowest D_{ct} rate. Accordingly, ClO₄ would be expected to form the strongest ion-pair with the positively charged sites in EVDQ²⁺ films and AsF₆⁻ the These data seemingly contradict conventional thinking weakest. which predicts that the anion movement will slow and become the rate limiting step for charge transport as anion binding increases; thus the smallest D_{ct} values should be expected intuitively for $ClO_4^$ and the largest for AsF₆. How can this disparity be explained?

Electron hopping between fixed sites attached to electrodes require an accompanying displacement of counterions to maintain charge neutrality. Recently Saveant has established that steady state currents obtained from immobilized sites on an electrode should be independent of counterion mobility. Furthermore, Andrieux and Saveant suggest that the current responses from transient techniques (like chronoamperometry) should increase as the mobility of the counterion decreases. Charge propagation is driven by a potential gradient established in the polymer film by an applied potential at the electrode. When counterions are mobile the potential gradient, which drives charge propagation through fixed polymer redox sites by site-to-site electron hopping, is diminished by the counterion

However, when counterions are immobilized the potential gradient can not be satisfied by ion movement. Therefore, for transient potential steps the electron hopping rate and D_{ct} will be driven by a larger potential field and thus charge transport is dominated by migration increasing the observed propagation rate. As ion mobility decreases, the potential gradient becomes larger and thus charge propagation rate increases. This increase in observed current from transient techniques, like chornoamperometry used in this study, results in larger calculated D_{ct} values (see eq 10, Section To our knowledge Tables 11 and 12 lists the first data that are I). consistent with this model. The anion's increasing ability to form tighter ion-pairs with positively charged polymers parallels increasing D_{ct} values. This implies that the currents measured for ClO₄ have the largest contributions from migration and AsF₆ lowest, resulting in larger calculated D_{ct} values for ClO₄. Saveant's model is further supported by the fact that for a given supporting electrolyte EVDQ²⁺ which has the tightest binding pocket exhibits larger D_{ct} values than PVDQ²⁺. Admittedly the Li⁺ and BF₄⁻ data on Tables on 11 and 12 are not in line with Saveant's model. The fact that Li⁺ and BF₄ are the smallest and least polarizable cation and anion studied respectively, may imply that more complex relationships between these counterions and polymer motion exists.

Of course the Saveant model will only apply for charge propagation along the polymer redox sites and not for the D_{app} of $W_6Br_{14}^{\ 2}$ because the monoanion can freely diffuse. Thus the charge propagation rate for cluster will always contain a diffusional component. Currents arising from the physical diffusion of ions as

the mode of charge propagation as opposed to site-to-site charge hopping can not be dominated by migration (diffusion and migration are competing processes). Therefore, the D_{app} 's of $W_6Br_{14}^{2-}$ should obey intuitive diffusional behavior *i.e.* tighter binding equals slower diffusion.

The charge transport rates, D_{ct} were determined for both EVDQ²⁺ and PVDQ²⁺ as a function of increasing $W_6Br_{14}^2$ concentration in acetonitrile containing 0.2 M TBAPF₆ and are listed in Table 13. On the basis of the Saveant model we would expect an increase in D_{ct} values from the films with tighter ion-pairs. shown in Figures 44 and 45, presumably due to its higher charge W₆Br₁₄²- binds more efficiently to the 2,2'-bipyridinium sites as compared to monoanionic electrolytes. The D_{ct} value for EVDQ²⁺ increases from 1.50 x 10⁻¹¹ cm²/s with only TBAPF₆ present to 4.39 x 10^{-11} cm²/s when 5 μ M $W_6Br_{14}^{2-}$ is added to the solution. Similar behavior is observed for PVDQ²⁺. These data clearly support the Saveant model. Eventually the D_{ct} values of polymer decrease with increasing concentration of W₆Br₁₄²- (however it should be noted that even with the observed decrease, D_{ct}'s are faster than that measured when no W₆Br₁₄² is present. As each 2,2'-bipyridinium site becomes bound by cluster, it is likely that the neighboring binding sites become diametrically opposed to each other across polymer chains in an effort to reduce W₆Br₁₄²-W₆Br₁₄²-Thus would perturb the polymers ability to establish interactions. proper orientation required for site-to-site electron hopping to occur.

Interestingly, the FWHM of the polymer reduction waves was noticed to parallel D_{ct} values in that as D_{ct} decreases, FWHM

Conc. of Added W6Br14 ² - µM	Γ _{corr} x 10 ⁹ moles/cm ^{2 a}	0.2 M Electrolyte	D _{ct} x 10 ¹¹ c m ² /sec ^b
EVDQ ²⁺			
0	1.3	TBAPF ₆	1.50
5	1.3	TBAPF ₆	4.39
10	1.3	TBAPF ₆	3.29
50	1.3	TBAPF ₆	2.19
PVDQ ²⁺			
0	1.0	TBAPF ₆	0.41
5	1.0	TBAPF ₆	2.33
10	1.0	TBAPF ₆	1.33
50	1.0	TBAPF ₆	0.79

^a The film coverage Γ_{corr} was determined using the electrochemically determined area of the Pt electrode. ^bD_{ct} is the apparent diffusion coefficient.

increases. The FWHM is controlled by interactions between neighboring charged sites to the extent that repulsive interactions are manifested in increasing FWHM. The predicted value for FWHM of 90 mV is only observed for thin films using ClO_4^- as the electrolyte. For a given electrolyte in Tables 11 and 12 the FWHM becomes larger for thicker films. This observation is expected because repulsive interactions between neighboring chains become more likely. These repulsive interactions between chains will be mediated by ion-pairing. Anions which bind tighter are more efficient at neutralizing charge and reducing repulsive interactions between polymer redox sites than weaker binding anions. On this basis the former would be expected to possess smaller FWHM values.

Moreover, as shown in Tables 11 and 12, the FWHM is always larger for the anodic wave then the cathodic wave. Because anion uptake has been established as the process by which charge neutrality is maintained upon oxidation of reduced polymer, it is likely that anion ejection controls charge neutrality for reduction of the polymer. The reduction of the film should occur rapidly because anions already in the film are simply ejected. However, reoxidation involves the uptake of anions thereby requiring swelling of the polymer to permit rentry of the anion into the film. This is a thermodynamically more difficult process producing equilibrium effects which cause multiple E⁰ values. Thus broadened waves are observed for the anodic component of the reduction wave.

C. Conclusion

This is the first reported example of a electrochemical sensor based on modified electrodes which can detect extremely dilute concentrations of monoanions in nonaqueous solutions. The characterization of electrolyte effects on the charge propagation rates support charge propagation driven by migration. In addition preliminary experiments demonstrate that these films work equally well with aqueous solutions over wide pH ranges. Further investigations of aqueous solutions are ongoing in our laboratory.

Ultimately development of practical sensors requires further development with emphasis on stability, impurity fouling, and low cost. However, the fundamental function of these polymer modified electrodes as novel sensor materials has been established.

CHAPTER VI

REFERENCES

- (a) Murray, R.W. Acc. Chem. Res. 1980, 13, 135-141. (b)
 Murray, R.W.; Bard, A.J. (Ed.) "Electroanalytical Chemistry"; M.
 Dekker: New York, 1984, 13, 191-392.
- 2. Snell, K.D.; Keenan, A.G. Chem. Soc. Rev. 1979, 8, 259-282.
- 3. Miller, J.S. (Ed.) "Chemically Modified Surfaces in Catalysis and Electrocatalysis"; American Chemical Society: Washington D.C., 1982, pg 1-301.
- 4. Albery, W.J.; Hillman, A.R. Ann. Rev. C. R. Soc. Chem. Lond. 1981, 377-385.
- 5. Faulkner, L.R. Chem. Eng. News 1984, Feb 27, 28-45.
- 6. Abruna, H.D. Coord. Chem. Rev. 1988, 86, 135-189.
- 7. Harrison, D.J.; Wrighton, M.S. J. Phys. Chem. 1984, 88, 3103-3107.
- (a) Fan, F.-R.F.; Wheeler, B.L.; Bard, A.J.; Noufi, R.N. J. Electrochem. Soc. 1981, 128, 2042-2045.
 (b) Fan, F.-R.F.; Hope, G.A.; Bard, A.J. J. Electrochem. Soc. 1982, 129, 1647-1649.
- (a) Noufi, R.; Tench, D.; Warren, L.F. J. Electrochem. Soc. 1980, 127, 2709-2713.
 (b) Noufi, R.; Frank, A.J.; Nozik, A.J. J. Am. Chem. Soc. 1981, 103, 1849-1850.
- 10. Rosenblum, M.D.; Lewis, N.S. J. Phys. Chem. 1984, 88, 3103-3108.
- 11. Nanthakumar, A.; Armstrong, N.R. J. Electroanal. Chem. 1988, 248, 349-362.
- 12. Gningue, D.; Horowitz, G.; Garnier, F. J. Electrochem. Soc. 1988, 92, 5221-5229.

- (a) Collman, J.P.; Denisevich, P.; Konai, Y.; Marrocco, M.; Koval, C.; Anson, F.C. J. Am. Chem. Soc. 1980, 102, 6027-6036. (b) Collman, J.P.; Anson, F.C.; Bencosme, C.S.; Durand, R.R.; Kirch, R.P. J. Am. Chem. Soc. 1983, 105, 2710-2718. (c) Collman, J.P.; Kim, K. J. Am. Chem. Soc. 1986, 108, 7847-7849.
- 14. Evans, J.F.; Kuwana, T.; Henne, M.T.; Royer, G.P. J. Electroanal. Chem. 1977, 80, 409-416.
- (a) Chang, C.K.; Liu, H.-Y.; Abdalmuhdi, I. J. Am. Chem. Soc.
 1984, 106, 2725-2726. (b) Liu, H.-Y.; Abfdalmuhdi, I.; Chang,
 C. K.; Anson, F.C. J. Phys. Chem. 1985, 89, 665-670.
- (a) Sullivan, B.P.; Meyer, T.J. J. Chem. Soc. Chem. Commun.
 1984, 1244-1245. (b) O'Toole, T.R.; Margerum, L.D.;
 Westmoreland, T.D.; Vining, W.J.; Murray, R.W.; Meyer, T.J. J.
 Chem. Soc. Chem. Commun. 1985, 1416-1417.
- (a) Cabrera, C.R.; Abruna, H.D. J. Electroanal. Chem. 1986, 209, 101-107.
 (b) Guadalupe, A.R.; Usifer, D.A.; Potts, K.T.; Hurrell, H.C.; Mogstad, A.-E.; Abruna, H.D. J. Am. Chem. Soc. 1988, 110, 3462-3466.
- (a) Stalder, C.J.; Chao, S.; Summers, D.P.; Wrighton, M.S. J. Am. Chem. Soc. 1983, 105, 6318-6320.
 (b) Stalder, C.J.; Chao, S.; Wrighton, M.S. J. Am. Chem. Soc. 1984, 106, 3673-3675.
- 19. Lieber, C.M.; Lewis, N.S. J. Am. Chem. Soc. 1984, 106, 5033-5034.
- Cosnier, S.; Deronzier, A.; Moutet, J.-C. J. Electroanal. Chem.
 1986, 207, 315-321.
- 21. Bettelheim, A.; Ozer, D.; Harth, R.; Murray, R.W. J. Electroanal. Chem. 1988, 246, 139-154.

- 22. Rault-Berthelot, J.; Mabon, G.; Sinonet, J. J. Electroanal. Chem. 1988, 240, 355-359.
- 23. Jiang, R; Dong, S. J. Electroanal. Chem. 1988, 246, 101-117.
- (a) Firth, B.E.; Miller, L.L.; Mitani, M.; Rogers, T.; Lennox, J.;
 Murray, R.W. J. Am. Chem. Soc. 1976, 98, 8271-8272. (b)
 Firth, B.E.; Miller, L.L. J. Am. Chem. Soc. 1976, 98, 8272-8273.
- (a) Komori, T.; Nonaka, T. J. Am. Chem. Soc. 1983, 105, 5690-5691.
 (b) Abe, S.; Nonaka, T.; Fuchigami, T. J. Am. Chem. Soc. 1983, 105, 3630-3632.
 (c) Komori, T.; Nonaka, T. J. Am. Chem. Soc. 1984, 106, 2656-2659.
- (a) Yamagishi, A.; Aramata, A. J. Chem. Soc. Chem. Commun.
 1984, 452-453. (b) Yamagishi, A.; Aramata, A. J. Chem. Soc.
 Chem. Commun. 1985, 449-452.
- 27. Tse, D.C.S.; Kuwana, T. Anal. Chem. 1978, 50, 1315-1318.
- 28. Fijihira, M.; Yokozawa, A.; Kinoshita, H.; Osa, T. Chem. Lett. 1982, 1089-1092.
- 29. Hazard, R.; Jaouannet, S.; Tallec, A. Tetrahedron 1982, 38, 93-102.
- 30. Salmon, M.; Bidan, G. J. Electrochem. Soc. 1985, 132, 1897-1899.
- (a) Landrum, H.C.; Salmon, R.T.; Hawkridge, F.M. J. Am. Chem.
 Soc. 1977, 99, 3154-3158. (b) Castner, J.F.; Hawkridge, F.M. J.
 Electroanal. Chem. 1983, 143, 217-232.

- (a) Eddowes, M.J.; Hill, H.A.O.; J. Am. Chem. Soc. 1979, 101, 4461-4464.
 (b) Albery, W.J.; Eddowes, M.J.; Hill, H.A.O.; Hillman, A.R. J. Am. Chem. Soc. 1981, 103, 3904-3910.
 (c) Allen, P.M; Hill, H.A.O.; Walton, O.J. J. Electroanal. Chem. 1984, 178, 69-85.
- (a) Chao, S.; Wrighton, M.S. J. Am. Chem. Soc. 1987, 109, 5886-5888.
 (b) Chao, S.; Simon, R.A.; Mallouk, T.E.; Wrighton, M.S. J. Am. Chem. Soc. 1988, 110, 2270-2276.
- 34. (a) Taniguchi, I; Murakami, T; Toyosawa, K.; Yamaguchi, H.; Yasukouchi, K. J. Electroanal. Chem. 1982, 131, 397-401. (b) Taniguchi, I; Toyosawa, K.; Yamaguchi, H.; Yasukouchi, K. J. Electroanal. Chem. 1982, 140, 187-193.
- 35. (a) Dhesi, R.; Cotton, T.M.; Timkovich, R. J. Electroanal. Chem.
 1983, 154, 129-139. (b) Cotton, T.M.; Kaddi, D.; Iorga, D. J.
 Am. Chem. Soc. 1983, 105, 7462-7464.
- 36. Elliot, C.M.; Martin, W.S. J. Electroanal. Chem. 1982, 137, 377-385.
- 37. Ye, J.; Baldwin, R.P. Anal. Chem. 1988, 60, 2263-2268.
- (a) White, B.A.; Murray, R.W. J. Am. Chem. Soc. 1987, 109, 2576-258l.
 (b) Oliver, B.N.; Egekeze, J.O.; Murray, R.W. J. Am. Chem. Soc. 1988, 110, 2321-2322.
- (a) Chidsey, C.E.D.; Murray, R.W. Science 1986, 231, 25-31.
 (b) Reed, R.A.; Geng, L.; Murray, R.W. J. Electroanal. Chem.
 1986, 208, 185-193. (c) Geng, L.; Reed, R.A.; Longmire, M.; Murray, R.W. J. Phys. Chem. 1987, 91, 2908-2914. (d)
 Wilbourn, K.; Murray, R.W. J. Phys. Chem. 1988, 92, 3642-3648.

- 40. (a) Wrighton, M.S. Science 1986, 231, 32-37. (b) Chao, S.; Wrighton, M.S. J. Am. Chem. Soc. 1987, 109, 2197-2199. (c) Natan, M.J.; Mallouk, T.E.; Wrighton, M.S. J. Phys. Chem. 1987, 91, 648-654. (d) Shu., C.-F.; Wrighton, M.S. J. Phys. Chem. 1988, 92, 5221-5229.
- 41. Fruge, D.R.; Fong, G.D.; Fong, F.K. J. Am. Chem. Soc. 1979, 101, 3694-3697.
- 42. White, H.S.; Abruna, H.D.; Bard, A.J. J. Am. Chem. Soc. 1982, 124, 265-271.
- (a) Noufi, R.N. J. Electrochem. Soc. 1983, 130, 2126-2128. (b)
 Rajeshwar, K; Kaneko, M.; Yamada, A.; Noufi, R.N. J. Phys. Chem. 1985, 89, 806-811.
- 44. (a) Dubois, D.L.; Turner, J.A. J. Am. Chem. Soc. 1982, 104, 4989-4990. (b) Dubois, D.L. Inorg. Chem. 1984, 23, 2047-2052.
- 45. (a) Sammells, A.F.; Ang, P.G.P. J. Electrochem. Soc. 1984, 131, 617-619. (b) Cook, R.L.; Sammells, A.F. J. Electrochem. Soc. 1985, 132, 2429-2431.
- 46. Yamamoto, T. J. Chem. Soc. Chem. Commun. 1981, 187-188.
- 47. Kaufman, J.H.; Chung, T.-C.; Heeger. A.J.; Wudl, F. J. Electrochem. Soc. 1984, 131, 2091-2093.
- 48. Simon, R.A.; Malleuk, T.E.; Daube, K.A.; Wrighton, M.S. *Inorg*. *Chem.* 1985, 24, 3119-3126.
- 49. Hagemeister, M.P.; White, H.S. J. Phys. Chem. 1987, 91, 150-154.
- 50. Holdcroft, S.; Morrison; Funt, L.B. *J. Electroanal. Chem.* 1988, 245, 191-199.

- 51. Jasinski, R.J. J. Electrochem. Soc. 1977, 124, 637-641.
- 52. Bruinink, J.; Kregting, C.G.A. J. Electrochem. Soc. 1978, 125, 1397-1401.
- 53. Cieslinski, R.C.; Armstrong, N.R. J. Electrochem. Soc. 1980, 127, 2605-2610.
- 54. Reichman, B; Fan, F.-R.F.; Bard, A.J. J. Electrochem. Soc. 1980, 127, 333-338.
- 55. Akahoshi, H.; Toshima, S.; Itaya, K. J. Phys. Chem. 1981, 85, 518-522.
- 56. Garnier, F.; Tourillon, G.; Gazard, M.; Dubois, J.C. *J. Electroanal.*Chem. 1983, 148, 299-303.
- Thackeray, J.W.; White, H.S.; Wrighton, M.S. J. Phys. Chem.
 1985, 89, 5133-5140. (b) Smith, D.K.; Lane, G.A.; Wrighton,
 M.S. J. Phys. Chem. 1988, 92, 2616-2628.
- 58. Viehbeck, A.; DeBerry, D.W. J. Electrochem. Soc. 1985, 132, 1369-1375.
- 59. Elliott, C.M.; Redepenning, J.G. J. Electroanal. Chem. 1986, 197, 219-232.
- 60. Yashima, H.; Kobayashi, M.; Lee, K.-B.; Chung, D.; Heeger, A.J.; Wudl, F. J. Electrochem. Soc. 1987, 134, 46-52.
- 61. Sugimoto, T.; Nagatomi, T.; Ando, H.; Yoshida, Z.-I. Angew. Chem. Ed. Engl. 1988, 27, 560-561.
- (a) Thackeray, J.W.; White, H.S.; Wrighton, M.S. J. Phys. Chem.
 1985, 89, 5133-5137. (b) Thackeray, J.W.; Wrighton, M.S. J.
 Phys. Chem. 1986, 90, 6674-6679. (c) Chao, S.; Wrighton,
 M.S. J. Am. Chem. Soc. 1987, 109, 6627-6631.

- 63. Marrese, C.A.; Blubaugh, E.A.; Durst, R.A. J. Electroanal. Chem. 1988, 243, 193-201.
- 64. Kasem, K.K.; Abruna, H.D. J. Electroanal. Chem. 1988, 242, 87-96.
- 65. Wang J.; Zadeii, J. Anal. Chim. acta. 1987, 188, 187-194.
- (a) Lane, R.F.; Hubbard, A.T. J. Phys. Chem. 1973, 77, 1401-1410.
 (b) Lane, R.F.; Hubbard, A.T. J. Phys. Chem. 1973, 77, 1411-1421.
- 67. Moses, P.R.; Wier, L.; Murray, R.W. Anal. Chem. 1975, 47, 1882-1886.
- Wrighton, M.S.; Austin, R.G.; Bocarsly, A.B.; Bolts, J.M.; Haas, O.;
 Legg, K.D.; Nadjo, L.; Palazzotto, M.C. J. Electroanal. Chem.
 1978, 87, 429-433.
- 69. Wrighton, M.S.; Palazzotto, M.C.; Bocarsly, A.B.; Bolts, J.M.; Fischer, A.B.; Nadjo, L. J. Am. Chem. Soc. 1978, 100, 7264-7271.
- 70. Bolts, J.M.; Wrighton, M.S. J. Am. Chem. Soc. 1978, 100, 5257-5262.
- Bolts, J.M.; Bocarsly, A.B.; Palazzotto, M.C.; Walton, E.G.; Lewis,
 N.S.; Wrighton, M.S. J. Am. Chem. Soc. 1979, 101, 1378-1385.
- 72. Bocarsly, A.B.; Walton, E.G.; Bradly, M.G.; Wrighton, M.S. J. Electroanal. Chem. 1979, 100, 283-306.
- 73. Wrighton, M.S.; Bolts, J.M.; Bocarsly, A.B.; Palazzotto, M.C.; Walton, E.G. J. Vac. Sci. Technol. 1978, 15, 1429-1433.
- 74. Fisher, A.B.; Kinney, J.B.; Staley, R.H.; Wrighton, M.S. J. Am. Chem. Soc. 1979, 101, 7863-7864.

- 75. Nakahama, S.; Murray, R.W. J. Electroanal. Chem. 1983, 158, 303-322.
- 76. Simon, R.A.; Ricco, A.J.; Wrighton, M.S. J. Am. Chem. Soc. 1982, 104, 2031-3034.
- 77. Ghosh, P.; Spiro, T.G. J. Am. Chem. Soc. 1980, 102, 5543-5549.
- 78. Ghosh, P.; Spiro, T.G. J. Electrochem. Soc. 1981, 128, 1281-1287.
- 79. Moses, P.R.; Murray, R.W. J. Electroanal. Chem. 1977, 77, 393-399.
- 80. Murray, R.W.; Leyden, D.E.; Collins, W. (Ed.) "Silayted Surfaces"

 Gordon and Breach: New York, 1980.
- 81. Finklea, H.O.; Abruna, H.D.; Murray, R.W. Adv. Chem. Ser. 1980, 184, 253-256.
- 82. Diaz, A. J. Am. Chem. Soc. 1977, 99, 5838-5840.
- 83. Abruna, H.D.; Meyer, T.J.; Murray, R.W. *Inorg. Chem.* 1979, 11, 3233-3240.
- 84. Abruna, H.D.; Walsh, J.L.; Meyer, T.J.; Inorg. Chem. 1981, 20, 1481-1486.
- 85. Kuo, K.; Moses, P.R.; Lenhard, J.R.; Green, D.C.; Murray, R.W. Anal. Chem. 1979, 51, 745-748.
- 86. Diaz, A.F.; Kanazawa, K.K. IBM J. Res. Dev. 1979, 23, 316-321.
- 87. Moses, P.R.; Murray, R.W. J. Am. Chem. Soc. 1976, 98, 7435-7436.
- 88. Watkins, B.F.; Behling, J.R.; Kariv, E.; Miller, L.L. J. Am. Chem. Soc. 1975, 97, 3549-3550.
- 89. Umana, M.; Rolison, R.; Nowak, R.; Daum, P.; Murray, R.W. Surf. Sci. 1980, 101, 295-310.

- 90. Fujihara, M.; Matsue, T.; Osa, T. Chem. Lett. 1977, 361-366.
- 91. Koval, C.A.; Anson, F.C. Anal. Chem. 1978, 50, 223-229.
- 92. Lennox, J.C.; Murray, R.W. J. Electroanal. Chem. 1977, 78, 395-401.
- 93. Lenhard, J.R.; Rocklin, R.; Abruna, H.; Willman, Kuo, K., Nowak, R.; Murray, R.W. J. Am. Chem. Soc. 1978, 100, 5213-5215.
- 94. Rocklin, R.D.; Murray, R.W. J. Electroanal. Chem. 1979, 100, 271-282.
- 95. Oyama, N.; Anson, F.C. J. Am. Chem. Soc. 1979, 101, 1634-1635.
- 96. Kuwana, T. J. Electroanal. Chem. 1978, 88, 299-303.
- 97. Tse, D.C.S.; Kuwana, T.; Royer, G.P. J. Electroanal. Chem. 1979, 98, 345-353.
- 98. (a) Miller, L.L.; Van De Mark, M.R. J. Am. Chem. Soc. 1978, 100, 639-640. (b) Van De Mark, M.R.; Miller, L.L. J. Am. Chem. Soc. 1978, 100, 3223-3225. (c) Miller, L.L.; Van De Mark, M.R. J. Electroanal. Chem. 1978, 88, 437-440.
- 99. Doblhofer, K.; Nolte, D.; Ulstrup, J. Ber. Bunsenges. Phys. Chem. 1984, 88, 345-351.
- 100. Pham, M.-C.; Lacaze, P.C.; Dubois, J.E. J. Electroanal. Chem.1978, 86, 147-157.
- 101. (a) Merz, A.; Bard, A.J. J. Am. Chem. Soc. 1978, 100, 3222-3223. (b) Itaya, K.; Bard, A.J. Anal. Chem. 1978, 50, 1487-1489.
- 102. (a) Tachikawa, H.; Faulkner, L.R. J. Am. Chem. Soc. 1978, 100, 4379-4385. (b) Tachikawa, H.; Faulkner, L.R. J. Am. Chem. Soc. 1978, 100, 8025-8026.

- (a) Nowak, R.; Schultz, F.A.; Umana, M.; Abruna, H.D.; Murray, R.W. J. Electroanal. Chem. 1978, 94, 219-225. (b) Murray, R.W. "Symposium on Silated Surfaces," Midland, MI. May, 1978.
- 104. Dautartas, M.F.; Evans, J.F.; Kuwana Anal. Chem. 1978, 51, 104-110.
- 105. Kerr, J.B.; Miller, L.L.; Van De Mark, M.R. J. Am. Chem. Soc.1980, 102, 3383-3390.
- 106. Rocklin, R.D.; Murray, R.W. J. Phys. Chem. 1981, 85, 2104-2112.
- 107. Oyama, N.; Anson, F.C. J. Am. Chem. Soc. 1979, 101, 739-741.
- 108. Oyama, N.; Shigehara, K.; Anson, F.C. *Inorg. Chem.* 1981, 20, 518-522.
- 109. Schneider, J.; Murray, R.W. Anal. Chem. 1982, 54, 1508-1515.
- 110. (a) Dautartas, M.F.; Evans, J.F. J. Electroanal. Chem. 1980, 109, 301-312. (b) Dautartas, M.F.; Mann, K.R.; Evans, J.F. J. Electroanal. Chem. 1980, 110, 379-386.
- (a) Rolison, D.R.; Umana, M.; Burgmayer, P.; Murray, R.W. Inorg. Chem. 1981, 20, 2996-3002. (b) Facci, J.; Murray, R.W. Anal. Chem. 1982, 54, 772-777.
- 112. Heider, G.H.; Gelbert, M.B.; Yacynych, A.M. Anal. Chem. 1982, 54, 322-324.
- 113. Rolison, D.R.; Unana, M.; Burgmayer, P; Murray, R.W. *Inorg.*Chem. 1981, 20, 2996-3002.
- 114. Abruna, H.D.; Denisevich, P; Umana, M.; Meyer, T.J., Murray, R.W. J. Am. Chem. Soc. 1981, 103, 1-5.

- (a) Diaz, A.F.; Logan, J.A. J. Electroanal. Chem. 1980, 111, 111-114.
 (b) Kanazawa, K.K.; Diaz, A.F.; Geiss, R.H.; Gill, W.D.; Kwak, J.F.; Logan, J.A.; Rabolt, J.F.; Street, G.B. J. Chem. Soc. Chem. Commun. 1979, 854-855.
- 116. Pham, M.-C.; Lacaze, P.-C.; Dubois, J.-E. J. Electroanal. Chem. 1979, 99, 331-340.
- 117. Kerr, J.B.; Miller, L.L. J. Electroanal. Chem. 1979, 101, 263-267.
- 118. Fuki, M.; Degrand, C.; Miller, L.L. J. Am. Chem. Soc. 1982, 104, 28-33.
- 119. Daum, P.; Murray, R.W. J. Phys. Chem. 1981, 85, 389-396.
- 120. Schroeder, A.H.; Kaufman, F.B.; Patel, V.; Engler, E.M. J. Electroanal. Chem. 1980, 113, 193-208.
- 121. Takiguchi, T.; Nonaka, T.; Fuchigami, T.J. Electroanal. Chem.1985, 195, 177-181.
- 122. Willman, K.W.; Murray, R.W. J. Electroanal. Chem. 1982, 133, 211-231.
- 123. Fan, F.-R.F.; Mau, A.; Bard, A.J. Chem. Phys. Lett. 1985, 116, 400-404.
- 124. (a) Ohsaka, T.; Sato, K.; Matsuda, H.; Oyama, N. J. Electrochem.
 Soc. 1985, 132, 1871-1879. (b) Oyama, N., Ohsaka, T.;
 Yamamoto, H.; Kaneko, M. J. Phys. Chem. 1986, 90, 3850-3856.
- 125. Burgmayer, P.; Murray, R.W. J. Electroanal. Chem. 1982,135, 335-342.
- 126. Mcquillan, J.A.; Reid, M.R. J. Electroanal. Chem. 1985, 194, 237-245.

- 127. Mengoli, G.; Muscani, M.M.; Zotti, G. J. Electroanal. Chem. 1984, 175, 93-104.
- 128. Diaz, A.F.; Martinez, A.; Kanazawa, K.K. J. Electroanal. Chem. 1981. 130. 181-187.
- 129. Waltman, R.J.; Bargon, J.; Diaz A.F. J. Phys. Chem. 1983, 87, 1459-1463.
- 130. Tourillon, G.; Garnier, F. J. Electroanal. Chem. 1984, 161, 407-414.
- 131. Oyama, N.; Ohsaka, T.; Shimizu, T. Anal. Chem. 1985, 57, 1526-1532.
- 132. Ohsaka, T.; Okajima, T.; Oyama, N. J. Electroanal. Chem. 1986, 215, 191-207.
- 133. Lewis, A.; White, H.S.; Wrighton, M.S. J. Am. Chem. Soc. 1984, 106, 6947-6952.
- 134. Gaudiello, J.G.; Ghosh, P.K.; Bard, A.J. J. Am. Chem. Soc. 1985, 107, 3027-3032.
- 135. Scott, N.S.; Oyama, N.; Anson, F.C. J. Electroanal. Chem. 1980, 110, 303-310.
- 136. Wan, G.-X.; Shigehara, E.; Tsuchida, E.; Anson, F.C. J. Electroanal. Chem. 1984, 179, 239-250.
- 137. Calvert, J.M.; Meyer, T.J. Inorg. Chem. 1981, 20, 27-33.
- 138. Potts, K.T.; Usifer, D.; Guadalupe, A.; Abruna, H.D. J. Am. Chem. Soc. 1987, 109, 3961-3967.
- 139. Ellis, C.D.; Margerum, L.D.; Murray, R.W.; Meyer, T.J. *Inorg*. Chem. 1983, 22, 1283-1291.

- 140. (a) Bidan, G.; Deronzier, A.; Moutet, J.-C. J. Chem. Soc. Chem. Commun. 1984, 1185-1186. (b) Cosiner, S.; Deronzier, A.; Moutet, J.-C. J. Phys. Chem. 1985, 89, 4895-4897.
- 141. Eaves, J.G.; Munro, H.S.; Parker, D. J. Chem. Soc. Chem. Commun. 1985, 684-685.
- 142. Margerum, L.D.; Meyer, T.J.; Murray, R.W. J. Electroanal. Chem. 1983, 149, 279-285.
- (a) Ikeda, T.; Leidner, C.R.; Murray, R.W. J. Am. Chem. Soc.
 1981, 103, 7422-7424. (b) Pickup, P.G.; Kutner, W.; Leidner, C.R.; Murray, R.W. J. Am. Chem. Soc. 1984, 106, 1991-1998.
 (c) Leidner, C.R.; Murray, R.W. J. Am. Chem. Soc. 1985, 107, 551-556.
- 144. Vining, W.J.; Surridge, N.A.; Meyer, T.J. J. Phys. Chem. 1986, 90, 2281-2283.
- 145. Guarr, T.F.; Anson, F.C. J. Phys. Chem. 1987, 91, 4037-4043.
- 146. Oyama, N.; Anson, F.C. J. Electrochem. Soc. 1980, 127, 247-250.
- 147. (a) Oyama, N; Shimomura, K.; Shigehara, K.; Anson, F.C. J. Electroanal. Chem. 1980, 112, 271-280.
- 148. Oyama, N; Ohsaka, T.; Ushirogouchi, T. J. Phys. Chem. 1984, 88, 5274-5280.
- 149. Niwa, K.; Doblhofer, K. Electrochim. Acta. 1986, 31, 553-549.
- (a) Ohsaka, T.; Anson, F.C. J. Phys. Chem. 1983, 87, 640-647.
 (b) Anson, F.C.; Ohsaka, T.; Saveant, J.-M. J. Am. Chem. Soc. 1985, 107, 4883-4892.
- 151. Sumi, K.; Anson, F.C. J. Phys. Chem. 1986, 90, 3845-3850.

- 152. Crouch, A.M.; Ordonez, I.; Langford, C.H.; Lawrence, M.F. J. Phys. Chem. 1988, 92, 6058-6065.
- 153. (a) Henning, T.P.; White, H.S.; Bard, A.J. J. Am. Chem. Soc.
 1981, 103, 3937-3938. (b) Krishnan, M.; White, J.R.; Fox,
 M.A.; Bard, A.J. J. Am. Chem. Soc. 1983, 105, 7002-7003.
- 154. (a) Buttry, D.A.; Saveant, J.-M.; Anson, F.A. J. Phys. Chem.
 1984, 88, 3086-3091. (b) McHatton, R.C.; Anson, F.C. Inorg.
 Chem. 1984, 23, 3935-3942.
- 155. (a) Martin C.R. Anal. Chem. 1982, 54, 1639-1641. (b) Penner, R.M.; Martin, C.R. J. Electrochem. Soc. 1985, 132, 514-515.
- 156. Lieber, C.M.; Schmidt, M.H.; Lewis, N.S. J. Am. Chem. Soc. 1986, 108, 6103-6108.
- 157. (a) Majda, M; Faulkner, L.R. J. Electroanal. Chem. 1984, 169, 97-112. (b) Jones, E.T.T.; Faulkner, L.R. J. Electroanal. Chem. 1987, 222, 201-222.
- 158. Vining, W.J.; Meyer, T.J. Inorg. Chem. 1986, 25, 2023-2033.
- 159. Nowak, R.J.; Schultz, F.A.; Umana, M.; Lam, R.; Murray, R.W. Anal. Chem. 1980, 52, 315-321.
- 160. Oyama, N.; Anson, F.C. J. Electroanal. Chem. 1980, 127, 640-647.
- 161. Daum, P.; Murray, R.W. J. Electroanal. Chem. 1979, 103, 289-294.
- 162. Kaufman, F.B.; Engler, E.M. J. Am. Chem. Soc. 1979, 101, 547-549.
- 163. Peerce, P.J.; Bard, A.J. J. Electroanal. Chem. 1980, 114, 89-115.
- 164. Laviron, E. J. Electroanal. Chem. 1980, 112, 1-9.

- 165. Andrieux, C.P.; Saveant, J.M. J. Electroanal. Chem. 1980, 111, 377-381.
- 166. (a) Ikeda, T.; Leidner, C.R.; Murray, R.W. J. Electroanal. Chem.
 1982, 138, 343-365. (b) Facci, J.S.; Schmehl, R.H.; Murray,
 R.W. J. Am. Chem. Soc. 1982, 104, 4959-4960.
- 167. Shigehara, K.; Oyama, N.; Anson, F.C. J. Am. Chem. Soc. 1981, 103, 2552-2558.
- 168. Lenhard, J.R.; Murray, R.W. J. Am. Chem. Soc. 1978, 100, 7870-7875.
- 169. Peerce, P.J.; Bard, A.J. J. Electroanal. Chem. 1980, 112, 97-115.
- 170. Angerstein-Kozlowska, H.; Klinger, J.; Conway, B.E. J. Electroanal. Chem. 1977, 75, 45-60.
- 171. (a) Brown, A.P.; Anson, F.C. J. Electroanal. Chem. 1978, 92, 133-145.
- Wrighton, M.S.; Austin, R.G.; Bocarsly, A.B.; Bolts, J.M.; Haas, O.;
 Legg, K.D.; Nadjo, L.; Palazzotto, M.C. J. Am. Chem. Soc. 1978,
 100, 1602-1603.
- 173. Sharp, M.; Peterson, M.; Edstrom, K. J. Electroanal. Chem. 1979, 95, 123-130.
- 174. Deronzier, A.; Latour, J-M J. Electroanal. Chem. 1987, 224, 295-301.
- 175. Oyama, N.; Anson, F.C. J. Am. Chem. Soc. 1979, 101, 3450-3456.
- 176. Kaufman, F.B.; Schroeder, A.H.; Engler E.M.; Kramer, S.R.; Chambers, J.Q. J. Am. Chem. Soc. 1980, 102, 483-488.
- 177. Denisevich, P.; Abruna, H.D.; Leidner, C.R.; Meyer, T.J.; Murray, R.W. *Inorg. Chem.* 1982, 21, 2153-2161.

- 178. Leddy, J.; Bard, A.J.; Maloy, J.T.; Saveant, J.M. J. Electroanal. Chem. 1985, 187, 205-227.
- 179. Oyama, N.; Ohasaka, T.; Yamamoto, H.; Kaneko, M. J. Phys. Chem. 1986, 90, 3850-3856.
- 180. (a) Chambers, J.Q.; Inzelt, G. Anal. Chem. 1985, 57, 1117-1121.
 (b) Inzelt, G.; Bacskai, J.; Chambers, J.Q.; Day, R.W. J. Electroanal. Chem. 1986, 201, 301-314.
- 181. Peerce, P.J.; Bard, A.J. J. Electroanal. Chem. 1980, 108, 121-125.
- 182. Samuels, G.T.; Meyer, T.J. J. Am. Chem. Soc. 1981, 103, 307-312.
- 183. Laviron, E. J. Electroanal. Chem. 1979, 105, 25-35.
- 184. Kaufman, F.B.; Schroeder, A.H.; Engler, E.M.; Kramer, S.R.; Chambers, J.Q. J. Am. Chem. Soc. 1980, 102, 483-488.
- 185. Henning, T.P.; Bard, A.J. J. Electrochem. Soc. 1983, 130, 613-621.
- 186. (a) Brown, A.P.; Anson, F.C. Anal. Chem. 1977, 49, 1589-1595.
 (b) Brown, A.P.; Koval, C.; Anson, F.C. J. Electroanal. Chem. 1976, 72, 379-387.
- 187. Smith, D.F.; Willman, K.; Kuo, K.; Murray, R.W. J. Electroanal. Chem. 1979, 95, 217-227.
- 188. Kuo, K.N.; Murray, R.W. J. Electroanal. Chem. 1982, 131, 37-60.
- 189. Laviron, E. J. Electroanal. Chem. 1980, 112, 11-23.
- 190. Faci, J.; Murray, R.W. J. Phys. Chem. 1981, 85, 2870-2873.
- 191. Dahms, H. J. Phys. Chem. 1968, 72, 362-364.

- 192. Laviron, E.; Roullier, L.; Degrand, C. J. Electroanal. Chem. 1980, 112, 11-23.
- 193. (a) Andrieux, D.C.; Saveant, J.M. J. Electroanal. Chem. 1978,
 93, 163-168. (b) Andrieux, D.C.; Dumas-Boouchait, J.M.;
 Saveant, J.M. J. Electroanal. Chem. 1980, 114, 159-163.
- 194. (a) Ruff, I. Electrochim. Acta. 1970, 15, 1059-1061. (b) Ruff,
 I.; Korosi-Odor, I. Inorg. Chem. 1970, 9, 186-188. (c) Ruff, I.;
 Friedrich, V. J. Phys. Chem. 1971, 75, 3297-3309.
- 195. Buttry, D.A.; Anson, F.C. J. Electroanal. Chem. 1981, 85, 2870-2873.
- 196. Facci, J.; Murray, R.W.; J. Phys. Chem. 1981, 85, 2870-2873.
- 197. White, H.S.; Leddy, J.; Bard, A.J. J. Am. Chem. Soc. 1982, 104, 4811-4817. (b) Martin, C.R.; Rubenstein, I.; Bard, A.J. J. Am. Chem. Soc. 1982, 104, 4817-4824.
- 198. Buttry, D.A., Anson, F.C. J. Am. Chem. Soc. 1983, 23, 685-689.
- 199. Anson, F.C.; Saveant, J.M.; Shigehara, K. J. Phys. Chem. 1983, 87, 214-219.
- 200. (a) Andrieux, C.P.; Dumas-Bouchiat, J.M.; Saveant, J.M. J. Electroanal. Chem. 1982, 131, 1-35. (b) Andrieu, C.P.; Saveant, J.M. J. Electroanal. Chem. 1982, 134, 163-166. (c) Andrieu, C.P.; Saveant, J.M. J. Electroanal. Chem. 1982, 142, 1-30.
- 201. Anson, F.C.; Saveant, J.M.; Shigehara, K. J. Am. Chem. Soc.1983, 105, 1096-1106.
- 202. (a) Andrieux, C.P.; Dumas-Bouchiat, J.M.; Saveant, J.M. J. Electroanal. Chem. 1981, 123, 189-243. (b) Andrieux, C.P.; Saveant, J.M. J. Electroanal. Chem. 1984, 171, 65-93.

- (a) Oyama, N.; Anson, F.C. Anal. Chem. 1980, 52, 1192-1198.
 (b) Tsou, Y.M.; Anson, F.C. J. Phys. Chem. 1985, 89, 3818-3823.
- 204. Leddy, J.; Bard, A.J. J. Electroanal. Chem. 1985, 189, 203-219.
- Feldman, B.J.; Ewing, A.G.; Murray, R.W. J. Electroanal. Chem.
 1985, 194, 63-81.
- 206. Ohsaka, T.; Okajima, T.; Oyama, N. J. Electroanal. Chem. 1986, 215, 191-207.
- 207. Sharp, M. J. Electroanal. Chem. 1987, 230, 109-124.
- 208. Facci, J.; Murray, R.W. J. Electroanal. Chem. 1981, 124, 339-343.
- 209. (a) Rubinstein, I; Bard, A.J. J. Am. Chem. Soc. 1980, 102, 6641-6642. (b) Kaifer, A.E.; Bard, A.J. J. Phys. Chem. 1986, 90, 868-873.
- 210. Montgomery, D.D.; Anson, F.C. J. Am. Chem. Soc. 1985, 107, 3431-3436.
- 211. (a) Oyama, N.; Ohsaka, T.; Kaneko, M.; Sato, K.; Matsuda, H. J. Am. Chem. Soc. 1983, 105, 6003-6008. (b) Ohsaka, T.; Okajima, T.; Oyama, N. J. Electroanal. Chem. 1986, 206, 191-207.
- 212. Doblhofer, K.; Braun, H.; Lange, R. J. Electroanal. Chem. 1986, 206, 93-100.
- 213. Lindholm, B. J. Electroanal. Chem. 1988, 250, 341-354.
- 214. Majda, M; Faulkner, L.R. J. Electroanal. Chem. 1984, 169, 77-95.
- 215. Chen, X.; Peixin, H.; Faulkner, L.R. J. Electroanal. Chem. 1987, 222, 223-242.

- 216. (a) Stalnaker, N.D.; Solenberger, J.C.; Wahl, A.C. J. Phys. Chem.
 1977, 81, 601-605. (b) Burstall, F.H.; Nyholm, R.S. J. Chem.
 Soc. 1952, 3570-3579.
- 217. Shilt, A.A. J. Am. Chem. Soc. 1960, 82, 3000-3005.
- 218. Dwyer, F.P.; Hogarth, J.W. Inorg. Synth. 1957, 5, 206-207.
- 219. Dorman, W.C.; McCarley, R.E. Inorg. Chem. 1974, 13, 491-493.
- 220. Bookbinder, D.C.; Wrighton, M.S. J. Electrochem. Soc. 1983, 130, 1080-1087.
- 221. Abruna, H.D.; Breikss, D.B.; Collum, D.B. *Inorg. Chem.* 1985, 24, 987-988.
- 222. Barrer, R.M.; Jones, D.L. J. Chem. Soc. A. 1970, 1531-1537.
- 223. Daum, P.; Lenhard, J.R.; Rolison, D.R.; Murray, R.W. J. Am. Chem. Soc. 1980, 102, 4649-4653.
- 224. Oyama, N.; Anson F.C. J. Electrochem. Soc. 1980, 127, 640-647.
- 225. Adams, R.N. "Electrochemistry at Solid Electrodes"; M. Dekker: New York, 1969.
- 226. Ghosh, P.K.; Bard, A.J. J. Am. Chem. Soc. 1983, 105, 5691-5693.
- 227. Ege, D.; Ghosh, P.K.; White, J.R.; Equey, J.-F.; Bard, A.J. J. Am. Chem. Soc. 1985, 107, 5644-5652.
- 228. Liu, H.Y.; Anson, F.C. J. Electroanal. Chem. 1985, 184, 411-417.
- 229. King, R.D.; Nocera, D.G.; Pinnavaia, T.J. J. Electroanal. Chem.1987, 236, 43-53.
- 230. (a) Fitch, A.; Lavy-Feder, A.; Lee, S.A.; Kirsh, M.T. J. Phys. Chem. 1988, 92, 6665-6670. (b) Fitch, A.; Faust, C.L. J. Electroanal. Chem. 1988, 257, 299-303.

- 231. Inoue, H.; Haga, S.; Iwakura, C.; Yoneyama, H. J. Electroanal. Chem. 1988, 249, 133-141.
- 232. Itaya, K.; Chang, H.-C.; Uchida, I. *Inorg. Chem.* 1987, 26, 624-626.
- 233. Shaw, B.R.; Creasy, K.E. J. Electroanal. Chem. 1988, 243, 209-217.
- 234. (a) Hernandez, L.; Hernandez, P.; Sosa, Z. Z. Anal. Chem. 1988, 331, 525-527. (b) Hernandez, L.; Hernandez, P.; Sosa Ferrera, Z. Z. Anal. Chem. 1988, 331, 756-759. (c) Hernandez, L.; Hernandez, P.; Lorenzo, E.; Sosa Ferrera, Z. Analyst. 1988, 113, 621-623.
- 235. Hernandez, L.; Hernandez, P.; Blanco, M.H.; Lorenzo, E.; Alda, E. submitted to Z. Anal. Chem.
- 236. (a) Miller, C.J.; Majda, M. J. Electroanal. Chem. 1986, 207, 4972. (b) Miller, C.J.; Majda, M. Anal. Chem. 1988, 60, 11681176.
- 237. Miller, C.J.; Widrig, C.A.; Charych, D.H.; Majda, M. J. Phys. Chem. 1988, 92, 1928-1936.
- 238. Lundgren, L.A.; Murray, R.W. J. Electroanal. Chem. 1988, 227, 287-294.
- 239. Murray, C.G.; Nowak, R.J.; Rolison, D.R. J. Electroanal. Chem. 1984, 164, 205-210.
- 240. De-Vismes, B.; Bedioui, F.; Devynck, J.; Bied-Charreton, C. J. Electroanal. Chem. 1985, 187, 197-202.
- 241. (a) Gemborys, H.A.; Shaw, B.R. J. Electroanal. Chem. 1986, 206, 95-107. (b) Sargeant, J.A.; Tirhado, M. J. Electrochem. Soc. 1988, 135, 869-876.

- 242. Murr, E.N.; Kerkeni, M.; Sellami, A.; Taarit, Y.B. *J. Electroanal.*Chem. 1988, 246, 461-465.
- 243. (a) Li, Z.; Mallouk, T.E. J. Phys. Chem. 1987, 91, 643-648. (b)
 Li. Z.; Wang, C.M.; Persaud, L.; Mallouk, T.E. J. Phys. Chem. 1988, 92, 2592-2597.
- 244. Lee, H.; Kepley, L.J.; Hong, H.-G.; Akhter, S.; Mallouk, T.E. J. Phys. Chem. 1988, 92, 2597-2601.
- 245. (a) Keita, B.; Nadjo, L.; Haeussler, J.P. J. Electroanal. Chem.
 1988, 243, 481-491. (b) Keita, B.; Nadjo, L. J. Electroanal.
 Chem. 1988, 240, 325-332.
- 246. Renneke, R.F.; Hill, C.L. J. Am. Chem. Soc. 1986, 108, 3528-3529.
- 247. Mizumo, N.; Watanabe, T.; Misono, M. J. Phys. Chem. 1985, 89, 80-85.
- 248. (a) Kulesza, P.J.; Faulkner, L.R. J. Am. Chem. Soc. 1988, 110, 4905-4913. (b) Kulesza, P.J.; Faulkner, L.R. J. Electroanal. Chem. 1988, 248, 305-320.
- 249. Itaya, K.; Uchida, I.; Neff, V.D. Acc. Chem. Res. 1986, 19, 162-168.
- 250. Thomas, J.M.; Whittingham, M.S. and Jacobson, A.J. (Eds)
 "Intercalation Chemistry" Academic Press: New York, 1982,
 Chpt. 3.
- 251. Fripiat, J.J.; Jell, A.N.; Poncelot, G.; Andre, J. J. Phys. Chem.1965, 69, 2185-2197.
- 252. Pinnavaia, T.J. Science 1983, 220, 365-371.
- 253. Yamagishi, A.; Aramata, A. J. Electroanal. Chem. 1985, 191, 449-452.

- 254. (a) Kanbara, T.; Yamamoto, T.; Tokuda, K.; Aoki, K. Chem. Lett.
 1987, 2173-2176. (b) Yamamoto, T.; Kanbara, T. Inorg. Chim.
 Acta. 1988, 142, 191-193. (c) Kanbara, T.; Yamamoto, T.
 Denki. Kagaku. Oyobi. Kogyo. Butsuri. Kagaku. 1989, 57, 91-92.
- 255. Aramata, A.; Yamagishi, A. Denki. Kagaku. Oyobi. Kogyo. Butsuri. Kagaku. 1987, 55, 422-427.
- 256. Ghosh, P.K.; Mau-A.W.-H.; Bard, A.J. J. Electroanal. Chem. 1984, 169, 315-317.
- 257. (a) Rusling, J.F.; Shi, C.-N.; Suib, S.L. J. Electroanal. Chem. 1988,
 245, 331-337. (b) Shi, C.; Rusling, J.F.; Wang, Z.; Willis, W.S.;
 Winiecki, A.M.; Suib, S.L. Langmuir 1989, 5, 650-660.
- 258. Kamat, P.V. J. Electroanal. Chem. 1984, 163, 389-394.
- 259. (a) Fan, F.-R.F.; Liu, H.-Y.; Bard, A.J. J. Phys. Chem. 1985, 89, 4418-4420. (b) Enea, O; Bard, A.J. J. Phys. Chem. 1986, 90, 301-306.
- 260. Kotkar, D.; Joshi, V.; Ghosh, P.K. Proc. Indian Natl. Acad. A 1986, 52, 736-743.
- 261. Rudzinski, W.E.; Bard, A.J. J. Electroanal. Chem. 1986, 199, 323-340.
- 262. Buttry, D.A.; Anson, F.C. J. Am. Chem. Soc. 1984, 106, 59-64.
- 263. Chan, M.-S.; Wahl, A.C. J. Phys. Chem. 1978, 82, 2542-2549.
- 264. Bard A.J.; Faulkner, L.R. "Electrochemical Methods.

 Fundamentals and Applications"; Wiley: New York, 1980, pg
 431.
- 265. Itaya, K.; Bard, A.J. J. Phys. Chem. 1985, 89, 5565-5568.

- Traynor, M.F.; Mortland, M.M.; Pinnavaia, T.J. Clays Clay Miner.1978, 26, 318-324.
- 267. Loeppert, R.H.; Mortland, M.M.; Pinnavaia, T.J. Clays Clay Miner. 1979, 27, 201-208.
- 268. Kadkhodayan, A.; Pinnavaia, T.J. J. Mol. Catal. 1983, 21, 109-112.
- 269. Cebula, D.J.; Thomas, R.K.; Middleton, S.; Ottewill, R.H.; White, J.W. Clays Clay Miner. 1979, 27, 39-52.
- 270. Van Olphen, H. "An Introduction to Clay Colloid Chemistry"; Wiley: New York, 1977, pg 27.
- 271. White, J.R.; Bard, A.J. J. Electroanal. Chem. 1986, 197, 233-244.
- 272. Carter, M.T.; Bard, A.J. J. Electroanal. Chem. 1987, 229, 191-214.
- 273. (a) Fan, F.-R.F.; Bard, A.J. J. Electrochem. Soc. 1986, 133, 301-304.
 (b) Castro-Acuna, C.M.; Fan, F.-R.F.; Bard, A.J. J. Electroanal. Chem. 1987, 234, 347-353.
- 274. Rudzinski, W.E.; Figueroa, C.; Hoppe, C.; Kuromoto, T.Y.; Root, D.
 J. Electroanal. Chem. 1988, 243, 367-378.
- 275. Inoue, H.; Yoneyama, H. J. Electroanal. Chem. 1987, 233, 291-294.
- Calvert, J.M.; Schmehl, R.H.; Sullivan, B.P.; Facci, J.S.; Meyer, T.J.;
 Murray, R.W. *Inorg. Chem.* 1983, 22, 2151-2162.
- 277. Denisevich, P.; Willman, K.; Murray, R.W. J. Am. Chem. Soc.1981, 103, 4727-4737.
- 278. Oyama, N.; Anson, F.C. J. Electroanal. Chem. 1986, 199, 467-470.

- 279. Oyama, N. Appl. Chem. Resour. 1987, 29, 138-141.
- 280. Faulkner, L.R. Int. Rev. Sci: Phys. Chem., Ser. Two 1975, 9, 213-263.
- 281. Pighin, A. Can. J. Chem. 1973, 51, 3467-3472.
- 282. Itoh, K.; Honda, K.; Sukigara, M. J. Electroanal. Chem. 1980, 110, 277-284.
- 283. Turro, N.J. "Modern Molecular Photochemistry";
 Benjamin/Cummings: Menlo Park, CA, 1978.
- 284. (a) Tokel, N.E.; Bard, A.J. J. Am. Chem. Soc. 1972, 94, 2862-2863. (b) Wheeler, B.L.; Nagasubramanian, G.; Bard, A.J.; Schechtman, L.A.; Dininny, D.R.; Kenney, M.E. J. Am. Chem. Soc. 1984, 106, 7404-7410.
- 285. Abruna, H.D. J. Electrochem. Soc. 1985, 132, 842-849.
- 286. Luong, J.C.; Nadjo, L.; Wrighton, M.S. J. Am. Chem. Soc. 1978, 100, 5790-5785.
- 287. Vogler, A.; Kunkely, H. Angew. Chem. Int. Ed. Engl. 1984,23, 316-317.
- 288. Ouyang, J.; Zietlow, T.C.; Hopkins, M.D.; Fan, F.-R.F.; Gray, H.B.; Bard, A.J. J. Phys. Chem. 1986, 90, 3841-3844.
- 289. Bonafede, S.; Ciano, M.; Bolletta, F.; Balzani, V.; Chassot, L.; Zelewsky, A. J. Phys. Chem. 1986, 90, 3836-3841.
- 290. Wallace, W.L.; Bard, A.J. J. Phys. Chem. 1979, 83, 1350-1357.
- 291. Itoh, K.; Honda, K. Chem. Lett. 1979, 99-102.
- 292. Kim, J.; Fan, F.-R.F.; Bard, A.J.; Che, C.-M.; Gray, H.B. Chem. Phys. Lett. 1985, 121 543-546.
- 293. Che, C.-M.; Atherton, S.J.; Butler, L.G.; Gray, H.B. J. Am. Chem. Soc. 1984, 106, 5143-5145.

- 294. Liu, D.K.; Brunschwig, B.S.; Creutz, C.; Sutin, N. J. Am. Chem. Soc.1986, 108, 1749-1755.
- 295. Mussell, R.D.; Nocera, D.G. J. Am. Chem. Soc.. 1988, 110, 2764-2772.
- 296. Rubinstein, I.; Bard, A.J. J. Am. Chem. Soc. 1980, 102, 6641-6642.
- 297. Rubinstein, I.; Bard, A.J. J. Am. Chem. Soc.. 1981, 103, 5007-5012
- 298. Buttry, D.A.; Anson, F.C. J. Am. Chem. Soc.. 1982, 104, 4824-4829.
- 299. Ghosh, P.K.; Bard, A.J. J. Electroanal. Chem. 1984, 169, 113-128.
- 300. Xun, Z.; Bard, A.J. J. Phys. Chem. 1988, 92, 5566-5569.
- 301. Abruna, H.D.; Bard, A.J. J. Am. Chem. Soc.. 1982, 104, 2641-2642.
- 302. Fan, F.-R.F.; Mau, A.; Bard, A.J. Chem. Phys. Lett. 1985, 116, 400-404.
- 303 Anson, F.C.; Ni, C.L.; Saveant, J.M. J. Am. Chem. Soc. 1985, 107, 3442-3450.
- 304. Fan, F.-R.F.; Reichman, B.; Bard, A.J. J. Am. Chem. Soc.. 1980, 102, 1488-1492.
- 305. Heller, A.; Miller, B.; Lewerenz, H.J.; Bachmann, K.J. J. Am. Chem. Soc.. 1980, 102, 6555-6556.
- Bookbinder, D.C.; Bruce, J.A.; Dominey, R.N.; Lewis, N.S.;
 Wrighton, M.S. Proc. Natl. Acad. Sci, UAS 1980, 77, 6280-6284.

- 307. Dominey, R.N.; Lewis, N.S.; Bruce, J.A.; Bookbinder, D.C.; Wrighton, M.S. J. Am. Chem. Soc.. 1982, 104, 467-482.
- 308. Bruce, J.A.; Murahashi, T. Wrighton, M.S. J. Phys. Chem. 1982, 86, 1552-1563.
- 309. Dabestani, R.; Wang, X.; Bard, A.J.; Campion, A.; Fox, M.A.; Webber, S.E.; White, J.M. J. Phys. Chem. 1986, 90, 2729-2732.
- 310. Shimidzu, T.; Ohtani, A.; Iyoda, T.; Honda, K. J. Electroanal. Chem. 1987, 224, 123-135.
- 311. Patil, A.O.; Ikenoue, Y.; Wudl, F.; Heeger, A.J. J. Am. Chem. Soc.. 1987, 109, 1858-1859.
- 312. Reynolds, J.R.; Sundaresan, N.S.; Pomerantz, M.; Basak, S.; Baker, C.K. J. Electroanal. Chem. 1988, 250, 355-371.
- 313. (a) Oyama, N.; Anson, F.C. J. Electrochem. Soc. 1980, 127, 249-250. (b) Shigehara, K.; Oyama, N.; Anson, F.C. Inorg. Chem. 1981, 20, 518-522.
- 314. Oyama, N.; Sato, K.; Matsuda, H. J. Electroanal. Chem. 1980, 115, 149-155.
- 315. Cox, J.A.; Kulesza, P.J. J. Electroanal. Chem. 1983, 154, 71-78.
- 316. Belanger, D. J. Electroanal. Chem. 1988, 251, 55-62.
- 317. Braun, H.; Storck, W.; Doblhofer, K. J. Electroanal. Chem. 1983, 130, 807-811.
- 318. Zumbrunnen, H.R.; Anson, F.C. J. Electroanal. Chem. 1983, 152, 111-124.
- 319. Doblhofer, K.; Braun, H.; Storck, W. J. Electroanal. Chem. Soc. 1983, 130, 807-811.
- 320. Bovey, F.A. "High Resolution NMR of Macromolecules";
 Academic Press: New York, 1972.

- 321. Mortimer, R.J.; Anson, F.C. J. Electroanal. Chem. 1982, 138, 325-341.
- 322. Bruce, J.A.; Wrighton, M.S. J. Am. Chem. Soc. 1982, 104, 74-82.
- 323. Miller, T.A.; Prater, B.; Lee, J.K.; Adams, R.N. J. Am. Chem. Soc.. 1965, 87, 121-122.
- 324. Kuwana, T.; Bublitz, D.E.; Hoh, G. J. Am. Chem. Soc.. 1960, 82, 5811-5817.
- 325. Osa, T.; Kuwana, T. J. Electroanal. Chem. 1969, 22, 389-406.
- 326. Winograd, N.; Kuwana, T. J. Am. Chem. Soc. 1971, 93, 4343-4350.
- 327. Samec, Z.; Nemec, C.I. J. Electroanal. Chem. 1971, 31, 161-173.
- 328. Bookbinder, D.C.; Wrighton, M.S. J. Am. Chem. Soc.. 1980, 102, 5123-5125.
- 329. Lewis, N.S.; Wrighton, M.S. Science 1981, 211, 944-947.
- 330. Bookbinder, D.C.; Lewis, N.S.; Bradley, M.G.; Bocarsly, A.B.; Wrighton, M.S. J. Am. Chem. Soc.. 1979, 101, 7721-7723.
- 331. Dominey, R.N.; Lewis, T.J.; Wrighton, M.S. J. Phys. Chem. 1983, 87, 5345-5354.
- 332. Ryan, T.M.; Day, R.J.; Cooks, R. Anal. Chem. 1980, 52, 2054-2057.
- 333. Ghosh, P.K.; Spiro, T.G. J. Am. Chem. Soc.. 1980, 102, 5543-5549.
- 334. Ghosh, P.K.; Spiro, T.G. J. Electrochem. Soc. 1981, 128, 1281-1287.
- 335. Willman, K.W. Thesis; University of North Carolina ,1981.

- 336. Haque, R.; Coshow, W.R.; Johnson, L.F. J. Am. Chem. Soc.. 1969, 91, 3822-3827.
- 337. (a) Spotswood, T.M.; Tanzer, C.I. Aust. J. Chem. 1967, 20, 1213-1225. (b) Spotswood, T.M.; Tanzer, C.I. Aust. J. Chem. 1967, 20, 1227-1234.
- 338. Wang, J.; Mahmoud, J.S. J. Electroanal. Chem. 1986, 208, 383-392.
- 339. Wang, J. "Stripping Analysis: Principles, Instrumentation, and Applications"; VCH Publishers: Deerfield Beach, Fla., 1985.
- 340. Wang, J.; Bard, A.J. (Ed.) "electroanalytical Chemistry"; M. Dekker: New York, 1988, 17, pg 1-88.
- 341. Cheek, G.T.; Nelson, R.F. Anal. Lett. 1978, 393-402.
- 342. Whiteley, L.D.; Martin C.R. Anal. Chem. 1987, 59, 1746-1751.
- 343. Guadalupe, A.R.; Abruna, H.D. Anal. Chem. 1985, 57, 142-149.
- 344. Murray, R.W.; Ewing, A.G.; Durst, R.A. Anal. Chem. 1987, 59, 379A-385A.
- 345. Wang J.; Greene, B.; Morgan, C. Anal. Chim. Acta. 1984, 158, 15-22.
- 346. Kalcher, K. Analyst 1986, 111, 625-630.
- 347. Ohsaka, T.; Okajima, T.; Oyama, N. J. Electroanal. Chem. 1986, 200, 159-178.
- 348. Nagy, G.; Gerhardt, G.A.; Oke, A.F.; Rice, M.E.; Adams, R.N.; Moore, R.B. III.; Szentirmay, M.N.; Martin, C.R. J. Electroanal. Chem. 1985, 188, 85-94.
- 349. (a) Saveant, J.M. J. Electroanal. Chem. 1987, 238, 1-8. (b) Saveant, J.M. J. Electroanal. Chem. 1988, 242, 1-21.

350. Andrieux, C.P.; Saveant, J.M. J. Phys. Chem. 1988, 88, 6761-6767.